FINITE ELEMENT ANALYSIS OF LAYERED ROAD PAVEMENTS

by

KENNETH LEWIS TAYLOR, B.Sc.

A thesis submitted to the University of Nottingham for the degree of Doctor of Philosophy

Department of Civil Engineering,
University of Nottingham

October 1971

ACKNOWLEDGEMENTS

The author wishes to thank Professor P.S. Pell, B.Sc.(Eng.), Ph.D., C.Eng., F.I.C.E. and Mr. C. Snell, M.Sc. for supervising his work and Professor R.C. Coates, B.Sc.(Eng.), Ph.D., C.Eng., F.I.C.E., F.I.Struct.E., M.I.Mech.E. for making available the facilities of the Department of Civil Engineering.

Development would not have been possible without the efficient system made available on a KDF9 computer by the Director and staff of the Cripps Computer Centre (Nottingham). The Support Group staff of SRC Atlas Laboratory, Chilton have also offered invaluable assistance.

The Science Research Council must be thanked for providing a Studentship, and the Institution of Civil Engineers for awarding extra assistance in the form of a Radley Research Studentship.

Miss Jane Clerbaut and Miss Catherine Hill are thanked for efficient typing.

SUMMARY

The recent interest in the application of classical structural design methods to the layered road pavement problem has made a demand for both realistic material structural properties and a method of structural analysis which can incorporate them. The Finite Element Method (FEM) offers this flexibility of approach. The purpose of this thesis is to develop and examine programs, based on this general method of analysis, which can then easily be used by future researchers.

An examination of a number of element forms has been made and one element, considered most suitable for the consideration of non-linear materials in layered systems, chosen for development. The mathematical behaviour, in iterative and incremental non-linear analyses, has been examined and the absolute importance of the non-linear material properties established. The lack of sufficient computing power inhibited the practical development of a fully three-dimensional approach to the problem. In the event of extra power being available, modification to the program will allow this more general problem to be tackled.

An attempt has been made to compare stresses and strains in a scaled down layered system with quantities calculated by FEM and incorporating any inferred non-linear elastic material properties. The effect a measured temperature distribution within an asphalt layer, had in weakening a typical pavement, and the change which was brought about in

the design parameters has been examined. The triaxial material test has been modelled by an FEM program, incorporating varying degrees of end frictional restraint. This has provided a method of analysis to assess the likely order of the errors involved in this usual method of material testing. A review of recent experimental work has been undertaken to establish the fundamental behaviour of soil materials, and suggestions have been made as to suitable tests which can characterise materials based on fundamental concepts of deformation behaviour.

The careful documentation of the more useful programs will enable future researchers to incorporate material properties as they become available.

CONTENTS

NOTATION

A	matrix containing terms derived from element node co-ordinates
a	radius of loaded area
B	matrix of strain coefficients
C_v	volume concentration of asphalt aggregate
D	stress-strain matrix
D_r	density
d	diameter of triaxial specimen
E	Young's Modulus
E_1, E_3	Young's Modulus in principal directions
E^{i+1}	Young's Modulus after i^{th} iteration
e	void ratio
F	load vector
G	Shear Modulus
J_1	sum of principal stresses $(\sigma_1+\sigma_2+\sigma_3)$, $J_1 = 3\sigma$
K	Bulk Modulus or Structural Stiffness Matrix
k_h, k_v	horizontal and vertical linkage stiffnesses
ℓ	length of triaxial specimen
M_r	resilient modulus of deformation
N	number of load cycles to failure
P	axial force on triaxial specimen or terms of assumed displacement polynomial
q	distributed or self weight load
R_e	set of nodal forces equivalent to distributed or self weight loading
r	radial distance from load axis
S	bitumen stiffness

t	time (seconds)
V	volume <u>or</u> nodal displacement vector
V_p	vector of displacements at any point in an element
z	depth below surface
α	column vector of coefficients
δ	represents small change to suffixed quantity
ϵ, ϵ_v	volumetric strain $\left(\frac{\delta V}{V}\right)$
ϵ	column vector of strains at a point
θ	tangential direction
μ	coefficient of friction
ν	Poisson's Ratio
ν_1, ν_3	Poisson's Ratio in principal directions
σ	Mean Normal Stress $\left(\frac{\sigma_1+\sigma_2+\sigma_3}{3}\right)$
	<u>or</u> column vector of stresses at a point
σ_r	radial
σ_θ	tangential
σ_z	vertical
τ_{rz}	shear stress
σ^{i+1}	mean stress after i^{th} iteration
σ'	effective normal stress
$\sigma_1, \sigma_2, \sigma_3$	major principal stresses, $\sigma_1 > \sigma_2 > \sigma_3$
τ	octahedral shear stress, 2nd stress invariant
τ_f	shear strength
Ω	region of integration for calculation equivalent nodal forces

CHAPTER 1

DESIGN OF LAYERED ROAD PAVEMENTS

1.1 The Layered Road Pavement

The function of the layered road pavement is to provide a level and durable surface allowing the free movement of traffic. Stiff upper layers are provided to reduce the stresses in the underlying geological strata to a level low enough to avoid excessive damage.

The soil foundation is termed the subgrade (Fig. 1.1), the the formation above it, the base. The base can consist of bitumen bound, completely unbound materials or a combination of the two, and serves to further spread the traffic stresses. Its thickness also protects the often saturated subgrade from the extreme effects of low temperatures, which could cause freezing and disruption of the pavement.

The stiffer surface layers may be composed of structural concrete or bitumen bound aggregates, sometimes termed asphalt concrete. In countries where the traffic loading is light, soil stabilised using cement or petroleum products is often used.

The higher loadings on roads and airfields in industrialised countries has led to the use of stronger materials in layered road construction.

Pavements which depend mainly on asphaltic materials for their load carrying properties have been found to be

"Flexible" Pavement

i) Unbound Base

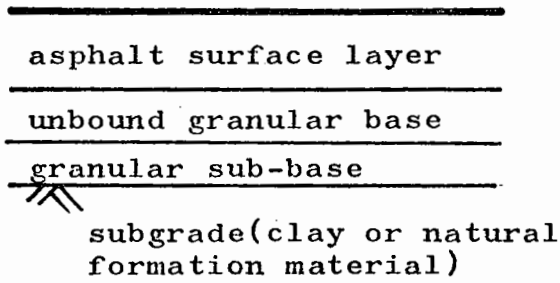

ii) Bitumen Bound Base

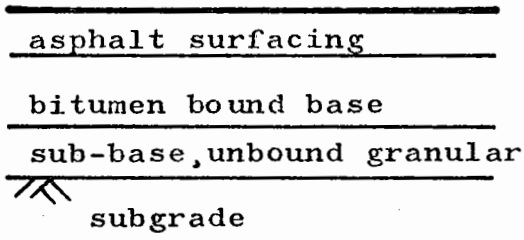

iii) Cement Bound Base

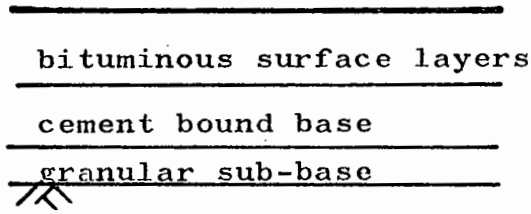

"Rigid" Pavement

Structural Concrete

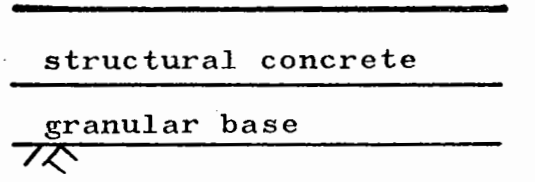

Fig. 1.1 Typical Layered Road Pavements

highly durable and are termed "flexible". Maintenance is less expensive than for concrete surfaced roads since the provision of only a surface overlay is often found quite adequate. Loss of subgrade support in a flexible pavement does not necessarily lead to cracking, which would reduce the serviceability of the road and could allow water access to the base and sub-base where it might cause further damage by freezing.

Bearing in mind the above factors, it is not surprising that the "flexible" pavement has become very widely used throughout the world. Since large sums of money are being spent on new road construction and major improvements (U.K. £90 million in 1970), any improvement in design efficiency would undoubtedly lead to a substantial financial saving.

1.2 Current Design Approaches

A design method must be employed so that a logical means exists to ensure that a pavement is made strong enough within itself and also sufficiently strong to limit stresses on the subgrade to an acceptable level. Permanent deformations may accumulate with each wheel load to reach unacceptable proportions if the pavement or subgrade is too weak to withstand the applied loading. Assessment of the interrelated factors of layer thickness and layer material properties under the dynamic loads a pavement experiences, has for long posed problems.

Most current design methods are empirical, being based on long practical experience, particularly the performance of full scale road experiments. Current British design

practice[1.1] is an example, relying heavily on the findings of the Road Research Laboratory in their full scale pavement experiments[1.2]. This data is taken together with results from California Bearing Ratio tests to establish the various layer thickness. This standard plunger test can be carried out on material from any of the layers of a pavement under construction to assess its ultimate strength. In the British design method, the test is carried out on a sample of the subgrade material. Traffic loading is reduced by equivalence factors (based on the AASHO Road Test findings) to a number of "standard axles". The sub-base and roadbase thicknesses for a particular subgrade CBR and "accumulative number of standard axles" over the design life, are presented in graphical form. In near saturated or saturated subgrade materials, increase in the pore-water pressure renders the test unreliable and recourse is made to values of the CBR based solely on soil classification. For a saturated subgrade the design method is thus based completely on soil classification and experience. Even when measured CBR values can be used in the design, some measure of the ultimate strength of the subgrade under one application of load is taken. Thus pavement behaviour at conditions other than failure and under many repetitions of load is not taken into consideration in the design method.

Empirical or semi-empirical methods of design depend heavily on experience which may not be applicable at other locations. Although such methods of design were adequate when traffic loads were light, experience of permanent

deformation in heavily trafficked roads seems to lead to the conclusion that a better understanding of the stresses, strains and displacements occurring in the layers is required. If it could clearly be established how these quantities lead to permanent deformations and the possible loss of pavement serviceability, then limitations could be imposed which would ensure a factor of safety against the "failure".

The full scale road experiments, which empirical methods often rely on, suffer the disadvantages that they are extremely expensive to construct and monitor, and results are not usually available for a number of years. The design often has to be decided upon long before the road construction takes place, and results are only available for a limited number of combinations of material thickness and properties. The uncontrollable nature of the pavement loadings further complicates the issue.

The results from these empirical tests cannot safely be extrapolated beyond the range of experience without some sound predictive theory being available. Given a means of predicting pavement behaviour, a more rational approach to the design problem based on structural design considerations may be possible.

Such a theory was used to produce design charts[1.3] by the Shell Company in 1963. Layered elastic theory (see later) was used to calculate the "critical" stresses and strains in typical pavements and a series of design charts produced. These depended on the limitation of the subgrade

vertical strain to acceptable levels and claimed that it was only necessary to know a dynamic subgrade modulus and traffic loading conditions to produce a design.

A method of analysis based on the failure of the complete pavement structure has been presented by Sebastyan[1.4]. By considering Mohr-Coulomb failure surfaces the method arrives at an ultimate load for a layered system by considering a series of wedge-like failures within the layers. Although some success was claimed in comparing theoretical solutions with full scale tests, the analysis can give no knowledge of behaviour other than at failure.

The Shell design method was, however, the first attempt to produce design charts based on the calculation of critical parameters. It was based on only two of the quantities thought to be important in controlling layered pavement behaviour, but did put a structural design approach to the layered pavement design problem into practice for the first time. It was based on the only quantities calculable at the time, revealing that the currently available methods of analysing layered systems were inadequate.

1.3 Structural Design Approach

The layered pavement may be thought of as any other structure; some loading is applied which gives rise to stresses, strains and displacements within it. Certain of the values of these variables may be critical when compared with the known strength of the materials and would lead to failure, (which in a layered pavement would be defined by a drop in the serviceability of the road to an unacceptable level).

The steps in a classical engineering structural design can be applied to the pavement problem and may be summarised as:

i) assume some structural form and define the behaviour of the constituent materials under the expected environmental conditions

ii) define the loading to be applied to the structure and the structural boundary conditions

iii) make a preliminary guess at the size of the components

iv) carry out an analysis to determine the critical stresses, strains and displacements based on the most accurate material characterisations available (from simple laboratory tests if possible)

v) assess whether the known strength of the constituent materials provides an adequate safety factor against the calculated critical stresses, strains and displacements.

If the design is not satisfactory, then steps iii) - v) are repeated.

The method is difficult to apply to the pavement problem since the structure is difficult to analyse, the loading difficult to define and the critical parameters difficult to identify. In order that solutions can be produced, simplifying assumptions must be made.

The assumption made in characterising the complex road making materials are examined in Chapter 3, and those made in the methods of analysis are discussed later (sections 1.4 onwards). So long as these assumptions are

proven valid the designer would have confidence in extrapolating beyond the limits of current pavement experience.

1.3.1 Validity of Assumptions

It has already been established that full scale pavement tests have serious disadvantages. They are expensive, difficult to control and give only limited basic information. Scaled down pavements offer a better solution. The applied loading can be controlled and measurements made under laboratory conditions. The validity of assumptions made about material properties from simple tests can be checked with these, more easily made, in-situ measurements of stresses and strains.

To this end, some measurement of the strains occurring under a rolling wheel load have been made[1.5] on a toroidal section of layered materials in the laboratory. The work was extended to full scale pavements using electric wire strain gauges to find the strains at the asphalt interfaces under rolling loads. Attempts to predict the strains using an elastic layered theory met with only limited success. To provide correlation between theory and practice, an in-situ dynamic elastic modulus, measured at a frequency of vibration relevant to the speed of the rolling wheel, was used in analysis. Uncertainty in choosing a value of the Poisson's Ratio for the complex asphaltic materials rendered comparison with measured strains difficult.

More comprehensive measurements of both the stresses

and the strains occurring in a layered system have been made by Brown[1.6/1.7]. Dynamic loads were applied to a layered soil system in a rigidly confined pit. The stress distribution set up was thus not exactly that under a rolling load. However, important factors emerged from the work - it was established that the structure seemed to obey some non-linear elastic law. Recent analysis of these results[1.8 and Chapter 5] has reinforced the views expressed in Chapter 3 on the effect of the stress and strain invariants on material properties. The above tests have been extended to a 3-layer system by including an asphalt surface layer[1.9]. Taken as a whole, these tests have shown that the accurate measurement of stresses and strains in-situ is an extremely difficult task, especially at low stress levels. The dynamic loading applied to the system resulted in an accumulation of permanent deformation and undoubtedly a change in the material properties throughout the test program. This type of testing on scaled down pavement sections, preferably using rolling loads and involving measurement of the accumulated displacement at various depths with load applications, would seem to offer the best method of checking theory with practice. Although expensive, such tests are cheaper and easier to construct and monitor than full scale road experients.

Simpler tests have been carried out on full scale road pavements in order to assess their response to loads similar to those experienced under traffic. A heavy vibration machine has been used by Heukelom and Klomp[1.10] to measure wave propagation and dynamic deflection in order

to determine the dynamic properties of road construction materials in-situ. Tests on subgrade materials revealed an approximate relationship between E (dynamic modulus of elasticity) and the CBR value. Although the test was cumbersome to perform, it did show that material properties and material interaction could be assessed without the complex instrumentation required to measure stresses and strains in-situ. A more recent series of tests by Isada[1.11] applied an impulsive load to the pavement surface. An "impulsive load stiffness" was defined based on the surface deflection response and an impulse load. This quantity varied at a location with season, and from location to location with the type of pavement construction employed. It was claimed that with some experience in the use of this device, empirical laws could be established and enable "good" or "poor" roads to be identified by the nature of their response to impact. Although vibrational testing methods are valuable in assessing the finished pavement performance, their semi-empirical nature gives only limited assistance to researchers attempting to identify the fundamental causes of pavement failure. Such dynamic tests on the finished pavement do, however, help to check the assumptions made about the individual layer material behaviour since they offer a relatively simple means of assessing the overall structural behaviour without complex instrumentation. No indication whatsoever can be derived as to which of the stresses and strains are critical and precipitate a drop in the serviceability of the pavement. It is to this problem attention will now be turned.

1.3.2 Critical Parameters

The resilient and permanent surface displacements in the pavement have often been thought of as the most important guide in assessing performance. Surface displacement is the easiest quantity to measure in the finished pavement. The Benkleman Beam deflection apparatus, as a means of measuring transient surface displacements, thus offers a valuable guide to the pavement performance.

Although rightly considered as a simple measure of performance[1.12/13], surface deflections only reflect the effects of strains deeper in the pavement. It has been suggested that the measurement of surface deflection without knowledge of layer geometry and material types is unlikely to be interpreted effectively[1.14]. An infinite variety of layer configurations and material types could lead to the same resilient and permanent deformations.

The Shell design charts of 1963[1.3] used the vertical subgrade strain as a main design criterion. The designs were based on computations carried out using a layered system analysis which was restricted in that it could not calculate shear stresses. The level of shear stress in the soil subgrade would have been of more use in assessing likely permanent damage (Chapter 3). Thus, restrictions imposed by the method of analysis dictated the design criterion. Later[1.14] it was established that consideration of the maximum shear stresses and strains at the base-subgrade interface was unlikely to effect the trend of the original design curves. The subgrade vertical strain does,

however, give an indication of the distortional effect of the interaction of the normal and shear stresses within the subgrade, but also depends on the strength of the upper stiff layers. Any weakness within these layers will lead to greater values of subgrade shear stresses and thus greater deformations in the subgrade. The vertical subgrade strain would increase accordingly, and retain its usefulness simply as an indication of the degree of subgrade support offerred to the increased stresses imposed by the base.

The mechanism of any weakening of the upper stiff layers of the road pavement is thought to be that of fatigue cracking in the direction of maximum tensile stresses[1.15]. The repeated flexure which the stiff layers undergo imposes a cyclic change in the stresses at the base of the asphaltic layers which it was claimed would eventually lead to an initiation of cracking after a particular number of load repetitions. The term fatigue was tentatively introduced based on the fact that the usual laws applying to fatigue in metals appeared to hold for a cyclic loading of asphaltic materials. For a particular controlled stress or controlled strain level of cyclic loading, failure occurred quite suddenly after a particular number of load repetitions. The following law appeared to hold

$$N = K\left(\frac{1}{\epsilon m}\right)^n \qquad 1.1$$

where N = number of load cycles to failure

ϵm = amplitude of applied tensile strain in the mix

K = a factor depending on the volume and grade of bitumen in the mix

n = a factor defined by the slope of the fatigue line : log strain v log cycles to failure.

The importance of limiting the tensile strain at the base of the bitumen bound layers was thus apparent. The limit would be such that the total number of load repetitions of a particular size and thus the "life" of the pavement was acceptable to the designer.

The possibility of the "healing" of bituminous materials has been examined by Bazin and Saunier[1.16]. It was established that samples tested, dynamically, almost to rupture and then allowed to "rest" for a number of days underwent a change. Their strength returned and greatly increased lives were predicted by subsequent testing. A small compressive stress acting on the specimen and higher temperatures increased this suspected healing. The question was posed as to whether sufficient pavement dead weights existed to produce large enough lateral compressions to heal damage caused by traffic at the base of the asphalt layers in a road. It thus may be possible that a "failure" of the pavement system as the result of cracking due to abnormally high loads might not greatly effect the future elastic properties of the pavement. Such cracking would, however, lead to at least a temporary weakening of the upper layers, and the transmission of higher stresses to the base and subgrade with the associated accumulation of further permanent deformations.

In summary, it appears that three main parameters are considered important to the pavement behaviour:

1. Surface deflection - This encompasses both the resilient and the accumulated permanent deformations. Displacements are more easily measured than stresses and strains and, along with surface cracks, are a critical factor in establishing whether the pavement is serviceable. Without information on layer materials and their geometry the surface displacement is simply an indicator of the resilient or permanent behaviour of the total structure and gives no information about the mode of failure of individual layers.

2. Asphalt tensile strain or stress - Knowledge of the magnitude of the repeated tensile stresses or strains could lead to some estimation of the period of time which will elapse before cracking will occur. The "life" of the pavement could thus be predetermined. Current repeated loading tests on these materials may, however, be unduly pessimistic since a "rest period" may allow some healing of cracks already initiated.

3. Vertical subgrade strain or stress - Excessive subgrade vertical strain due to weak upper layers will lead to permanent changes in the subgrade material. The magnitude of these strains may be limited, by increasing the design thickness or stiffness of the upper stiff layers.

Although these parameters, already well accepted in suggested "rational" design methods, do concentrate on the most critical parts of the pavement, the reason for their being important may be misunderstood.

It will be explained in Chapter 3 that unsaturated materials in compression and shear all obey the same conceptual law, except near failure. All round compression causes the material to compact and become stronger, shear stresses are disruptive and precipitate failure. The limitation of the shear stresses in the base and at the top of the subgrade, already suggested by Dormon and Edwards[1.14] is a partial recognition of this fact. It seems reasonable to suppose that the excessive vertical subgrade stress or strain or excessive strain in the base, which are to be guarded against, are the result of the interaction of normal and shear stresses which ought to be quantified.

The behaviour of materials in a state of all round tension is fundamentally different; rupture is simply thought to be due to the tensile stresses exceeding the strength of the material in simple tension (Chapter 3). The asphalt tensile strain criterion would thus seem to be founded on a sound basis. A more systematic approach to the whole problem of pavement design has recently been the subject of research.

1.3.3 Systems Approach

The basic core of the system has already been discussed. It can be reiterated by considering the layer configuration and material properties as the variables available in an optimisation problem and the criterion of limiting stresses, strains and displacements as constraints. The achievement of an optimal cost design would depend on the calculation of the stress, strain and displacement parameters and on assessing how important they are in damaging the pavement.

This general approach to the problem[1.17] includes the above vital factors. Performance, itself, was, however, defined in economic terms by the level of serviceability which could be expected from the road. This has been assessed quantitatively[1.18] and predictably found to depend on the axle load and number of applications and the thickness of the pavement. Extrapolation of the empirically calculated serviceability index to other materials and conditions would seem of dubious value.

Input to the total "system"[1.17] included loading and temperature, and construction and maintenance information.

Its characteristics were material geometry and properties. Decision criteria were included to establish the acceptability of the pavement design and included funding, cost, reliability and riding quality. These formed the basis for optimising the output of the system, the overall pavement performance. Each separate aspect of such a systems approach should, it was recommended, receive detailed attention. The indication is that work currently in progress (1971) at the University of California, Berkeley, includes study of sub-systems for permanent deformation and asphalt fracture or fatigue, these being considered as two of the critical design criteria.

Traffic density, and pavement weakness because of increased temperature, both being parts of the overall "system", have been incorporated into analysis by considering "traffic weighted mean stiffnesses"(1.19). In order not to overdesign an asphalt pavement by considering the maximum traffic density and maximum weakening of the pavement to occur at the same time, a formula was arrived at for stiffness which gives less weight to the figure when traffic density is low.

The input to the "system" thus appears to exist already in the form of spectra of loading and temperature, (although the important effect of temperature on design parameters is further emphasised in Chapter 6). A means of determining an acceptable level of serviceability of the complete road pavement structure based on economic terms has been outlined. The important area of the

identification of the critical stresses, strains and displacements has been considered. It remains to establish an adequate method of analysis to predict these possible design criteria.

1.4 Layered System Structural Analysis

1.4.1 Basic Methods

Two basically different methods of analysis of the layered system have been developed to date (1971).

i) Boussinesq[1.20] solved the general equations of elasticity for a semi-infinite elastic mass. More complex solutions involving layered systems were developed along the same lines, later being aided by the digital computer.

ii) The advent of the rapid digital computer has facilitated the more successful use of numerical methods. These include the finite difference and finite element methods which both subdivide the structural system with mesh points. The finite difference method depends on making approximations to the governing differential equations at each mesh point, whereas the finite element method assumes a displacement or stress pattern within each element defined by a number of mesh points. Each method relies on the solution of a large number of simultaneous equations to obtain the most accurate results.

1.4.2 General Assumptions

The accurate calculation of the stresses and displacements resulting from traffic moving at speed on a road surface is complex. Each method of analysis

involves a number of general assumptions, the particular assumption made by individual researchers are discussed later.

Most analyses assume, with justification[1.21], that wheel loads can be represented by a uniformly distributed circular load. The layer interfaces are usually assumed to be perfectly rough allowing complete continuity of radial and vertical displacements.

1.4.3 Viscoelastic Behaviour

The extent to which material behaviour may be considered as elastic has been examined by a number of workers. If the layered materials were linearly elastic the maximum instantaneous stresses under a moving load would virtually be the same as those under the same load when stationary[1.22]. If this assumption can be made, then the effects of multiple wheel loading can be considered by superposition of stresses, strains and displacements. For the purpose of the analyses carried out in this thesis, the time dependent properties of the materials have been simplified. For the asphaltic materials it has been assumed that for each particular rate of loading and temperature, elastic moduli can be assigned and analysis carried out using some elastic continuum theory (see Chapter 6).

Considerable effort is being made elsewhere to solve the layered problem using visco-elastic layered theories. Westman[1.23] demonstrated how to calculate the velocity range for which time dependent effects were of no importance. Very generally, if the wheel load moved faster, some speed

was eventually reached beyond which the materials were essentially elastic. Leger[1.24] developed a limited expansion for the calculation of the displacement at the surface of a visco-elastic half-space under a concentrated load moving at constant speed. The results were compared with the corresponding elastic case and the decrease of vertical displacement with increasing speed was shown to be dependent on the viscosity of the material. Recently, the failure criteria for a visco-elastic material have been examined[1.25].

These methods of analysis have so far only succeeded in producing solutions for a single layered system. In this early stage of their development they can, nevertheless, help the designer to realise the limitations of elastic theory, particularly when used to analyse situations involving slow-moving heavy loads.

1.5 Layered Elastic Solutions

1.5.1 Early Tabulations

Burmister first applied the theory of elasticity to a layered system[1.26] having the achievement of a pavement design as his objective. The pavement was represented by two layers of homogenous, isotropic and linear elastic material, the lower one being infinite in extent in both the horizontal and vertical directions. The analysis was later extended to include 3-layers[1.27]. Fox[1.28] evaluated stresses in a 2-layer system for various modular ratios and radii of loaded area using a relaxation method to provide more comprehensive information. Stresses were later obtained off the load axis by Acum and Fox[1.29], but

values were still restricted to those at the layer interfaces. Mehta and Veletsos[1.30] developed a more general solution to the layered problem allowing some variation of Poisson's Ratio. Computer programs were prepared for a system having a maximum of 5 layers and calculations were possible off the axis of symmetry. Comprehensive tables were later published by Ahlvin and Ulery[1.31] for the stresses, strains and displacements in a single layer system and the more difficult task of tabulating stresses in a 3-layer system was carried out by Jones[1.32] with the aid of a digital computer. The values he calculated were restricted to the layer interfaces on the axis of the load and Poisson's Ratio was set at 0.5. Twenty-six volumes of tables including variation of Poisson's Ratio in a 3-layer system were produced by Burmister[1.33] under contract to the US Navy at about the same time (1962).

Later in 1967 a 4-layer system was considered by Vertstraeten[1.34] following exactly the procedure used by Burmister. Plots of principal stresses were added and surface shear loads considered. Poulos[1.35] has considered a layer over a rough rigid base from Burmister's equations.

All these tabulations were made under difficult computational conditions involving great research effort for a small return. The recent development of computer programs based on layered theory, able to calculate stresses, strains and displacements at any point in the layers, for any values of Modulus and Poisson's Ratio has greatly eased the work load. The advance meant that, provided elastic theory is considered adequate, effort can be concentrated on the design problem rather than the development of the

means of calculating the critical parameters.

During the development of layered elastic analyses, several factors emerged, summarised by Nielsen[1.36]:

1. Vertical stresses in a layered system were found to have much lower values than the corresponding ones from Boussinesq theory.

2. The mechanism of how the stiff layers "spread" the load was more apparent. It was suggested that a very stiff upper layer could even have a detremental effect. A high vertical stress gradient was balanced by a high shear stress gradient which could affect the stability of the upper layer.

3. The critical shearing stresses at layer interfaces were thought to be deflection dependent.

4. The problem of pavement design was thus thought to be one of evaluating critical stresses and displacements so that the values were well below the breakdown values assigned to the materials.

1.5.2 Computer Programs for Layered Elastic Analysis

Computer programs which permit the direct calculation of stresses, strains and displacements at chosen points in an elastic layered system have recently become more generally available. A program commissioned by the Chevron Oil Company Inc.[1.37], and not available to the author, has been used by workers in California. Shell Research N.V. have produced a program[1.38] (BISTRO) which was used to make comparisons with the author's finite element programs. Recently, the Road Research Laboratory, Crowthorne, have refined an earlier computer program[1.39/1.40] which was designed for layered system analysis.

The author's experience is limited to the use of "BISTRO" which, in common with both of the other known programs, was based on the earlier work of Burmister. Hankel Tranform theory was used to enable the governing

partial differential equation, $\Delta^2 \Phi$ (r,z) = 0, to become an ordinary differential equation in the Hankel Tranform of the stress function, Φ. The integration constants to this tranformed ordinary differential equation depend on Young's Modulus (E) and Poisson's Ratio (ν) and were solved from the boundary conditions. It was assumed that layers remain in contact and that vertical stresses and displacements were continuous at the interfaces. Two further assumptions could be made about these boundary conditions - either no slip occurred at the interface or the layers could slip over one another without shear stresses acting.

The BISTRO program uses the principle of superposition to calculate the total stresses, strains and displacements at any point resulting from any number of vertical surface loads. Recently (1971) the program has been modified to include surface shear loads. It has been found by the author to suffer the disadvantages that:

1. The calculation of selected stresses, strains and displacements at each chosen point involves the complete recalculation of all integrals, making the demand for computer time high.
2. As the number of layers increases beyond 8-10, the time taken to calculate stresses becomes much greater. (This would discourage the use of the program for a problem to which it could have been suited, involving a modulus varying with the depth alone - e.g. temperature effect in asphaltic materials, Chapter 6.)
3. Quantities calculated near the surface are often

inaccurate, as sometimes manifested by an overflow occurring in the integral calculations. In short, there seems to be no guarantee that accurate answers are assured near the surface, even if no integral overflow message is printed by the program.

The Chevron program, based on the same theory, is claimed to produce answers more rapidly at the premium of only slightly less accuracy.

The earlier version of the R.R.L. Program suffered the disadvantage that it only calculated quantities on the axis. The most recent version (1971) calculates stress, strain and displacement at several places at once with a minimum amount of re-integration. Output of the stress invariants and some automatic graph plotting is incorporated. The Fortran IV program text is lengthy, requiring the overlay facility of the Road Research Laboratory's I.C.L. 4/70 Computer, thus casting doubt on its easy applicability to other computers.

The author experienced only limited compatibility problems with the FORTRAN IV "BISTRO" program text when loaded on to an I.C.L. KDF9 computer; some changes in "DATA" instructions were necessary.

The whole question of machine compatibility is the subject of difficulty and controversy but it would seem unwise to invest a great deal of development effort into a program which is dependent on facilities within a system unique to one type of computer which is little used elsewhere in the world. Such appears to be the case with the R.R.L. system.

It seems likely, however, that layered elastic analyses, although restricted to single modulus layered systems of infinite extent, will continue to play a vital part in the calculation of the critical design parameters. Further comparisons between the 3 programs available and finite difference and finite element methods are, however, needed. Some comparisons have been carried out between "BISTRO" and the finite element programs (Chapter 4). Comparison of the time taken to calculate the stresses, strains and displacements in a given non-layered system suggests that the whole system can be solved, throughout a suitable mesh, in the same time "BISTRO" takes to compute values at 10 or 15 points. Displacements calculated using the finite element method are, however, subject to certain basic inaccuracies (Chapters 4,6) because of

i) computer round-off when Poisson's Ratio is near 0.5

ii) the proximity of the boundaries in the geometrical idealisation.

The N-layer elastic solutions outlined above are restricted in the following ways:

1. a variation of modulus with radius cannot be dealt with
2. the method is restricted to elastic materials.

1.5.3 Non-linear Properties in N-layer Theory

The lack of a method of analysis which incorporated non-linear material properties led to the suggestion of an iterative procedure based on n-layer elastic analysis. Seed et al[1.12] and Kasianchuk[1.19] used such a method:

-stresses and strains were calculated using some initial layer modulus values.

-layer moduli were repeatedly modified according to these new stress levels until a satisfactory solution was reached.

The method has the important disadvantages that:

1. moduli could not vary with radius.

2. the many layers required for an adequate approximation to the modulus variation with depth, increased the computer time required to compute stresses for each iteration.

1.5.4 Anisotropy and Finite Difference Approximations

Anisotropy has been incorporated into an elastic analysis by Gerrard[1.41] based on similar integral transform techniques to those suggested by Burmister, but solutions were not extended to the layered problem.

Transformation of the equilibrium equations into linear finite difference equations has been carried out by Cumming and Gerrard[1.42] and extended to a cross-anisotropic half space and a 2-layer isotropic system by Gerrard and Mulholland[1.43]. Non-linear material properties which varied throughout the material have been incorporated (1969) using a stress dependent Young's Modulus, by Morgan and Gerrard[1.44].

A source of error exists in the finite difference approximation itself and also in representing a semi-infinite medium by a model having rigid boundaries at a finite distance from the loaded area. This latter error is also present in the finite element approximation.

Boundary conditions are, however, difficult to implement

in the finite difference method. An irregular boundary would lead to almost insuperable formulation problems. The development of a program using this method, flexible enough to incorporate general material properties and allow ease in specifying boundary conditions, has not yet been achieved (1971). The finite element method (Chapter 2) has received greater attention since it was first introduced in the early 1960's.

1.6 Finite Element Approximations

The finite element method of analysis has the basic advantages that:

1. each element can be assigned different material properties which are easily changed.
2. there is complete freedom of choice of boundary conditions including the type and number of loads.
3. a considerable amount of experience in the use of the method has been built up in the short time since its use has been made feasible by the digital computer.

Most unbound road pavement materials have been found to have modulus properties dependent on some measure of stress level, but in bituminous materials, the effect of temperature has been found to be far greater[1.13]. The effective examination of the importance of both of these factors demanded this flexible method of analysis (Chapter 2).

Waterhouse[1.45] first reported the development of a computer program specifically designed to consider the pavement problem. The program was based on the 3-node

axisymmetric triangle, but was not general in its stiffness formulation. The author stated the work to be incomplete. The more sophisticated program written by Wilson (see Chapter 4) based on the same element has been used by Duncan et al[1.46] to analyse a pavement system having non-linear elastic material properties. Dehlen[1.47] recently (1969) used the same program to analyse layered systems. The program relies on the 3-node axisymmetric finite element, but does not make provision for calculating the exact integrations for the stiffness of elements bounding on the axis of symmetry. The existance of a small cylindrical hole at the axis, not found necessary in the author's program, has been found to lead to inaccuracies. The main conclusion made by the above workers, using this program, was that the finite distance to the boundary was critical in determining displacements.

The main disadvantage of an axisymmetric analysis is that it does not model the true 3-dimensional behaviour of a pavement, and only single loads can be considered. Pretorius[1.48] considered the pavement edge effects using a program extended to 3 dimensions[1.49] using Fourier Series Analysis. He found that, for a uniform subgrade there was little difference in pavement stresses compared with axisymmetric analysis, 24 inches from the edge of an 11 in. thick pavement. Computation time for this analysis was high, rendering non-linear analysis prohibitively expensive.

1.7 Objectives

Since the author started work on the development of finite element programs (Oct. 1968), other workers have similarly examined the pavement problem. The objective of the author was primarily to lay the foundation for others at Nottingham by:

1. the development of versatile finite element programs by examining a number of element shapes.
2. the examination of the non-linear characterisation of soil materials and methods of testing to obtain fundamental properties.
3. the establishment of the importance of non-linearity compared with an n-layer elastic solution.
4. the tackling of a 3-dimensional pavement problem.

CHAPTER 2

THE FINITE ELEMENT METHOD

2.1 Introduction

The Finite Element Method has become widely used, having been recognized as a powerful means of calculating displacements, strains and stresses in structures having arbitrary shapes, boundary conditions and properties. Improvement in the speed and size of readily accessible storage of high speed digital computers has allowed the method to expand in use; its flexibility has meant that it has outstripped the Finite Difference Method as a means of solving the continuum problem.

Whereas the finite difference method makes a mathematical approximation to the continuum equations governing the structure, the finite element method defines the displacement or stress pattern within elements interconnected at their nodal points. The polynomial expression used to define the state of stress or displacement is truncated in an arbitrary way, which fact has led to controversy. The achievement of greater accuracy of displacements or stresses and strains depends on the type of formulation and the refinement of mesh. Nowhere has a satisfactory proof been presented to explain why the finite element method converges for the more complex formulations.

2.2 Types of finite element formulation

Two basically different methods exist for determining the

stiffness matrix of each element. A third is under development.

2.2.1. The method using an assumed displacement polynomial and adequately described by Clough[2.1] has become the most popular in current use. The number of terms in the polynomial expression is governed by the number of nodes in the element and the number of degrees of freedom at each node. The formulation suffers the drawback that continuity of displacement or slope (bending elements) is not assured between elements.

2.2.2. Another method derives a stiffness matrix from an assumed stress polynomial[2.2], based on the principle of complementary energy. Element interface continuity can be written into the formulation and the number of assumed stress coefficients is not limited by the number of nodal points in an element.

2.2.3. The displacement method has been found to yield less accurate strains and stresses, having discontinuities between elements[2.3]. Reduction of mesh size leads to a more accurate solution at the expense of greatly increased computer storage requirements. Improvement can be made using higher order elements but this requires more computational effort and reduces the possible variability of material properties by reducing the number of elements possible using the same computer storage.

Experience with elements derived using an assumed stress polynomial[2.3] has found slower convergence than that using

a displacement model. Results were, however, better for a simple element model but there are difficulties in formulation: the equilibrium equations must be satisfied exactly and it is difficult to establish a convenient co-ordinate system. Unless care is taken in the selection of constraint equations the banded form of the stiffness equations can be lost.

Since insufficient information is available which compares the stress model with the widely used displacement model and formulation of the method in a generally applicable computer program would seem to present problems, the displacement method was chosen as the tool of the author's work.

2.2.4. A third method is under development[2.4] which formulates the model in terms of both displacement and stress fields using the Hellinger-Reissner Theorem. It is claimed that since the stress field need not satisfy the equilibrium or compatibility equations or the stress boundary conditions and the displacement field need not satisfy the stress-strain-displacement relation or the displacement boundary conditions, the method represents a significant advance. The difficulty lies in establishing to what extent each condition is to be imposed on the co-ordinate functions. There appear to be no simple answers to this question and this generalised technique is still in the early stages of development posing theoretical as well as computational difficulties greater than those presented by the stress method.

2.3 Choice of element form

In deciding on an element form it is important to consider

shape and number of nodes and their relation to the quality and cost of the solution. The soils problem, however, demands non-linear properties which ideally should vary continuously throughout each element and the whole structure.

2.3.1. Elastic case

The simple, constant strain, plane triangle has increasingly been brought into disrepute and higher order elements found necessary. The 6-node triangle is claimed to increase the accuracy of an elastic solution even though less elements are possible within the same computer storage.

The same general rules apply to rectangular elements where the addition of mid-side nodes increase accuracy. The rectangular element, however, has boundary geometrical limitations which nevertheless can be considered acceptable in the layered road pavement problem. Both types of element produce a less accurate solution when the element includes very small angles or is elongated.

The recent availability of isoparametric element forms has increased the generality of element shape but at the expense of the increased computing time which is necessary to perform the numerical integrations.

2.3.2. Non-linear case

Integration to calculate the stiffness of an element with a non-linear stress-strain matrix would involve numerical integrations and increased computer time. An increase in the generality (more nodes or isoparametric form) of the element would probably render the time requirements excessive

since it would be necessary to calculate stresses and strains at many points in each element to completely define the non-linearity.

The alternative is to use simple elements and consider the structure as piecewise linear. A constant stress-strain matrix for each element would greatly simplify the necessary integrations. The road system is already layered and does not require generality in element shape, and thus the simple constant stress-strain element would seem to offer the best solution. Non-linearity can be built in by considering the constant stress-strain matrix within each element as dependent on a representative stress or strain level within the element.

Ideally, the road pavement should be represented by a number of simple rectangular 3-dimensional non-linear finite elements. The storage requirements are excessive, and demanded an axisymmetric finite element approach in order to obtain solutions for single loads in non-linear systems in the first instance.

2.4 Formation of element stiffness by displacement method

Loads are applied at the nodal points of the structure resulting in nodal displacements which depend on the structural stiffness

$$(F) = (K).(V) \qquad 2.1$$

F - load vector

K - structure stiffness matrix

V - nodal displacement vector

2.4.1. Assumed displacement pattern

It is assumed that the behaviour of the structure can be represented by the behaviour of the nodes in the mathematical model. The deformation pattern within an element is some polynomial in the variables used as a co-ordinate system (e.g. f(x,y,z)).

$$(Vp) = (P).(\alpha) \qquad 2.2$$

Vp is a column vector of displacements at any point in the element: $(Vp) = \begin{bmatrix} Vx \\ Vy \\ Vz \end{bmatrix}$

P = matrix of the terms of the assumed polynomial

α = column vector of coefficients

The matrix (P) must:

i) allow solid body movement of the element without incurring strain energy.

ii) be continuous with its first derivative within each element.

iii) ensure continuity of slope and displacement between elements (although some elements not 'conforming' to this requirement have given convergent solutions).

iv) allow uniform strain to be represented.

The matrix (P) thus contains terms of the form:

1, x, y, z, xy, yz, zx, x^2, y^2, z^2, xyz, x^2y, etc.

The number of terms taken is governed by the total number of degrees of freedom allowed by all nodes in the element. Thus a row of (Vp) will take the form:

$$Vp_i = \alpha_1 + \alpha_2 x + \alpha_3 y + \alpha_4 z + \alpha_5 xy + \text{etc.}$$

and define the displacement at any point within the element if the α_i terms are known.

2.4.2. Matrix (A)

The α_i terms are defined by a matrix (A) and the actual nodal displacements (V_i) for the element. The elements of the (A) matrix are those of (P) with the co-ordinate of each of the nodes of the element substituted:

$$(V_i) = (A).(\alpha) \qquad 2.3$$

V_i - nodal displacements for element.

A - matrix containing co-ordinate values substituted in (P).

$$\text{Thus} \quad \alpha = (A^{-1}).(V_i) \qquad 2.4$$

This means that (A) must be square and thus sets the limitation on the number of terms in the displacement polynomial in (P) and restricts its accuracy. The ordering of the rows in (A) may have significance, preventing its inversion by a matrix procedure which does not re-order the terms to select the maximum pivot at each stage. The choice of (P) can be influenced by the requirement that (A) is non-singular.

2.4.3. Strains

The strains are determined in terms of the coefficients (α) by differentiation of the assumed displacement polynomial (P), (Equation 2.2).

$$(\epsilon) = (B).(\alpha) \qquad 2.5$$

where (ϵ) = column vector of strains

(B) = matrix derived by the appropriate differentiations from (P).

2.4.4. Stresses

It is assumed that it is possible to define the relationship between stresses and strains in the element by a matrix (D) such that:

$$(\sigma) = (D).(\varepsilon) \qquad 2.6$$

where (σ) = vector of stresses.

2.4.5 Element stiffness

Stiffness means "force required at a nodal point to there produce unit displacement in the same direction". Defined for all the displacements in a structure, in a usual set of orthogonal axes, this leads to a structural stiffness matrix (K). By the principle of virtual work, the virtual internal energy in an element associated with virtual strains (ε') is:

$$\Delta W_{int} = \int_{vol.} (\varepsilon')^T.(\sigma)\ d\ vol. \qquad 2.7$$

But from 2.5 and 2.4 respectively:

$$(\varepsilon) = (B)(\alpha) = (B)(A^{-1})(V_i) \qquad 2.8$$

and substituting in 2.6

$$(\sigma) = (D)(\varepsilon) = (D)(B)(A^{-1})(V_i) \qquad 2.9$$

as in 2.8, virtual strains $(\varepsilon') = (B)(A^{-1})(V_i')$

$$\text{thus } (\varepsilon')^T = (V_i')^T(A^{-1})^T B^T \qquad 2.10$$

Substituting equations 2.9 and 2.10 into 2.7 the internal

virtual energy becomes:

$$\Delta W_{int} = (V_i')^T (A^{-1})^T \int_{vol.} (B)^T (D)(B)\ d\ vol.\ (A^{-1})(V_i) \qquad 2.11$$

The external work to produce this internal energy is:

$(V_i')^T (F_i)$ where (F_i) are the nodal loads.

Equating the two quantities:

$$(F_i) = \left\{(A^{-1})^T \int_{vol.} (B^T)(D)(B)\ d\ vol.\ (A^{-1})\right\}(V_i) \qquad 2.12$$

thus the stiffness for the element is defined as:

$$(K)_{el} = (A^{-1})^T \int_{vol.} (B^T)(D)(B)\ d\ vol.\ (A^{-1}) \qquad 2.13$$

2.4.5.1 Solution

The set of nodal displacements (V) for the total structure is found by solution of equation 2.1 given $(K)_{structure}$ assembled from many element stiffnesses $(K)_{el}$ as calculated in equation 2.13.

2.4.5.2 Strains and stresses

Strains at any point in any element are found from equation 2.8 and stresses from equation 2.9.

2.5 Boundary Conditions

2.5.1 Displacement restriction

To impose restriction on displacement being allowed to occur in either co-ordinate direction at a node it is necessary to delete rows and columns in the structure stiffness matrix

associated with the nodal point and direction in question. The associated zero stiffness prevents displacement provided the right hand side term is zero. The leading diagonal term must be set to unity to ensure the equations are non-singular.

2.5.2 Imposed loading

2.5.2.1 Point loads

Any simple nodal point loads are placed in the appropriate position in the load vector (F).

2.5.2.2 Distributed loading

This applies either to overburden loading imposed throughout an element with volume, or equally to a uniform distributed load on an area. Both are reduced to a set of equivalent nodal forces (R_e) by integrating over each element of the relevant loaded region in the following way:-

If (V_i') are a set of virtual nodal displacements

(V') virtual displacements with the element

(q) distributed loading or body forces

$d\Omega$ is the element of volume or area, as explained later:

then the External Work done on the element:

$$\Delta W_{R_e} = (V_i')^T(R_e) \qquad 2.14$$

Internal Work done by distributed load:

$$\Delta Wq = \int_\Omega (V')^T(q)\, d\Omega \qquad 2.15$$

from equations 2.2 and 2.4

$$(V) = (P)(A^{-1})(V_i)$$

$$\text{thus } (V')^T = (V_i')^T.(A^{-1})^T.(P)^T \qquad 2.16$$

$$\Delta Wq = \int_{region} (V_i')^T (A^{-1})^T (P)^T (q)\ d\Omega$$

$$= (V_i)^T (A^{-1})^T \int_{region} (P)^T (q)\ d\Omega \qquad 2.17$$

But $\Delta Wq = \Delta W_{R_e}$

thus:

$$(R_e) = (A^{-1})^T \int_{region} (P)^T (q)\ d\Omega \qquad 2.18$$

where (P) are the elements of the assumed polynomial.

The exact region of integration, Ω, is the volume if body forces are being considered, and the area if a uniformly distributed load is imposed.

The set of nodal forces (R_e) are placed into the relevant part of (F) the structure load vector.

2.6 Solution of structural equations (F) = (K).(V)

Although at first the solution was carried out using a standard direct inversion technique, computer storage restrictions demanded that the symmetry and banded nature of the equations be exploited. A procedure using the well known Banded Choleski Decomposition, modified from a routine in PAFEC[2.3], was used for all solutions presented here (Appendix A.7).

2.7 Displacement Method Flow Chart (Elastic)

The computations involved in a simple elastic finite element program are outlined in Fig. 2.1. The order of the

basic operations shown is that used in all programs developed by the author. Modifications to carry out calculations using non-linear material properties with iterative or incremental loading will be introduced in Chapter 4.

2.8 Finite Elements developed in programs

Since the production of a working finite element program could involve the use of considerable resources, let alone the author's time, a number of schemes written by other authors were examined[2.3/5/6/7] to see if they were easy to use and more important could be modified easily. It was eventually decided that only by writing working programs could the method be developed effectively.

Firstly a program was written for the axisymmetric 3-node triangle (Appendix, Prog. 1) aided by the experience of Zienkiewicz[2.8] and Wilson[2.5]. Although the element can be considered geometrically versatile the results were not found to be satisfactory for the computation time necessary.

The 4-node axisymmetric element after Clough[2.1] was found to be simple in formulation and led to equally acceptable results with the use of less computer time for the return obtained. As a result programs having the basic form of Program 2.1) (Appendix) were used for all of the tests on non-linearity (Chapters 4, 5), temperature effect on pavement strength (Chapter 6), and the analysis of the variables involved in the triaxial test (Chapter 7).

A program (Appendix, Program 3) was later written to investigate the feasibility of using a fully 3-dimensional

element. This would have the inherent advantages over an axisymmetric program of being able to carry out non-linear superposition and thus enable investigation of multiple wheel loading and the pavement edge effects. The lack of efficient enough computer software to enable the decomposition of a set of equations using disc or tape back-up prevented this program's use on practical problems. The main trouble being that each such decomposition would have involved a great deal of computer time and disc or magnetic tape storage. This would have to be repeated at least 8 times for non-linear elastic problems.

2.9 Verification of elements

2.9.1 Axisymmetric

The programs written for both the 3-node triangle (Appendix, Program 1) and the 4-node rectangle (Program 2) were verified by making comparison with the elastic stresses and displacements in an infinitely long thick ring under internal pressure. The exact solution to this plane strain problem is given by Timoshenko[2.9].

Apart from checking that the finite element approximations gave values of the correct order, it was thought necessary to examine the degree of stress continuity between elements and also make sure that as elements became smaller the solution became better (convergence).

The finite element idealisations in Fig. 2.2 were considered. Nodal loads were applied to represent an internal pressure of 2000 lbf/in^2 and boundary conditions were imposed

as shown in order to model an infinitely long thick walled cylinder. Radial nodal displacements (Fig. 2.3) and radial and hoop stresses at element centroids (Fig. 2.4) were compared with the exact elastic solution.

Stresses showed good agreement, the better agreement being obtained for the 4-node rectangle. To some extent this was no doubt due to the 3-node element representations not being geometrically symmetric about a line in the direction of increasing radius. Nodal displacements surprisingly did not compare with the elastic solution to the same degree of accuracy, although it was apparent that as the mesh became more refined answers improved.

An examination was made of stresses (at nodes and at element centroids) and nodal displacements for both element types to establish how well answers from each converged. Quite arbitrarily the point at r = 8 in. was chosen.

Element Mesh (in Fig. 2.2)	Finite Element $x10^{-4}$ (in.)	Elastic Solution $x10^{-4}$ (in.)	$\frac{\text{Fin El}}{\text{Elastic}}$ %
1. coarse 3N	6.0309	6.4444	93.6
2. refined 3N	6.1014	"	94.7
3. coarse 4N	6.0412	"	93.7
4. refined 4N	6.1001	"	94.6

Table 2.1 Radial Displacements at r = 8 in.

Radial displacements at this radius (Table 2.1) obtained from 3-node and 4-node elements (the 3-node values by

averaging displacements at that radius) showed a convergent trend with decreasing element size. However, there was no significant difference in displacements from the 3-node or the 4-node element.

Nodal stresses were calculated at the same radius by averaging stresses calculated at the node from all surrounding elements. These were compared with actual values of $\sigma_r = -833$ lbf/in^2 and $\sigma_\theta = 2167$ lbf/in^2 from elastic theory (Table 2.2). It can be seen that although there were large stress discontinuities at the boundaries (particularly with the 4-node element) decreasing mesh size improved the average values. It is perhaps surprising that with the refined 4-node element mesh, average radial and hoop nodal stress values were within as little as 4% and 1% respectively of the elastic theory value.

For both types of elements, stresses calculated at the centroid of an element were found to agree closely with the average of the nodal values.

Since the 3-node triangle was general in orientation, the program took longer to compute element stiffnesses and more elements (i.e. more computations) were required for a given problem. The rectangular element used by Wilson[2.5], and derived from 4 triangles, would have removed errors in calculated values due to lack of geometric symmetry of the finite element mesh, but would have required the averaging of stresses from surrounding element centroids. Although Wilson found this produced a satisfactory solution there was no theoretical justification given for the averaging process.

Element Mesh (in Fig. 2.2)	Radial Stresses at Nodal Point	Av. Radial Stress σ_r	$\sigma_r \frac{\text{Fin El}}{\text{Elastic}}$%	Hoop Stress at pt.	Av. Hoop Stress σ_θ	$\sigma_\theta \frac{\text{Fin El}}{\text{Elastic}}$%
1. coarse 3N	-1452 -345 -246	-681	81.8	1867 2342 2384	2198	101
2. refined 3N	-1145 -542 -519	-735	88.2	2020 2279 2290	2196	101
3. coarse 4N	-1651 -292	-972	117	1778 2360	2069	95.5
4. refined 4N	-1198 -536	-867	104	2000 2284	2142	99

Table 2.2 Radial and Hoop Stresses at r = 8 in.
(all stresses in lbf/in^2)

The 4-node rectangular element, as seen above, produced no better results than a combination of triangles but had the advantage of requiring less computer time. It was chosen for development.

2.9.2 3-dimensional element (8 node)

A program for the 8-node rectangular prism is given in the Appendix, Program 3. It is based to some extent on earlier work by the author[2.9].

Although the extension from the essentially 2-dimensional axisymmetric case to three dimensions is algebraically straight forward the logical problems are greater. Automatic data generation for a solid block of element was developed for the program which formed the upper band of the element stiffness matrix within the rapid access store.

The effort was undertaken in the expectation of a significant increase in computing power, and in addition to testing superposition of non-linear response, the practically important problem of the edge of the pavement could have been tackled.

Convergence and the absolute accuracy of the formulation were checked by considering a cantilever of material in bending (Fig. 2.5). Each of the three finite element models was made one element wide (y-direction) and acted on by 200 lbf distributed to the two lower nodes. Successive halving of the mesh size led to a rapid convergence toward the simple bending theory solution (Table 2.3). The explicit integrals and other matrices were thus proven accurate with some degree of confidence.

Element Mesh (Fig. 2.5)	Vert. Displacement at End. (δ_z in.) Fin. El. Solution	Simple Bending Theory ($P\ell^3/3EI$)	Fin. El./Bending %
1	-6.407×10^{-4}	-1.706×10^{-3}	37.6
2	-1.190×10^{-3}	"	69.8
3	-1.568×10^{-3}	"	91.9

Table 2.3 Vertical Displacements at End of Cantilever

In the event, the increased core store that is slowly becoming available is either associated with time sharing operations (ICL 1904E Loughborough, Chilton Atlas) making the use of the whole core plus backing store costly, or is not supported by adequate software to permit the exploitation of the Choleski decomposition for banded matrices. This is a disappointing situation as the program itself showed every indication that sensible 3-dimensional solutions could have been obtained.

Given efficient software, the decomposition of the structural equations would be ideally carried out in blocks using the back-up store, only the $(\text{bandwidth})^2$ being required as fast storage. The importance of the problem of size is illustrated as follows using (say) the fast store on an Atlas machine to retain the whole upper band of a symmetric stiffness matrix:

> Given a block of elements with ℓxmxn nodes in 3 orthogonal directions (where $\ell<m<n$) the minimum bandwidth is $3\ell m$ and the total number of unknowns $3\ell mn$. The number of structure stiffness matrix elements is $9\ell^2m^2n$.
>
> The Chilton Atlas computer has available 110x550 locations of rapid access store, e.g. if $\ell=m=n$, then $9n^5=110\times550$, i.e. $n = 8.3$.

This means that the largest block of elements which could currently be considered would be (8x8x8) in size, clearly not enough to derive useful solutions to the 3-dimensional layered problem.

Given adequate software support, which allowed decomposition in blocks on the same size of machine, the refinement of mesh would increase but in two directions be limited by the bandwidth and in the third by time or cost:

> The total fast store requirement is $(\text{bandwidth})^2$ i.e. $(3\ell m)^2$, thus $9\ell^2 m^2 = 100 \times 550$ if $\ell = m$ then $\ell = 9.06$.
>
> Mesh refinement in the n direction could be chosen at will and would increase the number of blocks to be considered. In consequence n would be restricted by the computer time available, and would depend for its large size on the efficiency of transfer software from backing to fast store.

It is clear that given an even larger fast store and the necessary software, an attempt can be made to model the three dimensional pavement in a realistic way, the n direction being that along the road pavement.

2.10 Conclusions

It has been established that simple elements appear to offer the most desirable solution to the non-linear finite element problem. The accuracy of the 3 and 4-node axisymmetric elements has been shown to be roughly comparable, but the 3-node triangle required more element stiffness calculation of a general kind and thus more computer time. Stress discontinuity at nodal points was shown to be more considerable for the 4-node element but values averaged from stresses given by all surrounding elements were found to be better using this formulation.

The program based on the 8-node rectangular prismatic element gave a convergent solution but awaits the development of efficient software. Inevitably such a solution procedure would be written in machine code and thus its form would depend heavily on the computer and its internal organisation. So that effort is not wasted it seems essential that a system with long life is chosen for which to develop the highly efficient coding necessary.

There is the danger however that given such a highly efficient tool, research workers would devote their time to solving more and more of the previously intractable problems without making an assessment of the very basic deficiencies of the finite element method itself. Although considerable resources have been used in developing complete finite element suites of programs based on the displacement method it must be borne in mind that increasing effort is currently being expended on other formulations and they will become more readily usable as experience of them is reported.

Fig. 2.1 Basic operations of finite element programs

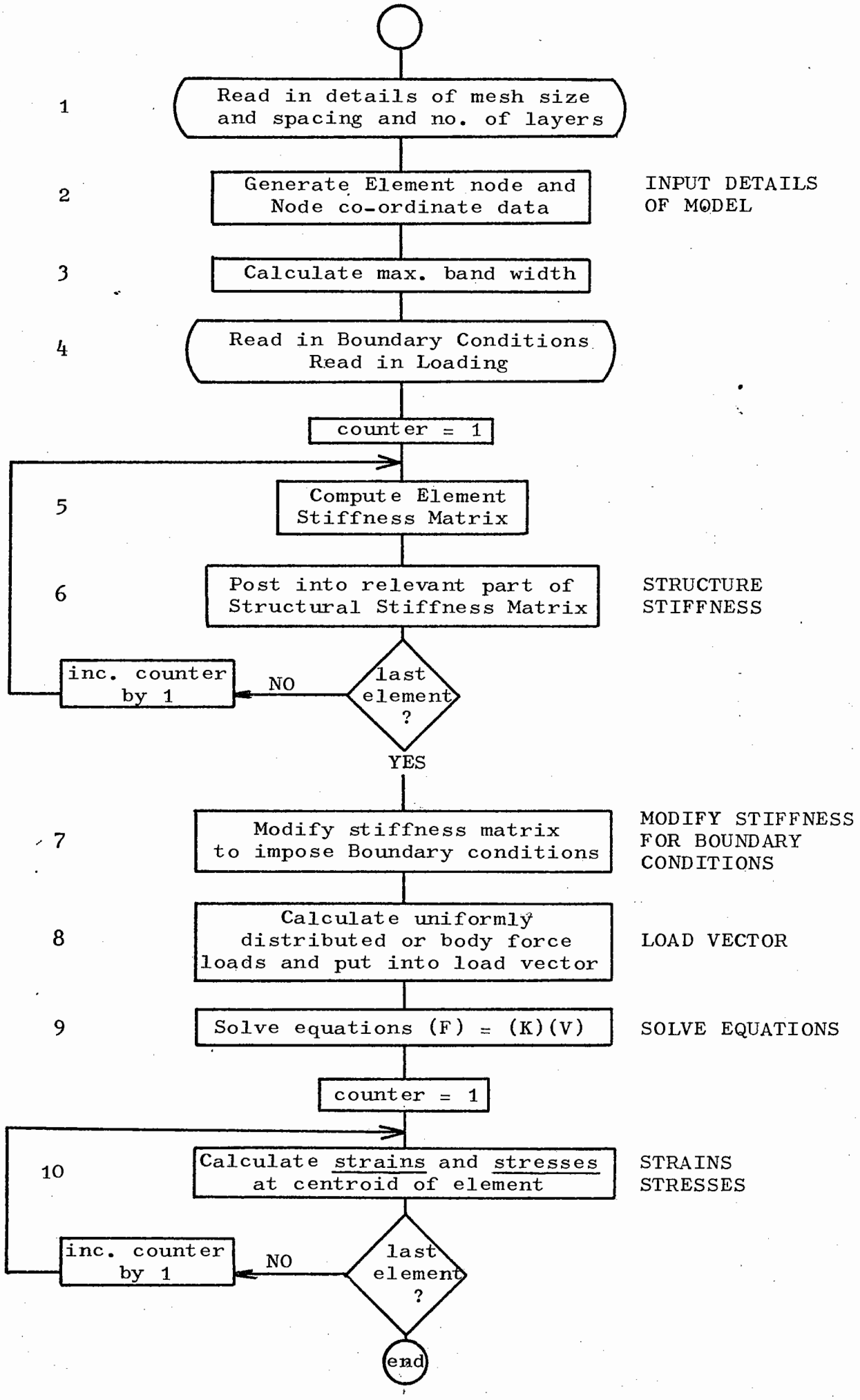

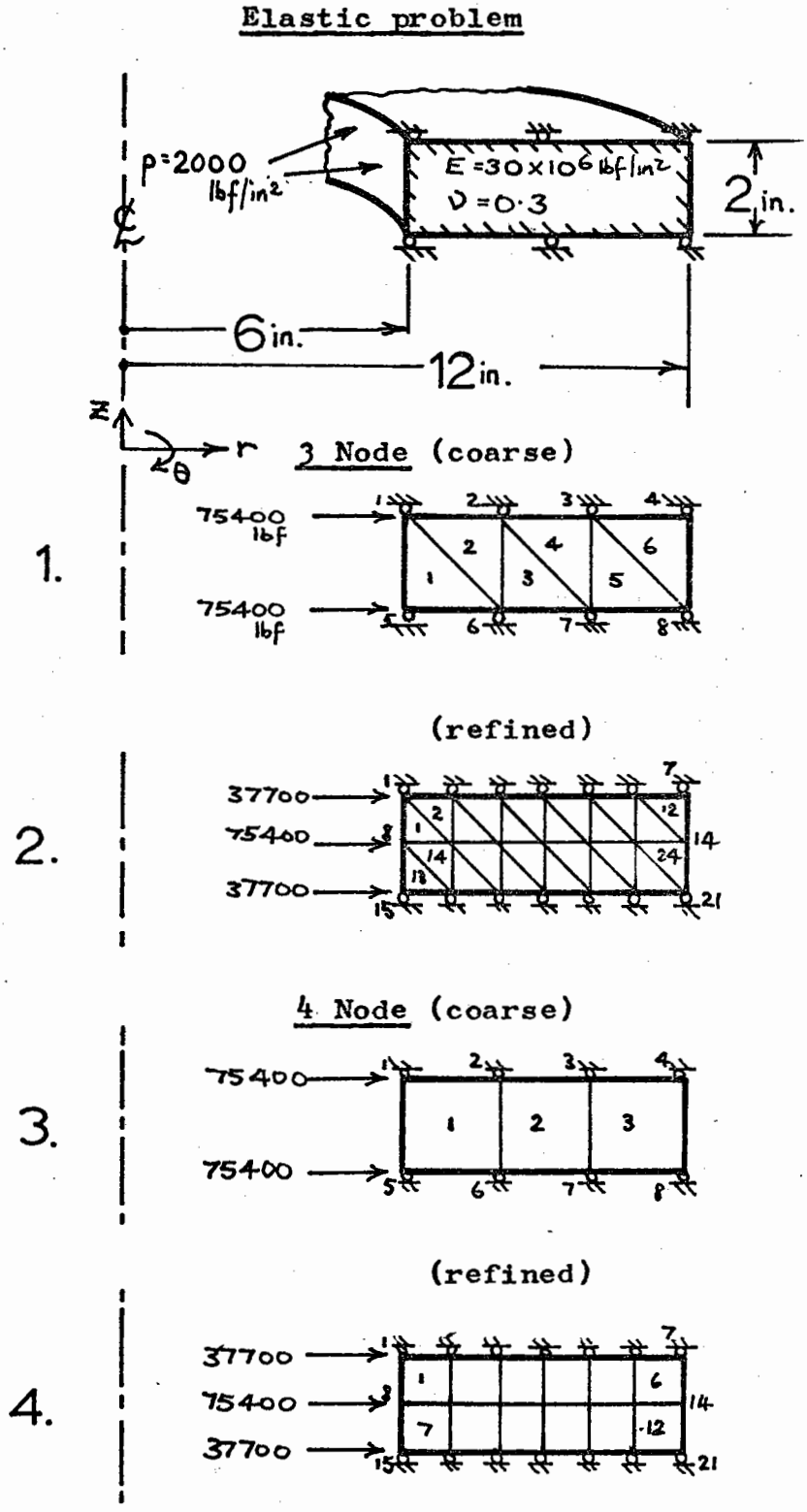

Fig. 2.2 Thick ring; actual and finite element models

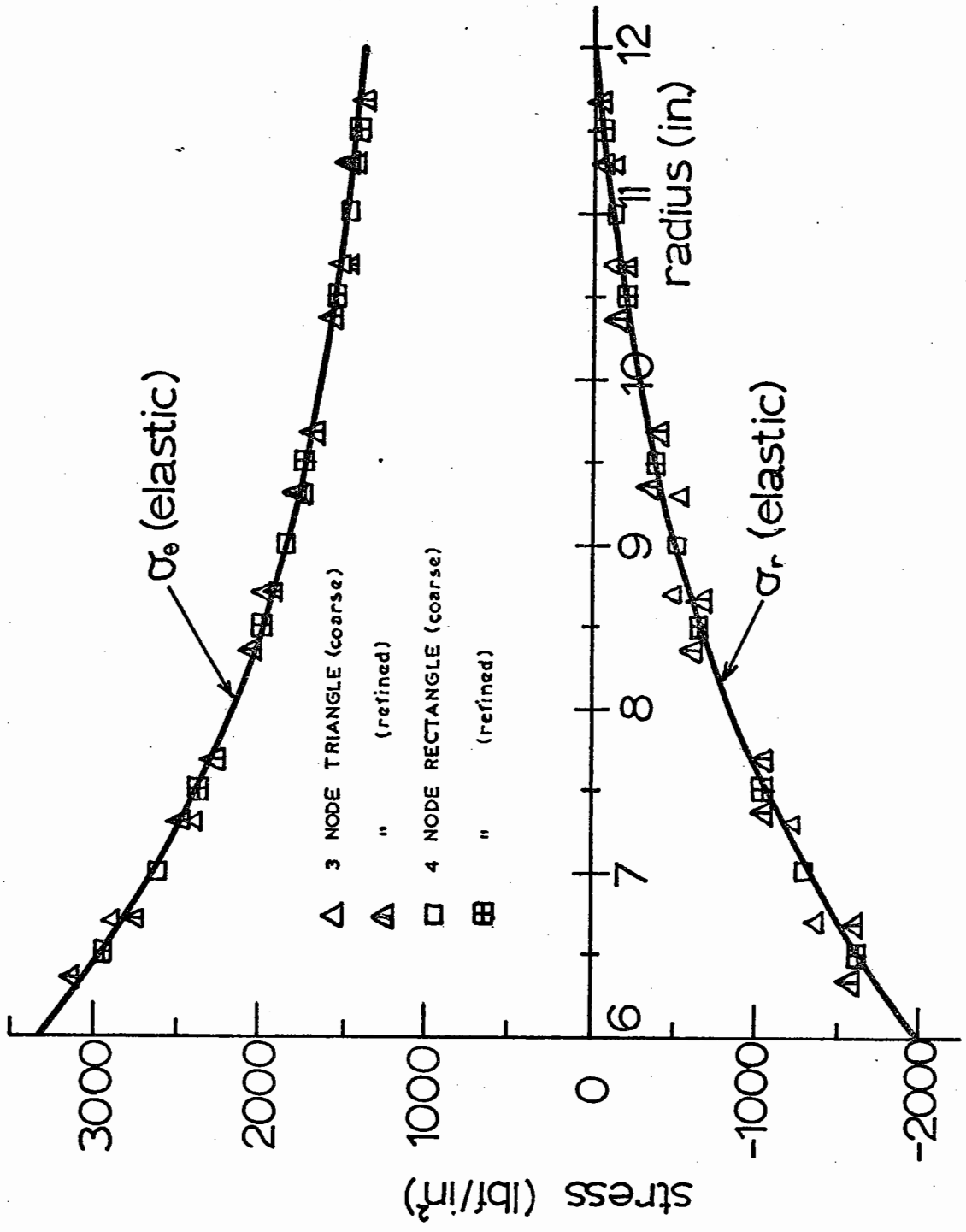

Fig. 2.3 Radial and Hoop Stresses in Thick Ring

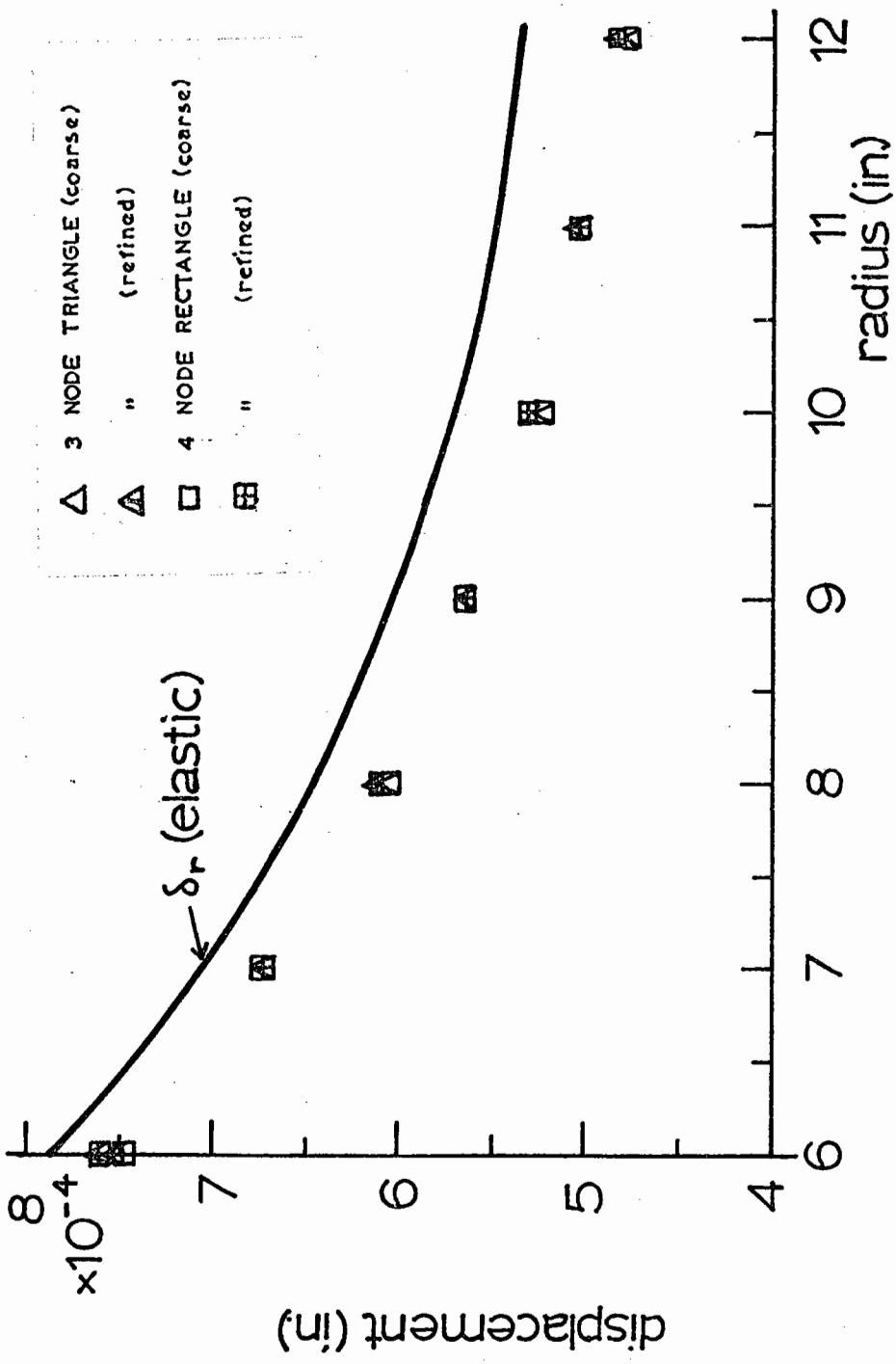

Fig. 2.4 Radial displacement of thick ring

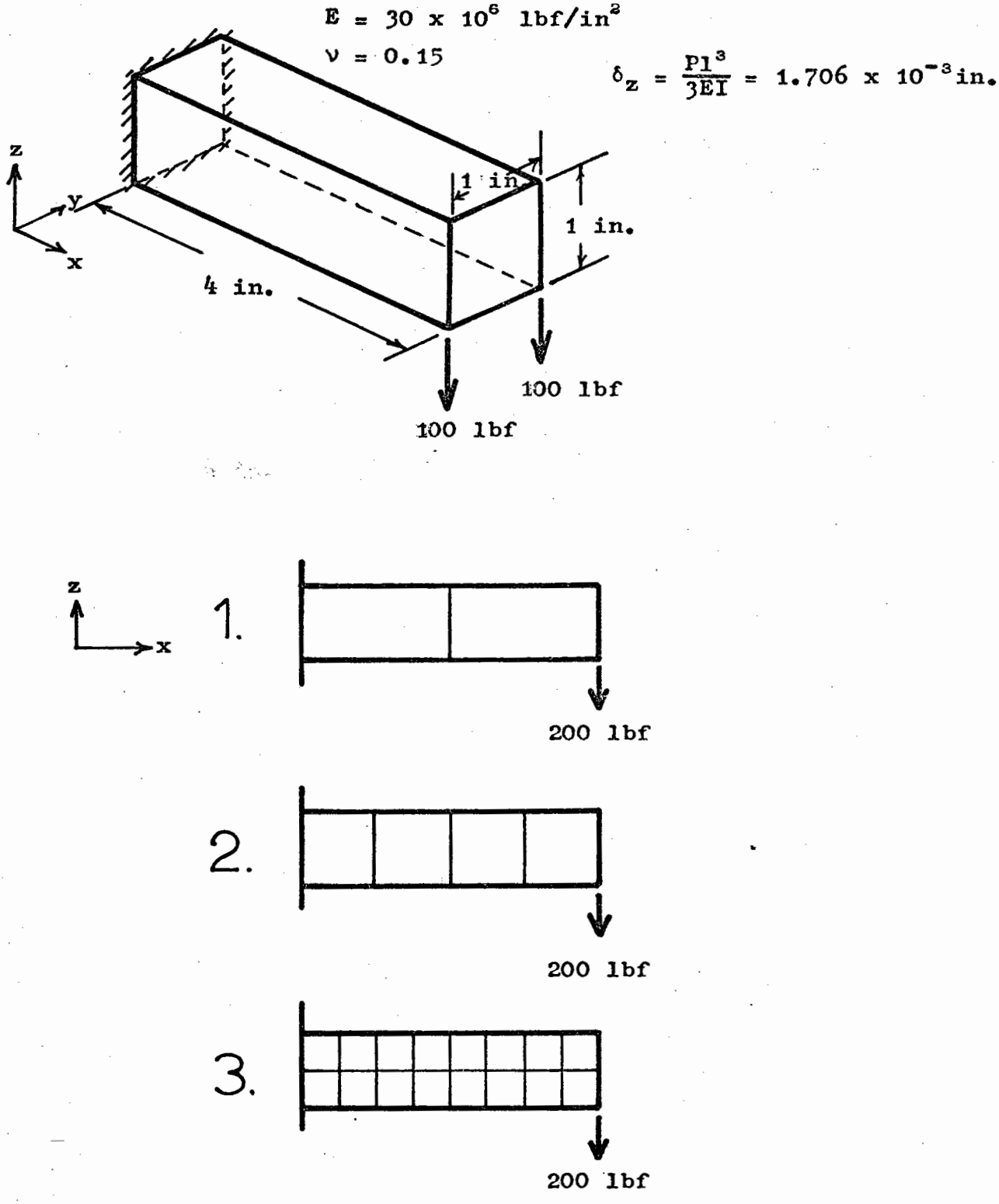

Fig. 2.5 Cantilever and solid finite element idealisations

CHAPTER 3

MATERIAL CHARACTERISTICS

3.1 Introduction

The objective of all pavement analysis is to predict displacements, stresses and strains as accurately as possible. To calculate these quantities the properties of the layer materials must be characterised so that the mathematical representation is as close as possible to the real behaviour. Road making materials have extremely complex properties and it is inevitable that all work for a long time henceforth will only produce an approximate material characterisation.

In this Chapter it is hoped to contribute to this by examining the fundamental properties of the materials. Experimental work[3.1,3.2] carried out recently on material characteristics has begun to fill in the gap which exists in our knowledge of soil properties. In roads, the major factors to be considered in the asphaltic material in predicting both resilient and long term deformations are the temperature and the rate of loading. However, for example, weakening of the asphaltic layers due to increased temperature may lead to increased stresses in the sub-base and subgrade and to a conventional soil mechanics failure of the system. It is thus clearly necessary to look at the conditions of deformation and stress in the pavement materials. In the past attention has been centred only on failure conditions and the early soil mechanics theories were based on this. It is now thought

important to observe the development of those stresses which lead to failure in the pavement and to be able to predict where it would occur within the pavement system.

To do this it is necessary to know the load deformation characteristics of the materials involved.

Roads are subjected to repeated loading and hence there are two phenomena to observe:-

(1) resilient behaviour - recoverable deformation occuring many times a minute under wheel loads, i.e. loading and unloading.

(2) long term deformation - non recoverable deformations occuring as a result of the effect of repeated loading to a particular stress level.

3.2 Materials in Road Pavements

The three basic materials widely used in layered road construction are: bituminous bound materials in the upper layers, a granular base, and a subgrade which in this country is often a clay.

3.2.1 Bituminous materials

The bituminous materials form both the wearing surface and the more highly stressed load spreading upper layers. The bitumen which forms the matrix of the asphalt or bitumen macadam has stiffness properties which vary very greatly with temperature (Chapter 6) and creeps with time under constant load. Simple viscoelastic theory has been used in layered systems[1.23/24/25] but the complex differential equations

which arise have inhibited work which otherwise would have led to the prediction of the permanent deformations within the upper asphaltic layers, and at the same time permitting realistic material properties in the lower granular and cohesive materials. Pagen[3.3] has defined the rheological response of a bituminous material over a wide range of loading times and temperatures and Gandi and Gallaway[3.4] have examined the effect of bitumen viscosity changes on the stress-strain behaviour of asphalt mixes. Terrel[1.13] found that temperature (and the attendant change in bitumen viscosity) was more important than stress level in governing asphaltic material behaviour.

For a long time measurement of the load-deformation characteristics was restricted to determining an axial modulus on a cylindrical specimen. Currently, dynamic tests more complete than the static tests of Gandi and Gallaway, are being carried out at Nottingham on specimens using the triaxial cell.

3.2.2 Granular base

The road-base is usually of crushed rock, a material which is often thought of as being able to take no tensile stresses. These granular materials have been found to have non-linear resilient stress-strain properties well below failure. In addition, any permanent deformations which occur may be caused by particles moving with respect to one another, alternatively, this could be explained by compaction or dilation due to repeated loading and unloading. The base is usually well drained so that pore water pressures do not pose a problem.

3.2.3 Subgrade

In this country the subgrade is usually composed of saturated or partially saturated clay. The California Bearing Ratio Test (CBR), as already mentioned, is often used to assess the subgrade strength in a failed condition. The test, however, does not give enough information about the material which would enable theoretical analysis of the whole pavement system to predict both the resilient and long term deformations under any loading up to failure.

The long term deformation, as in the case of the base materials under compression, can be thought of as that due to a contribution at each unload stage, i.e. the intensity of shear stress and effective bulk stress would be such that non-recoverable deformations occurred with each passing wheel load.

In this thesis the time and temperature dependent behaviour of bituminous materials has been simplified to that of an elastic modulus which is different at various rates of loading and temperatures (Chapter 6). The 'soil' materials are considered in a fundamental way and assumptions eventually made to enable their resilient properties to be incorporated into the finite element method of analysis. The non-recoverable behaviour has been considered but not incorporated into the analysis.

Until 1968 there is little published research describing experimental work leading to a material characterisation. Most of this is mainly concentrated on the calculation of an axial modulus from conventional soil mechanics tests. In the

years 1968-71 it has been more widely recognized that in this area inadequate information exists to permit computer analysis of soil structures and there has been a spate of unco-ordinated research effort, all of which, however, contributes to the whole.

3.3 Review of Recently Published Work

Road pavements in Britain are currently (1971) designed using the CBR test which characterises the subgrade under failure conditions. The CBR value has been related to a dynamic soil modulus by Heukelom and Klomp[1.10]. The concept of a dynamic soil modulus and its relation to past practice has been followed by major research investigations into road material behaviour.

It has long been known that the stiffness of roadmaking materials was dependent on stress level and thus elastic theory has been thought inadequate to predict stresses and displacements accurately. The response of a layered road to the cyclic loading it experiences is two-fold:

(1) resilient deformation which is thought to obey some non-linear stress-strain law and which might vary with age or the number of loading repetitions.
(2) long term damage, accumulated at each load cycle.

3.3.1 Material testing

As early as 1957 Hruban[3.5] had carried out incremental loading tests suggesting that a "modulus of deformation"

depended on stress level. He proposed that this modulus could be expressed as:

$$F_i = \frac{k|\sigma_1|^n}{\sigma_i^{n-1}} \qquad (3.1)$$

where n, k = constant, n > 1

σ_1 = major principal stress.

i defines direction of modulus.

The relationship shows a decrease in modulus with increased stress level for a clay. Hruban concluded that only further field observations could provide enough information for improved knowledge of material behaviour. He was concerned with soils under a "one-off" load increment and not with vibrational tests which give "dynamic characteristics". Although this was an early attempt to simplify, or make understandable, soil behaviour, effort did not become concentrated until the advent of the digital computer and the extensive development of continuum analysis programs demanded better material knowledge.

Non-linear resilient deformation received attention at the 1967 Ann Arbor Conference on the Structural Design of Asphalt Pavements. Monismith et al[1.12] showed that a tangent modulus of resilient deformation of a granular material under cyclic loading could be given by:

$$Mr = k\sigma_3^n \qquad (3.2)$$

n, k = constants.

σ_3 = confining pressure in the triaxial cell.

The tangent modulus, $\frac{d(\sigma_1-\sigma_3)}{d\varepsilon_1}$, increased with triaxial cell pressure at a decreasing rate. The tests were, however, carried out at constant cell pressure and thus did not model conditions in the pavement where horizontal stresses rise with load. The modulus is not necessarily a fundamental characteristic of the material except as representing repeated loading behaviour in the cylindrical test specimen.

Whereas Monismith et al. characterised the material from triaxial cell tests, Brown and Pell[1.7] derived a stress dependent "modulus" based on stress and strain measurements from a scaled down pavement section. They measured stresses and strains occuring in a granular basecourse and clay subgrade of a 2-layer pavement constructed in the laboratory subjected to a repeated pulse load. Instrumentation difficulties led to a very wide scatter of results. When linear elastic theory was assumed at each instrument point separately and then values of Young's Modulus and Poisson's Ratio calculated, Poisson's Ratio was found to vary eratically from 0.2 to 0.6 in the clay and decreased linearily with mean stress from 0.4 to 0.3 in the granular base. Using measured values of the maximum stresses and strains occuring in three-dimensions under the pulse load and by applying the equations of elasticity at a point, a "resilient Young's Modulus" was found. For each layer the modulus was expressed in terms of the sum of the principal stresses:

$$\text{granular base}, \quad E_{secant} = 2040\ J_1^{0.57}. \qquad (3.3)$$

$$\text{clay subgrade}, \quad E_{secant} = 28000\ J_1^{-0.61}.$$

where $J_1 = \sigma_1 + \sigma_2 + \sigma_3$ (3.4)

σ_i - principal stresses

These equations, it must be remembered, were the result of a regression analysis with a very wide scatter of results. It is shown in Chapter 5 that for similar test results the scatter is reduced if bulk and shear behaviour are characterised separately based on the derived values of bulk and shear stresses and strains. The equation for the granular base shows the same trend as that given by Monismith et al. In the clay subgrade, however, modulus decreased with the mean stress. The same trend was apparent from the measured stresses and strains of Brown and Pell when this secant modulus was expressed in terms of the 2nd stress invariant or octahedral shear stress. Thus, quite arbitrarily, the material could be characterised in terms of either the mean stress or shear stress.

Duncan et al[1.46] were concerned to find material characteristics which could be used in a finite element method of analysis. Conveniently the triaxial cell (where $\sigma_2 = \sigma_3$) at constant confining pressure yields a resilient tangent modulus equivalent to Young's Modulus defined: $M_R = \frac{d(\sigma_1 - \sigma_3)}{d\epsilon_1} = E_{tan}$. This was incorporated in finite element analysis. Although the balance between bulk and shearing stresses had been shown to be the fundamental factor in the behaviour of soils up to and at failure[3.6], Monismith et al[1.12] considered only quantities coming from the traditional triaxial test with pulsating loading, namely, "modulus" based on a peak to peak deviator stress and peak to

peak axial strain. This modulus has little meaning in terms of fundamental soils properties since it is defined $\frac{d(\sigma_1-\sigma_3)}{d\epsilon_1}$ and confuses shear stresses with an axial strain. Measurements of other, particularly radial, strains were not made presumably because of the practical difficulty involved. Difficult to measure within a triaxial cell under pressure, these radial strains, it would seem, are almost impossible to measure under pulsating loading conditions. Snaith[7.1] has evolved a technique involving measurement of volume change in a tube surrounding the triaxial specimen but the success of this is not yet certain.

The tests by Brown and Pell clearly show that stiffness was dependent on stress level in both granular and clay materials. The tests also showed that in a pavement the rate of loading influenced results. In the subgrade clay, stress increased and strain decreased with increased rate of loading, the effect on the strains being more marked. Although non-linearity was shown by the stresses in the clay not being proportional to surface contact pressure, they argued that elastic theory predicted maximum shear stresses adequately for design purposes. Later comment[3.7] again emphasised non-linearity. Under loading the clay showed a decrease in secant modulus with increased deviator stress at some confining stress, and an increase in modulus with increased confining stress. A more general description of the behaviour of the clay is therefore necessary and a simple functional relationship could be postulated as $E = f(\sigma, \tau)$. Here σ = all round stress is chosen, as opposed to any one normal stress and,

τ is a measure of the shear stress system, taken as the second stress invariant. With such a relationship isotropy is retained. Experimental evidence suggests that for a clay the shear (τ) is the dominant variable.

The earlier conclusion[1.7], that for a clay the modulus decreased with increasing confining stress was stated with a certain amount of confusion. In the layered system under test, normal loads at the surface led to ratios of mean normal/octahedral shear stress (Chapter 5) which did not vary greatly throughout the system for a given load, or at a given position for changes in the value of the normal load. Hence a relationship of the type, $E = 28000\ J_1^{-0.61}$, which describes the stiffness change in this type of stress system under these loading conditions does not model the clay under any general system of loads. Hence it does not model the fundamental characteristics of the material.

Huang[3.8] had first suggested a general set of postulates to cover both the granular and clay type materials. He assumed that under dynamic loads the effect of loading time on material properties could be ignored and the material could be considered as non-linear elastic. Clearly this excludes a rigorous consideration of asphaltic materials which because of their bitumen content have properties which are markedly time dependent. He also assumed that Poisson's Ratio (ν) was 0.5 so that the material could be described completely using one parameter E (Young's Modulus) or G (shear modulus). Huang stated that for granular materials, mean stress had a greater effect on E than octahedral shear stress

(Fig. 3.1 i)) but that increase in either stress led to increased E. It can be said for a clay that shear stress is the more important factor and reduces E (Fig. 3.1 ii)).

It can therefore be seen how tests carried out in instrumented scaled down pavement sections can obscure the understanding of the general behaviour. Brown and Pell produced a relation, $E = 28000\ J_1^{-0.61}$, but such was the similarity of σ/τ values within the pavement that the wrong conclusions were drawn. From Fig. 3.1 iii) it was inferred that E decreased with increasing σ, but since the ratio σ/τ varied only slightly in the material, the decrease was essentially due to the change in τ and the inferred dependence on σ incorrect. Huang contributes to the confusion by characterising the material in either of two ways:

$$E = k_1(\sigma)^{n_1} \qquad \text{or} \qquad E = k_2(\tau)^{n_2} \tag{3.3}$$

without recognising that k_1 and k_2 could not be true material constants.

Clough and Woodward[3.9] in carrying out an incremental finite element analysis on an earth dam, considered the more fundamental deformation properties of the soils. They stated that E and ν were not necessarily the most "convenient" measures of material properties. It was thought that in the field it was "more effective to deal with a bulk modulus (M_b) and a distortion modulus (M_d)". It was considered appropriate to consider the embankment problem as one of plane strain ($\varepsilon_2 = 0$); thus referring to the principal directions the stress-strain law could be written:

$$\begin{bmatrix} \sigma_1 \\ \sigma_3 \\ \tau_m \end{bmatrix} = \frac{E}{(1+\nu)(1-2\nu)} \cdot \begin{bmatrix} 1-\nu & \nu & 0 \\ \nu & 1-\nu & 0 \\ 0 & 0 & \frac{1-2\nu}{2} \end{bmatrix} \cdot \begin{bmatrix} \epsilon_1 \\ \epsilon_3 \\ \gamma_m \end{bmatrix} \qquad (3.4)$$

where τ_m and γ_m are the maximum shear stress and strain respectively.

The characteristic moduli were defined as follows:

$$\sigma_{bulk} = \frac{\sigma_1+\sigma_3}{2} = M_b(\epsilon_1+\epsilon_3) \qquad (3.5)$$

$$\sigma_{deviator} = \frac{\sigma_1-\sigma_3}{2} = M_d(\epsilon_1-\epsilon_3) \qquad (3.6)$$

By introducing equations 3.5 and 3.6 into 3.4, relationships between the moduli, as defined, and Young's Modulus and Poisson's Ratio were derived.

$$M_b = \frac{E}{2(1+\nu)(1-2\nu)} \qquad (3.7)$$

$$M_d = \frac{E}{2(1+\nu)} \qquad (3.8)$$

and equation 3.4 was expressed in terms of M_b and M_d only. In the triaxial test condition (where $\sigma_2 = \sigma_3$), $\epsilon_1 = \frac{1}{E}(\sigma_1 - 2\nu\sigma_3)$; thus provided the confining stress was held constant, $\frac{d(\sigma_1-\sigma_3)}{d\epsilon_1} = E_{tan}$. This ratio was defined as M_t by Clough and Woodward and from triaxial tests allowed the calculation of non-linear E and ν values for a finite element analysis.

Although the above simplification applies to the incremental behaviour of soils, secant characteristics necessary for an iterative analysis are less simple in definition (see later).

Clough and Woodward assumed an initial Poisson's Ratio of 0.44, arbitrarily, so that from the initial value of modulus

obtained from any one confining pressure and equation 3.8, an equally arbitrary value of M_d would be obtained for the incremental finite element analysis. It is shown in Chapter 4 that the correct choice of initial value is of critical importance in a numerical incremental treatment. In summary, the application of generalised Hooke's Laws using bulk and shear moduli derived from an incrementally loaded triaxial cell, without the measurement of ε_3 (radial strain), does not yield characteristics fundamentally different from an axial Young's Modulus. The results seem completely dependent on the aribtrary choice of Poisson's Ratio ($\nu = 0.44$) and this method of characterising soil behaviour would seem inadequate to model the fundamental behaviour.

Girijavallabhan and Reese[3.10] approached the problem of material characterisation in a more fundamental way. Two basic phenomena were recognised as being important.

(1) hydrostatic stress for volume change.

(2) deviatoric stress for change of shape.

It was also recognised that in soils volume change could occur as a result of shear stresses, thus adding a third variable to the relationship. The hydrostatic and shearing components of stress and strain were defined in terms of the first and second stress and strain invariants. These invariants in terms of principal stresses are:-

$$\sigma = \frac{\sigma_1+\sigma_2+\sigma_3}{3}$$

$$\tau = \frac{1}{3}\sqrt{(\sigma_1-\sigma_2)^2 + (\sigma_2-\sigma_3)^2 + (\sigma_3-\sigma_1)^2} \qquad (3.9)$$

$$\epsilon = (\epsilon_1+\epsilon_2+\epsilon_3)/3$$

$$\gamma = \frac{2}{3}\sqrt{(\epsilon_1-\epsilon_2)^2 + (\epsilon_2-\epsilon_3)^2 + (\epsilon_3-\epsilon_1)^2}$$

σ_1, σ_2, σ_3 are the principal stresses.

ϵ_1, ϵ_2, ϵ_3 are the principal strains.

σ and τ are mean normal stress and octahedral shear stress respectively. ϵ and γ are mean normal strain and octahedral shear strain.

For an isotropic elastic material the relations between stresses and strains are:

$$K \text{ (bulk modulus)} = \frac{1}{3}\frac{\sigma}{\epsilon} \qquad (3.10)$$

$$G \text{ (shear modulus)} = \frac{\tau}{\gamma} \qquad (3.11)$$

These relationships do not apply directly to all soils since they can change volume under shear. The ratio was replaced by function relationships which in the general form were written:

$$\epsilon = f_1(\sigma,\tau) \qquad (3.12)$$

$$\gamma = f_2(\sigma,\tau) \qquad (3.13)$$

The soft clay being considered was assumed incompressible ($\nu = 0.5$ and $K = \infty$). Since the Author's finite element method could not cope with this situation a value of 0.48 was chosen for Poisson's Ratio. Triaxial tests were carried out to establish the shear behaviour of the clay and the material characteristic obtained was used to analyse the load settlement behaviour of a circular footing in soft clay. Since the

material was considered as imcompressible, $2\epsilon_3+\epsilon_1 = 0$, and

$$\tau = \frac{\sqrt{2}}{3}(\sigma_1-\sigma_3)$$

$$\gamma \doteq \sqrt{2}\,\epsilon_1 \qquad (3.14)$$

thus $G = \frac{\tau}{\gamma}$ and $E = 2G(1+\nu) \doteq 3G$

For this saturated material, change of shape occurred under constant volume and the stress-strain curves were found to be independent of the confining pressure in the cell.

A second problem, that of a wall retaining sand, was considered by the finite element method. The material was assumed to suffer volume changes only under shear stresses and the pseudo-elastic constants E and ν derived from triaxial testing which involved the measurement of the volume change (δv). Thus shear stresses and shear strains were used to express the stress-strain relationship of the sand and σ used to represent the effect of the confining pressure on the relationship. The parameters E and ν were found as follows:

$$\nu = \frac{-\epsilon_3}{\epsilon_1} = \frac{1}{2}\left(1 - \frac{\delta V}{V}\frac{1}{\epsilon_1}\right)$$

$$E = 2G(1+\nu) \quad \text{where} \quad G = \frac{\tau}{\gamma} \quad \text{and}$$

$$\tau = \frac{\sqrt{2}}{3}(\sigma_1-\sigma_3) \quad \text{and} \quad \gamma = \frac{2\sqrt{2}}{3}\epsilon_1(1+\nu)$$

The variation in material properties was thus built into the analysis by varying both E and ν but relates only to the restricted stress state in the triaxial cell.

The authors make the comment that in the present state of experimental knowledge there may be no merit in ignoring

bulk action and explaining all volume change by shear action. The influence of confining pressure was, however, observed to result in a linear increase of the shear modulus.

Holubec[3.2] considered the elastic behaviour of cohesionless soils and described the volume change caused by shear through the void ratio (e). For any given initial void ratio he showed that the elastic properties of a granular material varied with σ and τ. He was concerned to obtain a soil characterisation which was based on an incremental stress-strain theory and thus claimed to show that the elastic properties were functions only of the state of strain of the granular material element and independent of how this state was achieved. Using a triaxial cell with frictionless end platens he obtained plots of deviator stress/axial strain and by unloading showed a permanent set. Graphs produced were similar to those of previous workers[3.9/10]. Holubec explains the unload and reload parts of the curve on the assumption that soil particles attain a critical equilibrium. Volume change occurs with shear because of the dilatant nature of the soil; the particles do not return to their original positions and irreversible deformations occur. The characterisation which Holubec sought was an incremental one which could model this permanent deformation as well as the resilient elastic behaviour. The experimental work, using the triaxial cell, established that the sand was anisotropic. The elastic axial modulus was found to be a function of the state of the soil element and more particularly, in the triaxial cell, a function of mean normal stress, octahedral shear stress and initial void ratio.

$$E_1 = f(\sigma, \tau, e_{init}) \qquad (3.15)$$

The anisotropy was described by four parameters E_1, ν_1 and E_3, ν_3 related to vertical and radial directions respectively. Fig. 3.2 (after Holubec) summarises the effect of stress level on E_1.

E_1 was seen to increase with σ and τ

E_3 increased with σ but decreased with τ but the change in E_3 was so small as to be regarded as insignificant

ν_1 decreased and ν_3 increased with σ and τ

The curves in Fig. 3.2 all represent a particular initial state (i.e. void ratio or density).

It has been suggested[3.11] that E_1 increased with τ_{oct} because small shear strains help individual grains to find positions of greater stability. Doubts were cast on Holubec's calculations showing anisotropy under the load but it was accepted as "intuitively reasonable" that anisotropy does occur. Coon and Evans[3.12] doubted whether Holubec was modelling elastic behaviour at all. (The fact that he was dealing with incremental loading and allowing irreversible deformations to occur by changing the E values does point to a confusion of two phenomena.) The need for more investigation of the purely recoverable part of the behaviour of cohesionless soils was also pointed out.

Whereas Holubec characterised the soil by E and ν, Domaschuk and Wade[3.1] returned to the more fundamental definitions set out by Girijavallabhan and Reese[3.10] earlier

used by Brown[1.6] to analyse results from in-situ 3-dimensional instrumentation. Bulk and shear modulus were given the definitions of classical elastic theory:

$$K = \frac{\sigma}{\frac{1}{3}\epsilon} ; \qquad G = \frac{\tau}{\gamma}$$

The ideal basis of the work was:-

(1) Bulk modulus (K) from triaxial tests in which only normal strains were permitted, i.e. isotropic consolidation.

(2) Shear Modulus (G) from triaxial tests in which only shear strains were allowed to occur. The condition to find bulk modulus was easy to simulate, that for shear modulus was more difficult since it was necessary to keep $\sigma = \frac{\sigma_1 + 2\sigma_3}{3}$ = constant. To calculate ϵ_1 and ϵ_3, a drained triaxial test with measurement of volume change was necessary. From volume change and ϵ_1, the lateral strain was deduced, presumably from, $\frac{\delta V}{V} = \epsilon_1 + 2\epsilon_3$. Hence the Bulk and Shear Moduli were obtained from their definition in terms of the first two stress invariants. Variation in the density of the sand was stated to be the 3rd factor which could vary K and G.

From isotropic consolidation tests a power law relation was proposed, $\epsilon = c\sigma^{\alpha}$, giving rise to a secant bulk modulus,

$$K = \frac{\sigma}{\epsilon} = \frac{1}{c}\,\sigma^{(1-\alpha)} \qquad (3.16)$$

Tests of the shear box type were found to give linear stress-strain curves in granular materials with the slope dependent on the applied normal pressure. Domaschuk and Wade

also discussed a dynamic shear modulus derived from repeated rotational testing where the shear modulus was found to depend on the confining stress alone (i.e. $G = c\sigma^{\frac{1}{3}}$). It is therefore implied that shear stress-strain behaviour does not depend on the magnitude of shear stress, but, of course, in almost any loading pattern shear stress increase is accompanied by changes in confining stress. Domaschuk and Wade, however, retained generality and defined a shear modulus from the triaxial test at various constant values of σ as $G = \frac{\tau}{\gamma}$ where τ and γ are octahedral shear stress and strain. Their findings are summarised in Fig. 3.3. Their experiments showed that for a sand:

> increased shear strain led to a lower shear modulus (softening)
> increased bulk strain led to a higher bulk modulus (stiffening),

and as might have been expected, modulus was increased by a lower void ratio or raised density.

In these tests σ and τ had taken various values depending on the stress path, but at failure σ/τ appeared to reach a constant value which depended on the overconsolidation ratio (Fig. 3.3 iii)). On this basis, if road materials did not dilate under shear then the location of regions succeptible to failure could be established with some confidence by theoretical analysis. The travelling load produces in the pavement a ratio σ/τ for any one point which varies with the passage of the load but its maximum value, neglecting time dependent properties, can be obtained from the maximum stationary load case. If the effective moduli are strongly

dependent on the stress path, the stress distribution would be affected. In real materials this leads to more difficult conceptual and computational problems which have not so far been examined.

It is generally accepted that volume changes occur under shear stress action thus prediction of the exact behaviour becomes complicated. For the sand considered by Domaschuk and Wade, failure occurred when σ/τ was less than about 0.8 for a dense sand and 1.0 for looser material. Their work appears to be the first separation of stress-strain behaviour into volumetric and deviatoric components in any fundamental sense.

$$K = f_1(\sigma, D_r)$$
$$G = f_2(\sigma, \tau, D_r) \qquad (3.17)$$

D_r = relative density

Since K and G are related to E and ν this shows that E and ν have a very wide range of values. K and G depend on fundamental soil stresses and strains which are measurable and independent of axis of orientation. Poisson's Ratio is difficult to define adequately in this context and difficult to measure.

In discussion of Domaschuk and Wade, Girijavallabhan[3.13] argued that the volumetric strain should be allowed to change as a result of shear stress (dilation), symbolically $\frac{dV}{V} = f(\sigma, D_r, \tau)$. He also made the valid conclusion that K and G values obtained from triaxial testing may not be valid for

states of stress where $\sigma_2 \neq \sigma_3$. It may be added that end restraint in the cell has an effect on the deformed shape and will cast doubt on estimates of ϵ_3 based on volume change and ϵ_1 (Chapter 7). Girijavallabhan also comments that Domaschuk and Wade do not explain precisely how ϵ_3 was calculated. He questioned the advantage of characterising the material using K and G. It was argued, what in linear elastic terms would be correct, that E and ν are only different versions of K and G and yield exactly the same results.

Chowdhury[3.14] doubted that the isotropic compression test and the constant mean normal stress test produced unique values of elastic moduli. He also stated that Domaschuk and Wade had nowhere justified the use of K and G as soil parameters except to say that they were more "appropriate". He recognized that the method of testing has an important bearing on the values of moduli obtained and would have preferred tests more closely related to the kind of stress system being modelled. A further criticism was that unloading characteristics were not produced. These are clearly important in showing to what extent dilation has caused permanent changes in the soil structure. Chowdhury was also interested in load and unload tests where deviator stress was increased, at constant mean normal stress, to a level well below failure. (He was presumably interested to know whether permanent deformation occurred due to shear at lower stress levels.) The rate of loading of the one-off tests carried out by Domaschuk and Wade was not specified.

Passing on from single loaded tests on both granular and cohesive soils, it is essential to consider repeated loading tests and to examine the nature of the characteristic parameters they have been able to yield. The Californian work on granular materials[1.12] yielded $M_R = k\sigma^n$, where M_R was defined as a modulus of resilience. For constant σ_3 in repeated load triaxial tests this yields a tangent Young's Modulus, $E_{tan} = \frac{d(\sigma_1-\sigma_3)}{d\varepsilon_1}$, which has been used in finite element analysis.

Vibration testing on clay materials has been reported by Hardin and Black[3.15] and Humphries and Wahls[3.16].

Hardin and Black recognised that in the early cycles of loading the clay underwent irreversible deformation so that for subsequent loadings the stress-strain relations changed. After about 100 repetitions the pattern settled to an almost steady, narrow hysteresis loop. (In the case of a sand this occurred after 10 or 20 repetitions.) It was claimed that, at a particular level of loading, any irreversible deformation had been completed and only the non-linear resilient behaviour under repeated loading remained to be observed. A shear modulus was measured in shear tests using a column of soil under repeated rotation and a "vibration shear modulus" found. A relationship was given:

$$G = A.f(e).\sigma^n \qquad (3.18)$$

where A depended on the amplitude of vibration.

e = void ratio.

n = constant (0.5 for angular sand).

It was emphasised that this vibration modulus did not depend on the octahedral shear stress and decreased with increasing void ratio. The modulus increased with mean normal stress by a square law but secondary increase occurred with time, which was thought to be a result of "sensitivity to particle disturbance". (There might well have been a volume contraction causing this stiffening.) The relationship for vibration modulus (Eq. 3.18) was found to be very similar to that earlier found by Hardin and other workers. In that case, G was found not to depend on the amplitude of vibration.

Humphries and Wahls[3.16] established a shear modulus from torsional tests on bentonite and kaolin. An increase in the all round pressure was applied and shown to produce an increase in shear modulus (defined in the same way as Hardin and Black). The new information given by Ref. 3.16 concerned the effect of amplitude on modulus. Dynamic shear modulus was found to decrease with increasing amplitude of rotational vibration. Again stress history, as simulated by all round pressure, and the void ratio were found to be the most important variables.

The above vibrational shear tests show that with repeated shear stress reversal a steady state is achieved and some characteristic resilient shear modulus can be determined. The modulus is <u>not</u> that defined by

$$G \text{ (shear modulus)} = \frac{d\tau}{d\gamma}$$

but some characteristic which is a function of this method

of dynamic testing.

Two recent papers[3.17, 3.18] have used soils tests to obtain a tangent modulus (E_{tan}) to be used in incremental finite element analysis.

Desai and Reese[3.17] carried out undrained triaxial tests and for various values of cell pressure determined the deviator stress, $d(\sigma_1-\sigma_3)$ - axial strain $d\varepsilon_1$, behaviour. If σ_3 = constant, $E_{tan} = \frac{d(\sigma_1-\sigma_3)}{d\varepsilon_1}$, thus enabling an incremental finite element analysis. Poisson's Ratio was arbitrarily assumed to have the value 0.485, for all stress conditions, in the absence of volume change measurements.

Duncan and Chin Yung Chang[3.18] made measurement of volume change in triaxial tests which were essentially the same as those of Desai and Reese and carried out at various constant cell pressures. The same incremental tangent modulus was obtained but an incremental Poisson's Ratio was calculated as follows:

from incremental generalised Hooke's law applied to the triaxial cell stress state ($\sigma_2 = \sigma_3$)

$$E\delta\varepsilon_1 = \delta\sigma_1 - 2\nu\delta\sigma_3$$
$$E\delta\varepsilon_3 = \delta\sigma_3 - \nu(\delta\sigma_1+\delta\sigma_3) \qquad (3.19)$$

but in these tests $\delta\sigma_3 = 0$ and $\delta\varepsilon_v = \delta\varepsilon_1+2\delta\varepsilon_3$ where ε_v is the volumetric strain

thus $$\nu = -\tfrac{1}{2}\frac{(\delta\varepsilon_v-\delta\varepsilon_1)}{\delta\varepsilon_1} \qquad (3.20)$$

For silica sand this ratio was found to increase with increasing "stress level" from ν = 0.11 to 0.65 over the range 2-7 kgf/cm^2. The tests are more complete than those of Desai and Reese in that the authors carried out unload and reload tests. On reload the range of Poisson's Ratio

became 0.15 to 0.4 and the range was "larger for unloading than reloading". It was, therefore, concluded that the material could not be characterised by one value of Poisson's Ratio and without regard to reload conditions. It was also pointed out that to represent materials which dilated or contracted under shear, more than two soil parameters were needed, even in the case of isotropic materials.

Gerrard[3.19] examined samples of sand for stress induced anisotropic behaviour. Initial anisotropy due to the method of packing of the sample was changed on the application of an all round pressure. The characteristics tended towards those of an isotropic material. For tests in which both deviator stress ($\sigma_1-\sigma_3$) and a torsion stress were applied a change in the nature of the anistropy was indicated by the increasing difference between "shear modulus" representing the deviator stress-strain behaviour, $G = \frac{1}{2}\frac{d(\sigma_1-\sigma_3)}{d(\epsilon_1-\epsilon_3)}$, and the shear modulus representing torsion stress-strain behaviour. Unfortunately, since unloading tests were not carried out it is not known whether the dilation that occurred was elastic or not.

In all the non-vibrational triaxial tests which have been examined under unload and reload conditions there has been a marked change in properties as measured by E and ν or K and G, however defined. Tests by Hardin and others have shown that after a number of repetitions of load a non-linear elastic property may be attributed to materials, but there is as yet no clear understanding of the mechanism whereby the material properties vary with stress level.

Gerrard[3.19] has demonstrated for sands that after repeated loading there is a degree of anisotropy which depends on the stress history. Holubec[3.2] confirms these findings and states that

> "cohesionless soil is isotropic for isotropic stress conditions and becomes anisotropic when sheared. The anisotropy increases with shear stress and the increase appears to be a function of σ/τ"

3.3.2 Elastic dilation and transverse isotropy

In a recent paper, Pickering[3.20] examines elastic dilation in terms of anisotropic parameters. He assumed that in a layered soil the governing parameters were independent of horizontal direction and that the vertical axis was an axis of radial symmetry. In the case of the stress dependent anisotropy observed by Gerrard this would not strictly be true away from the axis of a repeated load on a road pavement.

Twenty-one elastic parameters are needed to fully describe three dimensional anisotropy. If transverse isotropy is accepted as being a realistic description of the layered pavement materials under a large number of moving loads, then there is a reduction in the required material constants to 5. For such a material Pickering defined the limits of these parameters and stated that it was possible that a dilatant material could be treated by elastic methods and considered in this way in a finite element analysis. Suklje[3.21] has incorporated the same kind of anisotropy into relationships for the bulk and shear moduli of a material based on triaxial testing and allowing elastic

dilation. It is shown in the Appendix at the end of this Chapter that elastic dilation must be the result of interaction of the principal stresses only. Shear stresses in the plane of the principal stress axes do not lead to a volume change.

To summarise, an explanation of dilatant behaviour under shear stress or uniaxial compression demands anisotropic parameters. However, since dilatant behaviour in one-off loading tests is thought to be non-recoverable (e.g. in sand - riding over one another of particles) the relevance of elastic anisotropy is doubtful.

The material characterisations developed up to 1971 which use E-ν or K-G assume, either explicitly or implicitly, that the material is isotropic. Modification which allows the introduction of dilatant effects permits changes in moduli with either the density D_r or the void ratio e. This mechanism of change in characteristics seems most suited to the incremental analysis of once-loaded structures. Dilatant behaviour in this case would bring about permanent changes in structure and thus changes in "stiffness".

The situation under repeated loading is different. It has been shown that after a number of repetitions under the same load in laboratory conditions the behaviour can be explained by non-linear elastic deformation. Experimental evidence is not conclusive, but the elastic deformation may contain an element of recoverable dilation which could be modelled by anistropic parameters.

In full scale road tests it is well known that permanent damage occurs, even after many repetitions, since the pavement is not perfectly resilient. For numerical prediction it is therefore important to obtain additional experimental evidence on the variation in time of both resilient characteristics and the incremental permanent deformation per load cycle.

3.4 Summary of Basic Soil Characteristics

The behaviour of stress systems can be broken down into the separate effects of hydrostatic and shear stresses. These are thought to have fundamental significance in isotropic materials because of their invariance under changes of axes.

In soils the stress-strain characteristics under hydrostatic stress are very different from those under shear stresses, and from material to material the nature of these relationships will change.

For any stress system, the volumetric strain or volume change and the shear or distortional strain together completely define the state of strain. These strains each depend on the loading system imposed and in a soil the orientation of their principal directions will be different from that of the stresses if there are inelastic or anisotropic deformations.

A general loading on a layered system leads to the development of both normal and shear stresses with any one choice of axes. Thus the complete description of the behaviour of a soil which retains isotropy for an increment of load at

any already established state of stress can be stated as:-

(1) volume change with all round stress level:

$\left(\frac{\partial V}{\partial \sigma}\right)$ V - volume
σ - mean stress

The inverse of this quantity can be considered as a bulk modulus K.

(2) shear distortion with shear stress:

$\left(\frac{\partial \gamma}{\partial \tau}\right)$ γ - distortional strain
τ - deviatoric stress

The inverse of this quantity can be considered as a shear modulus G.

(3) volume change with shear:

$\left(\frac{\partial V}{\partial \tau}\right)$

The magnitude and sign of this quantity will depend on stress history. A heavily over consolidated clay will dilate under shear stresses whereas a normally consolidated sample would contract. At any state the material is at a particular density or void ratio, any volume change as a result of shear, changes this density and thus the bulk and shear moduli.

(4) The fourth possibility is distortional change with all round stress level. This is unlikely to occur in homogeneous materials.

Elastic theory, on which the continuum analysis in this thesis is based, defines the mean normal stress and octahedral shear stress invariants as:-

$$\sigma = \frac{\sigma_x + \sigma_y + \sigma_z}{3}$$

$$\tau = \frac{1}{3}\sqrt{(\sigma_x-\sigma_y)^2+(\sigma_y-\sigma_z)^2+(\sigma_z-\sigma_x)^2+6\tau_{xy}^2+6\tau_{yz}^2+6\tau_{zx}^2}$$

where x, y, z represents an orthogonal set of axes

These invariants as measures of the stress state are independent of the orientation of the axes to which they are referred and except in the case of isotropic materials the principal strain axis need not coincide with the principal stress axis.

A Bulk modulus (K) and a shear modulus (G) can be defined as:

$$K(\text{bulk}) = \frac{\text{bulk stress}}{\text{bulk strain}} = \frac{1}{3}\frac{\sigma}{\varepsilon} . \qquad (3.21)$$

$$G(\text{shear}) = \frac{\text{octahedral shear stress}}{\text{octahedral strain}} = \frac{\tau_{oct}}{\gamma_{oct}} . \qquad (3.22)$$

If the material is elastic, homogeneous and isotropic, these two parameters offer a complete description of the soil.

In real soils, each is dependent to some extent (which can be found from testing) on the two stress invariants σ and τ and on some factor to define the state of the material. It is possible that this third factor could be the density or void ratio, which would represent the state the material has reached in its history and would almost always be time dependent under repeated loading.

The outcome for isotropic materials is a two parameter description each of which varies with the state of stress and history of the material, i.e.

$$\left.\begin{aligned} K \text{ (bulk modulus)} &= f_1(\sigma, \tau, Dr) \\ G \text{ (shear modulus)} &= f_2(\sigma, \tau, Dr) \end{aligned}\right\} \text{ after Domaschuk}$$

Dr = relative density

The stresses occuring in an isotropic material dilating under shear will not be predicted accurately from linear elastic theory, but the use of a changing density or void ratio may lead to more acceptable results.

If the material was considered as generally anisotropic, with a stored energy, independent of stress path even though the anisotropy might be the result of the imposed stress system or stress history, 21 elastic constants would be required. If there is no recoverable work-energy concept, this number rises to 36. It would be outside the realms of practicality to carry out soils tests to establish all these parameters, even if it were possible with present equipment, and to handle the information to predict behaviour.

It is shown from analysis of insitu measurements (Chapter 5) that K and G, since they relate to fundamental modes of deformation, are informative about basic material behaviour. The triaxial cell can be used to measure all the quantities necessary to calculate K and G as defined above but in addition to the measurements commonly made in the past it would be necessary to measure the volume change of the sample or the radial strain. Because of its importance, a means of analysis of the triaxial test is given in Chapter 7. Finite Element Methods are used to examine the inaccuracies arising from end effects.

An approximate description of the deformation of the soil up to failure now seems possible given measurement of triaxial cell volume change.

3.5 Suggested Role of Triaxial Test

Since the test has the basic restriction that $\sigma_2 = \sigma_3$ a truly 3-dimensional stress state cannot be modelled.

Accurate material characteristics are, however, most desirable under the axis of a load on a pavement where the highest stresses occur. From symmetry, for the axis of the load only, the horizontal stresses are equal. The triaxial test would thus seem to give a reasonable prediction close to the axis of an on-off load. It would not accurately model the stress system with rolling or passing loads.

For a particular material it is desirable to find how the moduli vary with all round stress and shear stress. It seems that important information will be lost if assumptions are made about either Poisson's ratio values or bulk modulus. In the above mentioned research work stresses have been taken to be the effective values and not gross. The triaxial test for, say, wet clays introduces further parameters. In repeated loading tests on wet clays,drainage cannot occur to dissipate pore pressures in the time scale of the tests.

For a saturated soil it would be normal to define the effective stresses in terms of gross load divided by gross area (including voids), and to reduce this by the pore pressure. From the relative incompressibility of the pore fluid it could then be argued that for pulsating loads the

all round compression would be equilibrated by the pulsation of the pore pressure. This would equally occur in the test cell and in situ, in the road subgrade.

If there were long term or cumulative effects in situ, these could only be modelled under test conditions by allowing moisture movement to permit the appropriate dilation or consolidation.

The greater problem in subgrades, of seasonal variations in degree of saturation and the possibility of a partially saturated zone in the base and sub-base, is thought too difficult for most soil mechanics experiments and its consideration is often excluded. Apart from the comments above, the modelling of possible consolidation in saturated soil masses is also excluded from this thesis.

The basic material characteristics defined in terms of invariants when applied to the triaxial cell are:-

$$K = \frac{1}{3}\frac{\sigma}{\epsilon} = \frac{1}{3}\left(\frac{\sigma_1 + 2\sigma_3}{\epsilon_1 + 2\epsilon_3}\right) \tag{3.23}$$

$$G = \frac{\tau}{\gamma} = \frac{1}{2}\left(\frac{\sigma_1 - \sigma_3}{\epsilon_1 - \epsilon_3}\right) \tag{3.24}$$

where
$$\sigma = \frac{\sigma_1 + 2\sigma_3}{3} \qquad \tau = \frac{\sqrt{2}}{3}(\sigma_1 - \sigma_3)$$
$$\epsilon = \frac{\epsilon_1 + 2\epsilon_3}{3} \qquad \gamma = \frac{2\sqrt{2}}{3}(\epsilon_1 - \epsilon_3) \tag{3.25}$$

The cell pressure acts on the top of the triaxial specimen (Fig. 3.4) introducing experimental difficulties.

e.g. if it was desired that $\sigma_1 < 0$ then $\frac{P}{A} + \sigma_3 < 0$. This implies that for a positive cell pressure, P would be negative, clearly not feasible unless the specimen could be fixed to the end platen.

The following tests, although more complicated, might yield better material information by their concentration on the stress invariants.

3.5.1 Static tests (one off)

i) Constant Mean Normal stress (σ): requires $\sigma_1+2\sigma_3 = c_1$ (constant), where $\sigma_1 = \frac{P}{A} + \sigma_3$. For this condition:

$$\sigma_3 = \tfrac{1}{3}\left(c_1 - \frac{P}{A}\right) \qquad (3.26)$$

Thus to retain σ = constant, the cell pressure (σ_3) would have to be varied during the test according to the above equation. Separate tests would be carried out for a number of realistic values of c_1. During each test P would be varied over a range and simultaneously the cell pressure σ_3 changed according to equation (3.26).

With measurement of the volume change of the specimen the result would be; K and G with varying τ for constant values of σ.

ii) Constant Octahedral Shear stress (τ): requires $(\sigma_1-\sigma_3) = c_2$ (constant) where $\sigma_1 = \frac{P}{A} + \sigma_3$. For this condition $(\sigma_1-\sigma_3) = \frac{P}{A} = c_2$, implying that it is necessary to carry out tests at a number of constant values of P varying σ_3 each time over a realistic range.

The result would be; K and G with varying σ for constant τ.

iii) Strains

To obtain strain invariants, the radial strain must be

determined. Provided there is an appropriate correction made to account for change in shape of the specimen from cylindrical due to some end frictional restraint, volume change will provide radial strain.

If the specimen deformed in the shape of a cylinder the volume strain

$$\frac{\Delta V}{V} = \epsilon_1 + 2\epsilon_3$$

$$\text{i.e.} \quad \epsilon_3 = \tfrac{1}{2}\left(\frac{\Delta V}{V} - \epsilon_1\right) \tag{3.27}$$

and for zero volume change then $\epsilon_3 = -\frac{1}{2}\epsilon_1$ and the bulk modulus would be infinite.

The moduli defined from test measurements become

$$K = \tfrac{1}{3}\frac{\left(\frac{P}{A} + 3\sigma_3\right)}{\frac{\Delta V}{V}} \tag{3.28}$$

$$G = \frac{\frac{P}{A}}{\left(3\epsilon_1 - \frac{\Delta V}{V}\right)} \tag{3.29}$$

In the modulus definitions the possibility of dilation due to shear stress is not considered. Thus in a test where dilation occurred, whether recoverable or not, the volume changes would not be associated only with the mean normal stress whereas the definitions assume that they were. The volume changes could be separated by carrying out a hydrostatic compression test on the material, these being conditions where dilation could only occur in non-homogeneous material. The range of hydrostatic stresses used would be the same as the mean normal stress values in the above "static"

tests at constant σ or τ. The existence and magnitude of the dilation due to shear could therefore be determined from triaxial cell tests. Measurements of dilatancy would indicate whether further enquiries into the anisotropic parameters would be necessary.

Assuming, for example, an overconsolidated soil, $\frac{\Delta V}{V}$ as measured would be unreasonably high in the case where shear stresses accompanied and all round compression and the calculated values of K and G would be lower than if dilation had not occurred.

For a stiff clay (Keuper Marl), Brown[1.6] established curves of the type in Fig. 3.3i) and ii) for σ against ϵ and τ against γ (for one density only). K and G can be found from these curves. The effect of dilation on these material properties can be better explained by making diagrams of this type 3-dimensional and explaining volume change due to shear separately. In Fig. 3.5i), K will depend on stress history i.e. whether or not τ has undergone repeated reversal as in a road pavement. Shear modulus would be reduced if dilation were acknowledged (Fig. 3.5ii)) but increased if, for the material, σ increased G.

In general terms:

$$K_{apparent} = f(\sigma, \tau, \frac{\Delta Vd}{V}).$$
$$G_{apparent} = f(\sigma, \tau, \frac{\Delta Vd}{V}). \qquad (3.30)$$

where ΔVd is dilation volume change and depends on τ
Since in any material at given values of σ and τ dilation will depend on stress history, there are no unique equations

to describe K and G. Moving vehicle loading on pavements involves reversal of shear stress and would imply a completely different dilatant behaviour (the stress "path" is different). Dynamic moduli defined from equations (3.28/29) above and found from either full scale tests[1.6] or repeated load triaxial tests, do not simulate this shear reversal. Thus such tests do not model the true strain changes in the real pavement. Principal stresses are measured using the triaxial cell. Reversal of octahedral shear would imply interchanging σ_1 and σ_3 and necessitate a tensile force P being applied axially to the specimen. This is not feasible with present equipment.

The possible mechanism of dilation or consolidation in actual pavements may be missing from the present tests of a "triaxial" type. Thus present dynamic testing which could yield tangent bulk and shear moduli as modified by the dilatant effect might not be strictly correct for the pavement, which experiences passing traffic loading.

The development of a triaxial test where σ_1 and σ_3 can be interchanged would add materially to the confidence with which all tests could be extrapolated to pavements. Since such tests are not currently available the proposals for using more conventional dynamic tests are now considered.

3.5.2 Dynamic test

i) Constant Mean Normal stress (σ)

$\frac{P}{A}$ must be cycled but in order to retain σ as constant the cell pressure must be controlled such that $\sigma_3 = \frac{1}{3}(c - \frac{P}{A})$.

This follows directly from the reasoning in section 3.5.1. Similarly, if P cannot be negative (specimen can take little or no direct tension), then $(c - 3\sigma_3)$ must be kept greater than zero. Radial strains must come from cell volume changes or specimens heavily instrumented around the edge.

ii) Constant Octahedral Shear stress (τ)

$\frac{P}{A}$ must be kept constant (i.e. $\sigma_1 - \sigma_3$). This implies that σ_3 must be cycled in some chosen way and $\frac{P}{A}$ kept constant using some feedback device.

K and G are tangent moduli and expressed as peak-peak stress/peak-peak strain, implying the need to measure peak-peak volumetric strains. In conclusion it must be emphasised that although K and G fully describe an elastic material, soils exhibit dilation under shear. In road pavements shear reversal takes place. As yet neither dynamic nor static testing has simulated this in a specimen where σ and τ have been considered as fundamental material parameters and their effects examined separately.

3.6 Failure Criteria

Failure in a road pavement can be defined as occuring when permanent deformation renders it unsafe for traffic moving at its normal speed. Catastrophic failure may occur locally due to subgrade weakness but design against failure is mainly aimed at minimizing long term permanent damage.

Given that stresses and strains can be predicted accurately before a critical level of stresses is reached it

is necessary to examine what can be done to predict displacements after a "failure" has started and indeed to predict the level and type of stresses which exist at the critical state.

Early work was done on metals and two failure criteria emerge:

3.6.1 TRESCA yield is defined to occur when the maximum shear stress reaches a critical value, k. This yield function describes plastic behaviour in a material.

if $\sigma_1 > \sigma_2 > \sigma_3$ and F is the yield function
then $F = \sigma_1 - \sigma_3 - 2k = 0$

This criterion has been used to determine the yield point of elements in an ideal elastic-plastic soil model[3.22] analysed by the finite element method.

3.6.2 Von Mises

This criterion is defined in terms of the yield stress of the material in simple tension.

$$F = (\sigma_1-\sigma_2)^2+(\sigma_2-\sigma_3)^2+(\sigma_3-\sigma_1)^2-2Y^2 = 0$$

It must be noted that neither of these failure criteria contain terms for the influence of all round compression or specific volume. The Tresca yield function does not include the effect of intermediate principal stress and the Von Mises criterion equates a quantity proportionalto octahedral shear stress with a tensile yield stress for the material. The criterion can be rewritten as, τ^2 = constant, where this constant is some level of distortional energy.

3.6.3 Mohr-Coulomb

The Mohr-Coulomb theory of failure defines the limiting stress state by:

$$\tau_f = f(\sigma')$$

σ' = effective normal stress

τ_f = shear strength

The limiting stress envelope defined by this equation changes with various pre-consolidation pressures. Thus failure depends on both the shear and normal stresses taking particular values. A higher normal stress will permit higher shear stresses before failure occurs. A suggestion that this kind of relationship explained failure in concrete[3.23] was questioned by Bellamy[3.24]. It was doubted that octahedral shear stress could give a true distinction between safe and unsafe states of stress even though it provided a neat means of accounting for the intermediate principal stress. It was felt that "quantities directly proportional to stresses" would provide the soundest failure criterion. For soils, Domaschuk and Wade[3.1] found a definite relationship at failure (Fig. 3.3 iii)) between octahedral shear stress and mean normal stress. The envelope changed with different levels of compaction (consolidation ratios) and thus a soil would seem to obey a Mohr type of failure criterion.

3.6.4 Schofield and Wroth[3.6], however, found that a Mohr type of failure criterion led to unacceptably high rates of change of volume with shear distortion. In order to examine soil behaviour they define two hypothetical materials -

a rigid plastic gravel (granta)

an elastic plastic clay (cam)

The gravel (for example) was found to have a yield function defined:

$$F = q + Mp\left(\ell n \frac{p}{p_u} - 1\right) = 0 \qquad (3.31)$$

where $p = \sigma$

$q = \tau$

p_u = undrained critical state pressure = $\exp\left(\frac{\Gamma - v}{\lambda}\right)$

Γ = ordinate of crit. state line.

λ = grad. of compression line.

v = specific volume.

This defines a yield surface which takes account of both normal and shear stresses. The yield functions defined by Schofield and Wroth and the experimental findings of Domaschuk and Wade all lead to the same conclusion:

3.6.5 Failure appears to be dependent on a ratio of shearing stress to all round compression. · The lower this value, the more likely is failure to occur. Chapter 7 shows verification of this fact where the failure initiation of axial compressive loading in cylindrical specimens of bitumen-macadam was found to tie in well with stress distributions derived theoretically. Since stress invariants define stress level without reference to a set of axes these were considered as fundamental parameters. Thus the ratio was considered to indicate nearness to failure.

The mode of failure when the material is in a state of all round tension is, however, completely different. Compression failure requires that the particles ride over each other leading to dilation and an eventual weakening of the material. In tension, however, weakening of the material can be considered as the result of the breaking in interparticle bonds as a result of the direct tensile forces acting. Thus it would seem that failure should occur as a result of the maximum of the principal tensile stress, given a specimen in all round tension, as indicated by the mean normal stress.

Given the above evidence for compressive failure depending on some ratio between σ and τ and that the mode of failure in tension is fundamentally different (as verified in bituminous specimens, Chapter 7) the following conceptual diagram, in Fig. 3.6, can be considered as representing soil behaviour. To simplify the diagram and analysis σ_3 has been assumed zero. The material postulated has some limiting tensile strength $\sigma_1^{max} = \sigma_2^{max}$. The elipse is defined by assuming that failure in compression depends on the ratio of σ and τ, thus: $\frac{\sigma}{\tau} = k$ and if $\sigma_3 = 0$, then:

$$\frac{\frac{\sigma_1^2+\sigma_2^2}{2} + \sigma_1\sigma_2}{\sigma_1^2+\sigma_2^2-\sigma_1-\sigma_2} = k^2$$

which defines an elipse.

If adequate data could be obtained on the nature of this type of failure characteristic for each of the pavement materials, then it may be possible to accurately predict the pavement failure loading and hence redesign against it.

Appendix to Chapter 3

Dilation and transverse isotropy
(anisotropy of the horizontal layered type)

The principal directions are defined as 1 and 2 horizontal, and 3 vertical.

For transverse isotropy:

$$\begin{bmatrix} \epsilon_1 \\ \epsilon_2 \\ \epsilon_3 \\ \epsilon_{13} \\ \epsilon_{23} \\ \epsilon_{12} \end{bmatrix} = \left[\begin{array}{ccc|ccc} b_{11} & b_{12} & b_{13} & & & \\ b_{12} & b_{11} & b_{13} & & 0 & \\ b_{13} & b_{13} & b_{33} & & & \\ \hline & & & b_{44} & & \\ & 0 & & & b_{44} & \\ & & & & & 2(b_{11}-b_{12}) \end{array}\right] \cdot \begin{bmatrix} \sigma_1 \\ \sigma_2 \\ \sigma_3 \\ \sigma_{13} \\ \sigma_{23} \\ \sigma_{12} \end{bmatrix} \qquad (1)$$

Love (1892) showed that there are 5 independent elastic parameters for the transverse isotropy case.

In general:

$$\begin{aligned} E_1\epsilon_1 &= \sigma_1 - \nu_{12}\sigma_2 - \nu_{13}\sigma_3 \\ E_2\epsilon_2 &= \sigma_2 - \nu_{21}\sigma_1 - \nu_{23}\sigma_3 \\ E_3\epsilon_3 &= \sigma_3 - \nu_{31}\sigma_1 - \nu_{32}\sigma_2 \end{aligned} \qquad (2)$$

If the 1 and 2 directions have the same properties, then $\nu_{31} = \nu_{32} = \nu_3$ (say),

i.e. $E_3\epsilon_3 = \sigma_3 - \nu_3(\sigma_1+\sigma_2)$

In equation (1) $b_{11} = \frac{1}{E_1} = \frac{1}{E_2}$ $b_{12} = \frac{-\nu_{12}}{E_1}$ since $\nu_{12} = \nu_{21}$.

$b_{13} = \frac{-\nu_{13}}{E_1} = \frac{\nu_3}{E_3}$ $b_{33} = \frac{1}{E_3}$

Also $\nu_{13} = \nu_{23} = \nu_3 \frac{E_1}{E_3}$ (Love).

This gives:

$$\begin{aligned} E_1 \epsilon_1 &= \sigma_1 - \nu_{12}\sigma_2 - \frac{E_1}{E_3}\nu_3\sigma_3 \\ E_1 \epsilon_2 &= E_2 \epsilon_2 = \sigma_2 - \nu_{12}\sigma_2 - \frac{E_1}{E_3}\nu_3\sigma_3 \\ E_3 \epsilon_3 &= \sigma_3 - \nu_3(\sigma_1+\sigma_2) \end{aligned} \qquad (3)$$

thus there are 4 constants, E_1, E_3, ν_{12}, ν_3 and a shear modulus G defined:-

$$2G\epsilon_{13} = \sigma_{13}$$
$$2G\epsilon_{23} = \sigma_{23} \qquad \text{also} \quad \epsilon_{12} = 2\left(\frac{1}{E_1} - \frac{1}{E_3}\right)\sigma_{12}$$

The condition that the quadratic form (Eq. (1)) should be positive definite is that all the principal minors of the matrix are positive. This gives:-

1) $b_{11} - b_{12} > 0$ ie $\frac{1+\nu_{12}}{E_1} > 0$

2) $b_{44} > 0$ ie $G > 0$

3) $b_{33} > 0$ ie $E_3 > 0$

4) $b_{11}b_{33} - b_{13}^2 > 0$ ie $\frac{1}{E_1 E_3} > \left(\frac{\nu_3}{E_3}\right)^2$

5) $(b_{11}+b_{12})b_{33} - 2b_{13}^2 > 0$ ie $\frac{(1-\nu_{12})}{E_1 E_3} > 2\left(\frac{\nu_3}{E_3}\right)^2$

E_1, E_3 and G must be > 0, therefore

1) gives $\nu_{12} > -1$

4) gives $\frac{E_3}{E_1} > \nu_3^2$

5) gives $\frac{E_3}{E_1}(1-\nu_{12}) > 2\nu_3^2$

If a shear stress acts only in the plane of the 1, 2, 3 axes it follows that there is no volume change (ref. Eq. (1)).

A. Shear stress

For a general shear stress, s:-

with direction cosines defined as follows:

direction	normal, $\hat{n}$	in direction of shear, $\hat{s}$
1	ℓ_1	ℓ_2
2	m_1	m_2
3	n_1	n_2

then $\sigma_1 = 2\ell_1 \ell_2 s$

$\sigma_2 = 2m_1 m_2 s$

$\sigma_3 = 2n_1 n_2 s$

and $\epsilon_1 = b_{11}\sigma_1 + b_{12}\sigma_2 + b_{13}\sigma_3$

$= 2s(\ell_1 \ell_2 b_{11} + m_1 m_2 b_{12} + n_1 n_2 b_{13})$

and similarly for ϵ_2 and ϵ_3

Thus $\frac{dV}{V} = 2s n_1 n_2 (b_{33} - b_{11} - b_{12} - 2b_{13})$

$= 2s n_1 n_2 \left(\frac{1}{E_3} - \frac{1}{E_1} + \frac{\nu_{12}}{E_1} - \frac{2\nu_3}{E_3}\right)$

$= \frac{2s n_1 n_2}{E_3}\left((1-2\nu_3) - \frac{E_3}{E_1}(1-\nu_{12})\right)$ where $1-\nu_{12} > 0$ and $\frac{E_3}{E_1} > \nu_3$

Thus there are regions of negative and positive volume change depending on the values of the 4 material constants.

B. Uniaxial stress

If a uniaxial stress T acts in direction $\hat{n}$

$$\sigma_1 = \ell^2 T \qquad \sigma_2 = m^2 T \qquad \sigma_3 = n^2 T$$

and volume change, $\frac{dV}{V} = n^2 T\ (b_{33}+b_{13}-(b_{11}+b_{12}))$, which again can be positive or negative. It is therefore shown that anisotropy can produce dilation either from uniaxial compression (or pure shear provided that it is not along the preferred direction of the transverse anisotropy).

Bulk and Shear Moduli were derived by Suklje for the triaxial stress state and would incorporate dilation as defined above:

$$K = \tfrac{1}{3}\frac{\delta\sigma}{\delta\epsilon} \qquad G = \frac{\delta\tau}{\delta\gamma}$$

Thus: $$K = \tfrac{1}{3}\frac{2\delta\sigma_1+\delta\sigma_3}{2\delta\epsilon_1+\delta\epsilon_3} \qquad G = \frac{\delta\sigma_3-\delta\sigma_1}{2(\delta\epsilon_3-\delta\epsilon_1)}$$

From equations (3) this gives:

$$K = \frac{E_1}{3}(2\alpha+1).\frac{1}{\left[2\alpha(1-\nu_{12})+\frac{E_1}{E_3}(1-2\nu_3-2\nu_3\alpha)\right]} \qquad (4)$$

where $\alpha = \frac{\delta\sigma_1}{\delta\sigma_3}$

Similarly,

$$G = \frac{E_1}{2}(1-\alpha).\frac{1}{\frac{E_1}{E_3}(1-2\nu_3\alpha+\nu_3)-\alpha(1-\nu_{12})} \qquad (5)$$

If the material is simplified to isotropic (E, ν), equations (4) and (5) reduce to the well known:

$$K = \frac{E}{3(1-2\nu)} \qquad G = \frac{E}{2(1+\nu)}$$

i) granular (Huang)

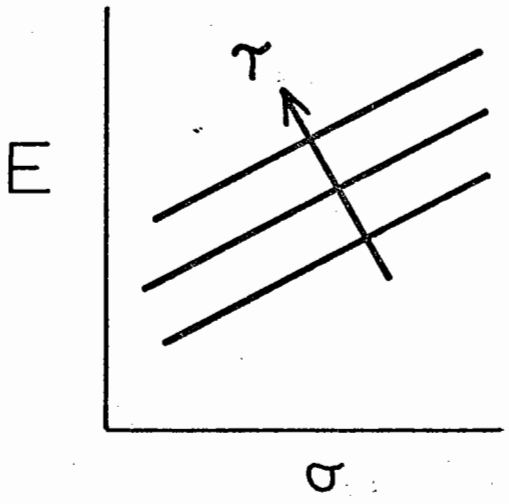

ii) clay (Brown and Pell)

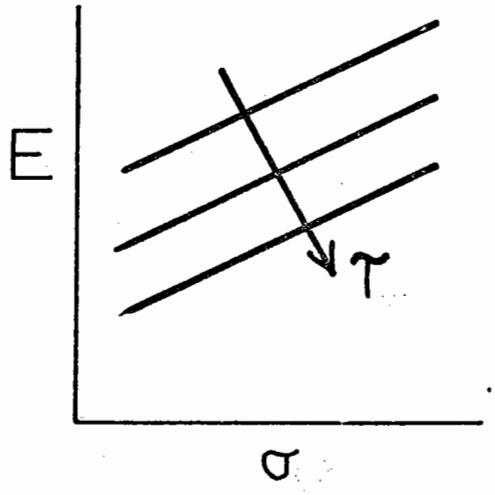

iii) clay - result from insitu measurements (Brown and Pell)

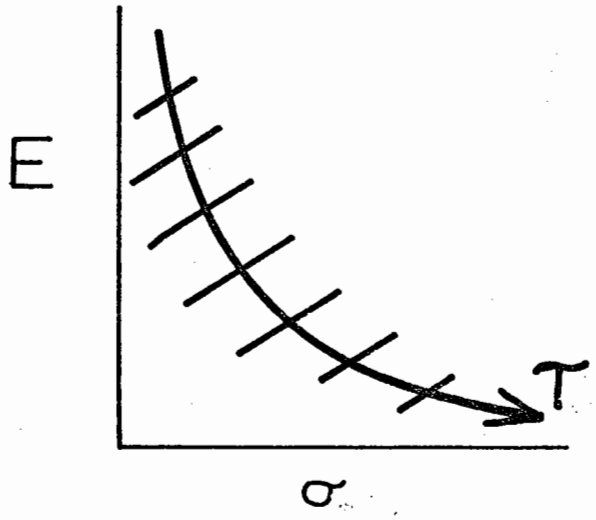

Fig. 3.1 Young's Modulus v Mean Stress and Shear Stress

i) Axial modulus with stress invariants

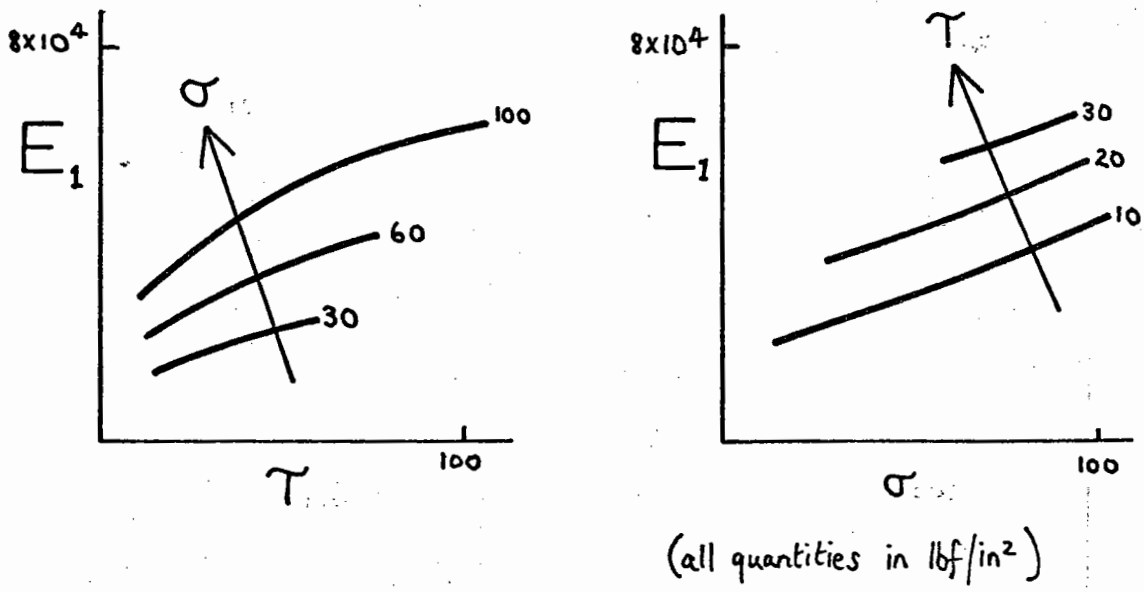

ii) In state space terms

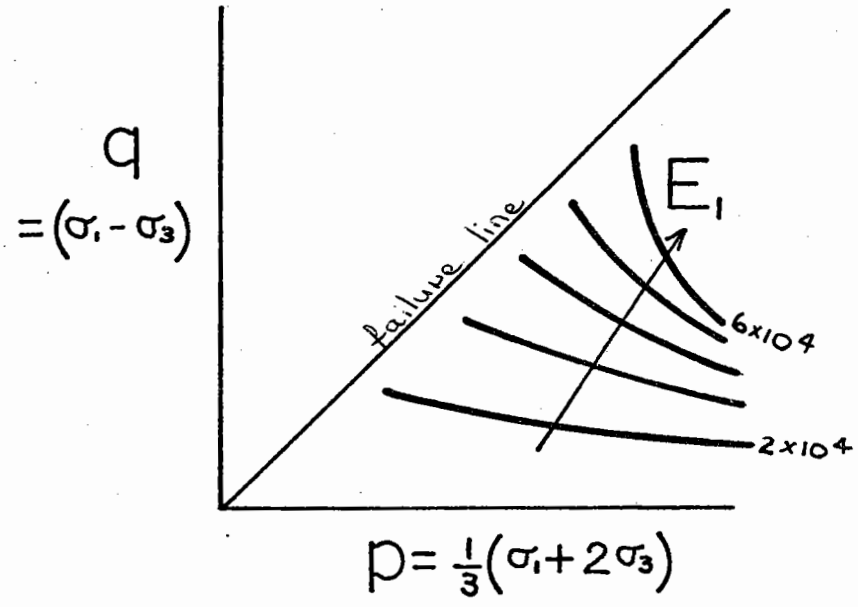

Fig. 3.2 Relation of Granular Material Characteristics to first two stress invariants (after Holubec)

i) Shear modulus (G)

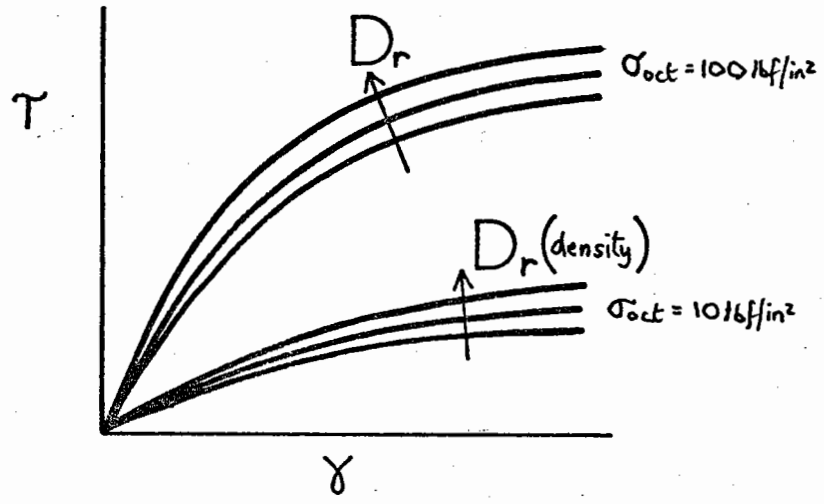

ii) Bulk modulus (K)

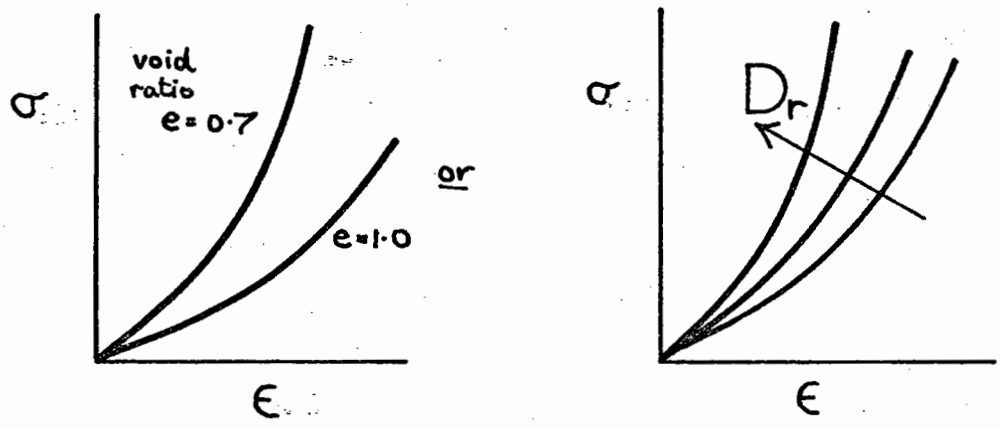

iii) Failure

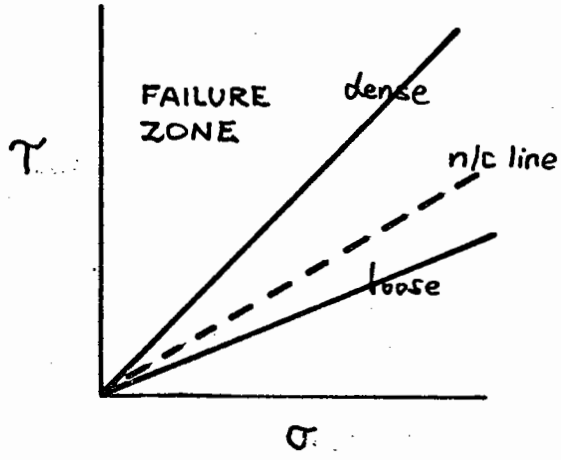

Fig. 3.3 Shear and Bulk Moduli and Failure in Granular Materials (after Domaschuk and Wade)

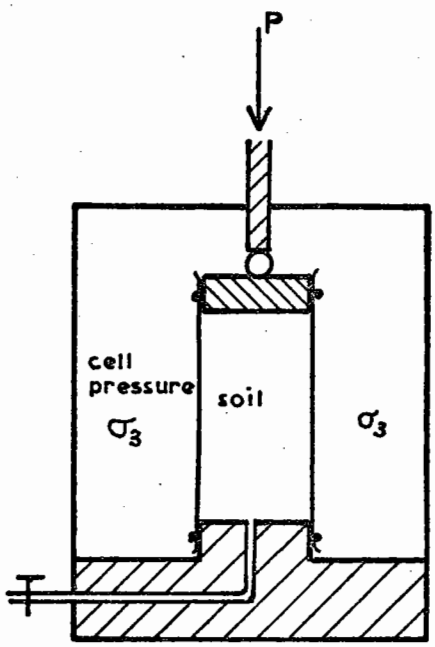

i) triaxial cell

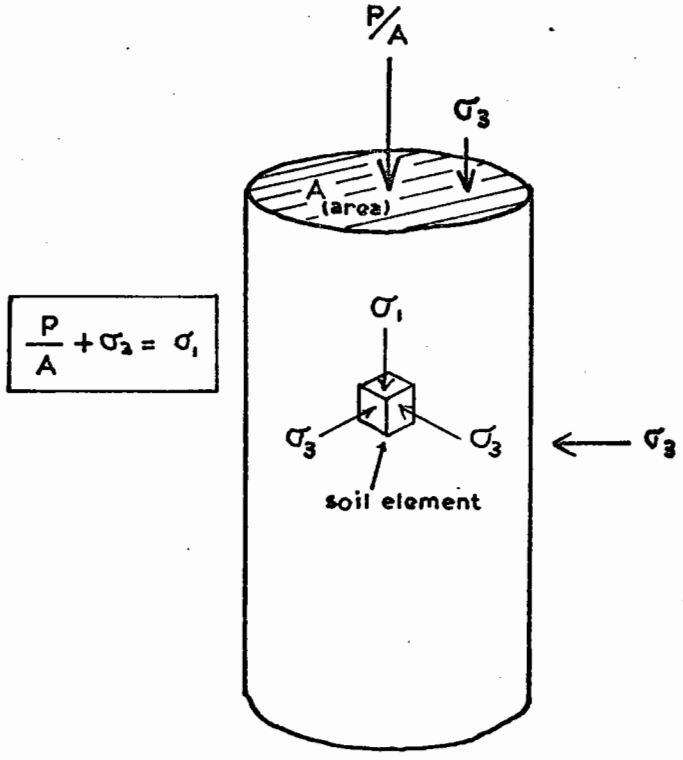

ii) soil sample

Fig. 3.4 Loading on the Triaxial Specimen

i) Bulk action $\left(K = \frac{\partial \sigma}{\partial \epsilon}\right)$

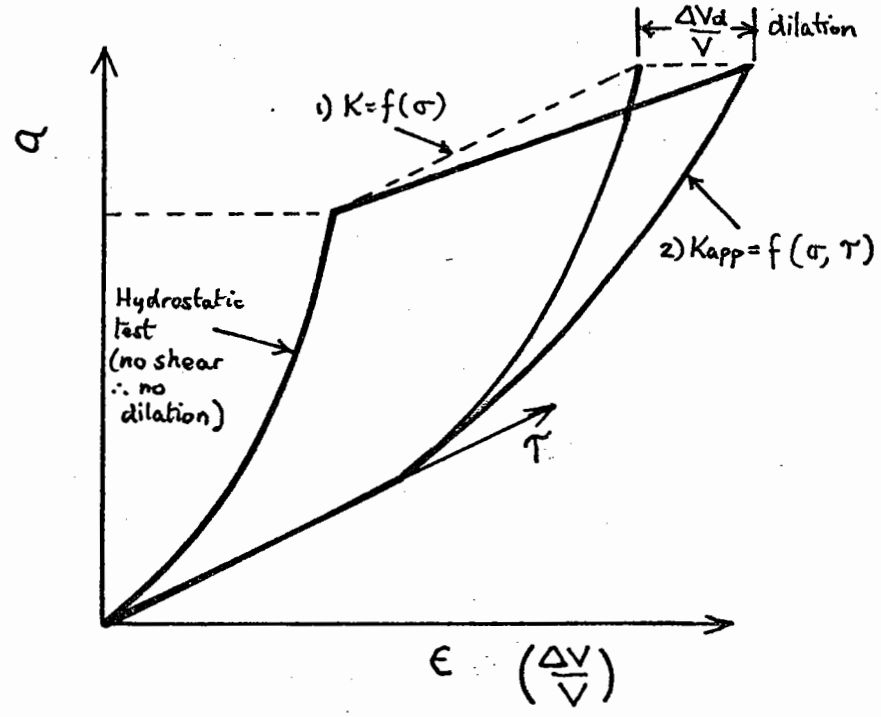

ii) Shearing action $\left(G = \frac{\partial \tau}{\partial \gamma}\right)$

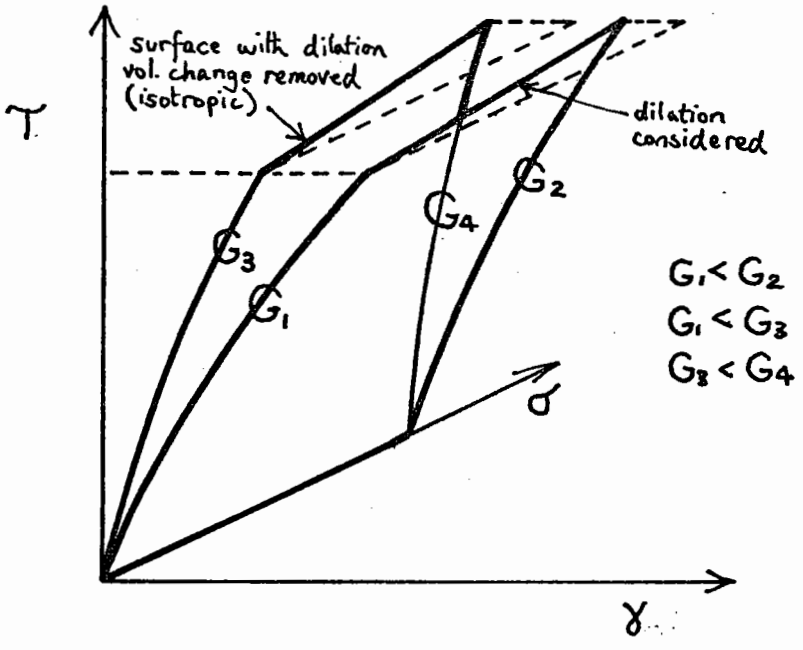

Fig. 3.5 Bulk and Shear Stress-Strain relations as Changed by Dilation (Conceptual)

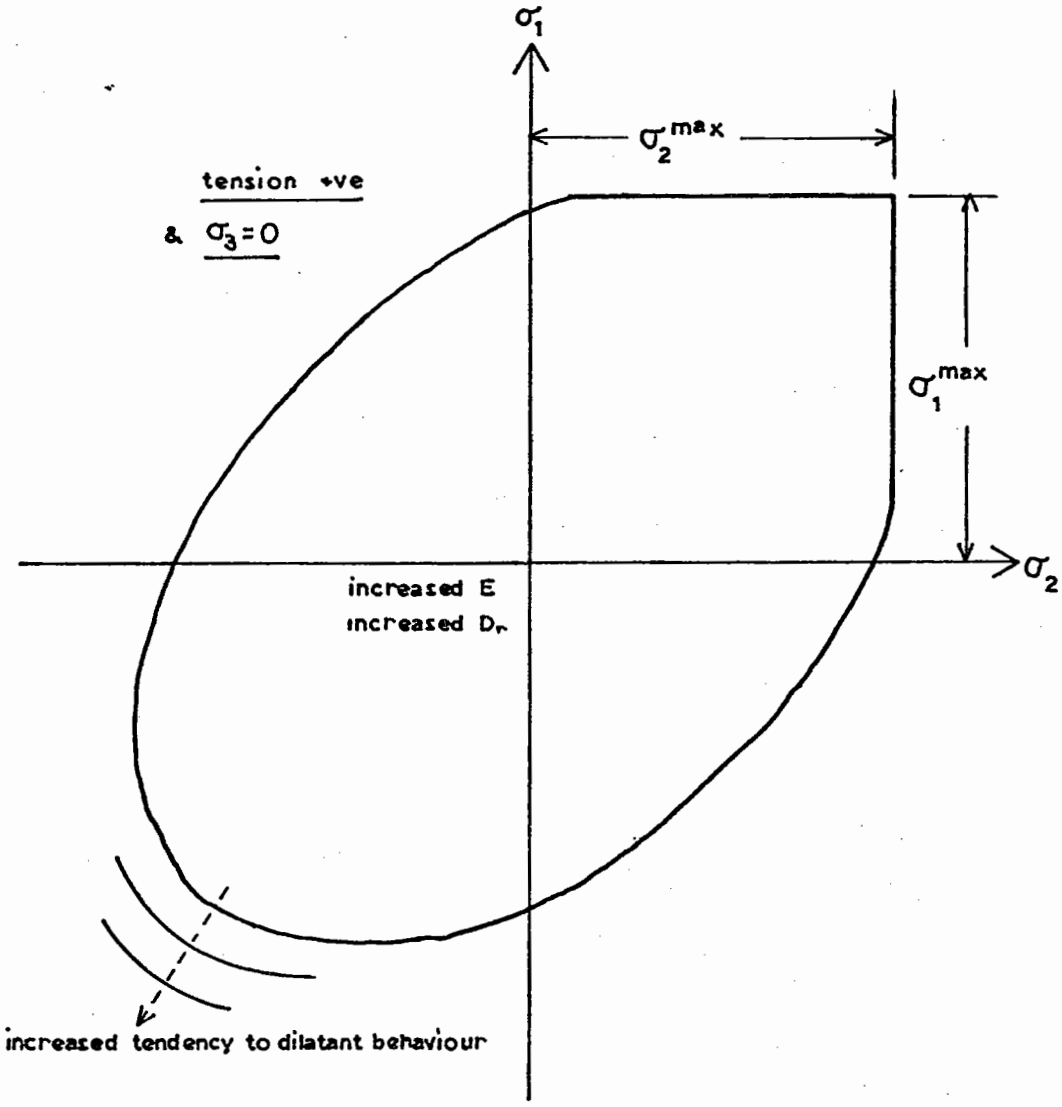

Fig. 3.6 Failure Criterion for Soil

CHAPTER 4

NON-LINEAR FINITE ELEMENTS IN LAYERED SYSTEMS

4.1 Introduction

In Chapter 3 suggestions have been made as to the additional information required on the material behaviour and the possible means of obtaining it.

Information is required for two conditions of test:

1. repetitive (cycling) loads to give dynamic resilience relevant to passing wheel loads in a road pavement,
2. an incrementally loaded test taking the path to failure of a once-loaded structure.

Under 1) information on the cumulative permanent strains is as relevant to pavement performance as the repeated stresses and strains resulting from traffic. The incremental loading test, however, gives an indication of material behaviour throughout a one-off loading up to failure. In the analysis of pavements, both are important in order to begin to understand the complex behaviour of the layered system as a whole. Each requires a different computational approach and presents different problems.

4.2 Basis of Iterative and Incremental Non-Linear Analyses

Both iterative and incremental analyses involve the solution of a series of linear boundary value problems. Iterative analysis is relevant to total stress-total strain non-linear elastic material tests, whereas an incremental analysis has the advantage of modelling intermediate behaviour and requires incremental stress-strain material tests.

Iterative analyses assume a unique state of stress-state of strain relation, or that sensible techniques lead to the correct result even where other false results could exist. They also assume that a final state of stress and strain does not depend on the "path" or history of intervening states of stress. These two inter-related assumptions are not in general true even when they related to a clearly defined unique load path.

4.2.1 Iterative Procedure

Material characteristics (moduli) are repeatedly modified in an iterative manner (Fig. 4.1) until element stress levels are compatible with the element moduli as defined by some functional relationship(s). The total load is applied at the outset and the path to a solution is purely a numerical process. Uniqueness of the solution is not guaranteed, but would seem likely to depend on the form of the functional relationships between moduli and stress level. Thus after a number of iterations, the iterative procedure may converge to a solution. Since total stresses and strain are being considered, secant moduli are used in the analysis.

Fig. 4.2(a) shows a possible functional relationship between (say) the stress and strain invariants of a material. If after the i^{th} iteration, the secant modulus of a particular element is E^{i}_{sec}, then a better approximation to the stress level is calculated to be σ^{i+1}. Reference to the stress-strain relationship for the element

(say $E = f(\sigma)$) would lead to a new modulus E_{sec}^{i+1}. Repetition of the process should lead to convergence of the iterative procedure and the production of a set of displacements, stresses and strains for the system.

4.2.2 Incremental Procedure

A predetermined number of linear analyses are carried out to enable the loading path for the material to be followed as closely as possible (Fig. 4.2(b)). At each step in the analysis the stress, strains and displacements are calculated for an increment of load. The linear analysis is based on an estimate of the modulus for the increment using the latest known material characteristics for the accumulated level of stress reached (Fig. 4.3). It is thus assumed that there is a set of moduli relevant to small stress increments which depends on the current state of stress (or strain), and not on the pattern of the increments. It follows that the modulus used for calculating stress and displacement for the next increment of load must be predicted as accurately as possible, as must the initial value chosen. To avoid taking very small increments, the chord modulus would seem to offer the ideal solution if the new expected stress level within the element could be predicted accurately. However, such an estimate can only be approximate since the increase in stress level due to an increment of load would appear difficult to predict in a markedly non-linear material. It seems reasonable to suppose that a predicted chord modulus would give better results since its attempts to keep the loading path on the stress-strain curve. This

is illustrated in Fig. 4.2. If the correct "chord" modulus for the so far accumulated level of stress (σ_i) resulted in an increment of stress ($\sigma_{i+1} - \sigma_i$) in the element, the strain increment would be predicted correctly. A tangent modulus taken at (σ_i) would result in an error of ε_{ei}.

However, in general, a predicted chord or current tangent modulus would give some error which would accumulate and the exact solution would never be reached.

The initial values chosen for the first step are clearly important; a bad choice of $E_{initial}$ (Fig. 4.2(b)) for each of an assembly of elements could lead to an immediate large error and to increased contribution to the errors at the later stages.

4.3 Earlier and Parallel Work

Iterative analysis was first employed in 1965 by Wilson[2.5] based on rectangular finite elements obtained from four triangles with the elimination of an internal node. He found that the procedure did not always converge to a steady state unless the non-linear effects were small. Later in 1967 Duncan et al[1.46] found that for a monotonic stiffening function, which had been proposed for a granular material, only "a possible convergent trend" could be identified. This appears to be contradicted by Dehlen[1.47] who, in 1969, using the same basic program and the same functional relationship, found convergence of the surface displacement after 6 iterations. Dehlen also claimed that this iterative method could be applied to markedly non-linear materials and the author's experience

supports that claim.

In published work using "Incremental" analysis, there has been little uniformity of treatment. The method necessitates knowledge of the material behaviour for small stress increments and for initial values depends on material properties at low stress levels. Where triaxial tests have been carried out at low stress levels[3.9,3.10,3.17] some confidence has been expressed in using initial values of moduli based on body force or self weight calculations. The halfspace problem was solved for overburden loadings only, and values of initial modulus assigned to elements according to these preliminary calculations of stress level. Recently (1969) a similar technique has been described for a finite difference formulation[1.44]. Other workers[3.18] have recently (1970) calculated the initial tangent moduli, based on a function of the confining stress (triaxial cell).

The above authors have used initial stress level due to overburden to choose the moduli for the first increment in stress due to the first increment in load. Where the two stress systems are very different this would clearly produce errors, and evidence is given later to demonstrate this. An alternative technique, used by Marcal and King[4.1] (1967), although for an elastic-plastic material, seems to offer most hope of producing an accurate incremental procedure but at the expense of increased computation time. At each incremental step an iterative analysis, to modify the moduli in relation to the observed stress incfement, was carried out. Such an expensive technique may be essential for problems which are highly dependent on stress path.

Akyuz and Merwin[4.2] (1968) used a similar technique on a material with an almost bilinear stress-strain relationship. The reasons it has been successful in elastic-plastic deformation would not necessarily extend to the monotonic stress-strain functions usually associated with soils.

Smith[4.3] (1970) has recently developed methods based on iteration within increments which avoids the re-formation of the structural stiffness matrix at each iteration and thus makes savings on computer time. The author's computer programs have been developed to incorporate very general non-linear, elastic functional relationships (Chapter 3) and it was possible to include incremental loading behaviour by making slight modifications (Appendix Prog. 2.2). The iterative non-linear behaviour of the 4 node axisymmetric rectangular element (Appendix Prog. 2.1) was examined in most detail since the 3 node element (Appendix, Prog. 1), although found to give satisfactory solutions, took a greater amount of computer time for the same number of iterations being a more general element.

4.4 Parameter Choice in Non-linear Elastic Analysis

Two parameters, which are usually taken in engineering literature to be E (Young's Modulus) and ν (Poisson's Ratio), are required to completely describe an isotropic elastic material. The finite element method applied to non-linear elastic problems in Chapter 5, consists of the solution of a sequence of linear analyses with the values of these parameters being repeatedly modified.

Chapter 5 describes computations with an equivalent

two parameter description. Bulk (K) and shear (G) moduli, derived from insitu measurements and both varying with stress level are used. Since the linear analyses which are being carried out at each stage retain the form of isotropic elasticity there is a direct relationship between K and G and E and ν; thus input parameters to the finite element analysis can be retained as E and ν. If more general forms of deformation laws were envisaged this would not be true.

The behaviour of the iteration to a solution in single and 2-layer systems with a variety of Young's Modulus V. stress level relationships were examined to see if the process produced a stable solution in all cases. The magnitude of the error involved in the stresses and displacements as the second parameter, Poisson's Ratio (ν), approached 0.5 was investigated. (It is at this value that the displacement method formulation breaks down due to a $(1-2\nu)$ denominator term.)

The incremental method was investigated with special reference to the importance of initial modulus values and the estimation of modulus throughout computation.

4.5 Iterative Method Computations (Single layer system)

All computations were carried out on the halfspace and loading shown in Fig. 4.4. The dimensions are conveniently those of the problem considered by Duncan et al[1.46], in order that comparison of behaviour with their differently formulated finite element would be free of other variables.

4.5.1 3-Node Triangular Element

In the halfspace shown in Fig. 4.4, the rectangles were subdivided to carry out analysis based on the triangular elements shown in Fig. 4.5(a). The program (Appendix, Program 1) was verified for the homogeneous case by comparison with the series type solution (BISTRO), known to be capable of high accuracy. The vertical displacement was found to be 92% of the solution from the n-layer elastic solution, which agreed with the simple Boussinesq theory. The contribution to vertical displacement of the material below the finite boundary of the "halfspace" (at 110 in. depth) would account for part of the discrepancy and is discussed in section 6.4.

Vertical stresses on the centreline (Fig. 4.5(b)) show a better agreement than the displacements.

Having established the order of the errors involved in this finite element approximation to the halfspace, a non-linear elastic analysis using this element was examined. A relationship of the form $E = k\sigma^n$, which represents a granular material[1.46] was used to modify stiffness according to stress level. Poisson's ratio was kept constant. It was found that even after 25 iterations the vertical surface displacement (Fig. 4.6) and vertical stress below the loaded area (Fig. 4.7) had not reached completely stable values, but after only 8 iterations the changes under successive iterations were within approximately $\pm 2\%$ for displacement and $\pm 3\%$ for stress. This would seem to be the best convergence of the iterative procedure which is possible using a 3-node element, although damping or feedback techniques described

later might offer an improvement.

The displacements were clearly about 8% low and steps to improve the accuracy did not seem worthwhile because of cost. (The full 25 iterations involved the use of 120 minutes of English Electric KDF9 time - 40 mins. for 8 iterations - which was considered excessive.)

4.5.2 4-Node Rectangular Element

The rectangular element (Appendix, Program 2.1) having sides parallel to the polar co-ordinate axes, involved relatively simple algebra and could be organised to use less computer time. With a layered road system it is not necessary to use a perfectly general element and the high cost seemed unwarranted. Again, a check with the classical series solution was undertaken. Results are given later in connection with the investigation into the effect of changing Poisson's Ratio.

The iterative behaviour of the 4-node element was in most cases stable, but for some materials produced an oscillating sequence. In most cases, damping the modulus change to half the expected value produced a stable solution (a fact also established by Dehlen[1.47] for the 3-node element).

Constituent relations for granular[1.46] and clay[1.6] materials show different trends, granular stiffening with increased mean stress level and clay materials softening. Both relations led to a satisfactory computation (Fig. 4.8) with surface vertical displacement reaching within about 1% of the final solution after 7 iterations. From published comment, it seemed prudent to minimise the risk of surge

by still further dampening the mathematical path by applying the load in 4 steps, i.e. ($\frac{1}{4}$, $\frac{1}{2}$, $\frac{3}{4}$, 1). There was thus no evidence of the erratic changes in displacement and stresses experienced with the 3-node element, and displacements for full load were found not to depend on the number of load increments. This may be because the stress distribution using an arbitrary initial modulus does not differ much from that after iteration using a modulus which was by then influenced by the modified moduli based on stress level (Fig. 4.9).

The behaviour of a large variety of hypothetical relationships (Fig. 4.10) between E (Young's Modulus) and σ (mean normal stress), together with the two known experimental curves, were examined to investigate the behaviour of the iterative procedure. The surface vertical displacement appeared to be a suitable guide to the convergence of the iterative procedure in a single layer system and this quantity is plotted against number of iterations in Fig. 4.11.

"Clay-like" relationships (softening) approached a solution from below (+ve change in displacement) regardless of the starting value of modulus and the converse was found for "granular" relationships. When plotted on a log basis, the percentage change in surface displacement with iteration was found to follow a straight line. In one case, where a strongly stress dependent modulus coincided with a region of high stress gradients, a minor oscillatory behaviour developed. All curves had roughly the same slope and changes became small after relatively the same number of iterations for all relationships (to

within 1% of final value at between 8-12 iterations).

From the straight line relationships predictor-corrector methods could lead to accelerated convergence. In modelling softening and stiffening materials, the behaviour is not so simple, and there seems to be no practical value in developing procedures applicable only to a single layer solution.

Smith[4.4] has recently reported work in progress to accelerate incremental finite element analyses on a single layer system.

4.6 Poisson's Ratio (ν)

Two parameters are required to describe the elastic behaviour of isotropic materials. A bulk modulus-shear modulus characterisation for in-situ test results will be shown in Chapter 5, but for purposes of computation this is identical to an E, ν material description.

An almost incompressible deformation can be defined through the Poisson's Ratio tending to 0.5. The state of stress can no longer be inferred from the displacement field if an all round compression produces zero strains, and this is physically reflected in the infinite value of the factor $\frac{1}{(1-2\nu)}$. Deformations of this type are certainly encountered in soil systems and investigation of the behaviour of finite element solutions as ν approaches 0.5 is warranted.

The mesh in Fig. 4.4 was used to examine the effect of changing Poisson's Ratio on displacements and stresses. Fig. 4.12 compares vertical displacement by different methods for varying ν. The consistent underestimate at low values

of ν is largely due to the missing contribution from material below the finite element boundary. The Boussinesq solution is exactly correct for the infinite halfspace. The 3-node element results were 2.1% lower than the 4-node at $\nu = 0.4$, and there is some measure of the errors from the element formulation.

Vertical displacements on and off-axis (Figs. 4.13, 4.14) show the same trend; a fairly constant error for low values with an added divergence as ν approaches 0.5. Very close to 0.5 the results are completely unreliable. Radial displacements (off-axis Fig. 4.14) are in good agreement with "n-layer" values except where $\nu > 0.45$ showing that the mesh boundary distance has little effect on the radial displacements, whereas vertical displacements are seriously affected.

Radial (Fig. 4.15) and vertical (Fig. 4.16) stresses at selected elements in the mesh in Fig. 4.4 are in close agreement with values from n-layer theory except for the large errors with ν near to 0.5. These begin to appear at $\nu > 0.4$; that is at a lower value of ν than had been found for the displacements. The errors in vertical stresses are not of constant sign, suggesting that boundary distance was not the major cause. The manner in which the error increases in a finite element solution (cf n-layer theory) is shown in the table:

ν	0.2	0.4	0.47
σ_r	0	+3	+35
σ_z	+3	+5	+13

Table 4.1 Percentage increase in FEM stresses over N-layer theory at centroid of element 23 (Fig. 4.4)

The n-layer solution, by computing more terms, seems well able to handle values of ν as shown by comparison with the exact Boussinesq solution for the halfspace (n = 1).

It is thus shown that the finite element method can yield quite inaccurate results where Poisson's ratio is near 0.5 and that values above 0.4 yield suspect solutions. It would seem likely that algebraic difficulties lead to round off errors in the matrix operations and contribute to the discrepancies. Double length or extended length arithmetic would probably improve the accuracy but at the cost of core store, and hence of size of problem handled.

The iterative behaviour of two completely dissimilar systems was considered by the mesh in Fig. 4.4:

i) where a 12 in. layer of granular material ($E = 70000^{0.55}$) overlaid a clay-like material.

ii) where a 12 in. layer of clay material ($E = 28000\ [3\sigma]^{-0.61}$) overlaid the granular material.

In case i) both surface and interface vertical displacements converged to a solution (Fig. 4.17). In case ii) where a clay-material was nearer the loaded

area, and thus had predicted a low modulus under the load, minor instability of the kind already experienced with this material in a single layer was again found to occur (Fig. 4.18).

This is consistent with the physically intuitive concept of the finite element iterative behaviour, namely that the softer material would appear more highly influenced by iterative steps which would be less stable. However, at stress levels of less than 1 lbf/in^2 the clay relationship is markedly more sensitive to stress changes than the chosen granular relationship and one would expect case i) to provide the more unstable situation. It would appear that instability does occur where this clay material spans the whole range from high stress level and low modulus to low stress level and rapidly changing, high modulus.

The danger of extrapolation of these functional relationships to stress levels over which they do not apply had thus been emphasised.

Brown[1.6] measured very few stresses below 0.5 p.s.i. and none above 10 p.s.i. in his in-situ tests. In this analysis, the absence of some cut-off stress level, beyond which the relationship should not apply, has severely tested the iterative behaviour of the finite element method but the results may have little relevance to a physical layered system. Even though an extreme range of modulus changes was allowed, the surface and interface displacements Fig. 4.18) in the unstable case still converged to a maximum change of 5% at the interface and 2½% at the

surface. This emphasises that in a layered system each interfacial vertical displacement should be monitored during the iterative computation since there is no assurance that variations in surface displacement will be the most critical.

The problem of limiting the range of stresses the relationships apply to and the importance of non-linearity as compared with an elastic solution will be examined in Chapter 5 where a practical 3-layer system[1.9] is considered.

4.7 Incremental Computations

A comparison of iterative and incremental methods was made to establish the amount of extra computation which would be required for incremental analysis and likely order of error in displacements and stresses. Computations were carried out using the finite element mesh in Fig. 4.4 and modifications made to the program to sum the stress and displacement increments (Appendix, Program 2.2).

The monotonic modulus v stress level relationship for a granular material after Duncan et al[1.46] was used to describe the material. This meant that:

$$E_{tan} = K\sigma^{n}.$$

$$E_{secant} = K(1 - n)\sigma^{n}.$$

$$E_{chord} = K(1 - n)\frac{(\sigma_{i+1} - \sigma_i)}{(\sigma_{i+1}^{(1-n)} - \sigma_i^{(1-n)})}.$$

(where σ_{i+1} is unknown and must be estimated).
All the above relationships are describing identically the same curve. Hence if accurate estimates of E_{tan} or

E_{chord} (initial and subsequent values) were made in an incremental analysis, some degree of agreement with an iterative calculation based on E_{secant} should be achieved.

Surface displacements directly under the loaded area are plotted in Fig. 4.19 and 4.20 with iteration or increment (depending on method).

It is demonstrated in Fig. 4.19 that there is a negligible difference in the incremental solution whether a tangent modulus or estimated chord modulus is chosen to represent behaviour. Although the difference is slightly greater in the case where only 5 increments were applied to achieve full load, it would seem acceptably small.

Two different initial (estimated chord) moduli were chosen to investigate how seriously this variation affected the solution. It was found that neither of the chosen initial E values produces a solution near to the "exact" iterative analysis (using $E_{sec} = 3150\ \sigma^{0.55}$). It may be noted that doubling the initial modulus value assigned to all elements changed the final displacement value by as much as 10%.

The accuracy in the initial modulus chosen is thus seen to be important.

Iterative analysis using a tangent modulus relationship yielded entirely incorrect displacements (Fig. 4.20), for a correct solution total stress-strain behaviour (i.e. secant values) must be used.

The suggestion that the moduli be calculated from gravity stress levels[1.47] was tested. Gravity stresses were calculated for a material of density 120 lb/cu.ft.

having linear elastic properties ($E = 1 \times 10^4$ lbf/in^2) and these were used to estimate the initial material properties. The poor agreement in Fig. 4.20 is not surprising - gravity stresses bear no relation to those due to the loading to be imposed on the structure. Indeed, the initial moduli predicted, using a stress stiffening material, are lower at the surface and higher at greater depth where gravity stresses are higher, but this is opposite to the situation in the fully analysed structure. It can be seen that initial moduli based on gravity stresses do not offer a good starting solution since the stress levels for each of the two systems are completely dissimilar and each covers a large range in magnitude.

The method which achieved a sound solution in 10 increments used secant (alternatively named "initial chord") modulus and 5 iterations within the first increment to improve the choice of the initial material chord properties. In subsequent increments the tangent modulus at each accumulated level of stress was used to estimate stresses for next increment of load. It was not found necessary to perform iterations within increments after the first time, and a satisfactory agreement with a full iterative analysis was found (Fig. 4.20) between a 10 increment loading and a full iterative analysis.

Although the incremental analysis above required 5 iterative steps within the first increment, as well as the 10 incremental steps, it correctly identified the stiffening material behaviour with increased stress level.

In this work a simple non-linear relationship between stress and strain was assumed to be valid over the full range of stresses experienced in the halfspace.

4.8 Conclusions

The behaviour of the finite element method in both kinds of non-linear analysis has been examined. It has been established that most monotonic stress-modulus relationships lead to a sound solution in iterative analysis, with relatively minor continuing oscillations existing in computations using strongly stress dependent relationships. In a layered system the convergence of the iterative procedure to a steady state can be inferred only from observance of the vertical displacements at all layer interfaces. The iterative procedures are unaffected by the initial choice of a constant modulus since in a linear elastic halfspace problem the stress distribution which governs the first modification to the element moduli is independent of modulus.

For an incremental analysis to be successful it is essential that a preliminary iterative analysis be carried out to establish starting values of moduli which are relevant to the total loading to be imposed. The incremental procedure can proceed without iteration for all increments except the first. Incremental analyses on this basis require more computer time (about 1.5 times that of a similar iterative computation) but are capable of giving the step by step loading behaviour of a non-linear structure as extra information.

The use of a single functional relationship for the

moduli poses problems which are discussed in Chapter 5, together with an assessment of the importance of non-linear behaviour.

Fig. 4.1 Iterative non-linear elastic analysis
(Modification to Fig. 2.1)

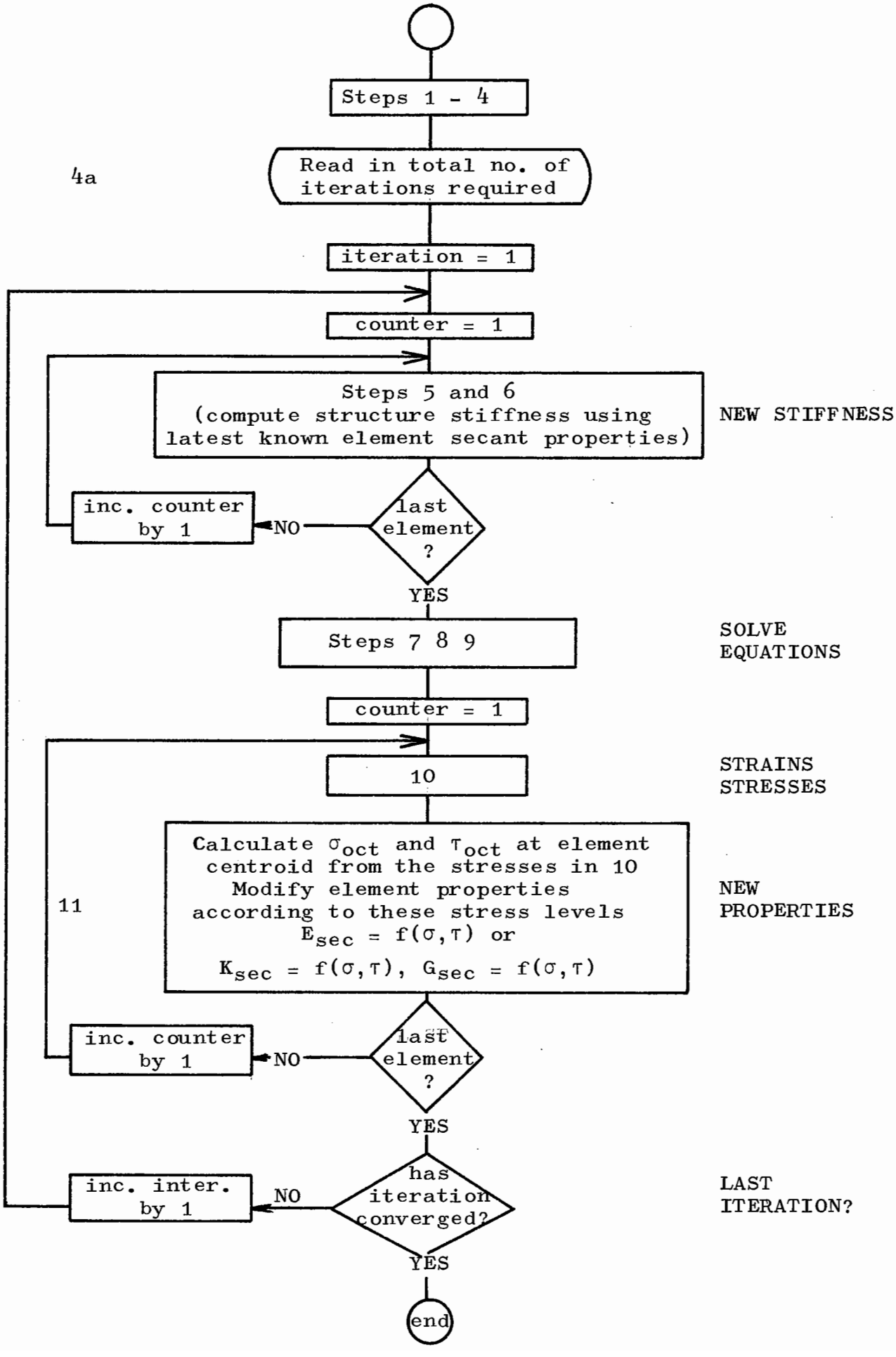

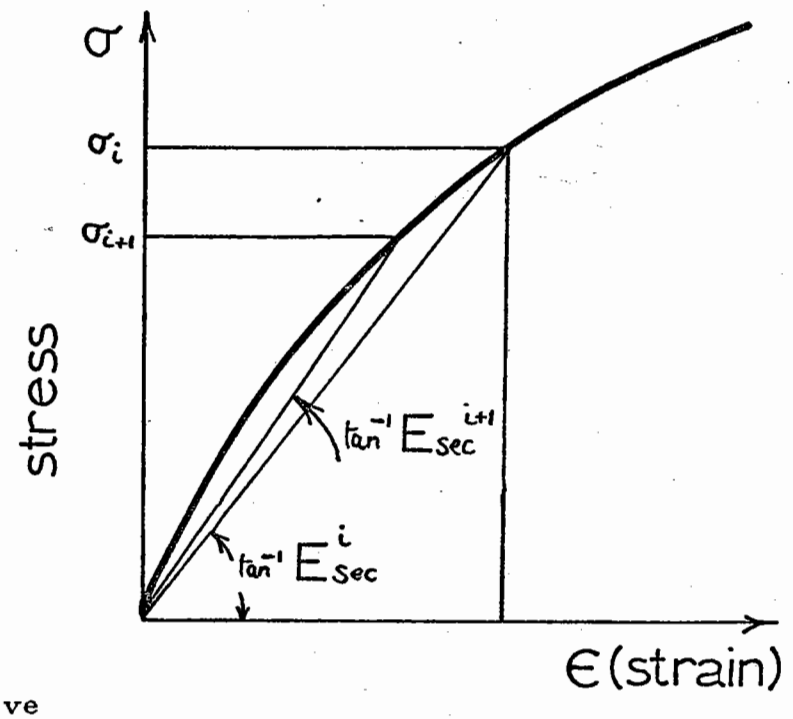

a) Iterative

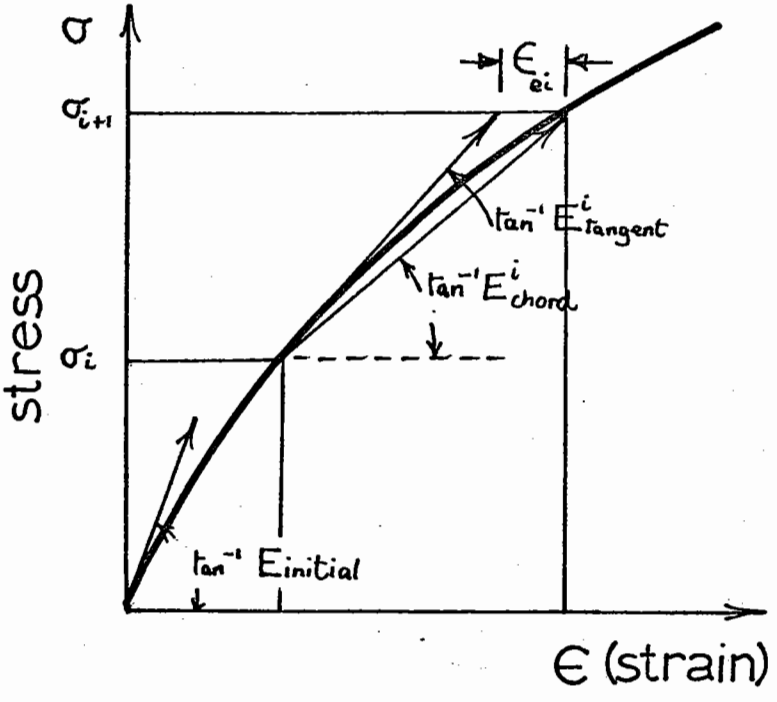

b) Incremental

Fig. 4.2 Iterative and incremental analysis

Fig. 4.3 Incremental non-linear elastic analysis
(Modification to Fig. 2.1)

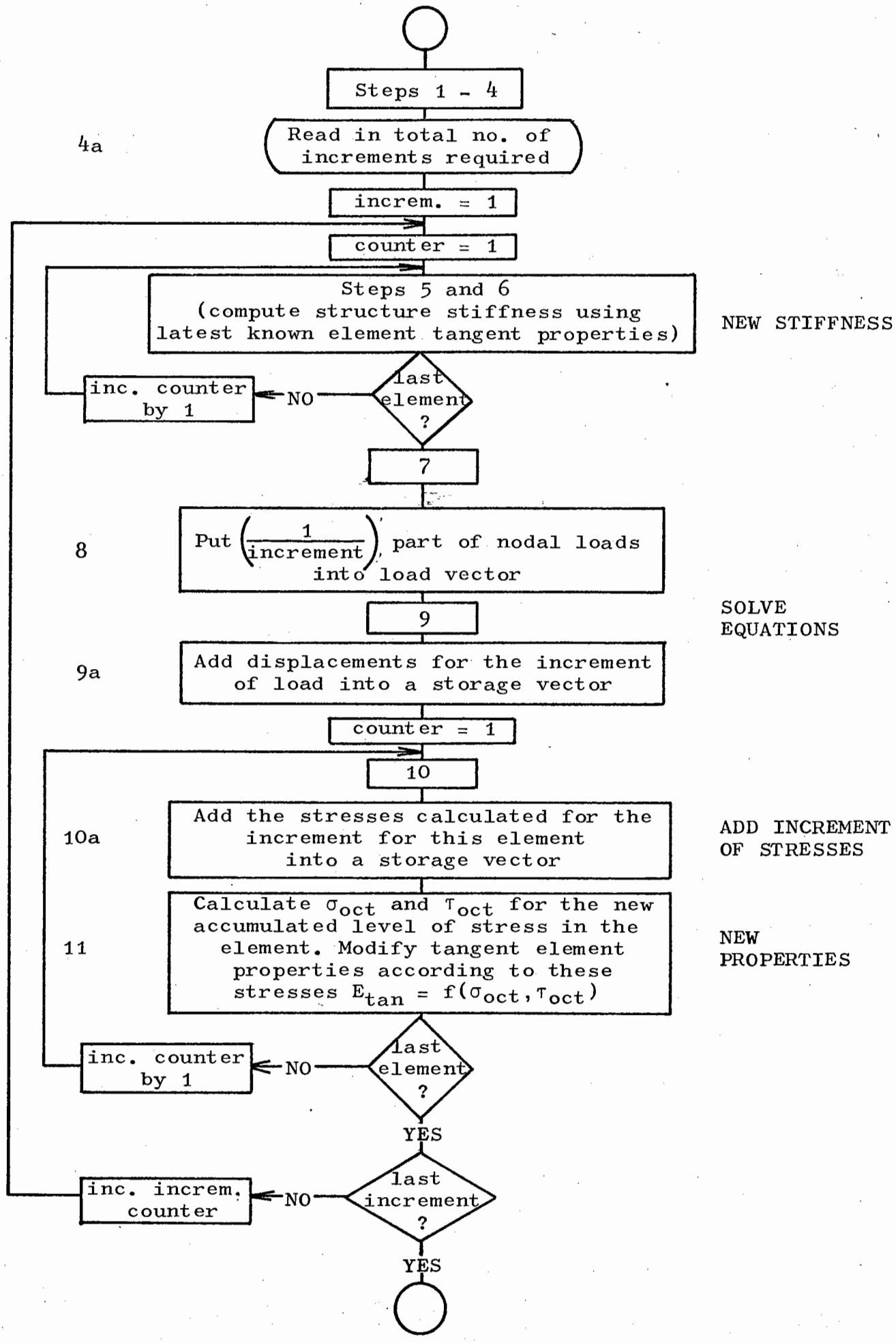

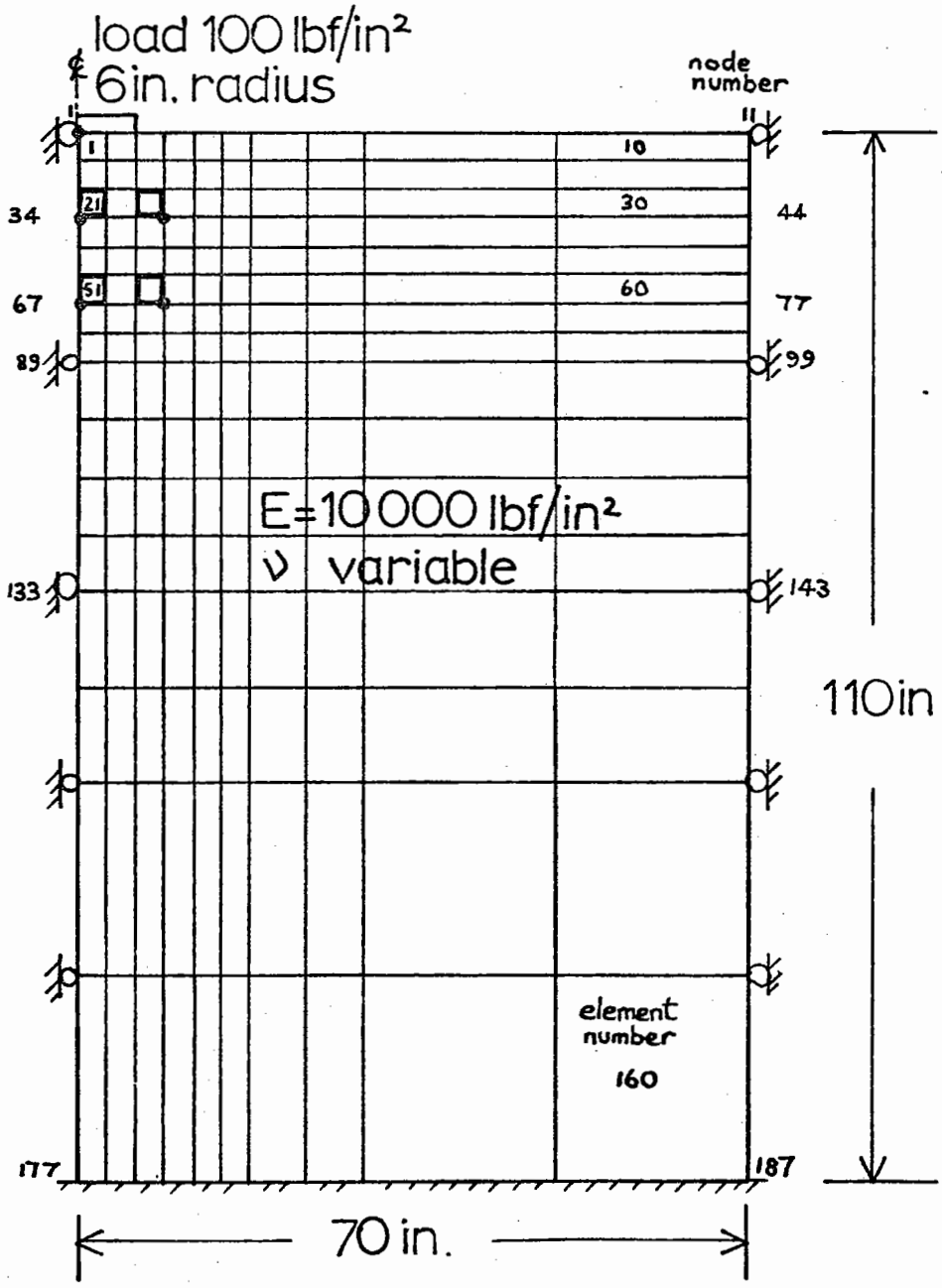

Fig. 4.4 Axisymmetric Finite Element Representation; loading and boundary conditions

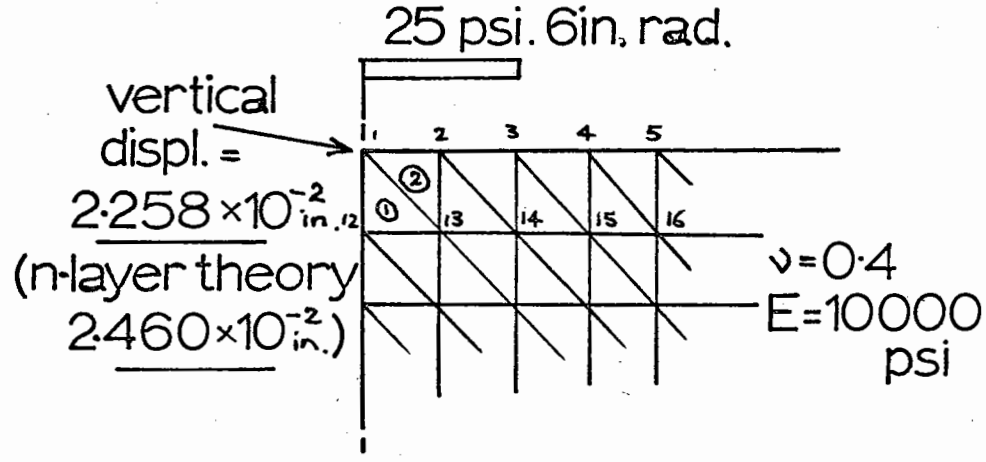

Fig. 4.5 a) 3-node triangular mesh, properties and loading

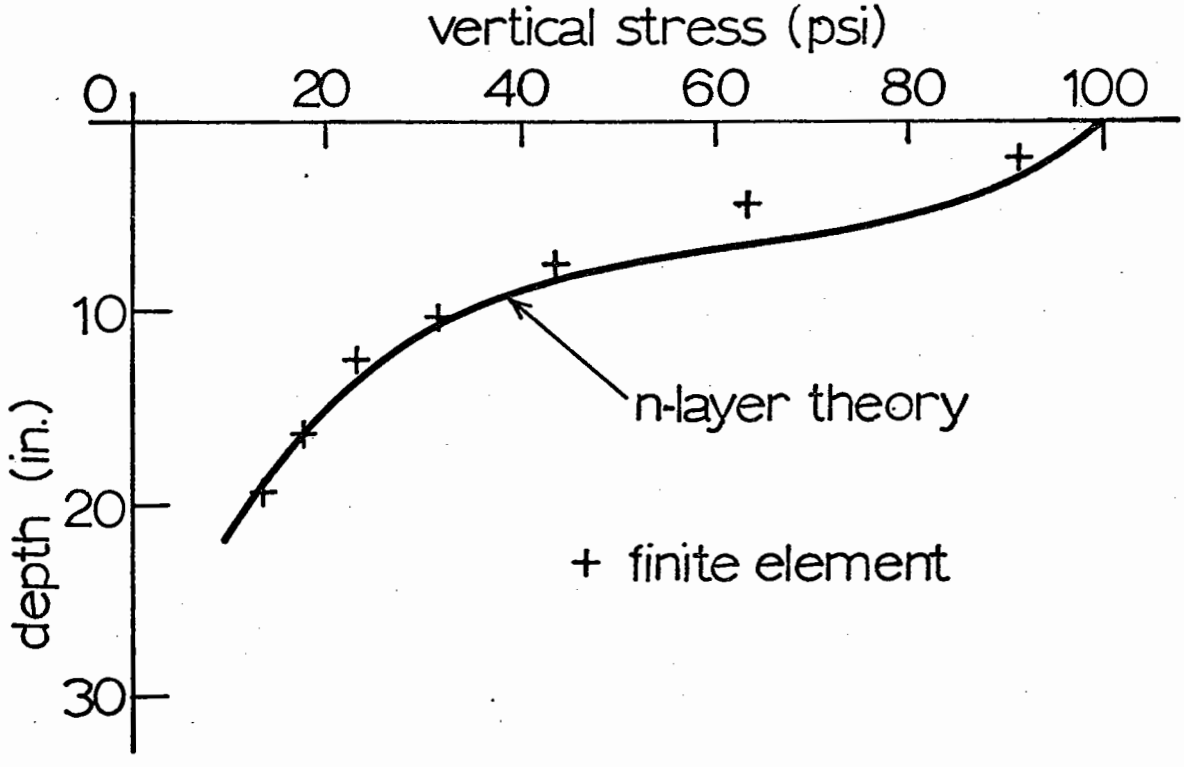

Fig. 4.5 b) Vertical stress close to centreline, under load

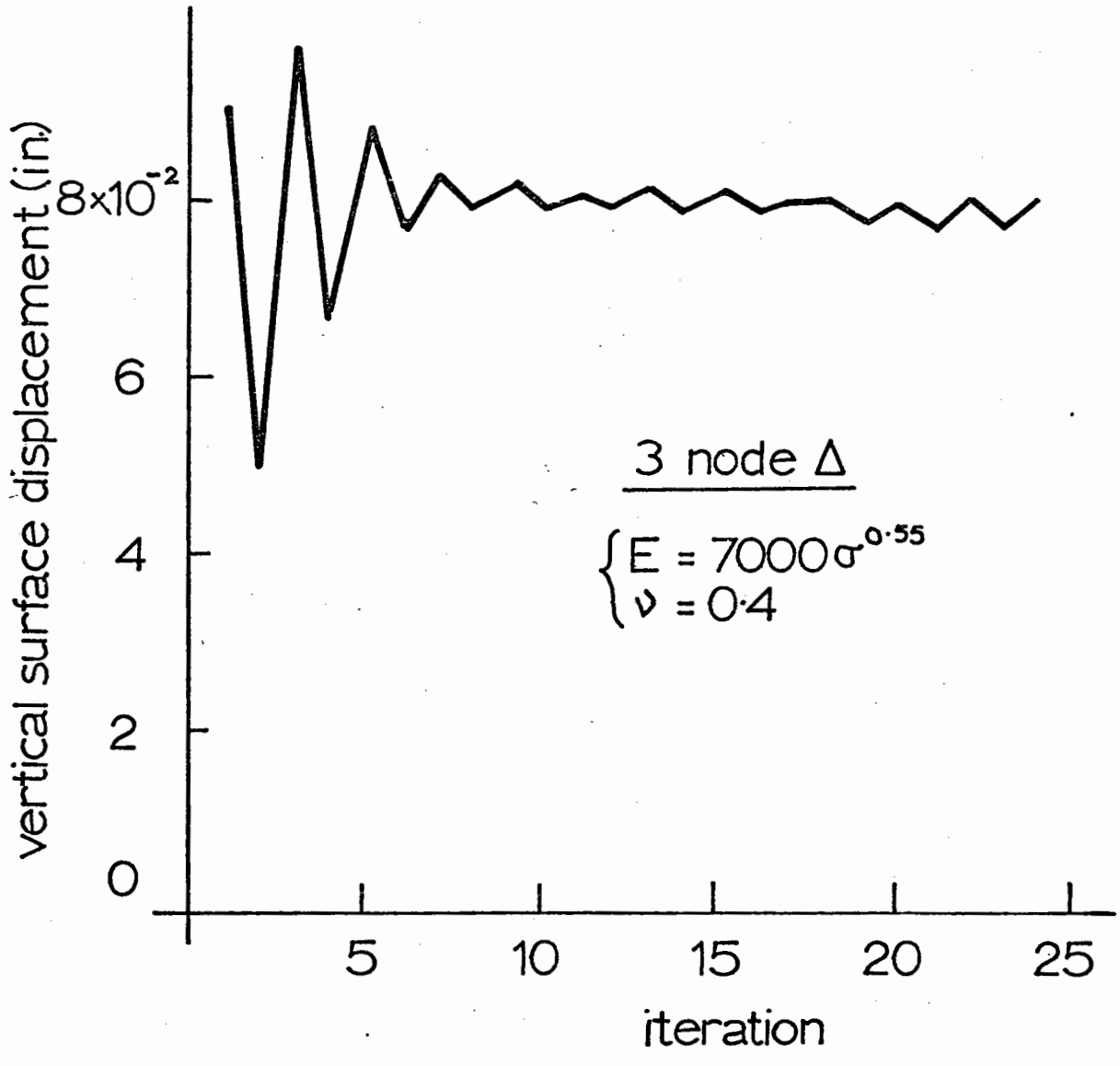

Fig. 4.6 Vertical surface displacement with iteration number

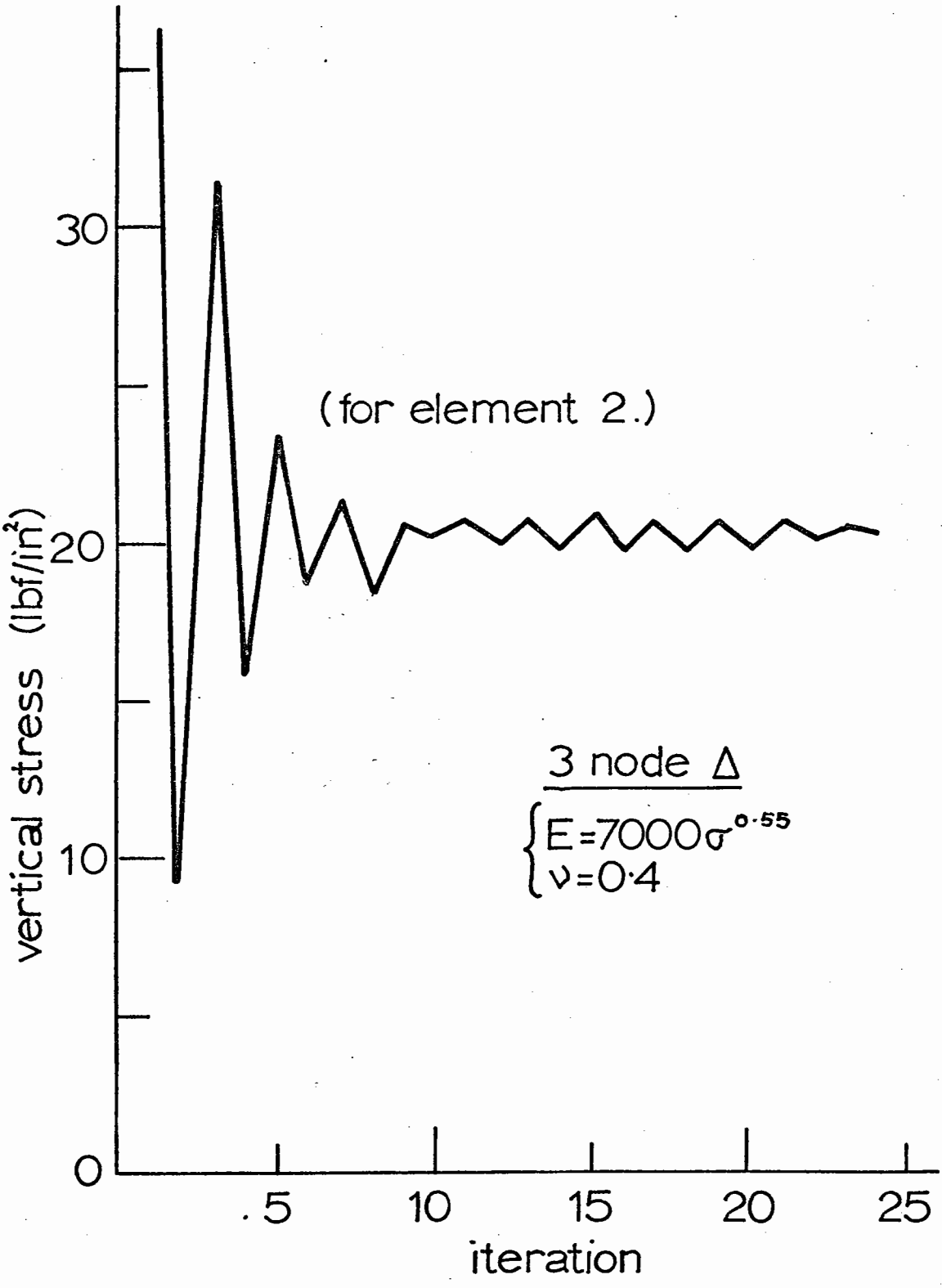

FIG. 4.7 Vertical stress beneath loaded area with iteration

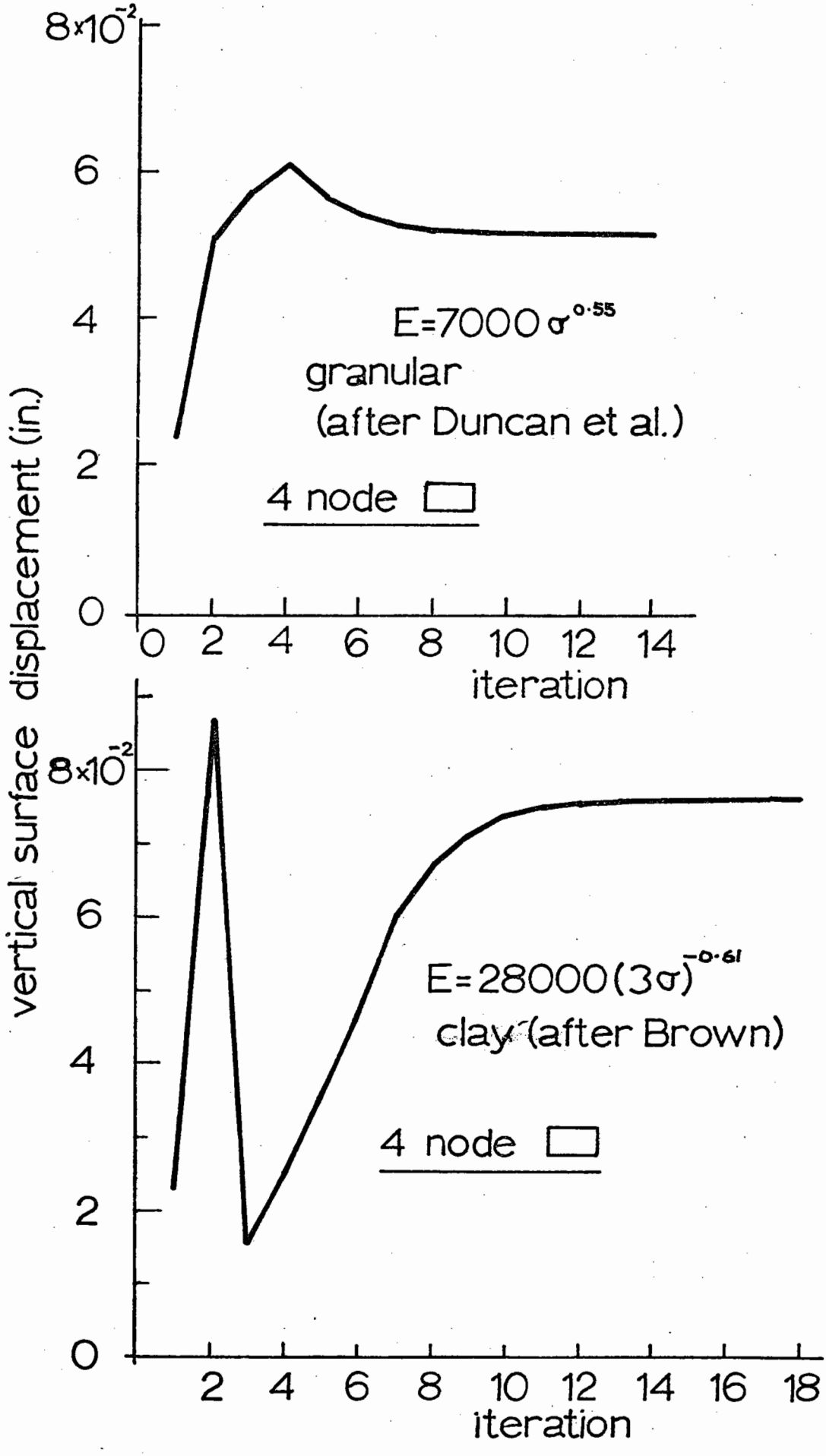

Fig. 4.8 Surface displacement with iteration (granular and clay)

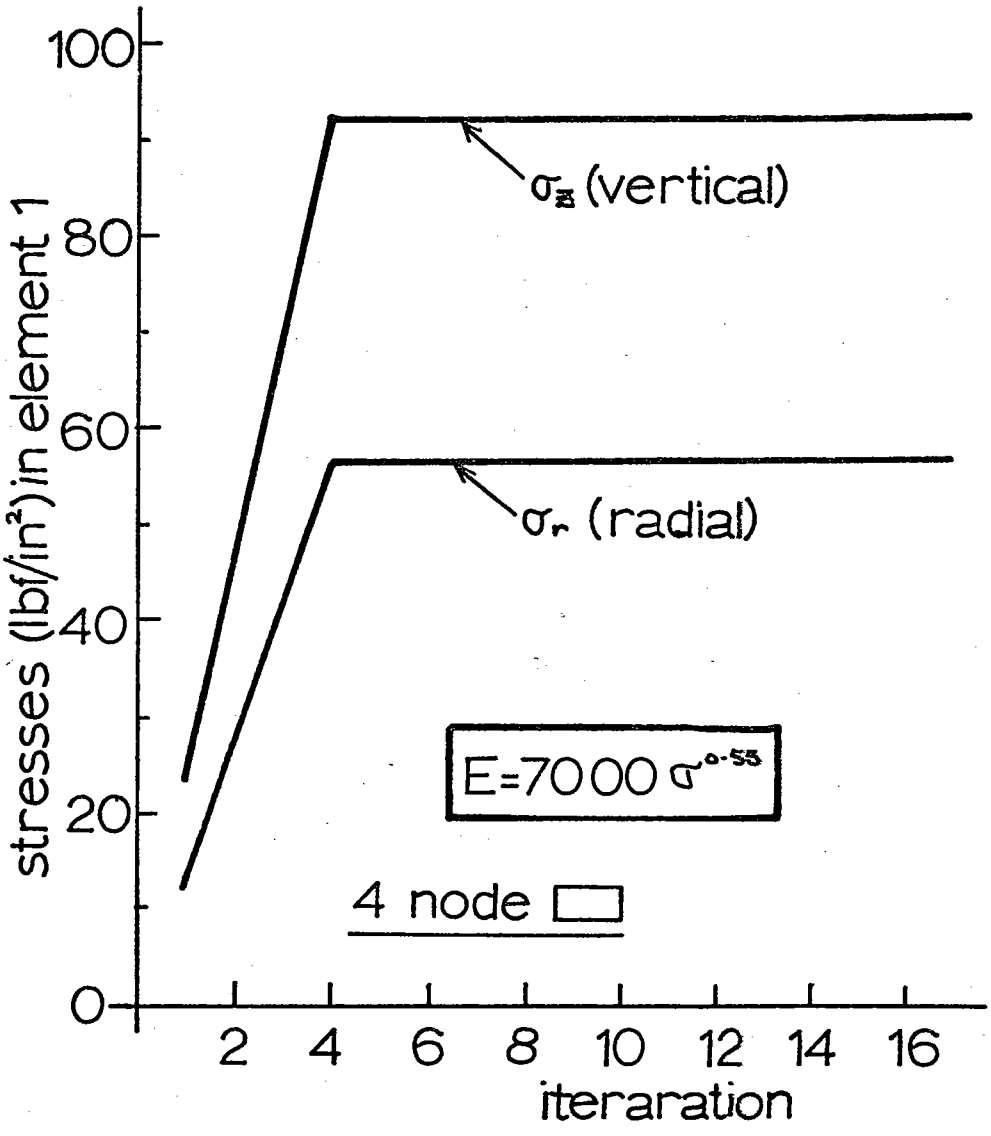

Fig. 4.9 Radial and vertical stresses under loaded area showing negligible change after full load applied

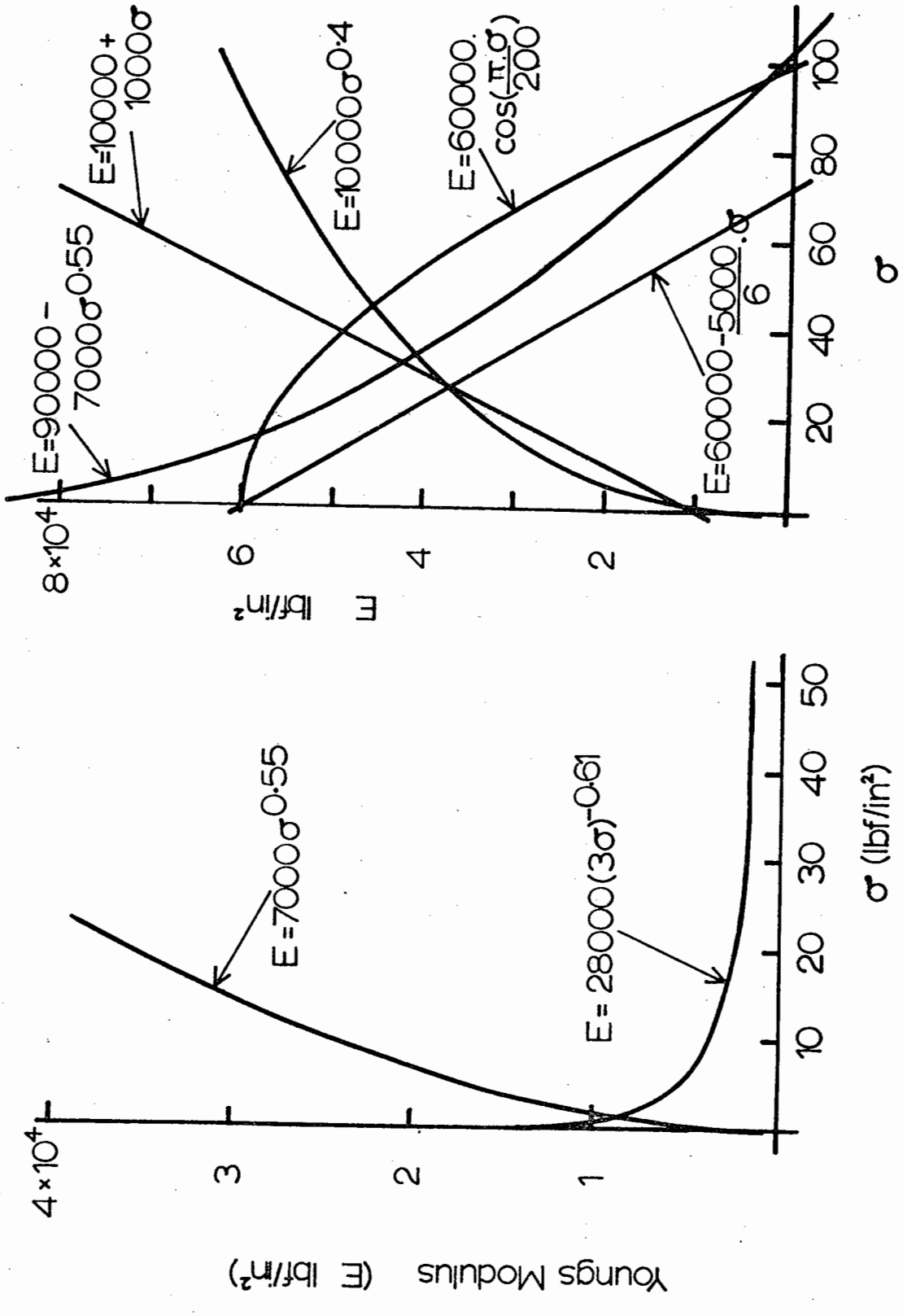

Fig. 4.10 Young's modulus v mean stress relationships

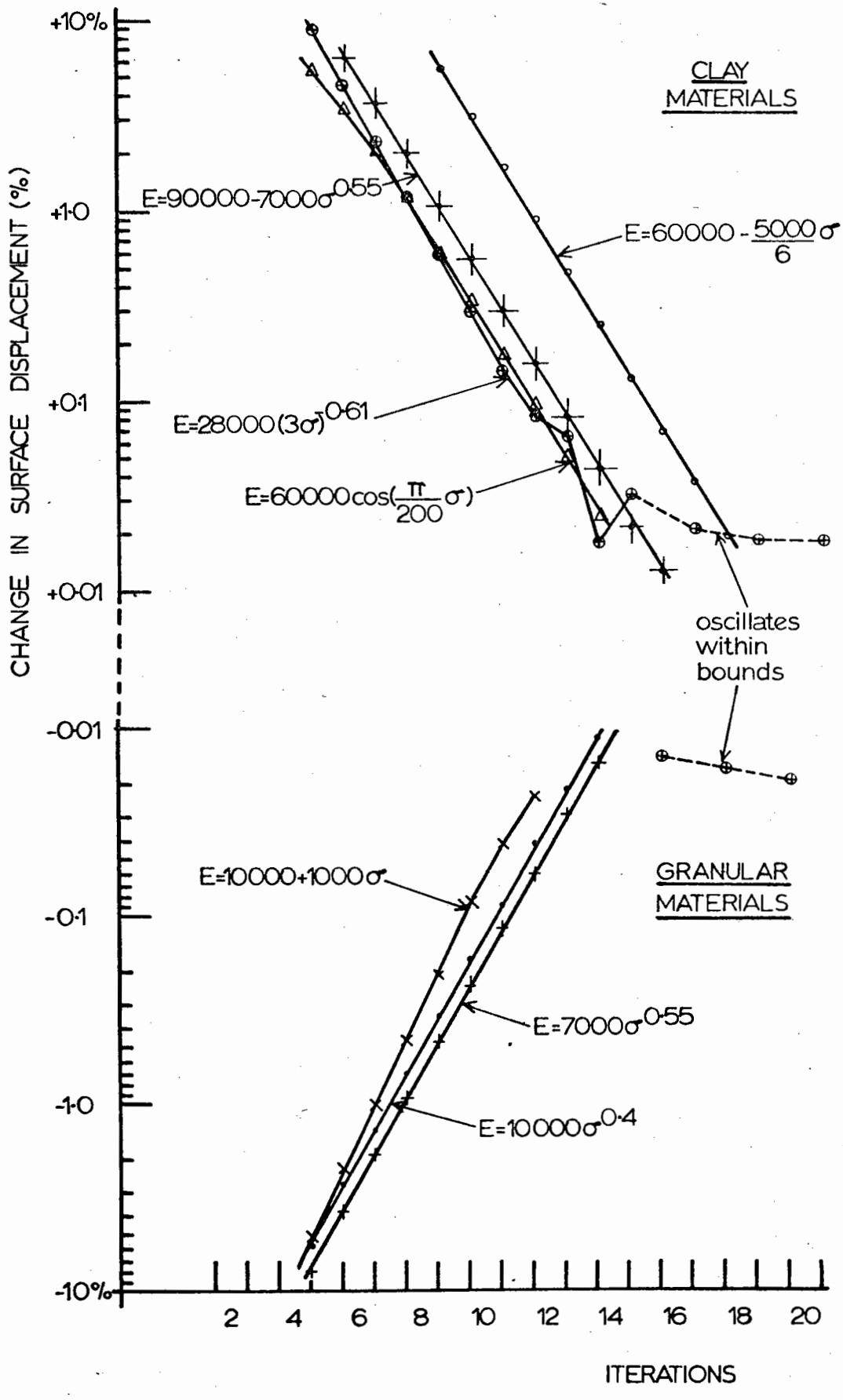

Fig. 4.11 Convergence of iteration, E = f(σ) relationships

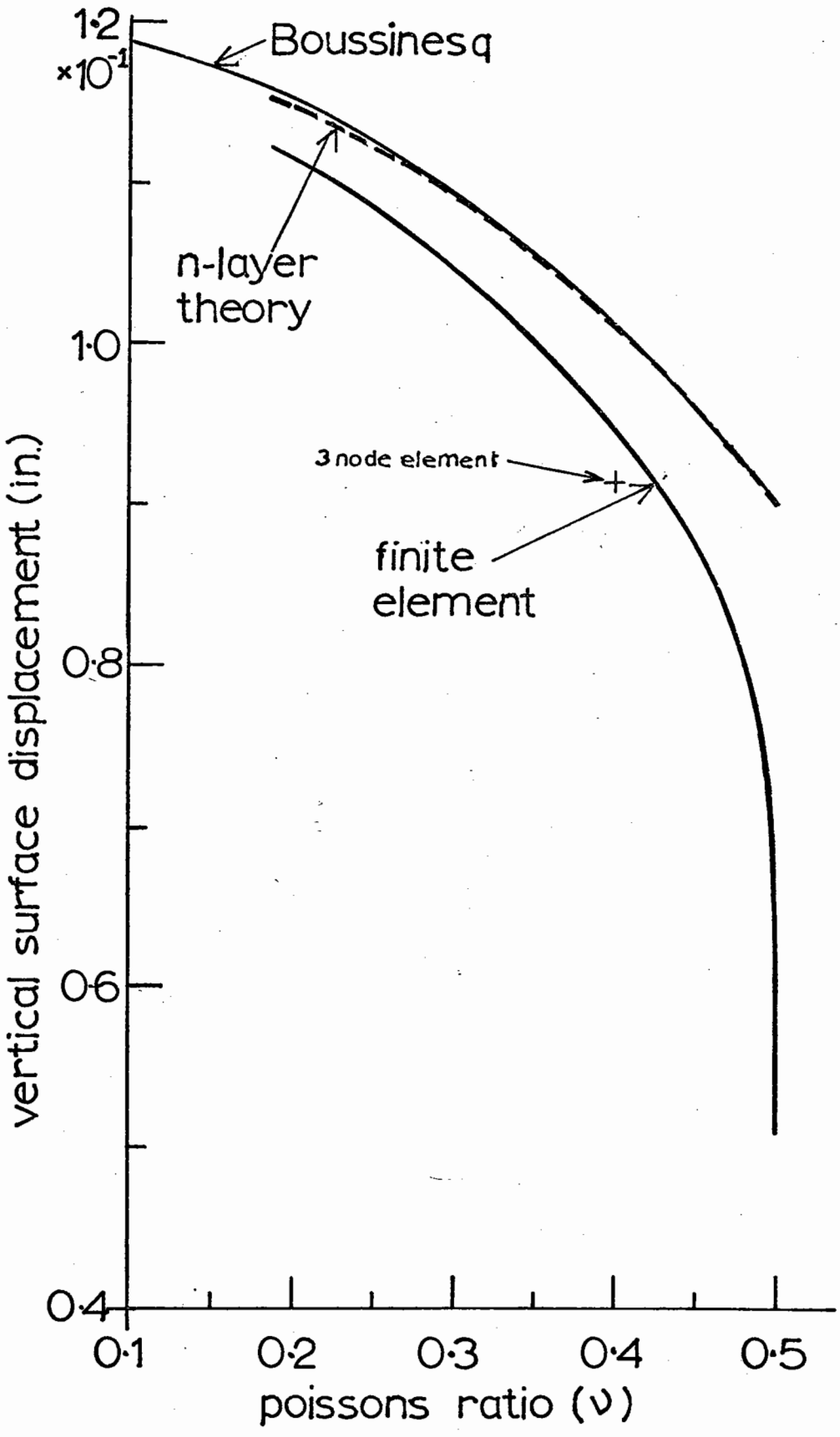

Fig. 4.12 Vertical surface displacement with Poisson's Ratio (4-node element)

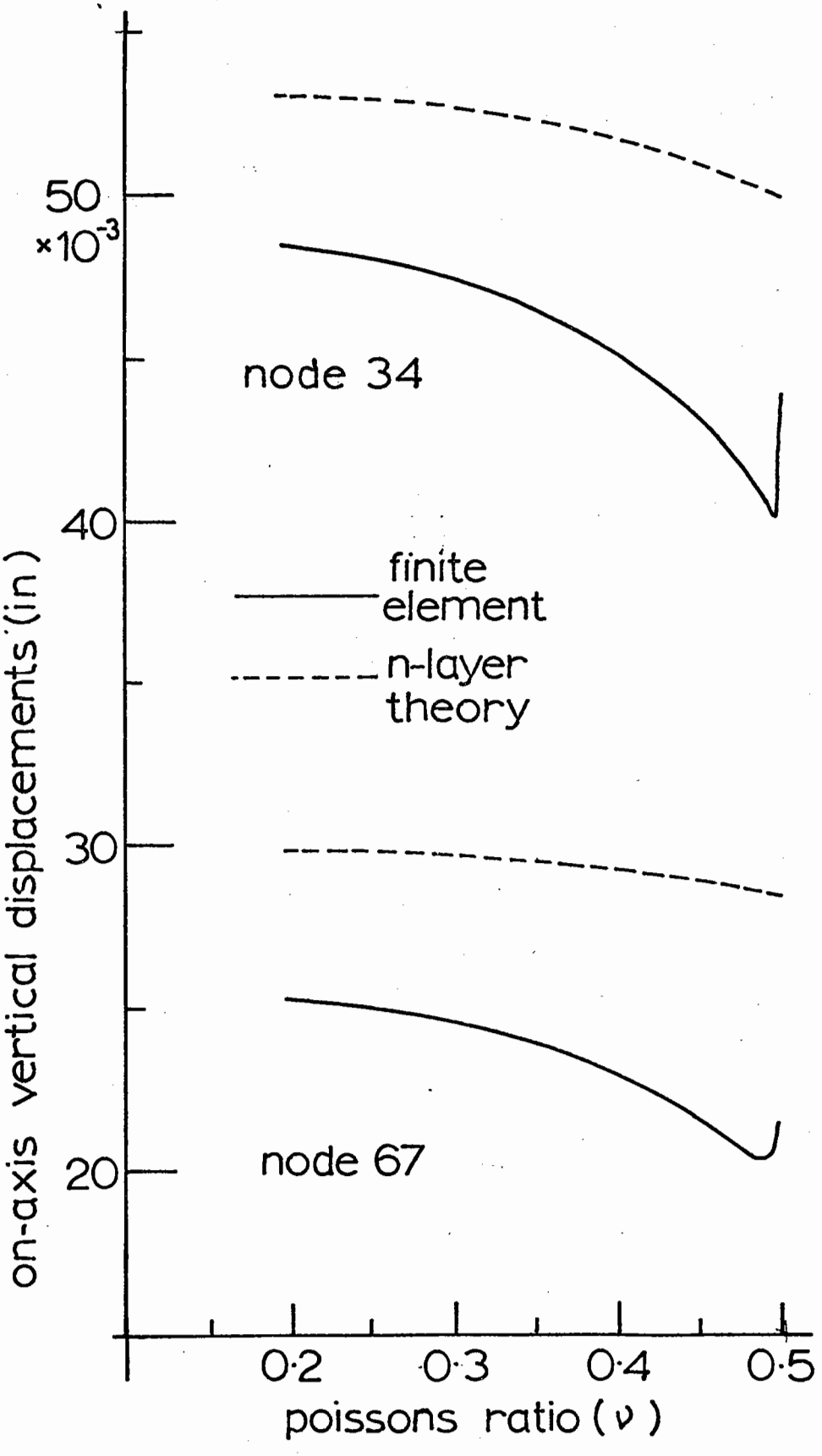

Fig. 4.13 Vertical displacement on axis

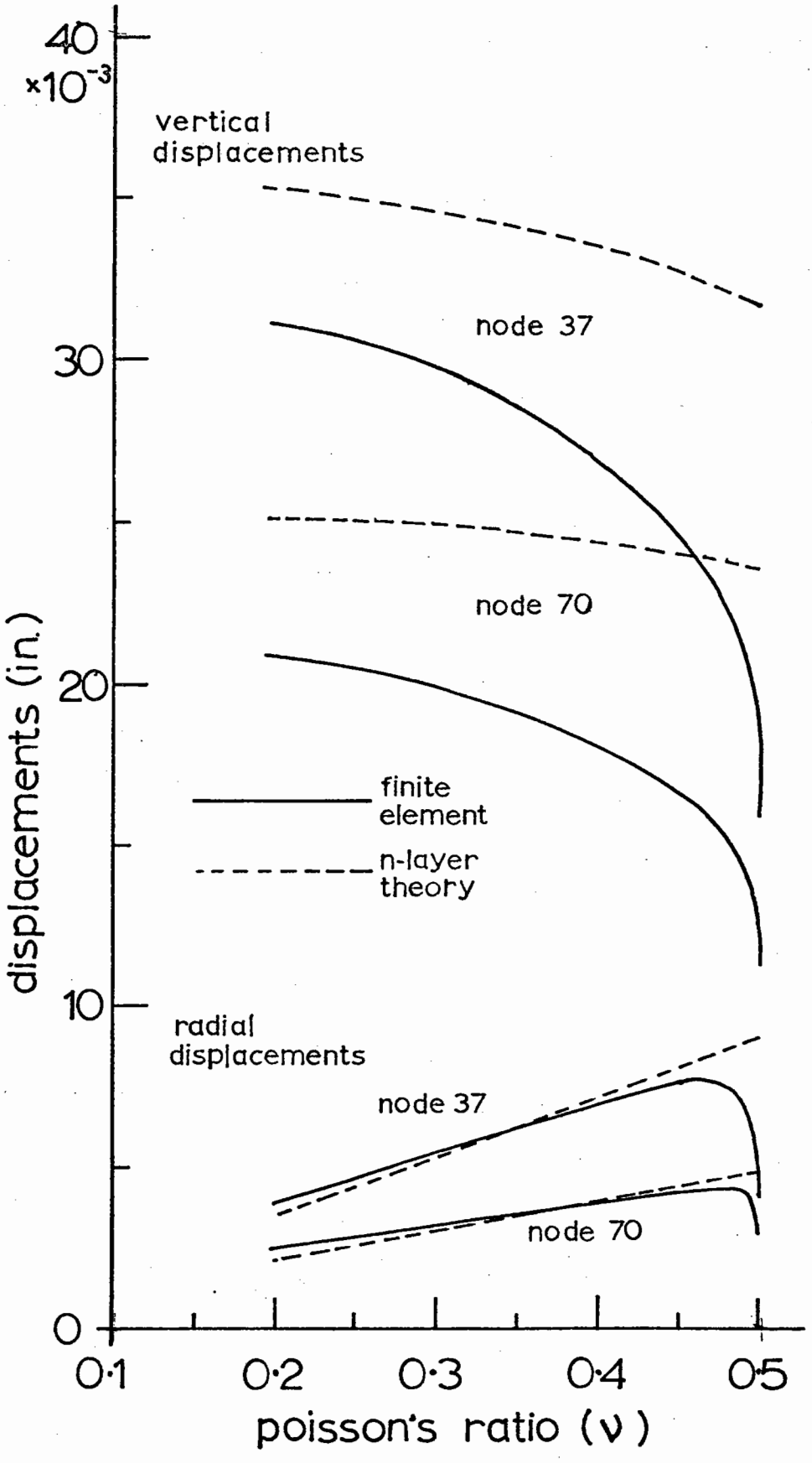

Fig. 4.14 Displacements off axis

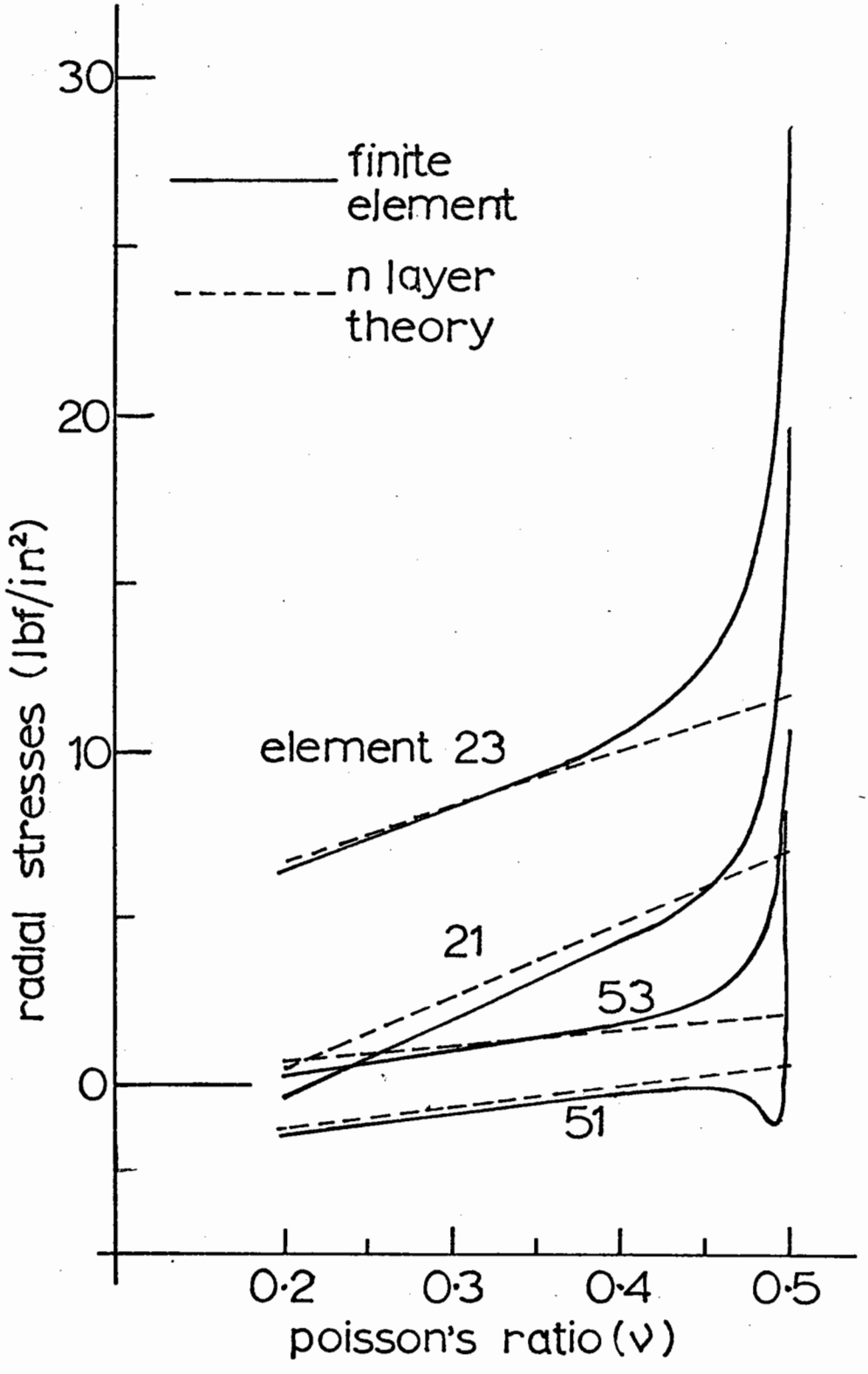

Fig. 4.15 Radial stress with variation of Poisson's Ratio

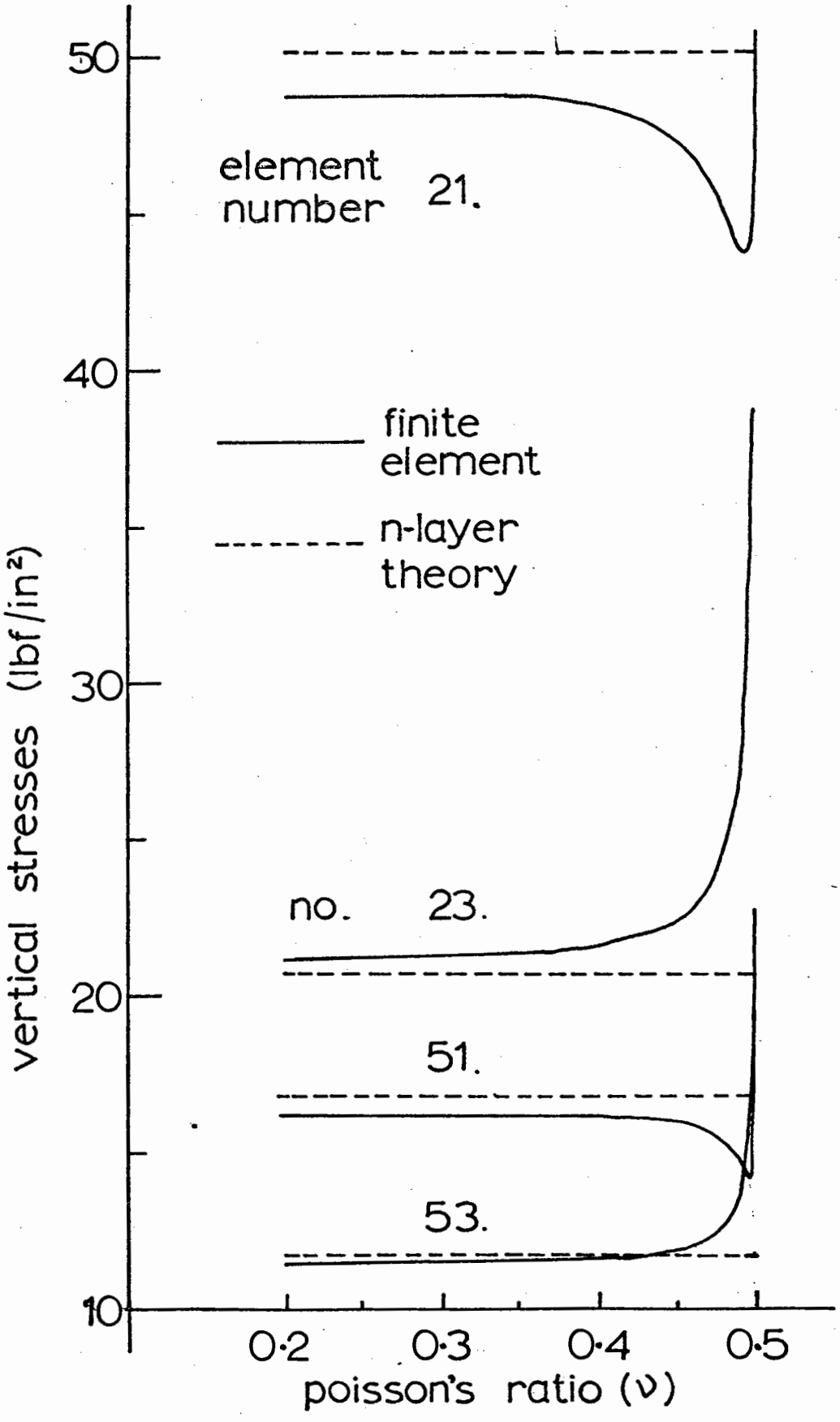

Fig. 4.16 Vertical stresses with variation of Poisson's Ratio

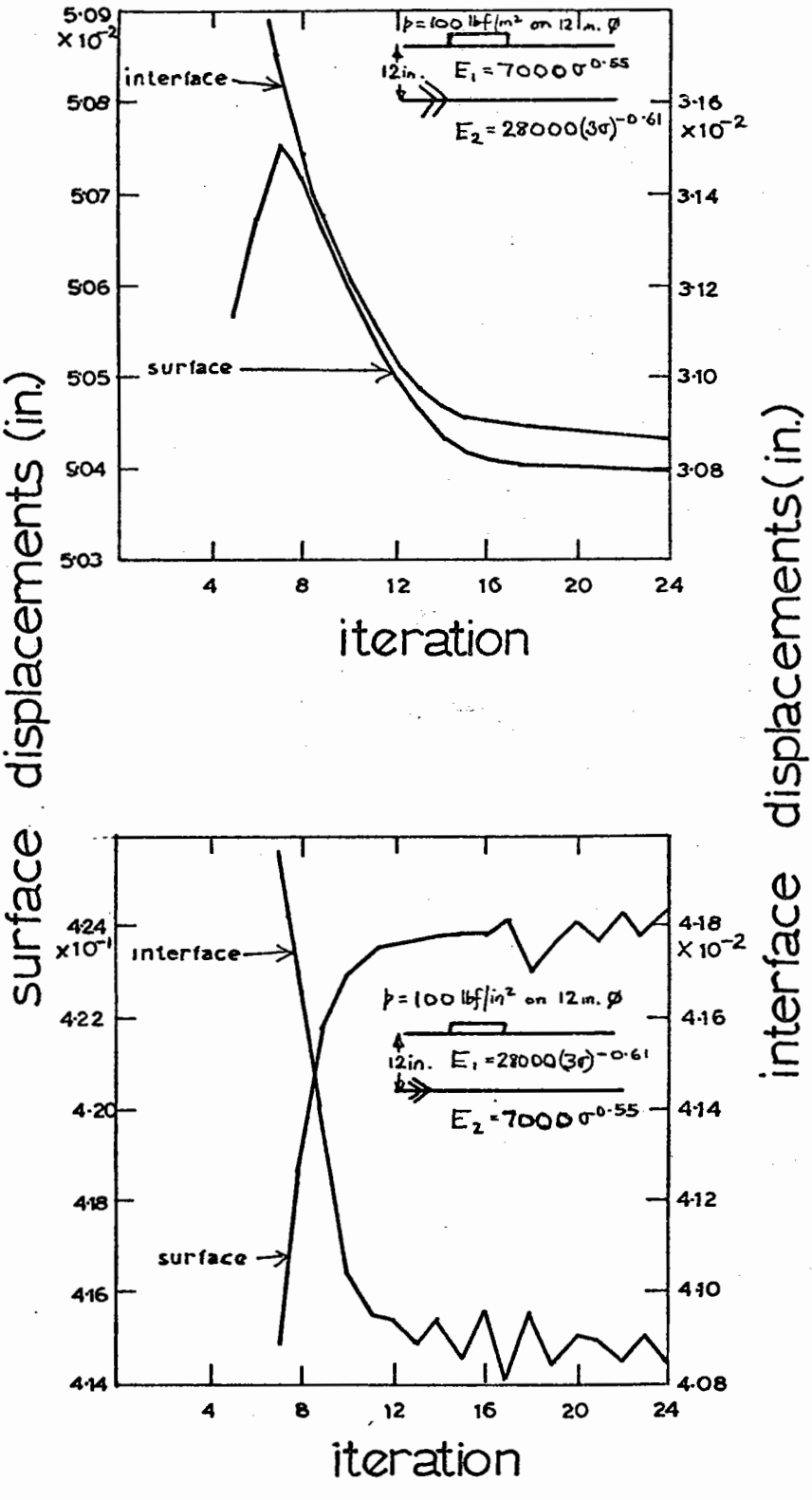

Fig. 4.17 Vertical displacements on axis (granular overlying)

Fig. 4.18 Vertical displacements on axis (clay overlying)

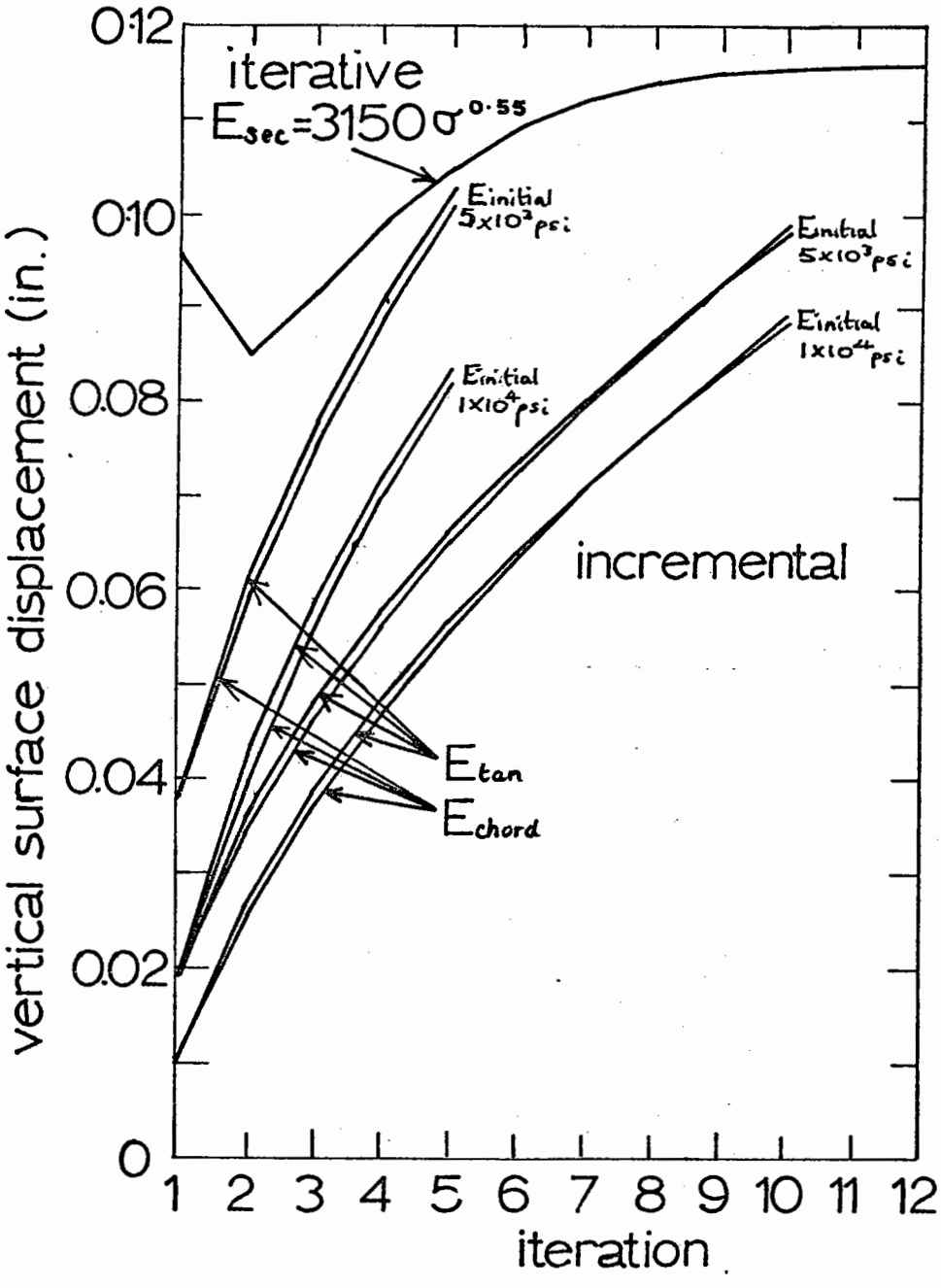

Fig. 4.19 Incremental behaviour: significant effect of initial values: tangent or chord values?

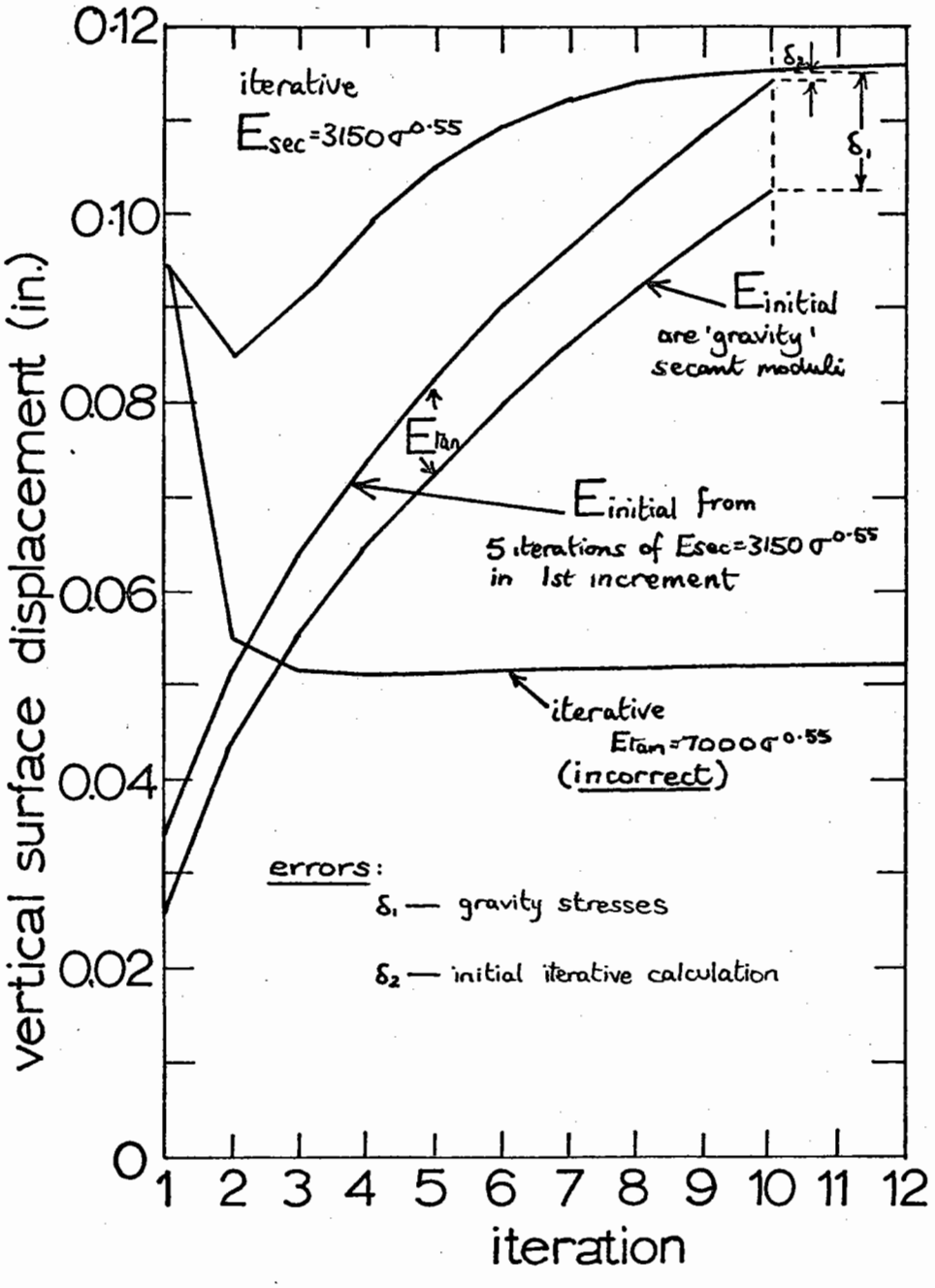

Fig. 4.20 Incremental behaviour - recommended initial values

CHAPTER 5

COMPARISON OF FINITE ELEMENT ANALYSIS WITH IN-SITU MEASUREMENTS

5.1 Introduction

As already mentioned, Brown[1.6] has made insitu measurements of stresses and strains under pulse loading on a scaled down pavement section contained in a rigid pit having dimensions 8 ft x 8 ft x 5 ft depth. Bush[1.9] repeated the two layer work and added a 3 in. surface layer of asphalt and made further measurements. From the measurements of the stresses and strains at a point it has been possible to calculate the first and second stress and strain invariants (σ, τ and ϵ, γ).

5.1.1 For the single layer system of Keuper Marl (silty clay), Brown calculated the Young's Modulus (E) at a point from the stresses and strains using linear elastic theory. A relationship between E and σ the mean normal stress was found, $E = f(\sigma)$, based on a best fit line to a very wide scatter of points. Poisson's ratio (ν) was found to vary erratically about the value 0.4.

An alternative formulation was found from the stress and strain invariants by fitting a curve by eye, thus giving values of the bulk and shear moduli, K and G, for varying stress level. The scatter of experimental results was great but nevertheless the bulk modulus was considered to be constant

and the shear modulus was found to fall with increase in the level of the octahedral shear stress, i.e. $G = f(\tau)$. (This emphasises a point made in Chapter 3, that the implied dependence of E on σ only, reflects the effect of shear stress on the material properties, and thus the $E = f(\sigma)$ relationship could not be applied to stress systems where shear stresses do not rise with mean normal stress in the way they do with this loading.)

Theoretical analysis of the system was carried out using the equations of Boussinesq since no method of analysis, which could incorporate the above non-linear properties, was available at the time. For each point the stresses and strains were calculated using an appropriate E value, constant over a semi-infinite halfspace. Better agreement was obtained between the measured and calculated stresses than similar comparison showed for strains. This was thought to occur since the calculation of strains required the absolute value of E, whereas the stresses rely only on the variability of E at the point.

The curves of modulus v stress level were based on many tests at two different rates of loading and two different contact pressures and thus would seem to represent an average behaviour of the material. Analysis incorporating these material properties should then have produced a solution which fell within the range of experimental measurements at each point.

The finite element method is here used to analyse the system, apparently having the following advantages:

i) allows continuous variation of material properties

ii) can model the rigid pit boundary

5.1.2 Bush extended the work of Brown, at first to a 2-layer system, and then finally added an asphalt surface layer. The maximum contact pressure applied to the final layered system (80 psi) was five times the maximum used by Brown (16 psi), that being the level of loading estimated as necessary to give stresses and strains which the instruments could measure accurately.

Bush attempted to predict the in-situ measurements in the 3-layer system using the Shell Company's (BISTRO) n-layer elastic theory program. The system was subdivided into 6 elastic layers given properties as follows:-

3 in. Asphalt layer: different mean E for each of two rates of loading (E = 137,000 lbf/in^2 for fast loading rate)

9 in. Meldon Dust base: divided into three 3 in. layers each assigned a mean modulus (E = 10,400 lbf/in^2)

∞ Keuper Marl subgrade: one 3 in. layer underlain by marl of infinite extent; each of these two 'layers' were assigned a mean modulus (E = 1300/5250 lbf/in^2)

Bush found that the measured strains and stresses could only be predicted to a reasonable degree of accuracy if it was assumed that the top of the subgrade was weak, probably due to the effects of moisture collecting there.

Re-analysis of Bush's 2-layer measurements of stress and strain invariants, using regression analysis and computer graph plotting, was undertaken to find Bulk and Shear moduli for use as characteristics for the prediction of stresses and strains in Bush's 3-layer system using the finite element

method. Analysis of the stresses and strains measured in the 3-layer system had led to an unacceptable experimental scatter of points.

5.2 Single Layer System

In comparing the results from non-linear finite element analyses with measured quantities it was considered important to establish:

(1) whether there was an improvement in the comparison with a linear elastic solution,

(2) whether it was necessary or even justified to use the modulus v stress level relationships over the whole mesh region, or could some part be considered as linear elastic,

(3) whether there was an improvement in the results if Bulk and Shear modulus relationships were used instead of a varying Young's Modulus.

The finite element mesh in Fig. 5.1 was chosen to represent the single layer system. In order that exact comparison could be made with Brown's results, element centroids were made to coincide with measuring points.

The non-linear elastic material properties for the marl were given by Brown as alternatively:

$$E = 28000\ (3\sigma)^{-0.61} \qquad \nu = 0.4 \qquad (5.1)$$

or

$$K = 6536, \quad G = \frac{10^6}{50+176\tau} \qquad (5.2)$$

where stresses were measured in the ranges:

σ : 1 - 12 lbf/in^2

τ : 1 - 5 lbf/in^2

Program 6 was used to calculate the stresses and strains occuring in the Keuper Marl, under a flexible loaded area of 6 in. radius, when separately characterised by E, ν or K, G, as above. A linear elastic analysis, using the properties suggested by the bulk and shear modulus relationship at low stress levels, (over most of the region), was carried out to investigate the error if the material was considered simply as linear elastic.

Bearing in mind that the non-linear elastic analysis used here assumes linear elasticity to hold within each element, the Bulk and Shear moduli imply a Poisson's ratio given by:

$$\nu = \frac{3K - 2G}{6K + 2G} \qquad (5.3)$$

Since the minimum measured level of octahedral shear stress was approximately 1.0 lbf/in^2, it was considered unreasonable to extrapolate the G = f(τ) relationship to lower stress levels. This implied a maximum value for G of 4444 lbf/in^2 and thus a minimum Poisson's Ratio of 0.22. The region calculated from the analysis as having these linear properties is shown in Fig. 5.1.

5.2.1 Comparison with insitu measurements

Plots, for various depth/radius of loaded area, of stresses as a percentage of the applied normal pressure, and strains per unit of normal pressure were compared with similar ones after Brown (Fig. 5.2) for various (depth (z)/radius of load area (here a = 6 in.)) ratios.

Stresses: Improvement in the prediction of radial stresses was observed using the non-linear elastic material properties

as compared with the elastic analysis after Brown. The discrepancy between the measured and calculated quantities was, however, still great. There was no perceptible improvement or deterioration in the prediction of vertical stresses, which in any case did not vary greatly from those given by an elastic analysis if examined at points greater than 6 in. from the loaded area.

It was noted that the apparently more fundamental description of the material (K and G) gave worse results than the E, ν characterisation. This also occurred in the strain comparisons and no reasonable explanation can be found, except that in this case K = constant and both characterisations effectively offer only a one parameter description.

Strains: The non-linear analyses gave a better prediction of strains at radii of less than 6 in. and depths less than 1.5 in. At greater distances from the loaded area (most of the pit) the non-linear solutions produced, and apparently inexplicably, worse predictions than Brown's approximate linear solution. Again the K, G characterisation increased the discrepancy (to as much as over 100%).

Although the instrumentation errors involved were suspected to be great by Brown, it is unlikely that they would completely explain these large discrepancies. The characteristics were based on all measurements, i.e. all speeds of loading, contact pressures and radii of loaded area; it could be argued that the average characteristic obtained could not be expected to predict the middle of the range of the measured quantities. It would, however, seem reasonable to

suppose that such large errors would not occur because of these factors alone.

5.2.2 Importance of non-linearity

The stresses (Fig. 5.3), and displacements (Fig. 5.4) nominally on the axis of the loaded area were examined in separate analyses to establish the absolute importance of the non-linearity. Where $\tau < 1$ lbf/in^2 then the material characteristics were considered linear and K and G assigned values appropriate to this stress level (Fig. 5.1).

Two kinds of analysis were carried out:

(1) Non-linear elastic over the shown region retaining the rest of the mesh as linear.

(2) The mesh completely linear and having the stiffer properties of the low stressed region (from (1)).

Stresses

Vertical stresses did not differ greatly over the non-linear region for the different characterisations, but a considerable difference (having its maximum effect as a 30% predicted drop in vertical stress at about 12-15 in. depth) was noted between the elastic and the non-linear analyses.

The non-linear analyses were also found to bring about a significant drop in the zone of radial tension below the loaded area.

Since a single layer system was being considered it is important to note that the stress distribution can not be affected by the absolute value of the constant modulus in the linear elastic analysis (Boussinesq). The stress plots

thus truly reveal the effect of the non-linear elastic material properties and the comparison is in no way affected by the choice of cut-off stress level which defined the geometrical limits of the non-linear region.

In a multilayer system comparisons to establish the effect of considering the non-linear properties are made difficult since the stress distribution relies on the ratio of moduli in layers, which thus must take realistic values.

Displacements

The difference between displacements calculated from a non-linear, the (K, G) characterisation and the equivalent linear analysis was only marked above the boundary between linear and non-linear regions.

The $E = f(\sigma)$ relationship led to much stiffer material and thus smaller displacements at depth.

5.3 Three-layer System

The 3-layer system of Bush[1.9] was also considered using the finite element method (Program 6).

5.3.1 Material characteristics

Measurements made by Bush in a 2-layered system were used to establish the Meldon Dust base and Keuper Marl subgrade properties in the absence of reliable findings from the 3-layer system. It was found that the experimental measurement of stress and strain resulted in a very wide scatter and no definite trend, if it was attempted to characterise the material by a curve of the form $E = f(\sigma, \tau)$. Fig. 5.5 shows

separate plots of E against σ and τ for the Keuper Marl subgrade. A trend exists, in that modulus decreases with increasing stress level, but this cannot be put into mathematical form. In neither of the plots was it possible to detect contours of the 3rd variable.

An alternative method of presenting the results does not involve the calculation of a modulus of elasticity at a point. In Fig. 5.6 i) the normal or bulk stress-strain relationship is shown and in Fig. 5.6 ii) the shear stress-strain relationship. The scatter on these plots is much less than in the log-log plots of Fig. 5.5 and no assumptions have been made about the material behaviour. This indicates that the use of bulk and shear moduli may be a better means of characterising the material than Young's Modulus and Poisson's Ratio. In using the results to obtain a mathematical function for use in finite element analysis it was only necessary to fit curves to the experimentally measured points shown in Figs. 5.6. For this purpose a standard regression analysis was used and the information automatically graph plotted for clarity. The fitted curves were constrained to pass through, or very close to, the origin. Visual inspection of increasing orders of curve enabled the simplest suitable relationships to be chosen.

In the case of the Keuper Marl (Fig. 5.6), the chosen curves were:

$$\epsilon = 0.4\sigma + 0.03\sigma^2$$
$$\gamma = 0.5\tau - 0.2\tau^2 + 0.08\tau^3 \qquad (5.4)$$

(where ϵ and γ are in microstrain)

giving Secant Moduli:

$$K = \frac{10^6}{1.2 + 0.09\sigma} \quad lbf/in^2$$

$$G = \frac{10^6}{0.5 - 0.2\tau - 0.08\tau^2} \quad lbf/in^2 \qquad (5.5)$$

For soils in general, the shear and normal stress effects cannot be entirely separated since shearing can cause volume change. Hence the shear and normal stress-strain relationships are not entirely independent. However, for the experimental points in Fig. 5.6 i) it was not possible to recognise a trend for differing shear stress nor in Fig. 5.6 ii) for differing bulk stress. This was though to be the result of the limited range of bulk/shear stress ratios resulting from insitu tests using only a load normal to the surface; e.g. in Meldon Dust σ/τ, 1 to 3, in Keuper Marl 0.25 to 1. The curves derived can thus only be justified when describing the material under vertical loading. If the action of surface shear forces had to be considered, then more definitive curves showing some inter-relationship between the bulk and shear behaviour would be required.

Using the same regression analysis technique, relationships were found for the Meldon Dust (granular) layer:

$$K = \frac{10^6}{107 - 2.8\sigma} \quad lbf/in^2$$

$$G = \frac{10^6}{276 - 5\tau} \quad lbf/in^2 \qquad (5.6)$$

The asphalt layer was given the linear elastic properties

chosen by Bush as appropriate to a "fast" loading time of 0.05 sec: i.e. $E = 1.37 \times 10^5$ lbf/in^2, $\nu = 0.4$.

The finite element mesh in Fig. 5.7 was used to represent the 3-layer system which was constructed by Bush to obtain insitu measured stresses and strains.

5.3.2 Range of applicability of material characteristics

The curves derived above from insitu measurements in a layered system, strictly can only be justified when used to represent the material behaviour at stress levels within the range they were measured. Some extrapolation could be argued for, however, if the particular modulus being considered did not vary greatly at the limiting stress level. In the material being considered here the measured ranges were:

Keuper Marl	σ	0.2 - 11.0
	τ	0.3 - 4.5
Meldon Dust	σ	0 - 16.0
	τ	0.5 - 17.0

(all stresses in lbf/in^2)

The value of Poisson's Ratio implied by the magnitudes of K and G for an element were considered. For the materials to be sensible in their behaviour it would be expected that $0.5 > \nu > 0$.

5.3.2.1 Meldon Dust

The relationships for the Meldon Dust in equations 5.6 imply that for ν to be greater than zero, then $\sigma > 2.6\tau - 98.9$. This is so for all σ and τ unless $\tau >> \sigma$, (which is never the case in this loading system). At low stress levels this

granular material is at its softest (i.e. for $\sigma = 0$ and $\tau = 0$, $\nu = 0.33$), at higher stress levels K and G would become negative, which is an unacceptable situation. The limits imposed by this condition are: if $K > 0$ then $0 < \sigma < 38.2$

if $G > 0$ then $0 < \tau < 55.2$

Calculations were, however, influenced by the former condition in only one or two highly stressed elements. In this case, when σ was greater than 38.2 the bulk modulus was set to the value appropriate to this cut-off stress level, which defined the upper limit of the applicability of equation 5.6.

The Meldon Dust relationships thus resulted in sensible material properties over the measured range, and could be extrapolated to higher stress levels, the limits being those above.

5.3.2.2 Keuper Marl

The values of ν implied by equations 5.5 were found to be very low or negative at low stress levels, and thus the fitted curves appeared not to be valid over the lower end of the measured range. For $\nu > 0$ then from the equation of K and G, approximately:

$$\tau > 3.5 + 0.128\sigma$$

This is clearly not so unless τ is greater than 3.5. It seemed appropriate to retain ν as positive and thus at low stress levels a cut-off was chosen where $\sigma = 0.1$ and $\tau = 3.6$. Below these stress levels the material was given the very stiff properties suggested by these values substituted in

equations 5.5. At higher stress levels the relationships behave satisfactorily.

The region where the Keuper Marl could be considered as non-linear thus became limited (Fig. 5.7), whereas the Meldon Dust relationships had been able to apply to virtually every element in the layer.

5.3.3 Iterative behaviour

The loading in Fig. 5.7 was imposed and iterative analyses carried out. These eventually incorporated the above restrictions when it became apparent that the stress levels in the system were outside the range over which the relationships could reasonably be extrapolated.

The behaviour of each of the layer interface vertical displacements was monitored (Fig. 5.8). The behaviour was found to be more erratic than that found in a single layer system (Chapter 4). This is thought to have been caused by the onset in particular elements of the above restrictions to the applicability of the relationships, during various stages of the iteration procedure. Nevertheless, the change in all the monitored displacements was found to be less than 1% beyond the 7th iteration. Bearing in mind that the basic innaccuracies involved in the Finite Element Method can lead to errors at least as large as this, this number of iterations would seem adequate for most purposes. The computing time taken for 7 iterations on the Chilton Atlas computer was approximately 20 minutes but the total execution time (time the 'job' spent in the machine) sometimes found to be as much as 70 minutes because the machine optimised the efficiency of

its operation by running several jobs at the same time. The demand on real computing time therefore does not seem excessive.

5.3.4 Comparison with in-situ stresses and strains

The iterative finite element analysis using material properties, as described above, was used to calculate stresses and strains in the 3-layer system. These calculated values are shown in Fig. 5.9 together with measured quantities relevant to the "fast" loading test being modelled. The n-layer elastic theory solution by Bush, containing a soft layer in the marl, is shown, and also a linear elastic finite element analysis based on material properties suggested by the best fit stress-strain relationships.

Bush found that by assuming the Keuper Marl to have a soft layer (above $z/a = 2.5$), with E arbitrarily chosen as one quarter of the general marl stiffness, he was able to obtain reasonable agreement with the measured quantities. The on-axis plots in Fig. 5.9 show that for the Keuper Marl stresses and strains this is so, but that the stresses in the upper part of the Meldon Dust layer were predicted very innaccurately.

Non-linear elastic finite element analysis, although accurately predicting the vertical stresses in the upper part of the Meldon Dust layer, failed to identify lower measured vertical stresses and higher radial and vertical strains in the region of the Meldon Dust-Keuper Marl interface.

Bush's attempt to explain the large discrepancies by the existance of a soft layer of Keuper Marl was followed in a

finite element analysis. An iterative analysis, carried out using a Keuper Marl having the same material functional form, but 1/10th the strength, brought about only a small increase in the vertical strains in the marl. A slight increase in the radial strain and a decrease in the vertical strain was observed, but otherwise the effect seemed negligible.

It can only be inferred that in practice the layer was very weak indeed for a considerable depth into the marl, and that it is not enough to assume that the material had the same functional properties but was weaker.

The linear finite element analysis carried out used constant moduli for the non-linear layer chosen as follows:

Meldon Dust: mid-range values found from non-linear analysis by inspection of element moduli:

$K = 10000 \qquad G = 4000$

Keuper Marl: cut-off values relevant to low stress level in Fig. 5.7:

$K = 830000 \qquad G = 1200000$

(all lbf/in^2)

These quantities were thus chosen from the functional relationships derived from the material, and the change in stress distribution they bring about demonstrates the absolute effect of considering the material as non-linear.

Bush used very different constant moduli. These gave subjective solutions more nearly agreeing with the majority of measured values, their choice being influenced by the degree of similarity between calculated and measured quantities. Although valuable in showing that some well chosen constant values of moduli could be made to give agreement (hence not

excluding layered elastic theory for design), the curves in Fig. 5.9 show clearly that the materials were sufficiently non-linear to influence the stress and strain distributions significantly. The vertical stress and vertical strain in the asphalt and Meldon Dust were the most changed as compared with the non-linear analysis.

Comparison of measured quantities with the linear analysis (which was based on each material's behaviour at low stress level) shows agreement, worse in the Meldon Dust layer and better in the Keuper Marl layer than non-linear elastic analysis.

Contours of the mean normal and octahedral shear stresses were plotted based on both the linear and non-linear finite element analyses (Fig. 5.10). These stresses were chosen since they are thought to be fundamental in governing material behaviour. The line printer plotting technique is incorporated in Program 6 (Appendix) and prints element stresses with spacings proportional to element size. The contours were then drawn by eye. It is apparent from the plots that there is a significant difference between solutions from linear and non-linear finite element analyses. This would have significance if the ratio σ/τ was being used to identify regions where failure was likely and changes were to be made to the material relationships accordingly. Non-linear analysis predicts low σ/τ at the middle of the Meldon Dust layer and the top of the Keuper Marl layer. Linear analysis, however, predicts higher values at these points and therefore stresses less likely to lead to significant permanent deformations.

In general it appears that the measured stresses and strains cannot be accurately predicted using either linear or non-linear finite element analyses based on the above material properties. It has been established that the non-linear properties are important and lead to significantly changed stress distributions. Further insitu measurement and supporting material characterisations from the triaxial test are required before better agreement between theory and practice can be expected.

5.3.5 Overburden stresses

In all layered systems, stresses caused by the weight of overburden are ever present. In a single layer system they add an all round compression which increases linearily with depth. It is of interest to know the magnitude of these stresses in the critical regions at the base of the bituminous layers in order to provide information to researchers examining healing effects in repeated loading tests with rest periods.

The program was re-run with the computed loads, due to the overburden densities given by Bush, added to the external loading (i.e. Asphalt 140 lbf/ft^3, Meldon Dust 116 lbf/ft^3, Keuper Marl 120 lbf/ft^3).

Predictably the general effect in the surface layers was to increase the vertical and radial compressive stresses and reduce the radial tensile stresses experienced at the base of the asphalt. The strains were found to be little affected. The all round state of compression due to overburden alone increased to a maximum of approximately 2.0 lbf/in^2 (vertical

stress, σ_z = 6.2 lbf/in^2) at the base of the system (depth 60 in.).

At the base of the 3 in. asphalt layer, for the loading and properties shown in Fig. 5.7, the horizontal tensile stress was reduced by the overburden compressive radial stress by 0.17 lbf/in^2. Bazin and Saunier[1.16] showed significantly different amounts of healing for rectangular bars of asphalt when left to rest either on end or flat. It seems reasonable to suppose that this healing involved very low self weight stresses possibly of the same order as those found in the above analysis. However, the bitumen used was very soft and may have given unreasonably high estimates of the healing capabilities of road making bituminous materials. Nevertheless the program's capability to calculate the overburden stresses in any layered system does offer researchers an easy method of obtaining the order of the stresses which may cause healing and would enable laboratory experiments to be designed to operate at realistic stress levels.

Since the order of the overburden stresses was such that healing could occur at the base of a 3 in. asphalt layer, it seems likely that the effect may be a significant factor in thicker, full scale road pavements.

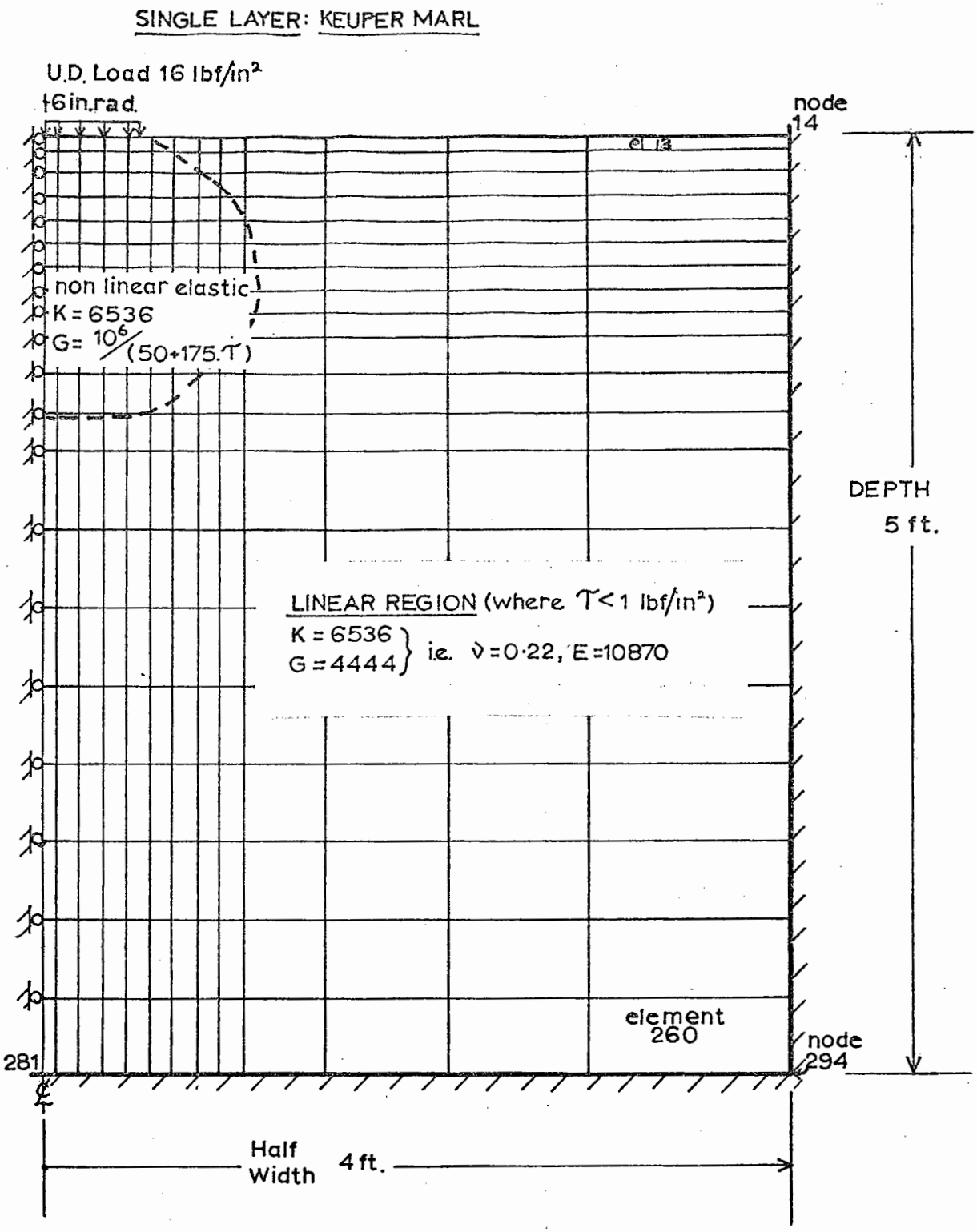

Fig. 5.1 Single layer system (after Brown 1967) showing: finite element idealisation, pit dimensions and area which can be considered as having non-linear elastic material properties.

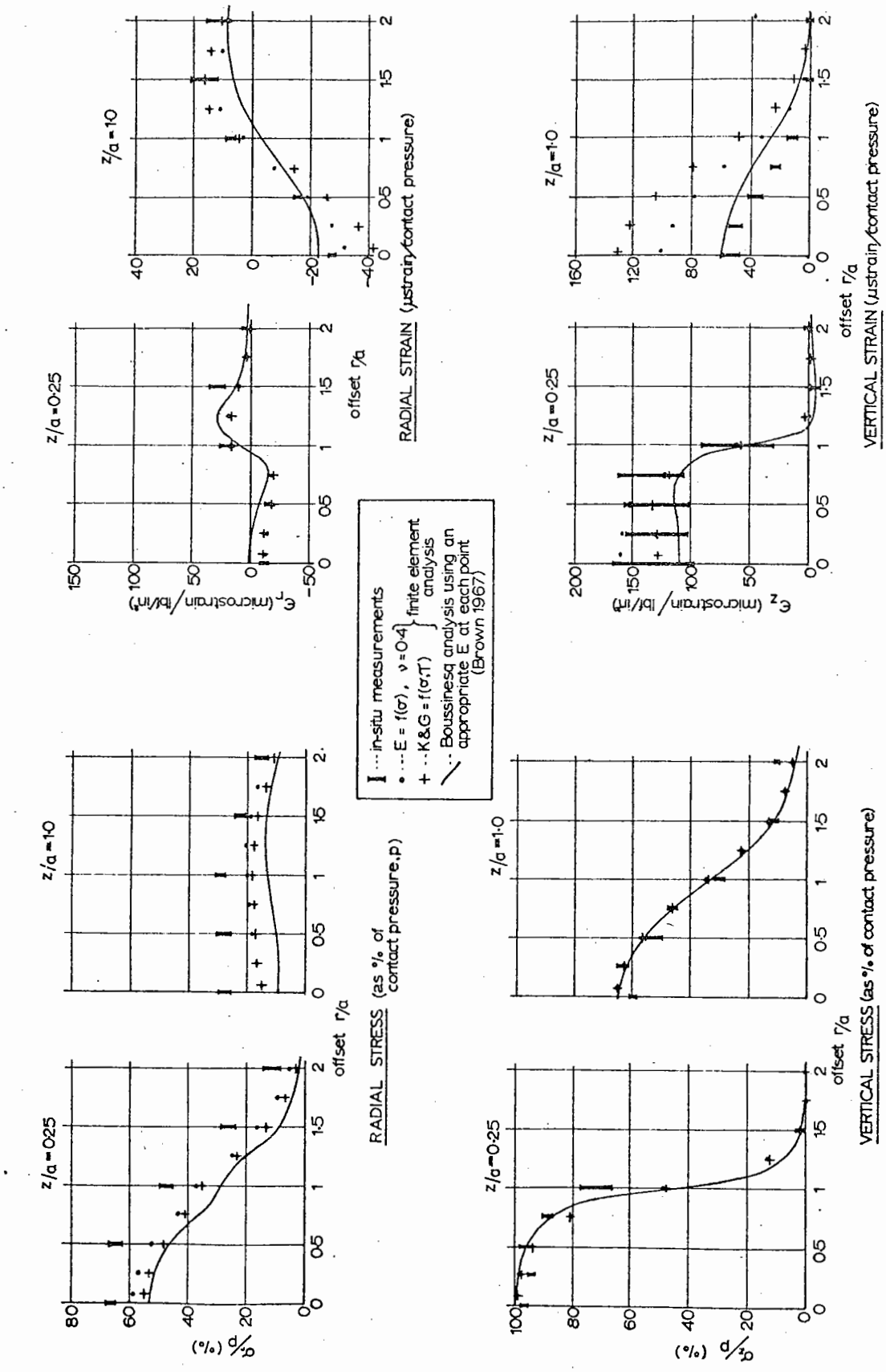

Fig. 5.2 SINGLE LAYER SYSTEM: FINITE ELEMENT ANALYSIS COMPARISON WITH IN-SITU MEASUREMENTS AFTER BROWN (1967)

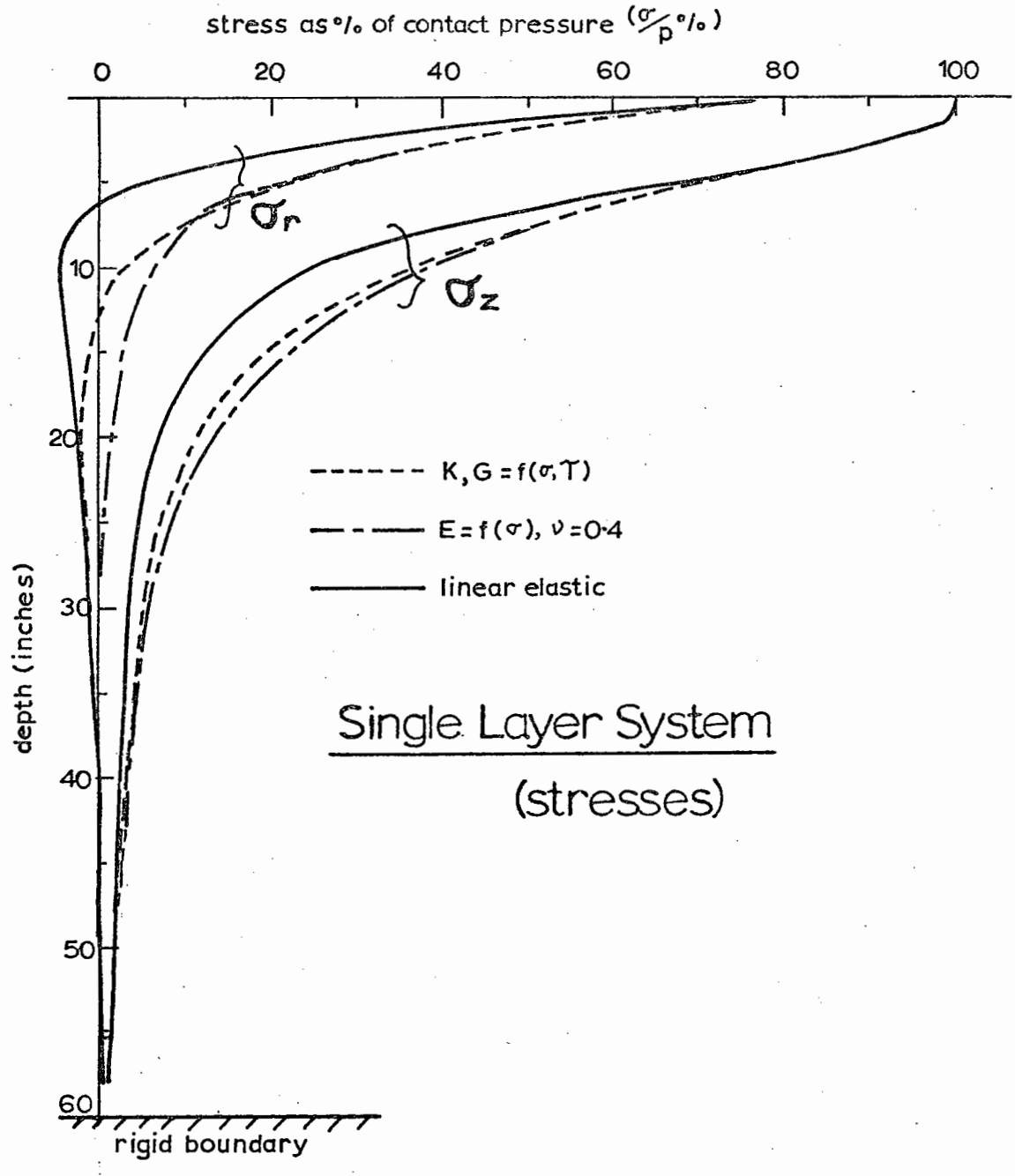

Fig. 5.3 Stresses on the load axis in single layer system - importance of non-linearity

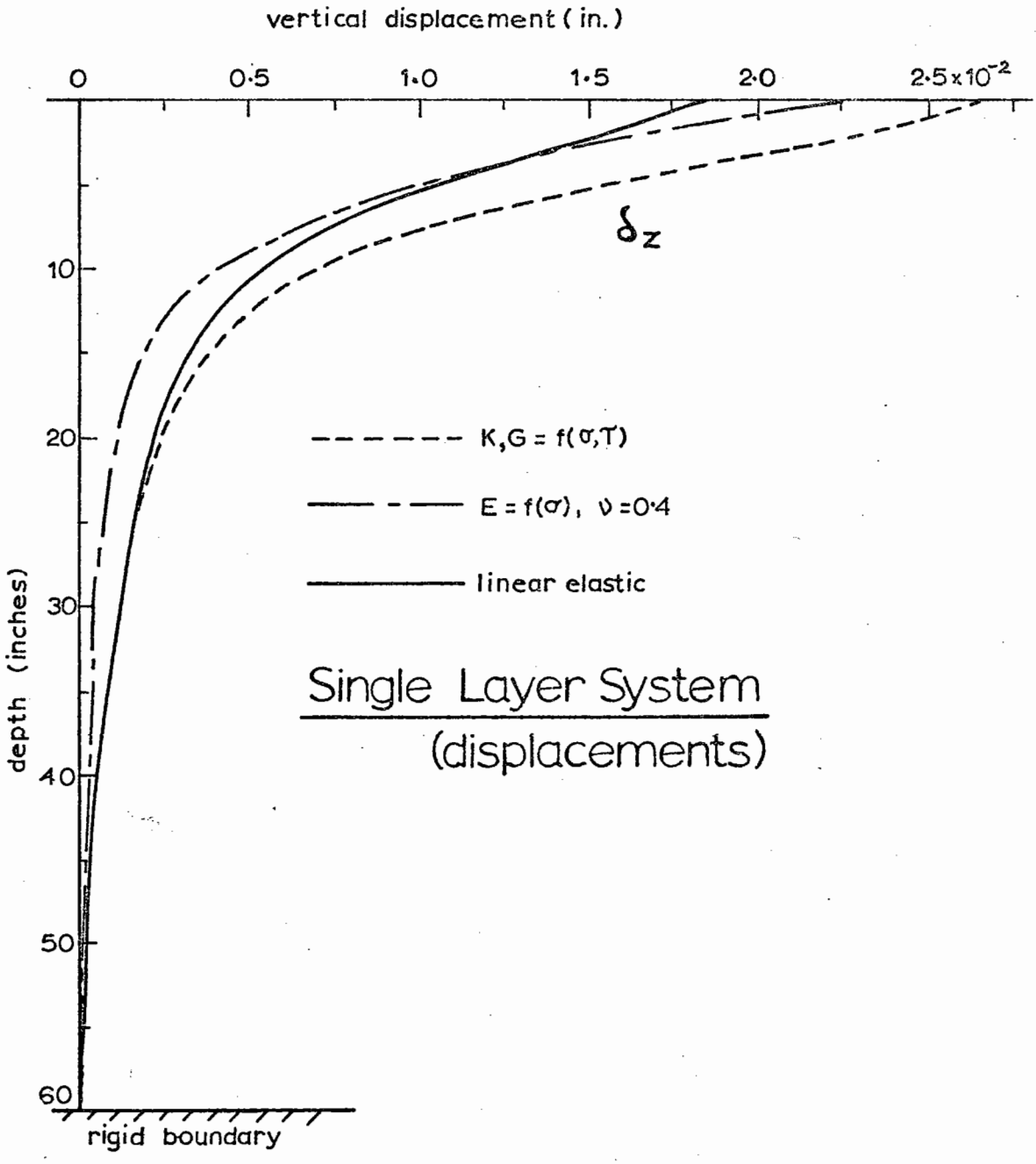

Fig. 5.4 Vertical displacements on the load axis in single layer system

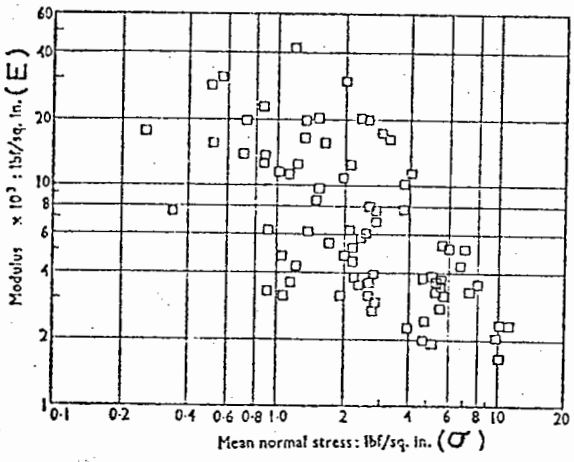

i) Variation of Young's Modulus with mean normal stress (σ)

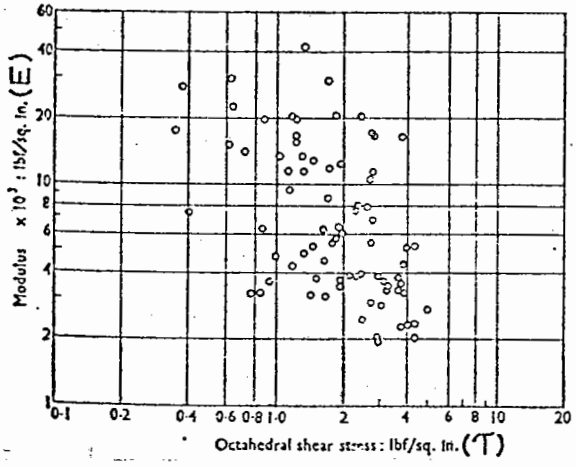

ii) Variation of Young's Modulus with octahedral shear stress (τ)

Fig. 5.5 Keuper Marl: Young's Modulus v Stress invariants from 2-layer system (after Bush 1969)

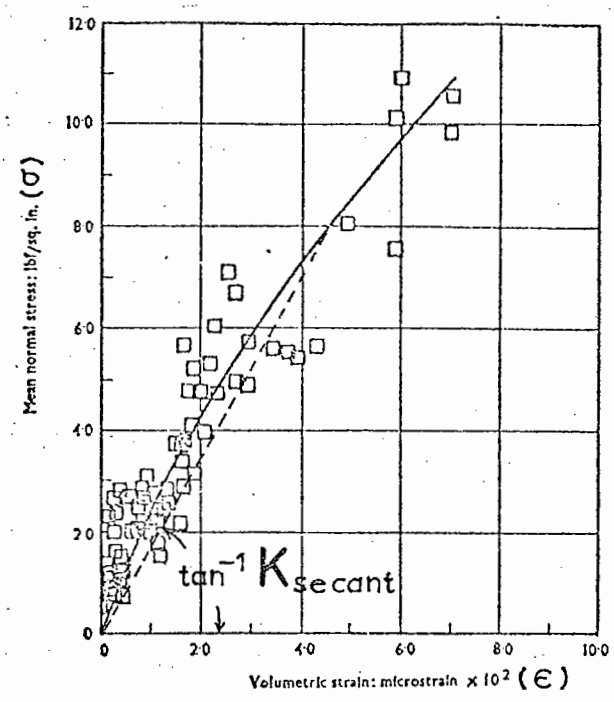

i) Bulk stress-strain behaviour

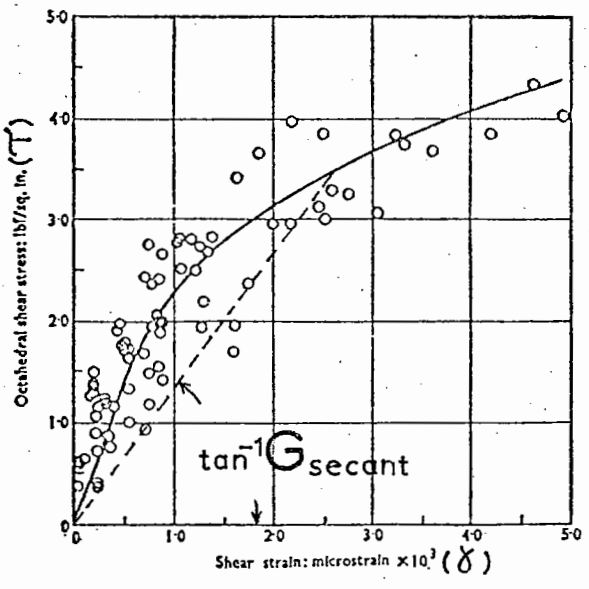

ii) Shear stress-strain behaviour

Fig. 5.6 Keuper Marl: Bulk and Shearing action from 2-layer system (after Bush 1969)

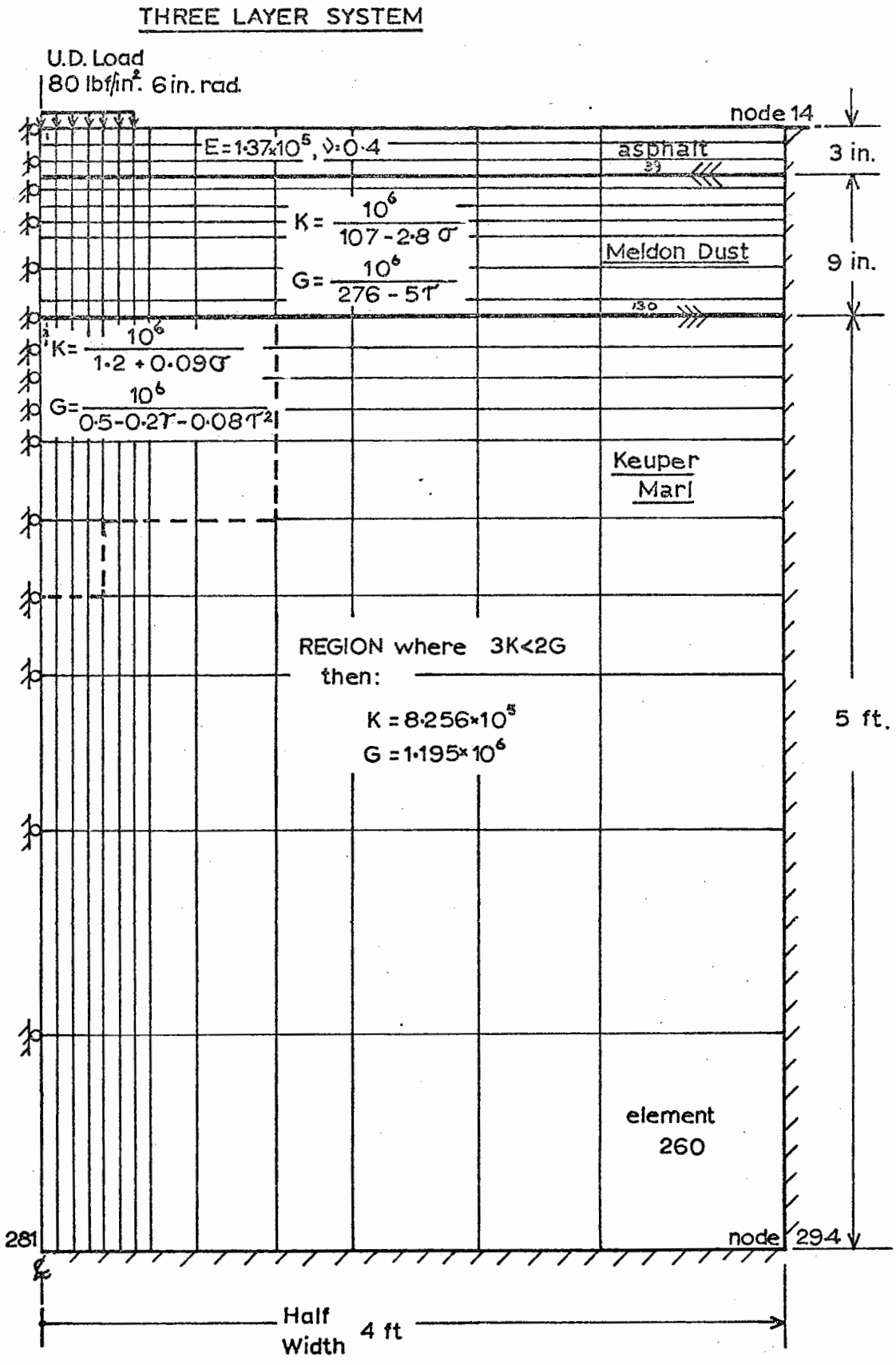

Fig. 5.7 Three layer system after Bush showing finite element idealisation and region of applicability of non-linear elastic material characteristics

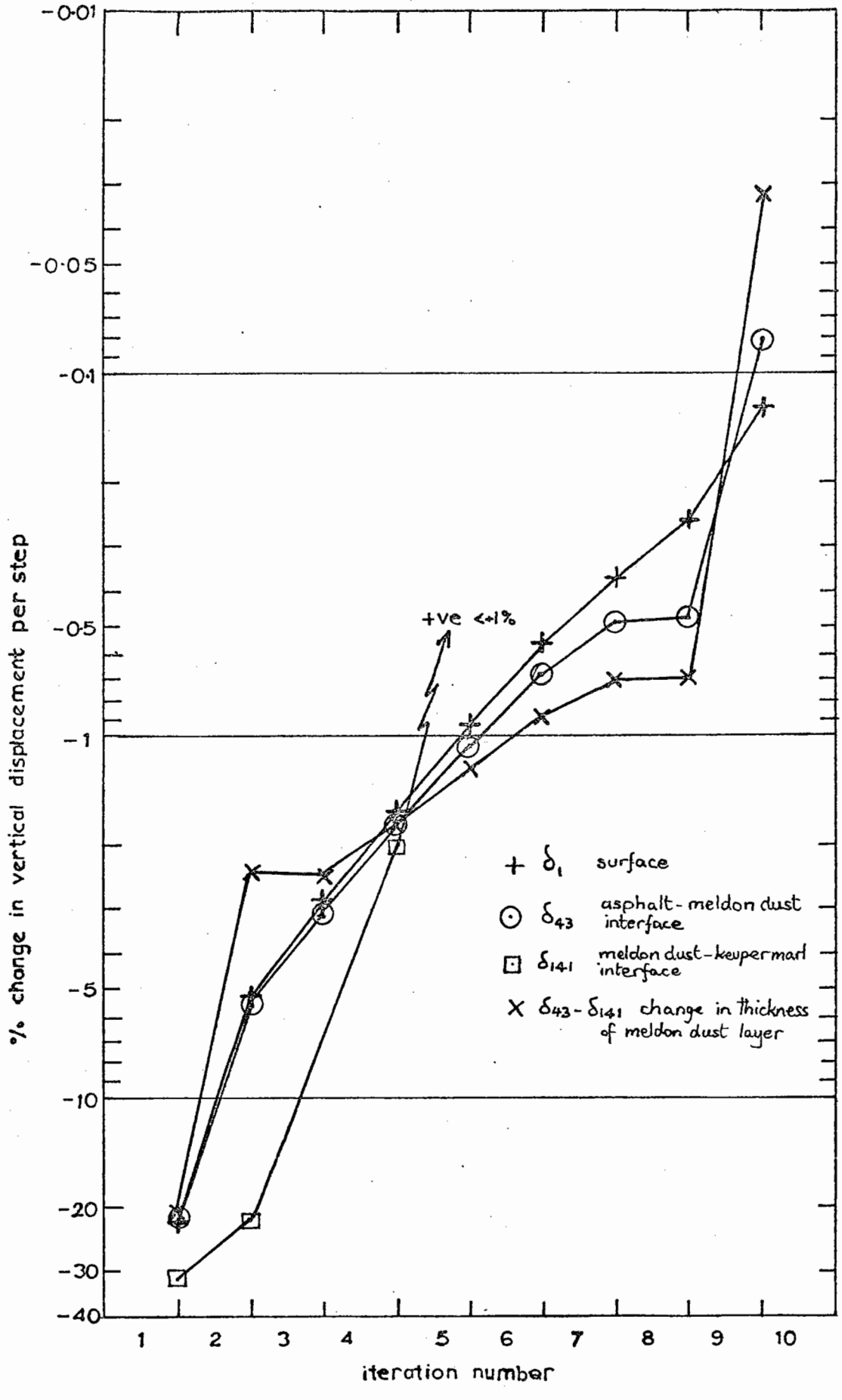

Fig. 5.8 Percentage change in interface vertical displacements with iteration step: 3 layer system

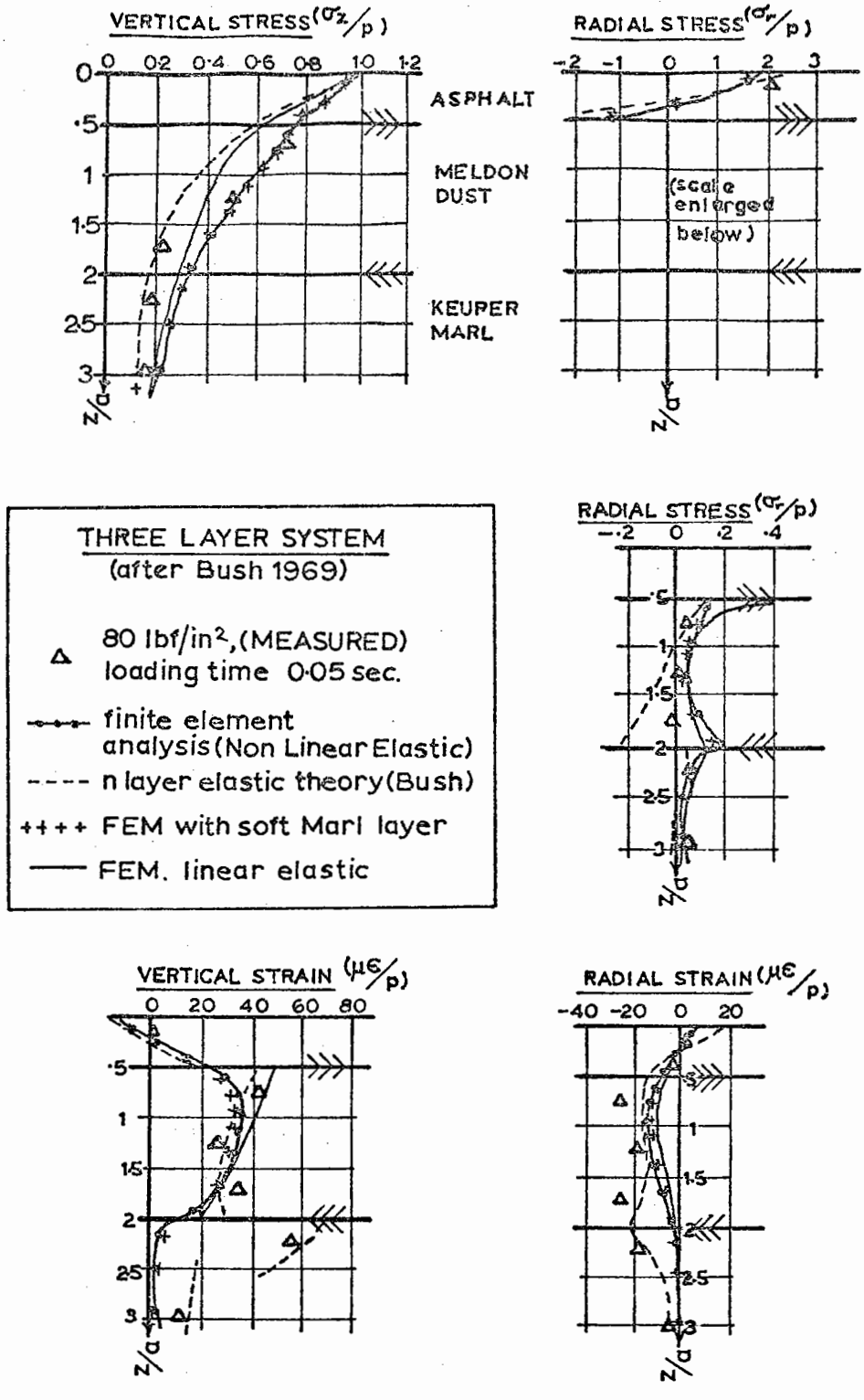

Fig. 5.9 Three layer system scaled down pavement system (after Bush 1969) - comparison of measured stresses and strains and analyses

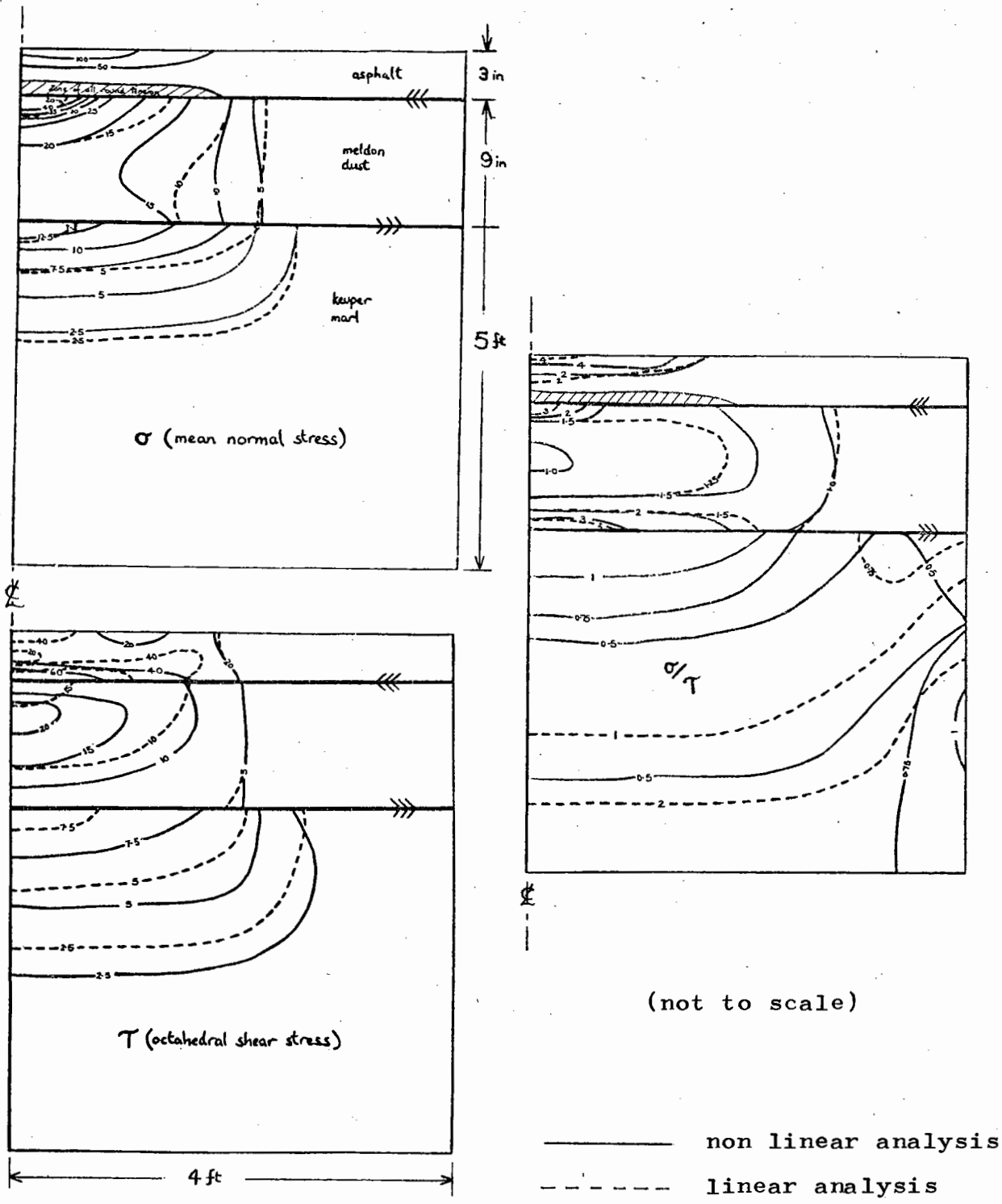

Fig. 5.10 Mean and shear stress in 3 layer system - linear and non-linear analysis

CHAPTER 6

THE EFFECT OF TEMPERATURE DISTRIBUTION AND VARIATION ON THE ELASTIC BEHAVIOUR OF THE LAYERED ROAD PAVEMENT

6.1 Introduction

It is well known that the bituminous layers in a pavement have temperature sensitive stiffness properties. Higher temperatures reduce the bituminous material stiffness and thus the load carrying capabilities of the road.

Improved design methods[6.1] for flexible pavement design involve an examination of the critical stresses, strains and displacements. It is shown here that these parameters vary considerably as a result of temperature variations which occur in a pavement section in the United Kingdom.

Data for obtaining the variation of temperature with depth in a pavement was made available to the Author by the Road Research Laboratory, Crowthorne (RRL), and was in the form of continuous temperature measurements at various depths. Stresses, strains and displacements under a representative wheel loading were calculated using both the finite element method and n-layer elastic analysis[1.38]. In this way, it was possible to demonstrate the inaccuracy involved if a mean stiffness value for the bituminous material was chosen instead of employing a more rigorous analysis taking account of the temperature (or stiffness) gradient in the layer. More

important, it was possible to determine the change in the elastic stresses, strains and displacements which were implied by measured temperature variations.

The effect of measured temperatures on the surface deflection of pavements has been investigated before by Southgate and Deen[6.2]. Benkelman beam deflection measurements have highlighted the importance of the effect of temperature on pavement behaviour and a means of adjusting deflection measurements for temperature has been presented. This work relied on the prediction of temperature at depth as a function of air temperature history and the surface value, substantiated by field measurements. AASHO Road Test Data was analysed using layered elastic theory and a temperature-deflection-modulus correlation between field data and theory found to exist. Extrapolation of the temperature with depth estimation to other locations would seem suspect since factors other than air temperature influence the variation within the pavement.

Knowledge of this variation was sought at the RRL[6.3] and temperature duration measured at a limited number of depths in a test section of pavement.

Using climatic data and material thermal properties temperature has been predicted recently[6.4]. The work emphasised wind speed and air temperature as climatic factors and thermal conductivity and heat absorption as pavement factors. All vary widely, even in the same pavement, thus much more field data is required before temperature variation can be estimated in this way.

For the purposes of the analyses the author carried out, access was allowed to continuous records of temperature at various depths now (1971) being made by the RRL[6.5].

6.2 Variation of Temperature with Depth

The RRL continuous temperature recording stations have been set up in locations with as widely different environmental conditions as the Highlands of Scotland, Southern England and tropical Africa. At various depths in untrafficked pavement sections, thermocouples have been placed and produce a continuous pen record of temperatures throughout the year. The objective of the author was to investigate the effect of changes in bituminous layer stiffness as a result of temperature changes on the resilient pavement behaviour. The effect on design parameters of considering a temperature (and thus stiffness) gradient in the analysis and not only a mean value in the layer was also considered.

For design purposes the critical stresses, strains and displacements occur in a pavement at high temperature. Vertical subgrade stress and vertical subgrade strain, the radial strain at the base of the bituminous layers and the surface deflection are all likely to have their maximum values when the pavement is in its hottest and thus weakest state. By inspection of the RRL temperature records it was seen that the most extreme gradients of temperature also arose during very hot days. Analysis was thus carried out using temperature variations from the hottest day at the pavement location, RRL Crowthorne, namely 7th July, 1970.

Data was most complete for a 10 ft. x 10 ft. x 12 in. thick layer of asphalt overlying Bagshot Sand, thus records for this section were used. The subgrade temperature (Fig. 6.1) beneath each of the test sections at the location were approximately equal and varied throughout the chosen year. It is apparent from the figure that there was a change in winter temperature from 1969-1970, which emphasises the importance of making continuous records over many years. The daily variation of subgrade temperature was found by inspection of the records to be negligible; the important variation was in the 12 in. asphalt layer (Fig. 6.2).

Each curve represents the variation of temperature at a particular time of the day. These times were chosen by inspection as being of most interest for the following reasons:

05.00 - coolest throughout - coolest surface temperature

14.30 - hottest at surface

17.30 - intermediate case - becoming hotter deeper in asphalt

22.30 - hottest at base of asphalt - surface temperature lower

Air temperatures were added to Fig. 6.2 showing the vast difference between those and the pavement surface temperature. This emphasised that many factors influence the quantity of heat transferred to the pavement, the most important, it is known, being surface texture and colour.

The finite element program required definition of temperature with depth in the bituminous layer in order to assign stiffness values to elements. Linear approximations (Fig. 6.3) were made to the curves of temperature with depth

but care was taken to ensure that the essential differences between the distributions for each chosen time were retained. Curves of the form $t^{o}C = f(z)$ (where z = depth) were incorporated in the program (Appendix, Program 4).

6.3 Material Properties

In an elastic isotropic material, behaviour can be defined completely using the two parameters, Young's Modulus (E) and Poisson's Ratio (ν). Bituminous materials are, however, viscoelastic and require more parameters to describe them. Heukelom and Klomp[6.6] have described a procedure to establish an elastic modulus for the bituminous material given the time of loading, the temperature and the mix and bitumen specifications. The term, stiffness (S), was given to the property of the material, which for a particular time of loading can be considered as an elastic modulus representing resilient dynamic behaviour of the material.

The following expression was given:

$$\frac{S_{mix}}{S_{bitumen}} = \left(1 + \frac{2.5}{n} \cdot \frac{C_v}{1-C_v}\right)^n \qquad (6.1)$$

where S_{mix} = stiffness of bituminous mix (kgf/cm^2) or E

S_{bit} = bitumen stiffness determined from the nomograph after Van der Poel or as modified by Heukelom and Klomp (kgf/cm^2)

C_v = volume concentration of aggregate

$$n = 0.83 \log_{10}\left(\frac{4 \times 10^5}{S_{bit}}\right)$$

The bitumen properties are defined by the ring and ball test temperature and the penetration index. These values together with a representative loading time enable the nomograph to be used to find bitumen stiffness (S_{bit}).

The 12 in. layer of asphalt at RRL, Crowthorne was constructed to the specification given in Chapter Appendix 6.2. Necessary measured bitumen properties are given in Chapter Appendix 6.3.

A loading time of 1/100th sec was considered representative of normal road traffic and $S_{bitumen}\left(E_{\frac{1}{100}}\right)$ was found from the Heukelom and Klomp nomograph for temperatures in a range which could be expected in the United Kingdom. S_{mix} was calculated from Eq. 6.1, and a quadratic function fitted to the values when plotted on a log-linear scale was found adequate to produce a best fit line:

$$S_{mix} = \text{asphalt mix stiffness} = E_{\frac{1}{100}}\text{th sec}$$

$$= e^{(14.648-0.0435t-0.00066t^2)} \text{ lbf/in}^2 \qquad (6.2)$$

(See Fig. 6.4)

where t = temperature in degree centigrade.

The equations of temperature with depth together with this equation define the asphalt stiffness with depth at the given times of the day.

In the finite element analysis, modulus values were assigned to elements in the asphalt layer according to the temperature at the element centroid. The model thus could

only approximate the change in elastic modulus to a step function.

Asphalt Poisson's Ratio (ν) has been found to vary with temperature and rate of loading[6.7] (for 40°F to 140°F the value changed from 0.37 to 0.498 for a $\frac{1}{100}$th sec loading time). Since no means exists to quantify the value accurately over the intermediate range a constant value of 0.4 was chosen.

The subgrade was given properties representative of a dense sand:

$$E = 10{,}000 \text{ lbf/in}^2 \qquad \nu = 0.4$$

6.4 Method of Analysis

The 4-node axisymmetric finite element was used in the analysis to find stresses, strains and displacements under the different asphalt stiffness conditions which were dictated by temperature variation.

The effect of a single uniformly distributed load of 100 lbf/in^2 acting over a 6 in. radius surface area was considered. The pavement configuration analysed was as that at RRL, a 12 in. asphalt layer with stiffness properties varying with temperature, overlying a dense sand. Fig. 6.5 shows a typical finite element model of this. Finite boundaries must exist thus leading to inaccuracy in displacements, stresses and strains when the finite element solutions were compared with those from the n-layer elastic program. To combat this and investigate whether inaccuracy could be reduced, the area covered by the mesh idealisation was extended. This was at the expense of making each element

bigger since computer storage restrictions did not allow a more refined mesh. Comparison with n-layer elastic theory is shown in Chapter Appendix 6.4 where improving agreement with n-layer theory using an extended mesh area is apparent.

6.5 Results

The investigations of the effect of the different pavement stiffness conditions at different times of the day and the effect of considering temperature gradient as opposed to a mean value (see Fig. 6.3) in the layer were possible using results from the finite element model only. Automated graph plotting was used to examine stresses and displacements to establish the significant trends.

Vertical displacements on the axis below the centre of the loaded area (Fig. 6.6) changed by a maximum of 100% at the surface as a result of asphalt stiffness changes between 05.00 and 17.30. This clearly demonstrated the very significant effect of change of temperature on asphalt pavement behaviour.

The radial and vertical stresses (Fig. 6.7) changed significantly and in a predictable manner. As the asphalt layer became hotter at the surface, the radial compressive stresses at the surface were reduced and the tensile stresses at the base of the layer increased. Vertical stresses increased throughout the upper layer and subgrade as the asphalt layer became weaker.

The difference between solutions computed using an accurate temperature gradient and the simple assumption of a

mean temperature within the asphalt layer was of interest. At 14.30 the maximum gradient existed and, as might be expected, the maximum difference in solutions was found. This applied both to vertical displacements (Fig. 6.8) and stresses (Fig. 6.9). The error involved in making the simpler assumption;that one value of stiffness could be used for the layer,was very small at 05.00 but at 14.30 became significant. The radial stresses (Fig. 6.9 i)) demonstrate this with an estimate 20% low at the base of the layer using a mean value.

From the above selected plots it can be seen that both absolute temperature changes and the simplifying assumption of a single layer stiffness value are significant. A structural design approach to pavement design involves the limiting certain stress and strains, Tables 6.1-4 show the variation of these values, with the time of day and the assumption made in the analysis. All values are the maxima experienced in the analysis, being directly under the loaded area. The strain values were calculated at the centroids of finite elements and are thus not exactly the maximum values which would be experienced in the system. They are, however, satisfactory for the purpose of the comparisons being made in Tables 6.1-4.

The temperature has a less steep gradient at 05.00 and 22.30 which reflects itself in there being little difference in values whether the gradient is taken into consideration or simply the mean value taken. Radial strains (Table 6.1) are most changed by considering gradient.

Tables 6.1-4 a) Variation in design parameters throughout the day

b) Comparison of results by considering a gradient of stiffness through asphalt layer with mean stiffness solution

(All analyses by Finite Element Method)

Table 6.1 Radial strain at base of layer (ϵ_r)

	Time	Temperature gradient, varying stiffness	% inc.	Mean temperature, constant stiffness in the layer
	05.00	6.715×10^{-5}	-6.0	6.313×10^{-5}
% inc.		+114		+185
	14.30	1.440×10^{-4}	+18.0	1.797×10^{-4}
% inc.		-9.0		+3.7
	17.30	1.311×10^{-4}	+29.0	1.863×10^{-4}
% inc.		-12		-35
	22.30	1.158×10^{-4}	+4.4	1.211×10^{-4}
% inc. to 05.00		-42		-48

Table 6.2 Subgrade vertical stress (σ_z) lbf/in^2

	Time	Temperature gradient, varying stiffness	% inc.	Mean temperature, constant stiffness in the layer
	05.00	-2.73	0	-2.73
% inc.		+116		+120
	14.30	-5.89	+2.0	-6.01
% inc.		+3.7		+2.8
	17.30	-6.11	+1.1	-6.18
% inc.		-28		-28
	22.30	-4.40	+0.5	-4.42
% inc. to 05.00		-38		-38

Table 6.3 Vertical strain in subgrade (ε_z)

	Time	Temperature gradient, varying stiffness	% inc.	Mean temperature, constant stiffness in the layer
	05.00	-2.306×10^{-4}	-1.7	-2.266×10^{-4}
% inc.		+112		+144
	14.30	-4.898×10^{-4}	+13	-5.538×10^{-4}
% inc.		+6.1		+3.1
	17.30	-5.198×10^{-4}	+9.8	-5.708×10^{-4}
% inc.		-25		-35
	22.30	-3.888×10^{-4}	-4.0	-3.732×10^{-4}
% inc. to 05.00		-41		-39

Table 6.4 Surface displacement (δ_z) ins

	Time	Temperature gradient, varying stiffness	% inc.	Mean temperature, constant stiffness in the layer
	05.00	8.300×10^{-3}	-0.1	8.295×10^{-3}
% inc.		+108		+97
	14.30	1.725×10^{-2}	-4.9	1.641×10^{-2}
% inc.		+1.4		+2.7
	17.30	1.750×10^{-2}	-3.7	1.685×10^{-2}
% inc.		-29		-26
	22.30	1.238×10^{-2}	-0.6	1.245×10^{-2}
% inc. to 05.00		-33		-33

After the hottest time of the day (14.30) the assumption that a single value of stiffness can be used for the whole layer becomes unreasonable. Radial strain would be predicted 18% high and surface displacement 5% low. These large discrepancies are carried over to 17.30. The importance of taking the temperature gradient into account is thus clearly demonstrated.

6.6 Implication on Design

The implication on design of the variation of pavement stiffness throughout the day is marked. The effect on all of the design parameters is virtually the same. From 05.00 to 14.30 an increase of over 100% was found to occur. If a mean value of stiffness was considered, then the effect was more erratic. The change in radial strain at the base of the layer, the vertical strain in the subgrade and the subgrade vertical stress were all predicted as higher.

Except for the radial strain, all values increase further to the time 17.30, thereafter decreasing to 05.00. The total changes are thus predicted as follows:

Table 6.5 Maximum changes in design parameters derived from Tables 6.1-4

Design Parameter	Time change	% change for loading considered
(i) Radial strain at base of layer	05.00-14.30	+114
(ii) Subgrade vertical stress	05.00-17.30	+120
(iii) Vertical strain in subgrade	05.00-17.30	+118
(iv) Surface displacement	05.00-17.30	+109

The implications on pavement design methods based on a structural design approach are important. If the radial tensile strain at the base of the layer is considered as the criterion for design[6.1], then pavement life as predicted is reduced by the temperature rise in the asphalt. In detail, for a bituminous material close to that used in the RRL test sections (curve 2 given by Brown and Pell, Fig. 4, Ref. 6.1), a relationship between fatigue life and the maximum applied strain was given as:

$$N(\text{cycles}) \propto \left(\frac{1}{\varepsilon}\right)^{3.4}$$

Using the maximum variation in the radial strain given in Table 6.1 this results in

$$\frac{N_{05.00}}{N_{14.30}} = \left(\frac{\varepsilon_{14.30}}{\varepsilon_{05.00}}\right)^{3.4} = \left(\frac{144}{67.2}\right)^{3.4} = 15.5$$

Life, expressed as load cycles to failure, was thus predicted as 15 times longer with the stiffer pavement given by the temperature distribution at 05.00 than that at the hottest time of the day. This is obviously very significant and possibly more important than the effect of material non-linear elastic properties (Chapter 5).

An approach to the prediction of pavement life based on the vertical compressive strain[6.8] in the subgrade yields a 56 times change in number of axle load applications to failure.

$$\frac{N_{05.00}}{N_{17.30}} = \frac{1.8\times10^{8}}{3.2\times10^{6}} = 56$$

However, in absolute terms life was predicted as much longer by the latter approach. At 05.00 a vertical subgrade strain of 2.31×10^{-4} predicts a life of 1.8×10^{8} applications. This is approximately 500 times the life of 3.5×10^{5} cycles predicted by consideration of the maximum tensile strain in the asphalt layer (ref. 6.1).

6.7 Conclusions

The mix used at the RRL in a 12 in. thick layer thus yielded a situation where asphalt tensile strain would have been the critical factor in design. The comparison of the two design criteria showed, however, that vertical subgrade strain was more sensitive to the temperature changes experienced than radial tensile strain at the base of the layer. The predicted change in road pavement life was high showing temperature to be a very important factor.

There is a need for more widespread measurement of temperatures occuring within road pavements and the environmental factors associated with them. In many parts of the world pavement temperatures and their gradients are likely to be much higher than in the United Kingdom, and the implications on design would appear more important. However, in hotter countries it is usual for bituminous layers to be thinner and thus for the non-linear properties of sub-base and subgrade materials to be more important in design.

In this exercise no account has been taken of a likely traffic spectrum. This either could reduce or increase the effect depending on whether maximum loading occurred at the

hottest or coldest time of the day. Kasianchuk[1.19] has quantified the effect of traffic density using his "traffic weighted mean stiffness" concept.

The Author has simply calculated the likely order of magnitude of the effect on design of temperature changes experienced in the United Kingdom and found it to be significantly high and meriting further investigation.

Appendix 6.1: Equations of curves for temperature with depth in asphalt: 7th July, 1970

12 in. asphalt layer RRL Crowthorne

Curves in Fig. 6.3

Notation t = temperature (°C)

z = depth below surface (inches)

Time	Equation	Range of z values valid
05.00	$t=20+{}^{5}/_{12}z$	0 - 12
14.00	$t=50-{}^{25}/_{12}z$	0 - 12
17.30	$t=47-z$	0 - 3
	$t=50-2z$	3 - 9
	$t=41-z$	9 - 12
22.30	$t=30+\frac{2}{3}z$	0 - 6
	$t=38-\frac{2}{3}z$	6 - 12

Appendix 6.2: Asphalt specification

12 in. layer

$1\frac{1}{2}$ in. Rolled Asphalt wearing course

30% stone ($\frac{3}{4}$" max. size)

40/60 pen. binder

Table 7(a) BS 594 1961

TLA Blend (Table 1 Col 3)

$2\frac{1}{2}$ in. Rolled Asphalt base course

65% stone (1 in. or $\frac{3}{4}$ in. max. size)

40/60 pen. binder

Table 7(b) BS 594 1961

8 in. Rolled Asphalt base

1 in. max. size

other data as base course

Appendix 6.3: Measured properties

Ring and Ball test temperature	65°C	} bitumen
Penetration index	0.5	
C_v = 0.84		} asphalt

Appendix 6.4: Effect of extended finite element mesh area

The mesh size within 12 in. of the loaded area was retained, the boundaries were extended by increasing the size of subgrade elements.

Mesh	Extent of Mesh
1	110 x 70 in. (Fig. 5)
2	220 x 140 in.
3	440 x 280 in.

Time 05.00 Surface displacement (δ_z) ins

Mesh	Mean stiffness used Fin. E1, δ_z (in.)	% increase	Mean stiffness used N-layer elastic, δ_z (in.)
1	8.30×10^{-3}	+42	1.18×10^{-2}
2	9.92×10^{-3}	+19	"
3	1.07×10^{-3}	+10	"

Time 05.00 Radial strain at base of layer (ε_r)

Mesh	Mean stiffness used Fin. E1, ε_r	% increase	Mean stiffness used N-layer elastic, ε_r
1	6.31×10^{-5}	+13	7.13×10^{-5}
2	6.80×10^{-5}	+4.8	"
3	6.54×10^{-5}	+9.1	"

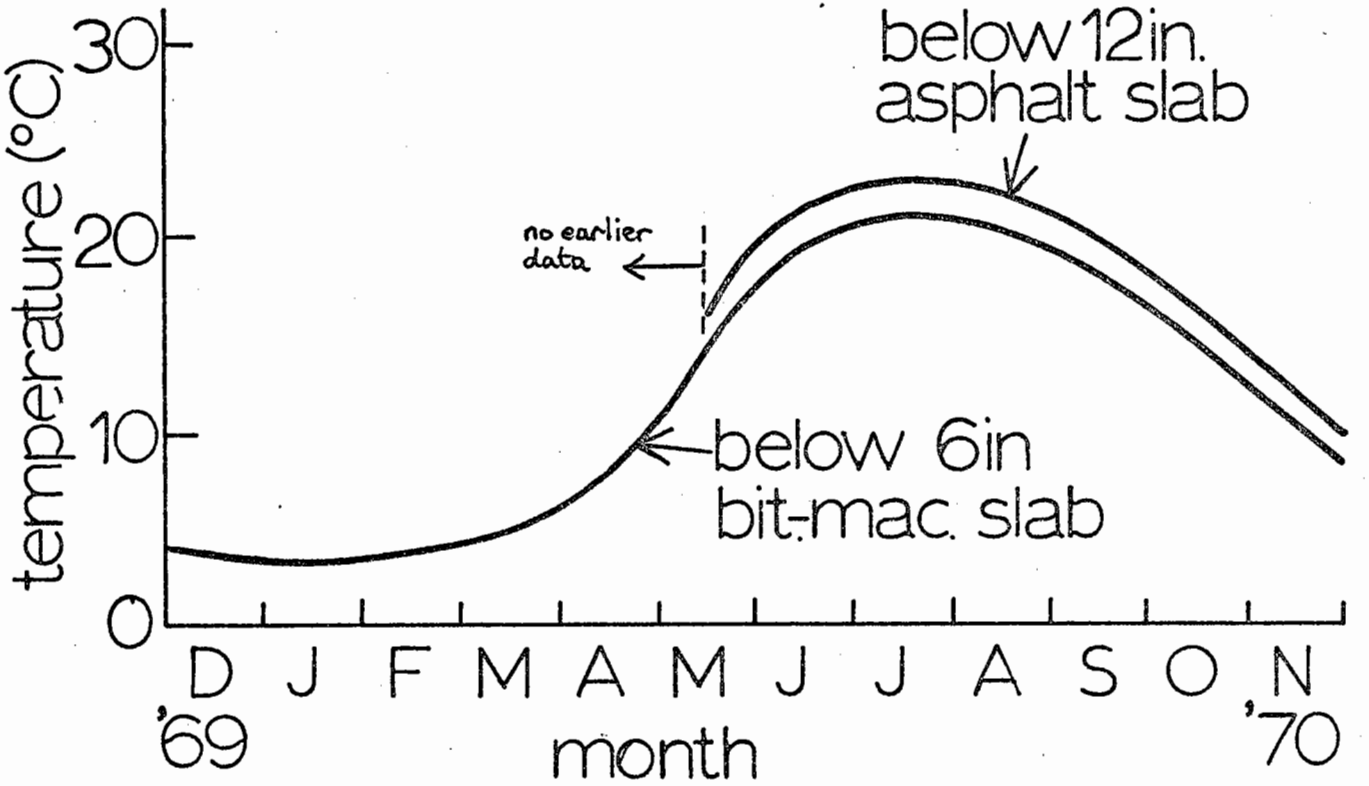

Fig. 6.1 Subgrade temperature variation at 2 ft depth (invarable throughout each day)

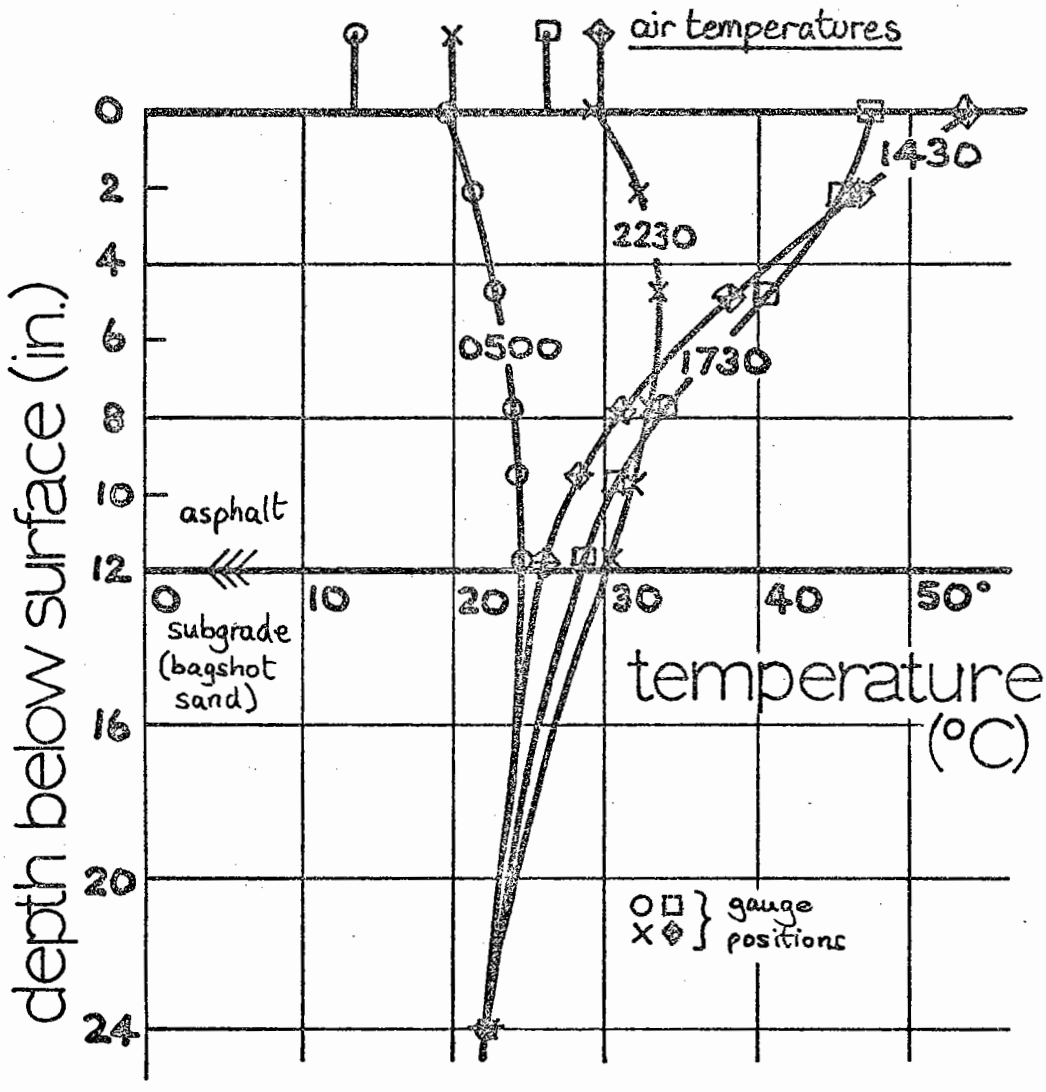

Fig. 6.2 Asphalt temperature (7 July 1970) at chosen times

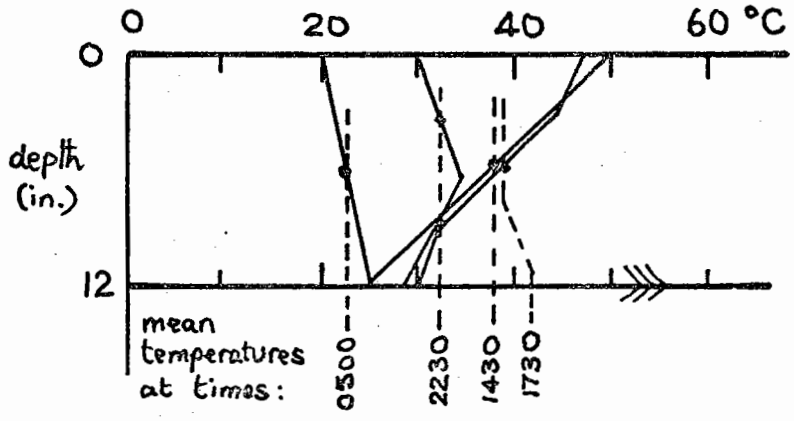

Fig. 6.3 Linear approximations to temperature gradients and average temperatures

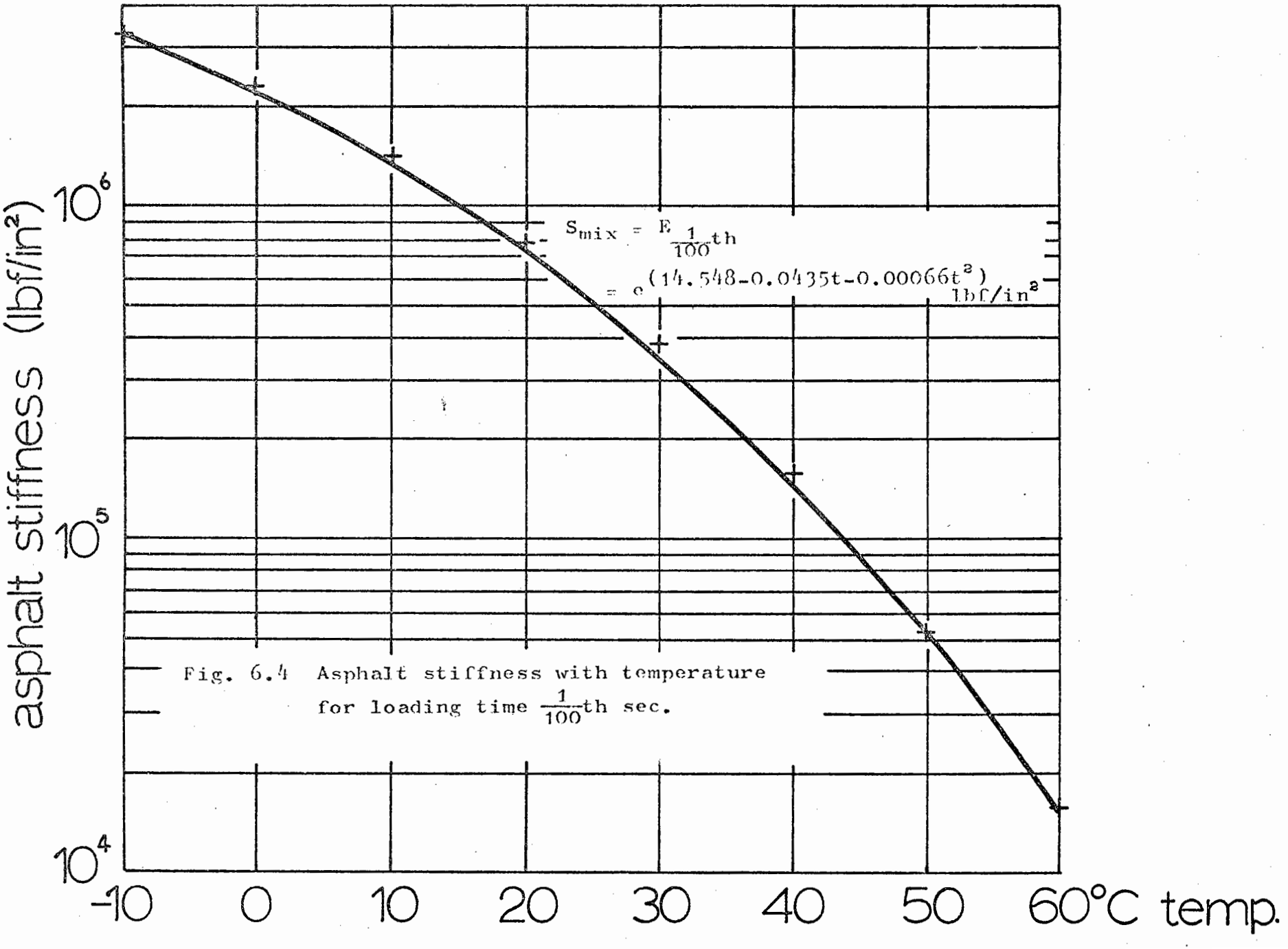

Fig. 6.4 Asphalt stiffness with temperature for loading time $\frac{1}{100}$th sec.

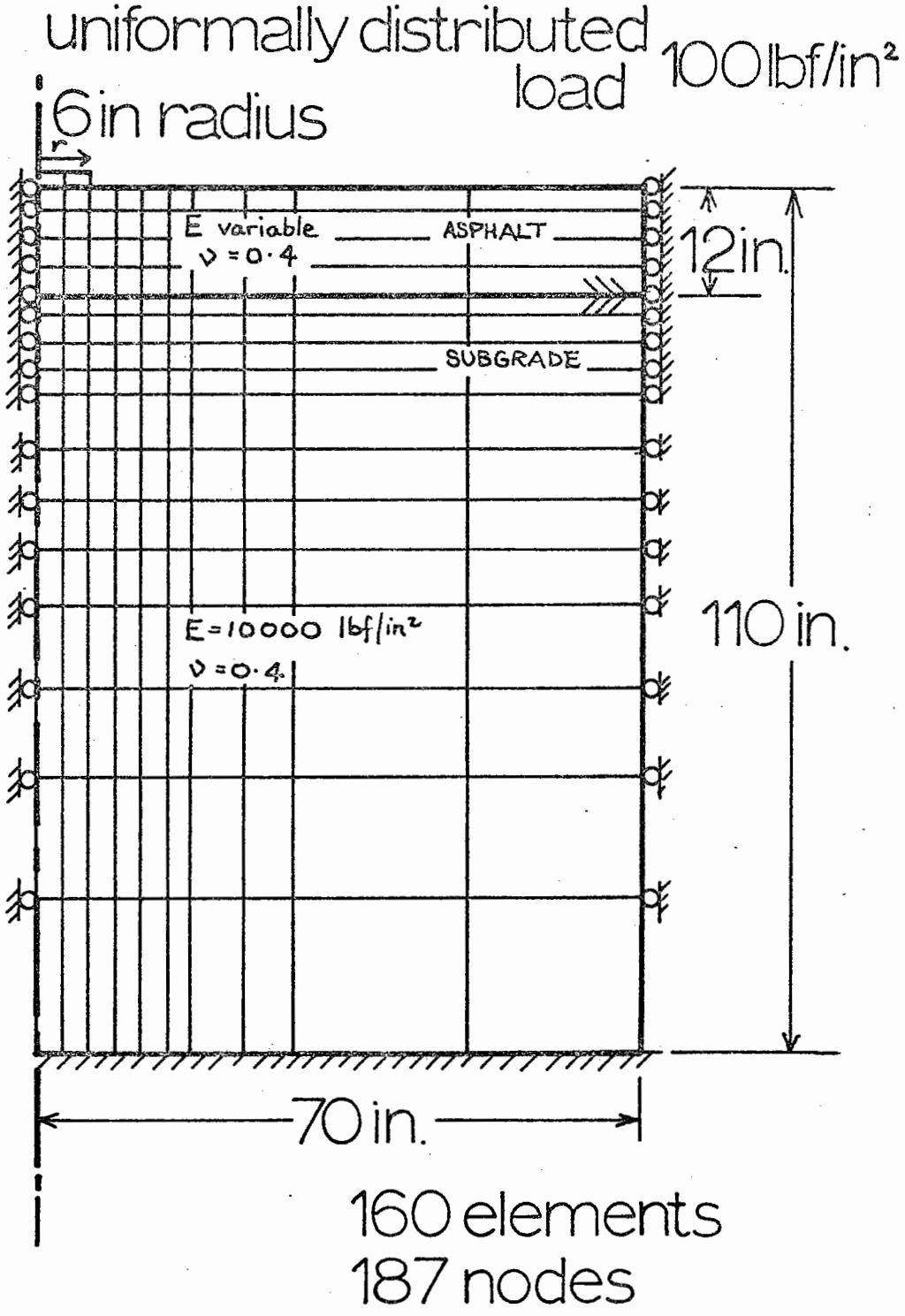

Fig. 6.5 Finite element model and loading

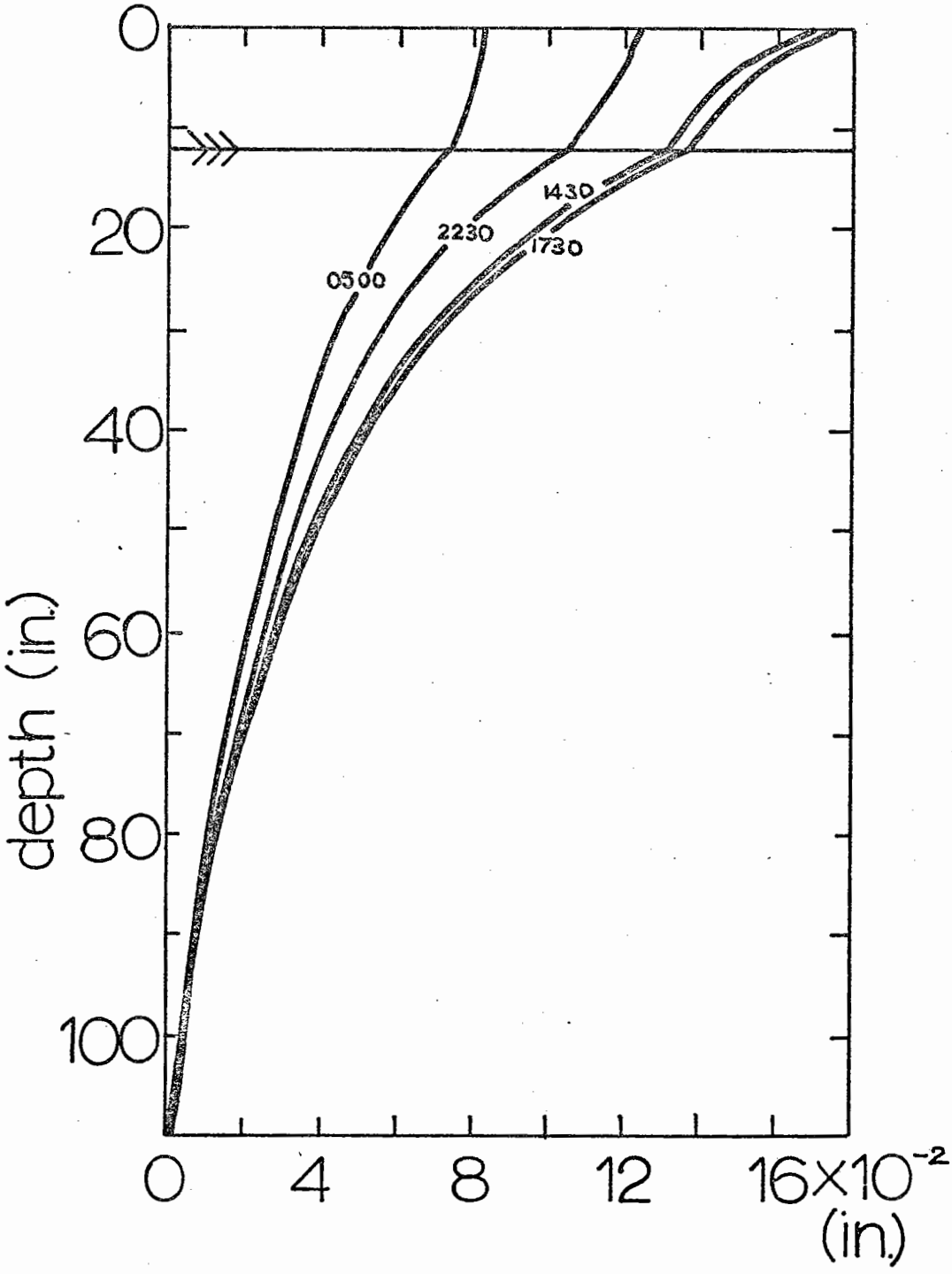

Fig. 6.6 Vertical displacement on centre line at different times using accurate temperature gradient analysis (Finite Element Method)

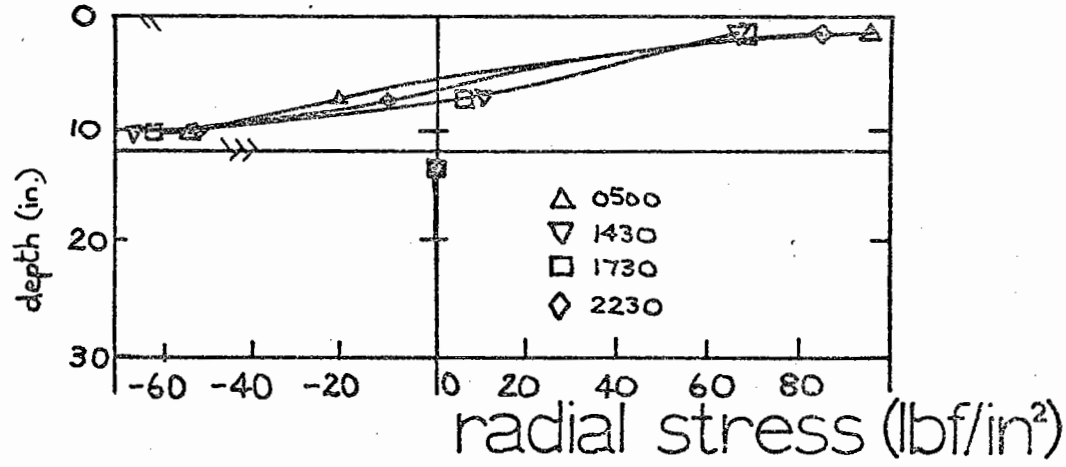

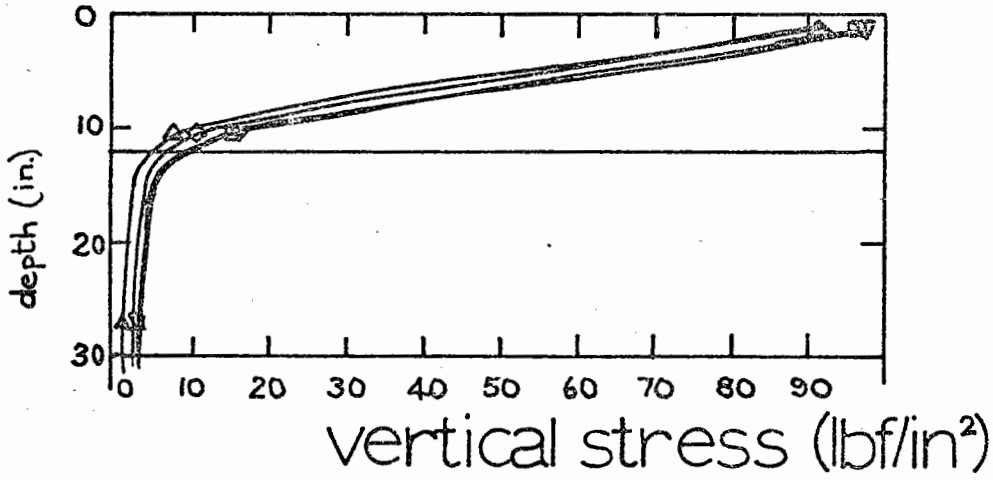

Fig. 6.7 Radial and vertical stresses on centre line at different times using accurate temperature gradient analysis (Finite Element Method)

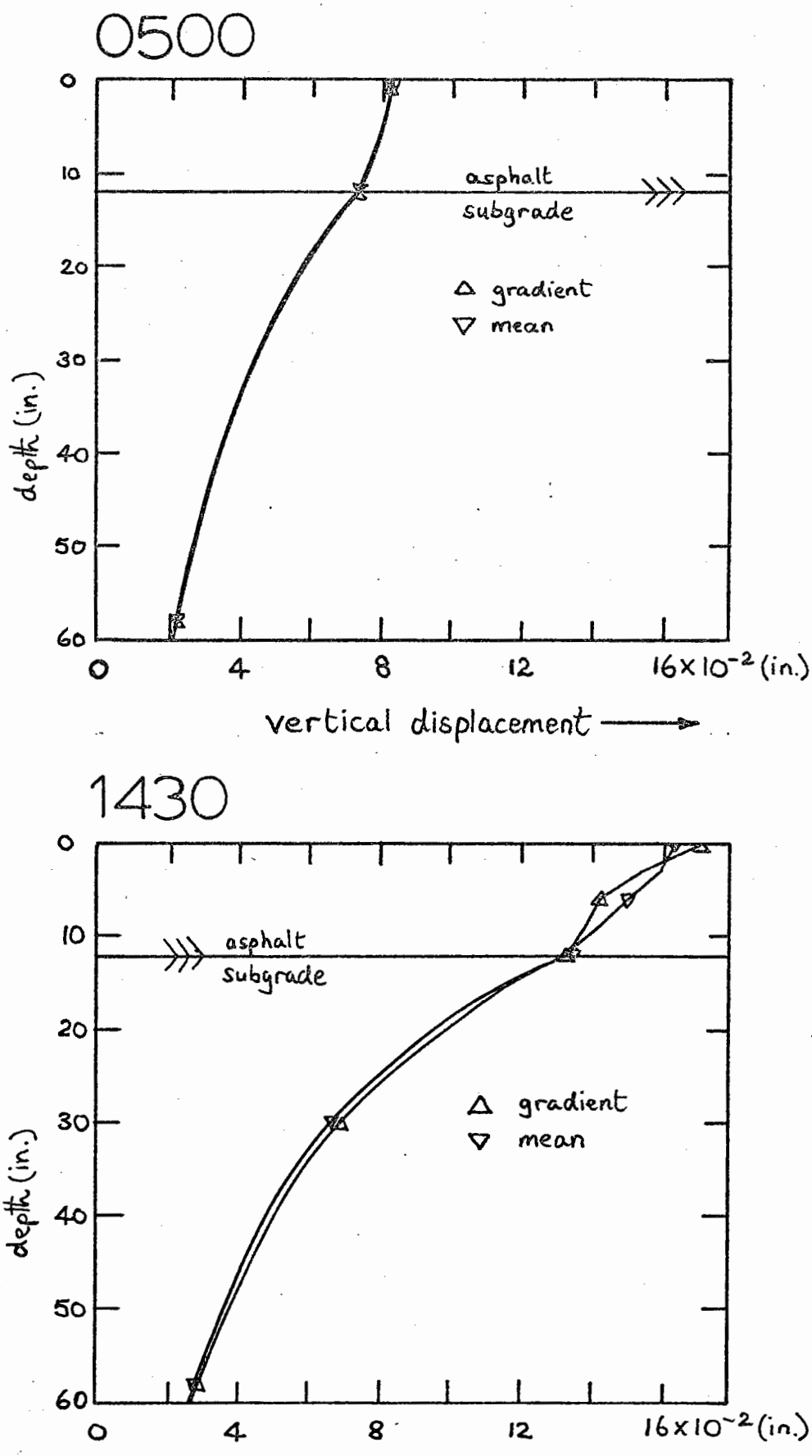

Fig. 6.8 Vertical displacements on centre line at two times of the day, calculated using gradient of stiffness and compared with values if mean stiffness assumed

i) Radial stresses

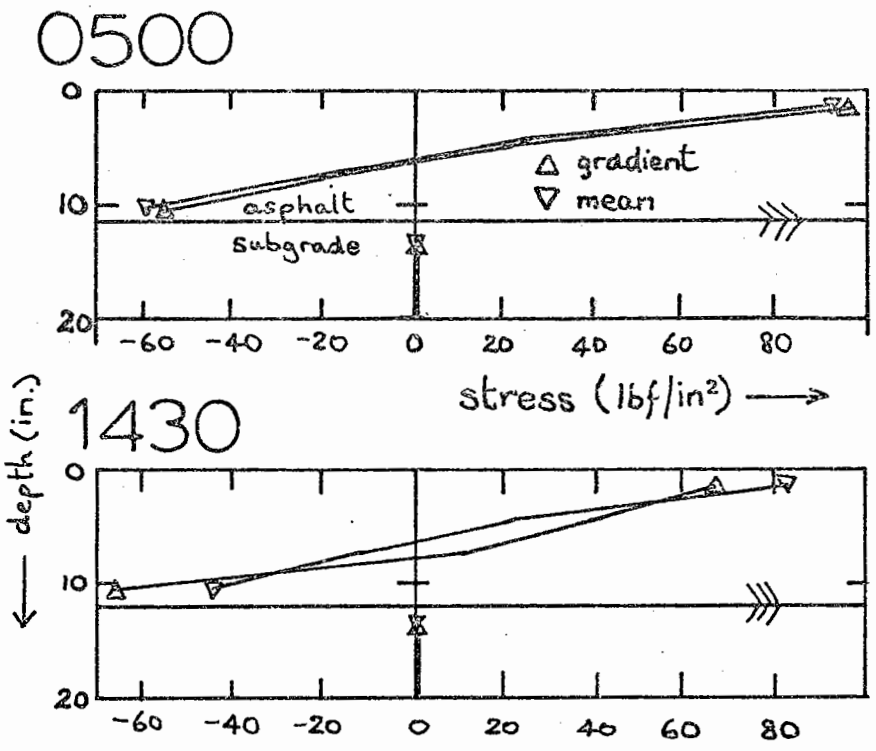

ii) Vertical stresses

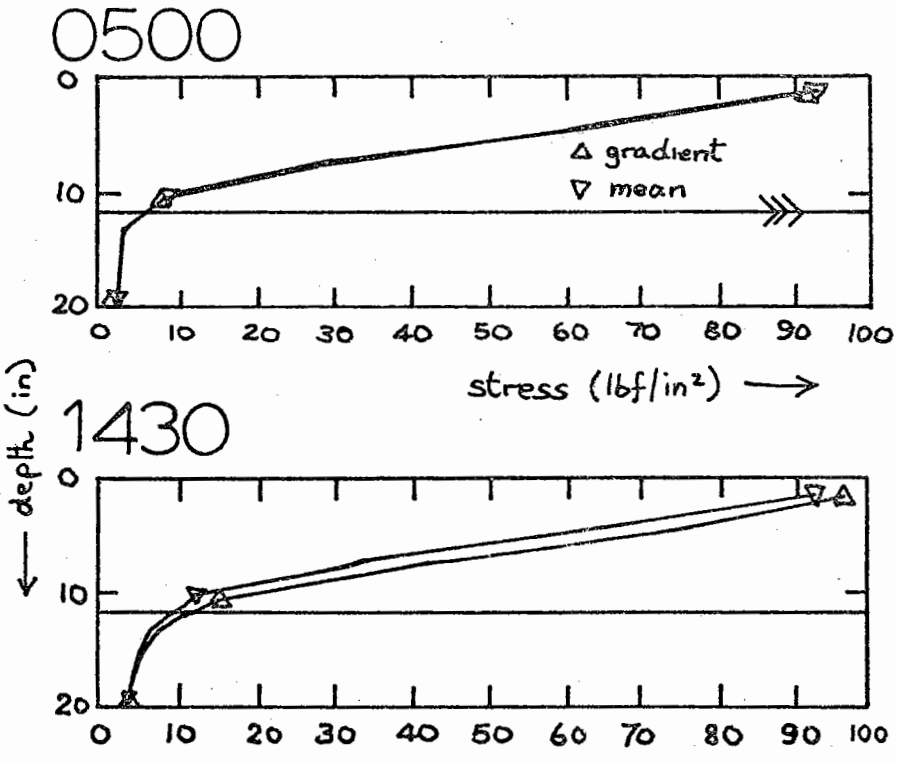

Fig. 6.9 Stresses from solutions using temperature gradient compared with single mean value solution (Finite Element Method)

CHAPTER 7

THE TRIAXIAL TEST

7.1 Introduction

The triaxial test is extensively used to establish the characteristics of a soil or bituminous material in either static or dynamic loading tests. It was explained in Chapter 3 that in order to obtain suitable characteristics for a soil some measurement of the volumetric strain is required. End frictional restraint is known to cause a barrelling of the cylindrical specimen and thus complicates any correction being made for change in cross-sectional area. The barrelled shape is itself caused by a change in the distribution of stress within the specimen away from the values which would nominally be applied, as if by a rigid end platen.

Theoretical stress distributions were produced by the finite element method which was modified to take account of frictional forces between the end platen and specimen and base. Mean normal stress and octahedral shear stress, explained to be fundamental in influencing failure in Chapter 3, were paid particular attention. The mode of failure of cylindrical bituminous material specimens tested in unconfined repeated load tests[7.1] were compared with the theoretical stress and strain distributions. Any conclusions about failure, however, could only be expected to be qualitative since the finite element analysis used considered only the

elastic properties of the materials. The errors likely in the measured material characteristics as a result of end frictional restraint and specimen geometry are presented as being of most interest.

7.2 Previous Findings

Work has already been done on the calculation of stress distributions in the triaxial specimen. Balla[7.2] produced equations for the stresses, strains and displacements in a cylindrical specimen based on Elasticity Theory. He tabulated stress as characterised by the octahedral shear stress for $\ell/d = 2$ and total end fixity. The integrals involved in calculation were complex and required a computer program for their solution and boundary conditions were difficult to change. Balla did not attempt to model an end platen but assumed the nominal distributed load acted directly on the specimen. Triaxial testing to investigate the effect of end restraint[7.3] concluded that the use of well lubricated end caps was only necessary if volumetric strain measurements were required for large values of axial strain. Another useful contribution was made earlier[7.4] when experimental evidence was given showing failure in cone shaped zones where end restraint existed. It was assumed that this occurred because of the concentration of dilation into local zones thus causing the premature development of a failure surface. Multiple failure surfaces were considered desirable and the means of achieving this found to be lubricated end platens.

Although experimentally it was shown that failure was

different and less desirable when end restraint existed, no theoretical analysis was readily available to establish which stresses were governing failure and were changing when end fixity changed.

A Coulomb failure criterion had already been shown[7.5] to be inadequate to define failure as rigid-plastic. It was found necessary to incorporate some non-linear stress-strain relationship to define behaviour more precisely.

Recently work in progress, and allied to this, has been reported[7.6] (1971) where the soil behaviour in the triaxial cell has been modelled using incremental finite element loading techniques. This work is aimed at "once-loaded" tests on soils, whereas the main interest in layered road pavements is for modelling of the materials under dynamic conditions.

Non-linearity of the deformation characteristics would seem to be of most importance in a heavily stressed sub-base or subgrade material. The bituminous layer structural properties are more influenced by temperature, than stress level (Chapter 6 and ref. 1.19).

Linear elastic analysis of the test, given the advance of being able to model end frictional restraint was thus considered of interest. The versatility of the finite element method, particularly the ease with which geometry and boundary conditions can be changed, made it a useful tool to theoretically analyse test specimens and help decide on the magnitude of factors such as the ℓ/d ratio and the thickness of the end platen for laboratory testing.

7.3 Finite Element Representation

7.3.1 The finite element idealisation (Fig. 7.1) represents, in shape and properties, bitumen-macadam specimens being tested under dynamic loading at Nottingham. A 1 in. thick steel end platen, acted on by a point load at its centre, distributes the load to the 4 in. diameter cylindrical specimen. The 4-node axisymmetric rectangular finite element was used in the analysis with certain modifications in order to mobilise interface frictional forces at the top and bottom of the specimen (Appendix, Program 5).

Values of the friction constant (μ) derived from tests at Nottingham[7.1] were used in the analyses as given in Table 7.1. In addition the extreme values, $\mu = 0$ and full fixity were considered.

End platen	μ
mild steel	0.25
hardened steel	0.1
lubricated	0.005

Table 7.1 End platen - bitumen macadam friction

7.3.2 End frictional forces

The basic finite element method relies on the composition by superimposition of a structural stiffness matrix and on the solution of this set of equations for nodal displacements given a vector of loads. In order to incorporate forces mobilised by friction at an interface, it was necessary to

provide two sets of nodal points at each interface (Fig. 7.1) and in addition join the two separate parts of the structure using dummy (linkage) stiffnesses. This was identically the technique used in finite element analysis of bond in reinforced concrete beams by Ngo and Scordelis[7.7]. A connection stiffness was derived from this work for the particular case where the interface is parallel to the co-ordinate axes:

$$\left[\begin{array}{cc|cc} k_h & 0 & -k_h & 0 \\ 0 & k_v & 0 & -k_v \\ \hline -k_h & 0 & k_h & 0 \\ 0 & -k_v & 0 & k_v \end{array}\right]$$

k_h = horizontal dummy stiffness

k_v = vertical dummy stiffness

Each pair of nodes was thus joined, both in the radial and vertical direction by an 'element' of no dimension but having stiffness. For a pair of nodes this can be visualised as Fig. 7.2 i). By giving the stiffness a high enough value in comparison with the adjoining material, the deformation between the nodes was found to be negligible. (A value of 10^{10} lbf/in^2 was found satisfactory for this purpose.)

Freedom of horizontal movement between nodes on the interface (equivalent to $\mu = 0$, Fig. 7.2 iii)) was achieved

by setting $k_h = 0$. The intermediate cases, $0 < \mu < 1$, required mobilisation of horizontal frictional forces, Fig. 7.2 ii). However, these could not be calculated unless the nodal displacements were known (Eq. 2.12), and therefore an iterative procedure was required.

Starting from the situation in Fig. 7.2 iii), with $k_h = 0$ and $k_v = 10^{10}$ lbf/in^2, the set of vertical nodal forces (F_i) along the interface, as a result of the point load alone, were calculated. The frictional forces, μF_i, were then placed in the load vector, along with the external load, and the equations resolved. New forces were calculated and the process repeated until successive sets of forces were found to agree to the 3rd significant figure.

The iterative behaviour of the computation of the interface friction forces for the two extreme values of coefficient of friction, 0.25 and 0.005, was as presented in Table 7.2. Nodes and elements referred to in the tables are shown in Fig. 7.1.

It is apparent that 5 iterations were necessary for the case, μ=0.25, and 3 for $\mu = 0.005$. Although the vertical displacement under the load was changed little in the final iterations, the radial stresses near the interface were changed markedly during the computation and their rate of change closely followed that of the frictional forces.

This technique for incorporating frictional forces in the finite element method was thus proven feasible.

7.3.3 Special features in finite element program (Appendix, Program 5)

i) automatic data generation modified (GEN4NM) to

Table 7.2 Iteration for frictional forces (6x4 in. specimen)

i) $\mu = 0.25$

Iteration number	Vertical displacement under load in.x10^{-3}	Radial Friction Forces (lbf)		$\sigma_{r_{33}}$ lbf/in^2 element 33 (centre)	$\sigma_{r_{40}}$ lbf/in^2 element 40 (edge)
		node 45	node 270		
1	-3.25	36.1	-37.8	-6.58	-0.08
2	-3.14	51.0	-53.4	-77.7	-5.97
3	-3.13	52.7	-55.3	-72.0	-10.66
4	-3.13	52.9	-55.4	-72.1	-11.27
5	-3.13	52.9	-55.5	-72.1	-11.31
ii) $\mu = 0.005$					
1	-3.25	0.723	-0.756	-6.58	-0.08
2	-3.25	0.729	-0.762	-8.00	-0.20
3	-3.25	0.729	-0.762	-8.00	-0.20

provide double row of nodes at interfaces.

ii) post dummy stiffnesses to structure stiffness matrix (LINK)

iii) modified loading procedure (LOADM, LOADFR) to place structure loads and last calculated frictional forces into load vector

iv) calculation of frictional forces on interfaces (FORCES)

One further procedure (FXTEST) was incorporated which ensured that no loads were applied at nodes in a direction already specified by procedure (FXBDIT) to have zero displacement. This applied in the case of radial friction forces at the centre line (where only vertical movement was allowed).

7.4 Theoretical Investigations

7.4.1 End platen imposed stresses

A point load applied vertically on the centre of the end platen was chosen in order to give a nominal vertical stress on the specimen of 100 lbf/in^2. Computations incorporating the various degrees of end frictional restraint were carried out and revealed a deviation from the mean value due to both distortion of the end platen and changes in the frictional restraint. Plots of the vertical stress immediately beneath the end platen (Fig. 7.3) for 4, 6 and 8 in. long specimens showed this. It can be seen that there was no significant change in the distributions as a result of change in specimen length, Figs. 7.3 i), ii) and iii) have substantially identical appearance.

The frictionless case ($\mu=0$) showed an increase in stress at the centre of the end platen of 10%. This must isolate the effect of end platen flexibility, since no frictional forces are acting. At the edge of the end platen a 4% reduction of vertical stress took place.

Increasing frictional restraint reduced the discrepancy in stress level below the centre of the end platen so that the fully fixed case showed a reversed trend. The vertical stress was less than the nominal value, reaching a maximum discrepancy of -8% at about $\frac{2}{3}$ of the radius from the centre-line. Very near to the outer edge of the specimen a sharp increase in stress took place predicting values 20% higher than nominal. The varying degrees of frictional restraint caused stress distributions lying between the above extremes with $\mu=0.1$ giving a distribution approximately nearest the nominal value. The sense of the increases or decreases in the nominal value of vertical stress are perhaps predictable, the magnitude is not. Here it has been demonstrated that using a standard end platen the specimen has imposed on it, stress levels considerably different from those expected. Frictional restraint has been shown to reduce the vertical stress acting over most of the surface of the specimen but increase that at the edge considerably. The above gives an indication of the order of magnitude of the changes in nominally applied stress at the point of application; some mention of the likely effect on material characteristics is warranted before further detailing stress and strain changes.

7.4.2 Displacements

The calculation of an axial modulus (e.g. in repeated load tests on bituminous materials) or bulk and shear moduli (as described in Chpt.3) relies on the stress distribution in the specimen under test being that nominally applied. If it was assumed that the end platen was infinitely stiff, perfectly lubricated and no Poisson's ratio effect existed, an axial modulus could be calculated as:

$$E = \sigma.\frac{\ell}{\delta}$$

σ - imposed vertical stress

ℓ - length

δ - axial displacement

These are the assumptions used in calculating the final column in Table 7.3.

size (in.) \ μ	fixed	0.1	0.005	0	∞ stiff end platen μ=0
4x4	1.911	1.990	2.046	2.048	2.001
% inc. from ∞ stiff solution	-4.5	-0.5	+2.3	+2.4	
6x4	2.909	3.004	3.046	3.049	3.001
% inc.	-3.1	-1.0	+1.5	+1.6	
8x4	3.906	4.004	4.047	4.049	4.001
% inc.	-2.4	+0.7	+1.1	+1.2	

Table 7.3 Vertical axial displacement for varying size of specimen and end frictional restraint ($x10^{-3}$ in.) +% deviation from simple elastic calculation

Table 7.3 shows axial displacement for varying length of specimen and frictional restraint and demonstrates that

the above assumption could lead to discrepancies in "modulus" based simply on axial displacement. The percentage increase in displacement compared with the simple calculation is given. The solutions gave axial displacements both higher and lower than that using this "simple elastic calculation", since the assumptions themselves were not being adhered to. A value of $\mu=0$ (4x4" specimen) led to a vertical displacement 2.4% higher than that using the simple calculation, confusing the effects of end platen flexibility and Poisson's Ratio. However, the "fully fixed" calculation led to displacements 4.5% lower than the simple calculation, or about 7% lower than the finite element computation for $\mu=0$.

The implication was that end platen flexibility effects would have lowered the apparent axial modulus of the specimen and increase in end friction have raised it.

Increased specimen size had the effect of decreasing both the discrepancy with a simple elastic calculation and the difference between the solution from a fully fixed and "perfectly lubricated" finite element model. This occurred since a greater length of the specimen away from the ends was at nearer nominal stress conditions; as will be shown.

The radial displacements at the edge of the specimen, (Fig. 7.4), show the deformed shape becoming increasingly non-cylindrical with increasing end restraint. Any measurement of radial deformation would of necessity require care. If the volume change in a triaxial cell was measured to obtain radial strain measurements (as would be required if bulk and shear modulus were being measured (Chapter 3)), then, either

corrections would be required or, more desirably, friction should be reduced to a minimum.

If tests were required to establish the tensile characteristics of bituminous materials, and ends were of necessity fixed, then it is suggested by Fig. 7.4 that measurements of both axial and radial deformations would be better made in the region further than 1.5 in. from the ends of the modelled specimen. Uniform radial displacement does exist over the remaining length of the specimen. This length varied for different size of specimen since the region influenced by the end restraint was roughly constant for a particular size of end platen.

Finite element analyses of this kind have thus influenced the positioning of instrumentation in tests on bituminous specimens at Nottingham[7.1].

7.4.3 Stress distribution within specimen

The vertical compressive stress on the centreline and at the edge of a 6 in. long specimen was affected by the end platen flexibility and end constraint. Stresses on the vertical axis (Fig. 7.5i) were consistently higher than the nominal 100 lbf/in^2 except at the ends where radial frictional restraint caused a lowering.

At the base the effect of end restraint was more marked with 10% reduction in vertical stress. This was countered by an increase at the edges (Fig. 7.5ii). At the base of the specimen the effect of frictional forces was isolated (since the base was considered as virtually rigid). The top end platen flexibility caused a 10% increase in the vertical

stress under the load with no friction present, but it is notable that within 2 in. of the end the nominal value had been reached and maintained down through the specimen to the rigid base.

Complete end restraint led to a 5% increase in vertical stress at the middle of the specimen and at 5% decrease at the edge, nearer the ends the situation was worse.

The radial stress on the centreline (Fig. 7.5iii) became compressive in the region of the ends, indicating that here existed a state of all round compression which was acting as an extended end platen. Low values of tensile stress were experienced near the surface at the middle of the specimen, which in the case when the end restraint was high, became greater. This would indicate that the load required to cause a tensile or hoop stress failure at the specimen edge would be lower than if there was no end restraint.

7.4.4 Stress invariant distributions

Since it was considered that the first two stress invariants influenced failure of a specimen (Chapter 3), their distributions for varying degrees of end friction and specimen length were examined. Figs. 7.6 and 7.7 show σ (mean normal stress) and τ (octahedral shear stress). The hatched regions had imposed on them levels of stress more than approximately 5% above or below the nominal value,

i.e. σ nominal $= \frac{1}{3}(100+0+0) = 33.3$ lbf/in^2

$$\tau \text{ nominal} = \tfrac{1}{3}\sqrt{(100-0)^2+(0-0)^2+(0-100)^2}$$

$$= 47.1 \text{ lbf/in}^2$$

σ/τ nominal = 0.705

Both plots showed that a lubricated end platen (μ=0.005) would lead to a greater length of the specimen being near the nominal stress value. The 4 x 4 in. specimen with fixed ends, for example, was predicted as having only a very small region where either σ or τ was near nominally stressed. The importance of lubricated end platens or more important the considerable deviation from the norm in fixed-end tests were thus clearly demonstrated. The small deviation in the "free" case could only be due to end platen flexibility and would be removed by strengthening it.

7.4.5 Failure

Plots of σ/τ (Fig. 7.8) clearly would suggest different types of failure for varying end restraint. (Lower values indicate regions more likely to be critical.)

In the case of full end fixity, a conical zone of higher values existed near the end platens and failure would be predicted to occur outside this zone. The testing of bituminous material specimens by Snaith at Nottingham[7.1] has verified that this occurs (Fig. 7.9). With lubricated end platens barrelling of the specimen did not occur (Fig. 7.10) and failure was observed to be preceeded by the appearance of vertical cracks which started about 1.5 in. from the ends of the specimen. Heukelom[7.8] observed the same type of failure in such specimens and concluded the cracks to be due to excessive hoop strain.

Fig. 7.5 iv shows that if some end restraint exists then

hoop strains at the specimen edge are greatly reduced and thus explains why cracks did not extend to the ends. The radial strains at the outer edge of the specimen (Fig. 7.5v) were found to be lower than the hoop values and thus, accepting a strain criterion of failure for bituminous materials, are of no significance. The horizontal strains at the centre of specimens with full end restraint (Fig. 7.5vi) were predicted as higher than the hoop values at the specimen edge. It is thus likely that the actual failure of a bituminous material would be on the centreline under the point load due to excessive tensile strain.

Soils which have little tensile strength are known to behave differently. The failure of clays in compression, for example, is thought to be primarily due to excessive shear stresses. If shear stresses were the only factor involved, then failure predicted by the distributions in Fig. 7.7 certainly would not predict the typically found conical failure in the case of full end restraint. The highest shear stresses in this case existed on the centreline of the specimen at slightly greater than half the length from the base, and not along a sloping line. Acceptance of failure being governed by both normal and shear stresses, however, (Fig. 7.8) in the "fixed end" case, would lead to the more realistic prediction of a conical region near the ends where failure was less likely (similar to Fig. 7.9).

7.5 General Observations

The finite element method has been used to calculate

stresses, strains and displacements and assist in the design of satisfactory testing methods for the triaxial testing of bituminous materials. The importance of the end platen flexibility and end platen/specimen interface frictional forces on the stress and strain distributions have been established. The effective length of the specimen where gauges to measure radial deformation could be placed has been established.

The likely effect of the end effects on "elastic modulus" values for different ℓ/d ratio specimens has been established to be no greater than 7% at the most.

The mode of failure in compression has been accurately predicted for a bituminous material specimen giving confidence in the common failure criterion supported by Domaschuk and Wade[3.1] and Schofield and Wroth[3.6], namely that failure in compression is dependent on σ (mean normal stress) as well as τ (octahedral shear stress).

Failure in tension in bituminous materials has been found to lead to a plane fracture at 90° to the axis of applied principal tension. This demonstrates the point made in 3.6.5 that failure in tension and compression is fundamentally different. In tensile tests, fixed end platens are obviously essential and stress conditions would be as in Figs. 7.6/7/8 ("fixed" case), but with opposite signs. The applied tensile stress would lead to a simple tensile failure when the limiting value for the material was exceeded.

The "dead" conical area of all round compression in fixed ended specimens under axial compression could have

important significance in repeated load tests. If failure could be considered as the result of deformations accumulated at each load cycle,or as the gradual absorption of energy, then failure would occur prematurely in "fixed end" tests. All work would have been done (or all shear deformation occurred) away from the conical regions of all round compression and have led to a local failure in the specimen rather than an overall breakdown.

7.6 Extension to Pavement Analysis

Accepting σ/τ in compression and limiting tensile stress in states of all round tension (see section 3.6.5) as criteria for failure,the possibility of being able to identify the likely critical regions in a layered pavement exists. The comparison of σ/τ values found to be critical from lubricated end triaxial tests of the materials,could be compared with the values obtained from the finite element analysis of a pavement system,and lead to the prediction of likely zones of failure.

7.7 Reservations

No attempt has been made to model the test beyond the elastic range since tests on bituminous materials[7.1] have shown elastic behaviour close to failure.

In soils, large deformations occur as the result of dilation under shear stresses, which in a pavement would result in the accumulation of permanent deformation at well below a failure load. Attention is being paid to this problem by

the use of incremental loading techniques in finite element[7.6] but is limited to the simulation of once-loaded tests.

The resilient part of the deformation of road pavement materials under repeated loading is known to behave in a non-linear elastic manner. Bituminous materials are known to have properties so temperature sensitive as to make investigation of any non-linear elastic properties of minor importance[1.19]. Thus lack of necessity and the high cost of the computer time to carry out an iterative analysis (within the iteration required for mobilisation of frictional forces) have negated such investigation.

Whereas one can have confidence that frictional forces are mobilised between a steel end platen and the triaxial specimen there appears to be no justification for assuming that anything but total continuity exists between layers in a road pavement. If such an analysis was ever thought justified then it would have to be borne in mind that the passage of a wheel load would cause reversal of the frictional forces at a layer interface. It is thus apparent that experimental determination of the magnitude of the mobilised interfacial friction in layered pavements is required.

7.8 Conclusions

The triaxial specimen has clearly been shown to experience the nominally applied stresses if end friction is low and the end platen thick. The implication of friction and ℓ/d ratio on failure mode has been shown to be as important as the errors in the measured material characteristics if

specimen deformation was assumed perfectly cylindrical where high frictional forces were mobilised. These errors in the case of an axial modulus have been shown to be no greater than 7%.

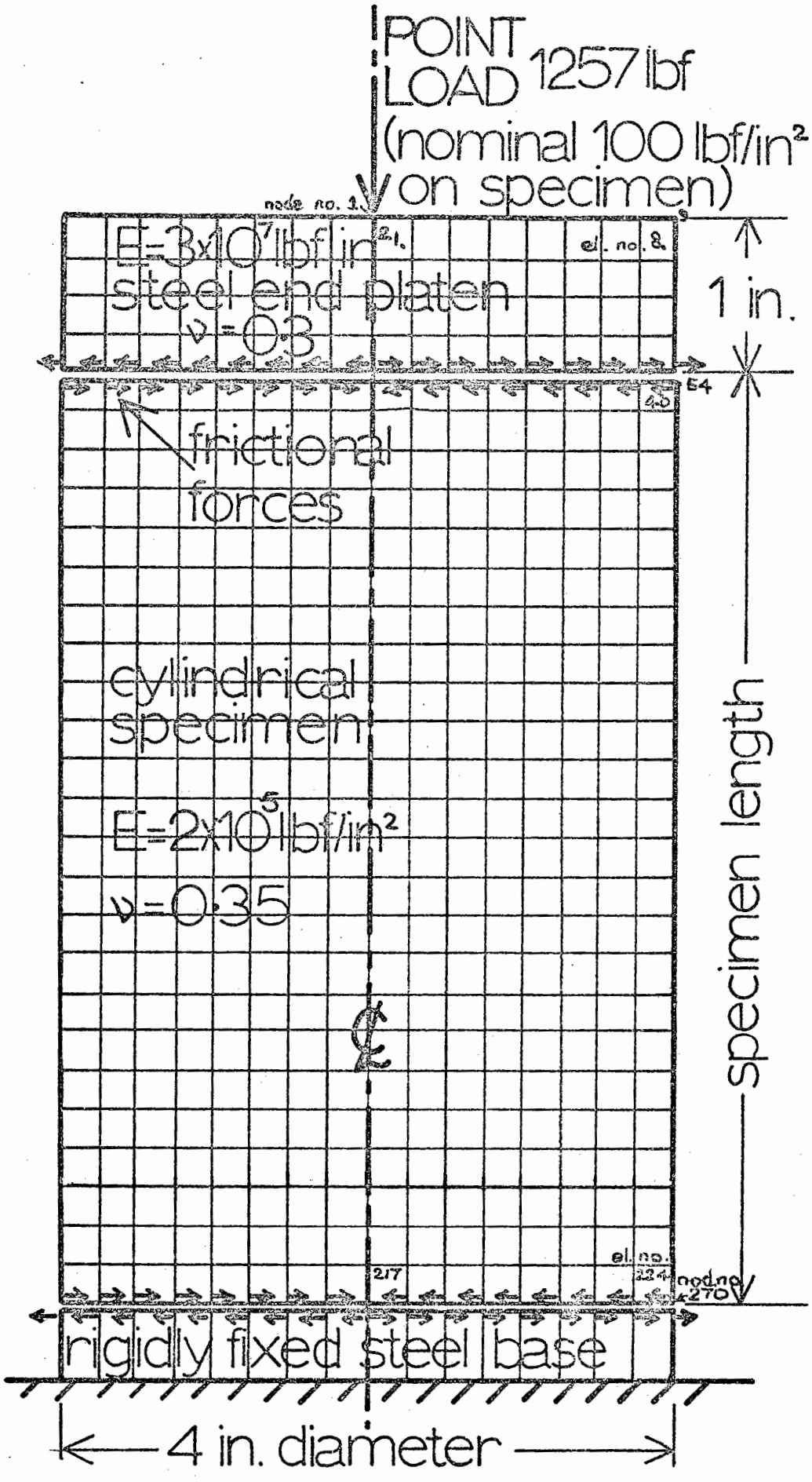

Fig. 7.1 Finite Element Idealisation of triaxial specimen with end friction restraint

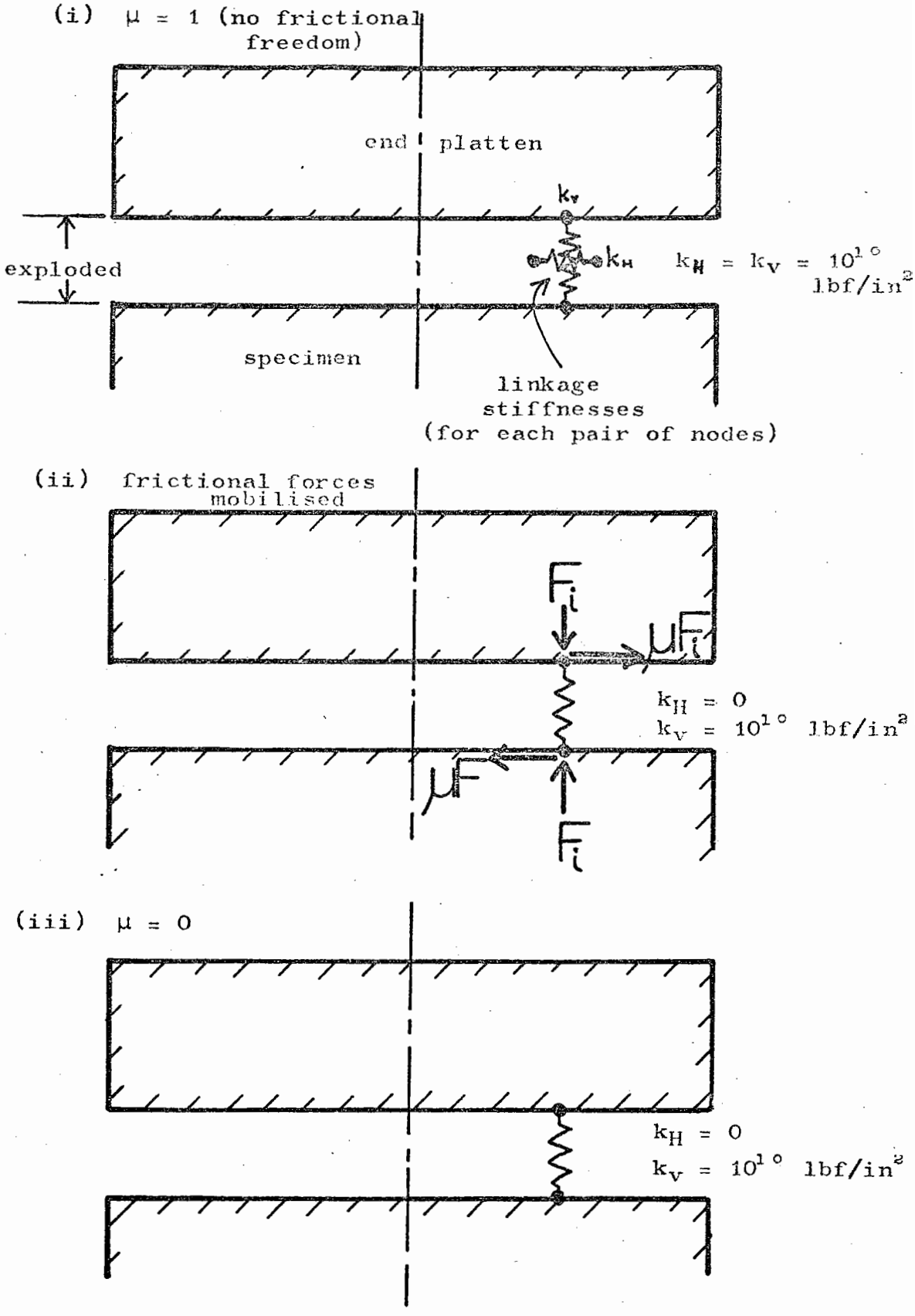

Fig. 7.2 Frictional restraint and structural linkage

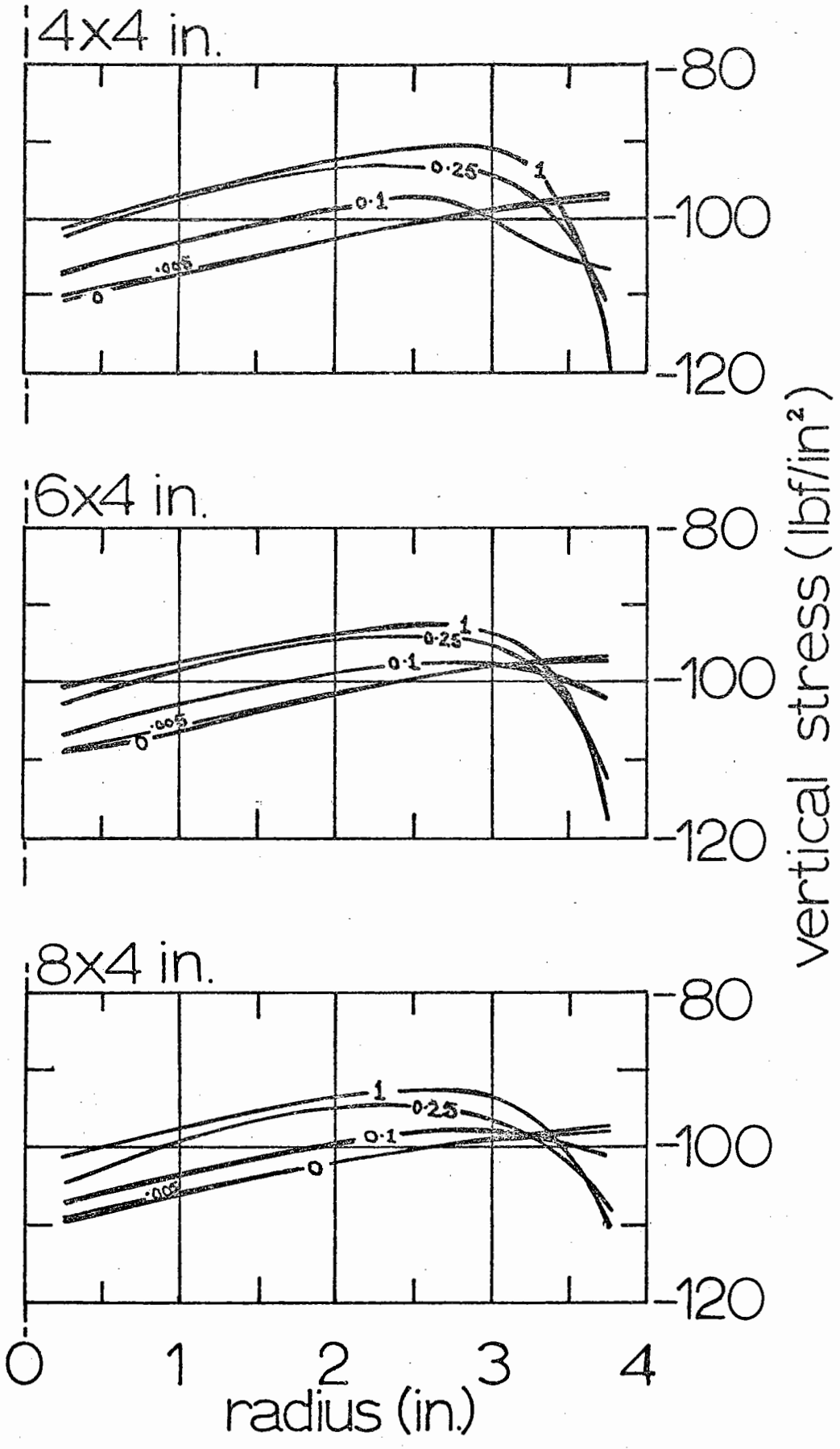

Fig. 7.3 Vertical stresses imposed by end platen at top of specimens with varying end frictional restraint

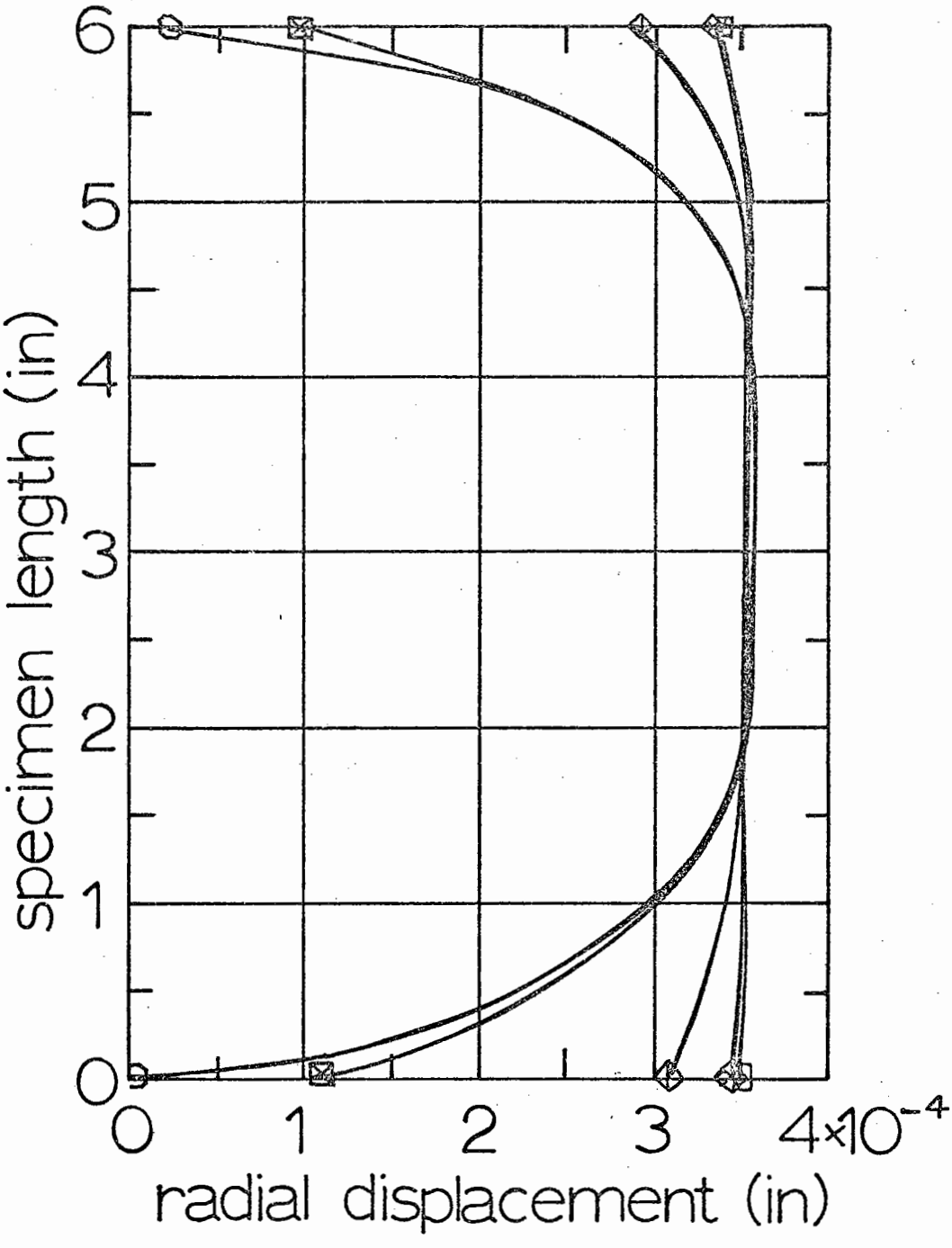

Fig. 7.4 Radial displacement at edge of 6 x 4 in. specimen

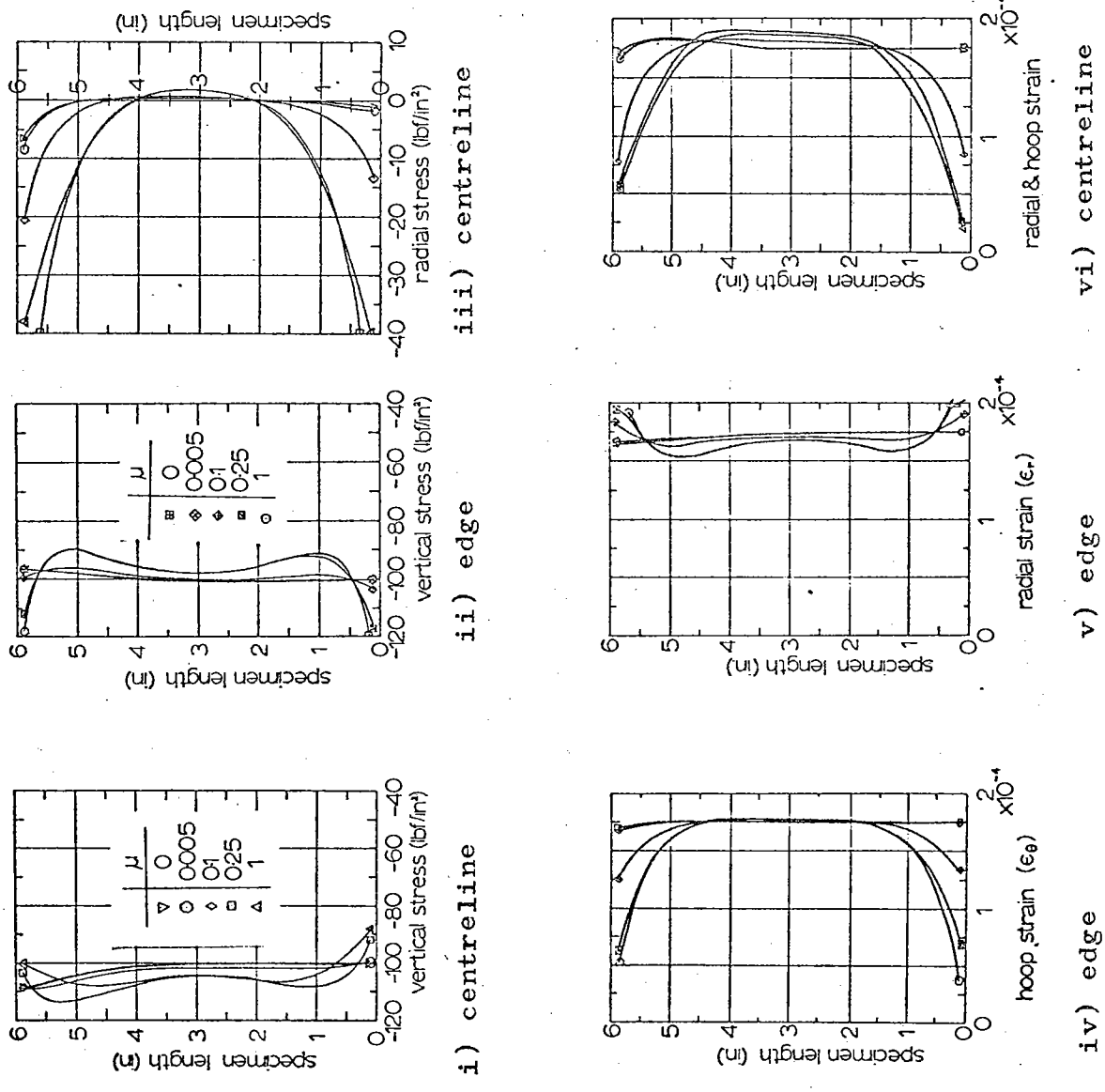

Fig. 7.5 Stresses and strains on centreline and at edge of specimen

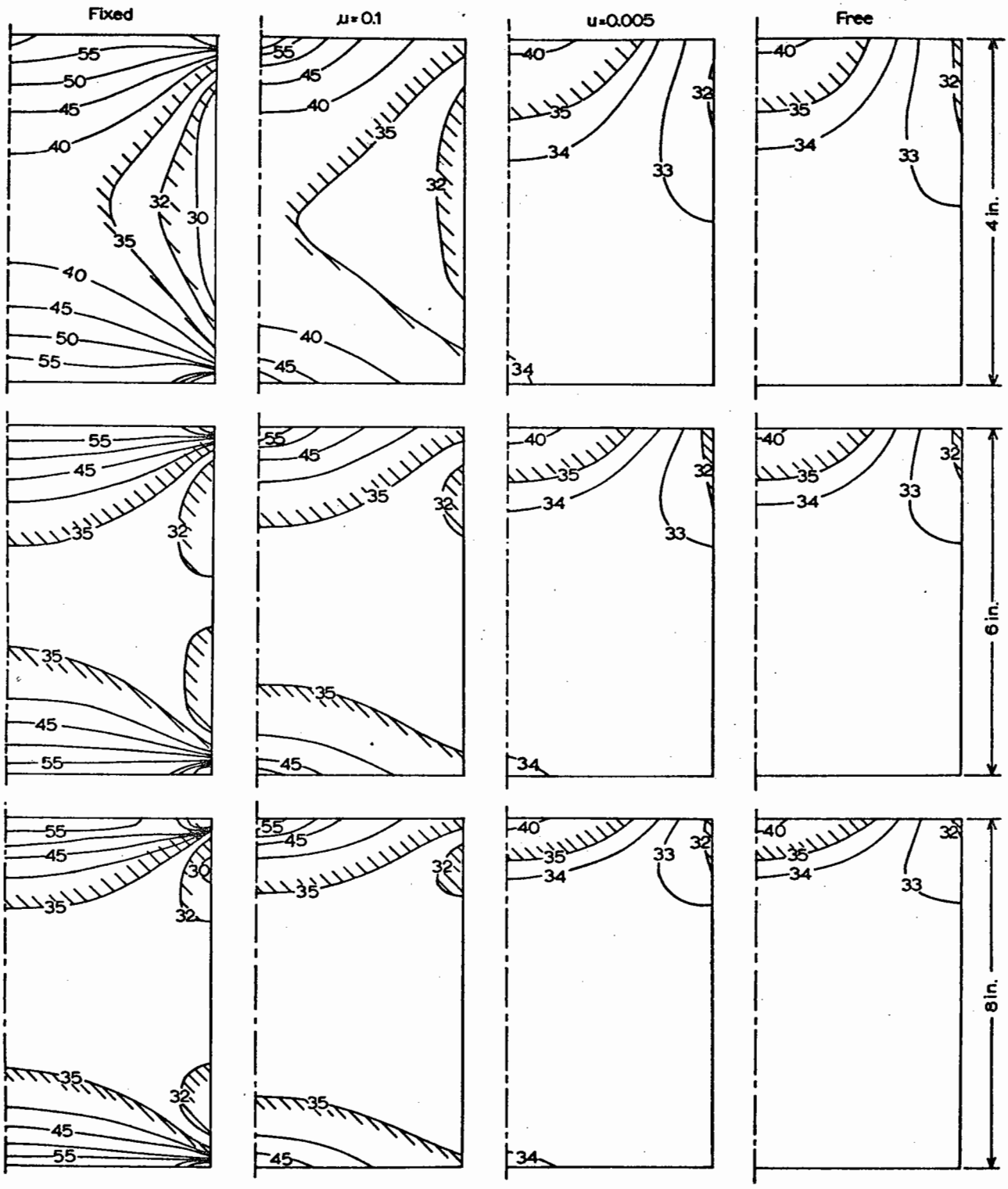

Fig. 7.6 Mean Normal Stress distribution for different specimen size and end restraint

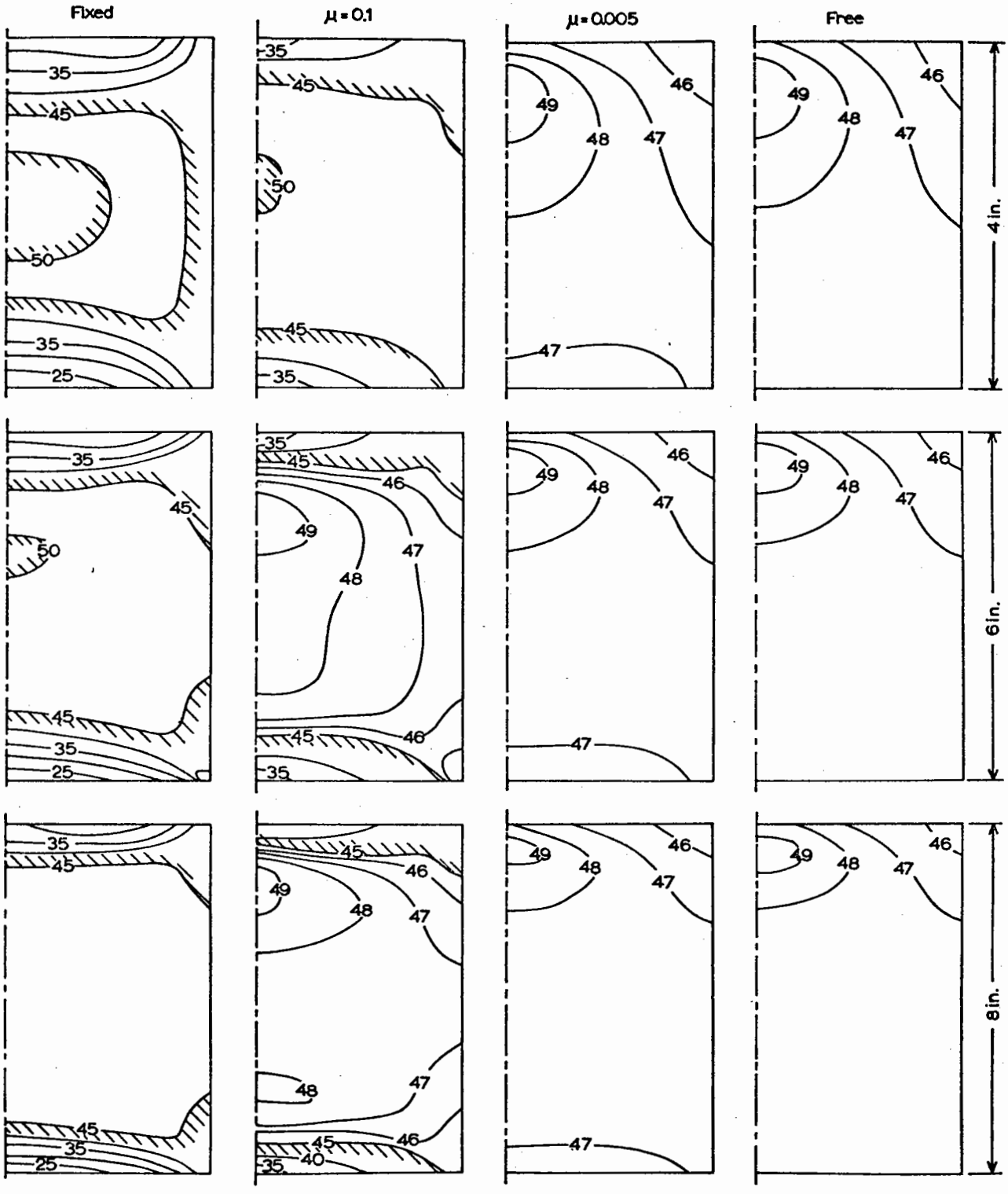

Fig. 7.7 Octahedral Shear Stress distribution for different specimen size and end restraint

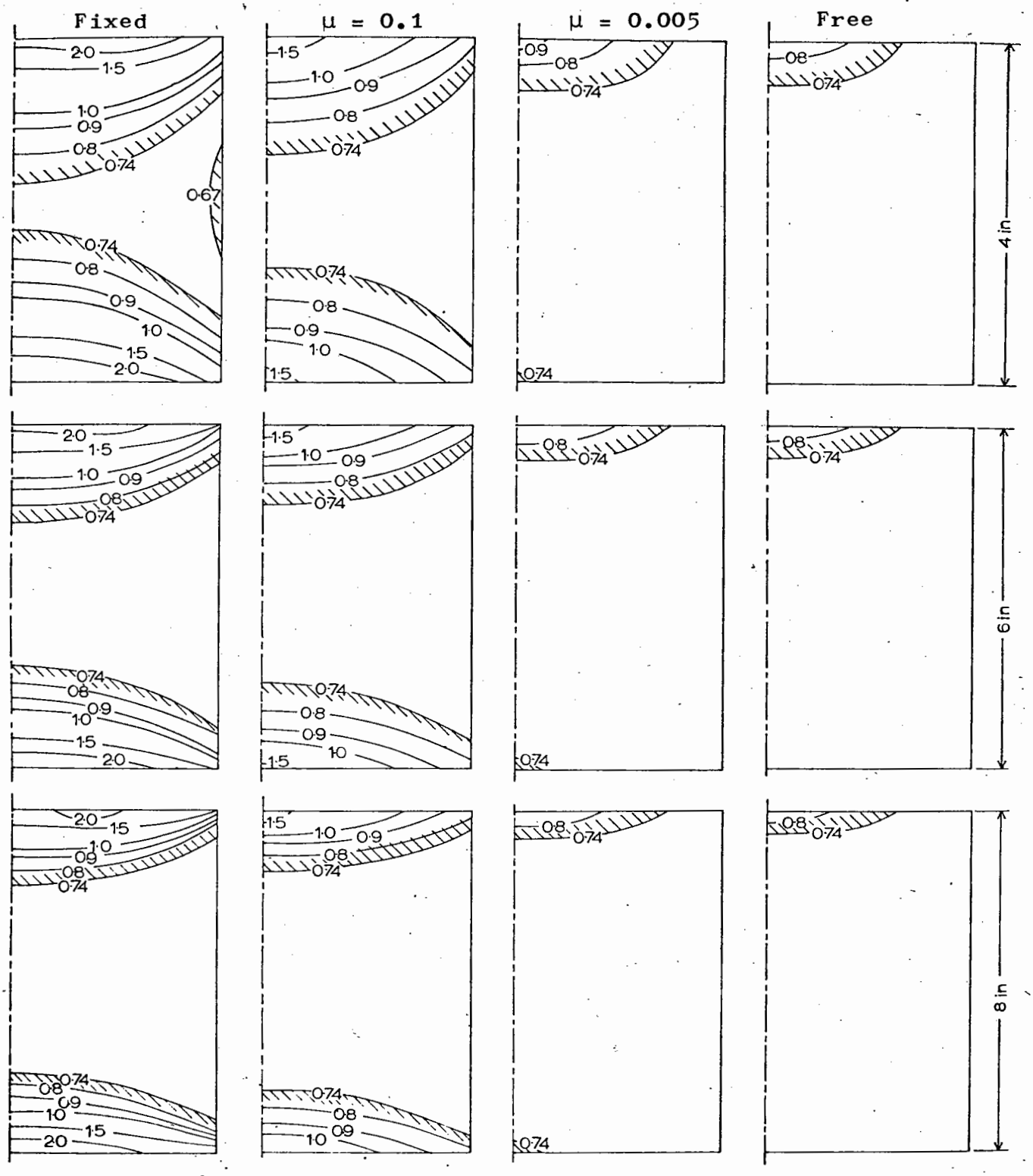

Fig. 7.8 Ratio Mean Normal Stress to Octahedral Shear Stress (σ/τ), showing conical zone of all round compression for fixed or near-fixed ends

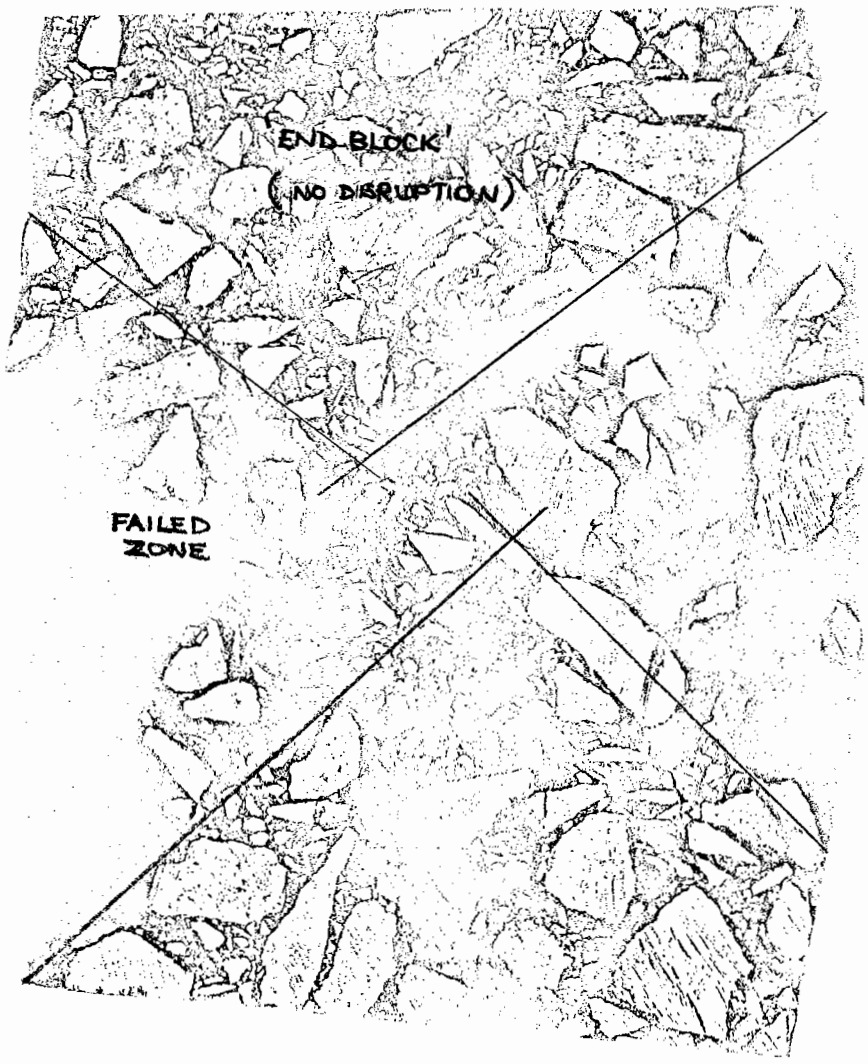

FULL END FIXITY (full scale)

Fig. 7.9 Full end fixity on nominally 6x4in. asphalt specimen

Fig. 7.10 Lubricated ends on 9x6in. specimen showing vertical cracks

CHAPTER 8

CONCLUDING DISCUSSION

8.1 The Finite Element Method

It is suggested that continuous variation in material properties is best represented by many simple finite elements, each of which has different material properties which depend on a representative stress or strain level and environmental conditions. The simple 8-node rectangular cuboid element makes excessively great demands on computer storage and time, using present day machines. In representing the physically layered system encountered in road pavements the 4-node axisymmetric element, with side parallel to horizontal and vertical co-ordinate axes, was found more suitable than a more general 3-node element. For the same number of mesh points, the 4-node element required less stiffness computations and did not involve the theoretically doubtful practice of averaging the stresses or strains from surround elements, which has often been found expedient by other workers.

The program based on the truly 3-dimensional element awaits the development of a system with long life which is supported by software which can carry out rapid transfer of information from fast to backing store in a way relevant to the Choleski decomposition method of solution.

Preliminary investigations into the behaviour of the finite element method can be carried out using a coarse

mesh, but the analysis of a real system to provide comparison with in-situ values demands as refined a mesh as is possible. The axisymmetric formulations used here offered this accurate approach as a starting point to understanding layered system behaviour. The more ideal 3-dimensional elements are, however, restricted by the size of fast store available and a highly refined mesh in all directions, accepting high cost, is not possible. The imposition of displacement boundary conditions, calculated from a preliminary analysis, may, however, allow these more realistic computations to be carried out.

The displacement method of finite element analysis was chosen for development in the absence of detailed descriptions of other formulations. It seems likely that such formulations will have advantages which may be exploited when detailed programming is reported.

Examination of the behaviour of the axisymmetric formulations using simple non-linear material properties showed that all manner of monotonic modulus-stress level relationships lead to a stable solution. Any secondary instability as a result of a strongly stress dependent modulus was acceptably small. In a single layer system some pattern of convergence was established which potentially would lead to an acceleration of the iterative procedure. Investment in developing such a method was not considered worthwhile since it was found that a multilayered system led to a less regular process. In a layered system the convergence of the iteration procedure could be established by monitoring all interfacial

surface displacements. After as little as six iterations, it was found that the change of vertical displacement between successive iterations at any interface was less than 1%, which seemed adequate.

The iterative procedure in a single layer system was unaffected by the initial choice of a constant modulus for all elements since the stress distribution which governs the first modification to element moduli is independent of modulus.

For a successful incremental analysis, a preliminary iterative analysis, during the first increment, seems essential to establish the initial tangent moduli. These moduli were thus relevant to the stress distribution in the structure under the imposed external loads. The procedure demanded a knowledge of both the resilient secant and tangent properties of a material but had the advantage that it could proceed without iteration within increments beyond the first.

The finite element method suffered the disadvantage that vertical displacements were found to be greatly affected by the proximity of the lower boundary of the mesh at a finite depth. Stresses were little affected however. Certain non-linear relationships may predict Poisson's Ratios near to 0.5. At this value the finite element formulation breaks down. There can be little confidence in the accuracy of solutions with ν greater than 0.45 but improvement could probably be obtained at greater expense using double length arithmetic.

8.2 Non-linear material properties

Reference to literature has established that the stress invariants are fundamental in governing material behaviour both up to and at failure. Both the resilient and incremental material properties have dependence on these stress levels.

A third factor, that of dilation or compaction with shear stress, has not been incorporated, due to lack of experimental data, but seems likely to become more significant at stress levels near to failure (or when permanent deformations become excessively large). A means is suggested whereby this phenomenon could be isolated in material tests and incorporated as a change in resilient moduli which depended on the number of load repetitions already applied to the structure. These changes in material properties may not have been significant after the limited number of load repetitions applied by Brown or Bush. In a full scale road pavement the change in properties could become significant.

It is possible that the resilient material behaviour may contain an element of elastic dilation over a limited history of the total loaded life of the material. It is shown how this can be modelled in a pavement using five anisotropic parameters.

The two stress invariants, σ and τ, also influence material failure and thus can be used in theoretical analysis to predict zones of weakness in any given structural system. Given a relationship between σ and τ at which failure occurs for each material, attempts at identifying the load for failure could be made.

It is shown how the triaxial test could be used to reveal the variation of a bulk and shear modulus with a wide variety of mean and shear stresses. This can be extended to the dynamic testing of soils provided the axial load and cell pressure can be cycled in a specified way and the resilient radial strains can be measured.

The program developed to analyse the triaxial specimen, and which models end frictional effects, greatly improves understanding of the mechanism of failure and offers a tool which can assist in the design of experiments. Failure is simple to observe in the test, thus a reliable failure criterion for materials can be established. Its applicability to the layered pavement should strictly be limited to the axis of load where a 'triaxial' stress system exists. Confidence can be expressed in considering the ratio σ/τ as one of the parameters fundamental in leading to permanent changes in the resilient properties of materials under dynamic loading.

Even though a specimen with ℓ/d ratio = 1 was found to have a very limited region at near nominal stress conditions, the error in a measured axial modulus was limited to 7%. The program offers the possibility of providing more accurate material properties by taking into account variations caused by end platen flexibility and end frictional restraint.

8.3 Insitu measurements

It has been shown in Chapter 5 that even more fundamental approaches to the problem of material characterisation did

not lead to a significantly more accurate prediction of the stresses and strains measured in a scaled down layered system. Comparisons were made using measurements made in a scaled-down pavement in the laboratory. This system was subject to many experimental errors and thus any conclusions drawn are not necessarily directly applicable to the practical layered system.

The consideration of non-linearity was clearly shown to be important, however, but the choice of linear properties which afforded the comparison was in some degree, subjective. The choice made by the author was based on the properties suggested by the characterising functions used in non-linear analysis. For the Keuper Marl, high values relevant to low stress levels, which themselves were not adequately supported by measured stresses and strains, were used. This extra-polation was necessary because of the lack of measured low level stresses and strains. This deficiency is all important since most of the material in the finite element idealisation was at a low stress level.

The accuracy of the measured quantities is in serious doubt since embedded instruments could not be inspected through-out a whole series of tests. During the life of a pavement the material properties would gradually change and lead to significantly different stress distributions being imposed throughout its life. This factor may have had some influence on the accuracy of the results obtained from the scaled-down pavement tests with their only limited number of load repetitions.

The change in structural properties brought about by temperature changes has been found to be very significant indeed. The high gradients of temperature experienced in a test section have been shown to require the finite element method of analysis since linear elastic theory led to unacceptable innaccuracy. The absolute change in the design parameters which was brought about by temperature change was found to be far more significant than the errors introduced by non-linearity. However, any weakness brought about by increased temperature in the bituminous layers would increase the stresses in the lower layers rendering a non-linear analysis, which could incorporate permanent change in a near critical material, more important.

Increased temperatures in the bituminous layers would also enhance their healing properties. Opposed to this is the problem that before any healing could take place permanent changes would have occurred in the lower layers and contributed to unwanted permanent surface displacements.

The temperature measurements now being made on a variety of pavement types and thicknesses by the Road Research Laboratory can be used in analysis together with information from healing tests to assess the likely importance of these problems.

The importance of the weakening effect increased temperature in the bituminous layers of a pavement have cannot be over-emphasised. Temperature distributions, recently measured in realistic layered systems, have brought about highly significant changes in the quantities thought of as

critical in a structural design approach to the pavement problem.

The short term implication would seem to be that more effort should be made to measure practical temperature distributions. At the same time engineers can establish the more detailed implications on current pavement design by making use of the widely available n-layer elastic theory analyses.

8.4 Suggestions for further research

There is a need for in-situ measurements of the stresses and strains in a layered system to be carried out in such a way that the change in resilient material properties with number of load repetitions can be established. A series of bulk and shear stress v normal and shear strain relationships could be obtained. It would be desirable that there are enough instrument points to detect a wide enough range of stresses and strains to identify the effect of the 3rd variable on each plot. After a particular number of load repetitions it would be hoped that a characteristic could be obtained which would recognisably differ from that from another series of tests further on in the life of the pavement. The repeatability of such tests could only be established by digging up the tested pavement and repeating the series of tests in a layered system having a similar initial compaction. It would also be hoped to identify whether elastic dilation (or compaction) took place as well as the dilation causing permanent changes in the resilient properties of the materials.

Since a heavily instrumented system would be required, a preliminary theoretical investigation into the effect of the gauges as rigid inclusions should be undertaken using the finite element method.

The cost of this suggested test would be greater than that undertaken by Brown or Bush, but would afford a better understanding of the change in material properties with repeated loading, and allow measurement of the all important permanent deformations in a layered system. This type of pulse load testing is objected to on the grounds that it does not set up a transient stress system similar to that under a moving wheel. It can be argued, however, that the cost of moving wheel apparatus is much greater and that theoretical analyses to simulate moving loads on multilayered systems are not yet available. Since reliable fundamental material properties have not yet been established for soils in general, it also seems unjustified to carry out tests on very complex systems which undergo complicated changes in stress distribution.

The triaxial cell is the most readily available means of characterising soil materials. In the long term the test should give comprehensive material properties, which when used in theoretical analysis, can be verified to predict in-situ measurements of stresses and strains. To assist this development, there is required an accurate means of measuring sample volume change or radial strains under dynamic loading conditions.

Investigation is also required to establish whether stress

induced anisotropy is significant in a layered pavement. If this were the case then computer programs would have to be modified to account for the extra parameters, and testing methods would of necessity become more complex. This step may be necessary since moving or stationary loads normal to the surface lead to unequal vertical and horizontal stresses.

It can be seen that the pavement problem is by no means solved, nor can be without human intervention offering judgement based on experience and intuition. The three main areas of interest are:-

(1) Simple material test to find properties.

(2) Structural analysis to calculate critical parameters and evolve designs and an accurate specification of "failure" in the structure.

(3) Verification by in-situ measurement.

It is hoped that light has been thrown on each of these problems and that the flexible finite element programs contained in this thesis will assist future experimental work. It has been demonstrated that these programs offer a powerful analytical tool, whose exploitation is currently limited only by the knowledge of material properties and size of computer core store for efficient computations.

REFERENCES

1.1 "A guide to the structural design of pavements for new roads", Road Note 29, Dept. of the Environment, RRL.

1.2 Page, M.E., "A summary of RRL pavement design experiments", RRL Tech. Note, in preparation.

1.3 "Shell 1963 Design Charts for Flexible Pavements", Shell Int. Petroleum Co., London 1963.

1.4 Sebastyan-Yishai, G., "Flexible pavement design based on the element method of analysis", Ph.D. Thesis, Univ. of Michigan, 1963.

1.5 Klomp, A.J.G. and Niesman, Th.W., "Observed and calculated strains at various depths in asphalt pavements", Proc. 2nd Int. Conf. on Struct. Design of Asphalt Pavements, Ann Arbor, Mich., 1967.

1.6 Brown, S.F., "Stresses and deformations in flexible layered pavement systems subjected to dynamic loads", Ph.D. Thesis, Univ. of Nottingham, 1967.

1.7 Brown, S.F. and Pell, P.S., "An experimental investigation of the stresses, strains and displacements in a layered pavement structure subjected to dynamic loads", Proc. 2nd Int. Conf. on the Struct. Design of Asphalt Pavements, Ann Arbor, Mich., 1967.

1.8 Brown, S.F. and Taylor, K.L., "Discussion of 'Developments in pavement design in the USA - Flexible pavements' by R.G. Ahlvin", Symp. on Aircraft Pavement Design, Inst. Civ. Engineers, Nov. 1970.

1.9 Bush, D.I., "Behaviour of flexible pavements subjected

to dynamic loads", Ph.D. Thesis, Univ. of Nottingham, 1970.

1.10 Heukelom, W. and Klomp, A.J.G., "Dynamic testing as a means of controlling pavements during and after construction", Proc. Int. Conf. on the Struct. Design of Asphalt Pavements, 1962.

1.11 Isada, N.M., "Impulsive load stiffness of flexible pavements", ASCE, SM2, March 1970.

1.12 Seed, H.B., Mitry, F.G., Monismith, C.L., Chan, C.K., "Prediction of flexible pavement deflections from laboratory repeated load tests", NCHRP Report No. 35, Highway Research Board, Washington, 1967.

1.13 Terrel, R.L., "Factors influencing the resilient characteristics of asphalt treated aggregates", Ph.D. Thesis, Univ. of California, Berkeley, Aug. 1967.

1.14 Dormon, G.M. and Edwards, J.M., "Developments in the application in practice of a fundamental procedure for the design of flexible pavements", Proc. 2nd Int. Conf. on the Struct. Design of Asphalt Pavements, Ann Arbor, Mich., 1967.

1.15 Ibid Pell, P.S., "Fatigue of asphalt pavement mixes".

1.16 Ibid Bazin, P. and Saunier, J.B., "Deformation, fatigue and healing properties of asphalt mixes".

1.17 Hudson, W.R., Finn, F.N., McCullough, Nair, K., Vallerga, B.A., "Systems approach to pavement design", Interim Report, NCHRP Project 1-10, Highway Research Board, March 1968.

1.18 Konder, R.L. and Krizek, R.J., "Factors influencing

flexible pavement performance", NCHRP Report No. 22, Highway Research Board, 1966.

1.19 Kasianchuk, D.A., "Fatigue considerations in the design of asphalt concrete pavements", Ph.D. Thesis, Univ. of California, Berkeley, 1967.

1.20 Boussinesq, J., "Application des potentiels a l'étude de l'équilibre et du mouvement des solides élastiques", Gauthier-Villare, Paris, 1885.

1.21 Lister, N.W. and Nunn, D.E., "Contact areas of commercial vehicle tyres", RRL Report LR172, Crowthorne, 1968.

1.22 Lister, N.W. and Jones, R., "The behaviour of flexible pavements under moving wheel loads", Proc. 2nd Int. Conf. on the Struct. Design of Asphalt Pavements, Ann Arbor, Mich., 1967.

1.23 Westmann, R.A., "Visco-elastic layered system subjected to moving loads", ASCE, EM3, June 1967.

1.24 Leger, P., "Massif visco-elastique indéfini soumis à une charge roulante", Annales des points et chaussées, No. 1, Jan-Feb 1968.

1.25 Soydemir, C. and Schmid, W.E., "Deformation and stability of viscoelastic soil media", ASCE, SM6, Nov. 1970.

1.26 Burmister, D.M., "The theory of stresses and displacements in layered systems and applications to the design of airport runways", Proc. Highway Research Board, Vol. 23, pp. 126-149, 1943.

1.27 Burmister, D.M., "The general theory of stresses and

displacements in layered systems", Journal of App. Phys., Vol. 16, No. 2, Feb. 1945, pp. 89-94; No. 3, Mar. 1945, pp. 126-127; No. 5, May 1945, pp. 296-302.

1.28 Fox, L., "Computation of traffic stresses in a simple road structure", Dept. of Scientific and Industrial Research, Road Res. Tech. Paper No. 9, 1948.

1.29 Acum, W.E.A. and Fox, L., "Computation of load stresses in a three-layer elastic system", Geotechnique, Vo. 2, No. 4, pp. 293-300, 1951.

1.30 Mehta, M.R. and Veletsos, A.S., "Stresses and displacements in layered systems", Structural Research Series No. 178, Univ. of Illinois, Urbana, Ill., June 1959.

1.31 Ahlvin, R.G. and Ulery, H.H., "Tabulated values for determining the complete pattern of stresses, strains and deflections beneath a uniform circular load on a homogeneous halfspace", Bulletin 342, High Research Board, Washington, p. 1-13, 1962.

1.32 Jones, A., "Tables of stresses in three-layer elastic systems", Paper presented to the 1962 Annual Meeting of the Highway Research Board, Washington D.C., Bulletin 342: "Stress distribution in earth masses".

1.33 Burmister, D.M., "Flexible pavements for airfields", Interim Report on Contract NBy-13009 to the Dept. of the Navy, Bureau of Yards and Docks, Columbia Univ., New York, May 1962.

1.34 Verstraeten, J., "Stresses and displacements in elastic layered systems", Proc. 2nd Int. Conf. on the Struct. Design of Asphalt Pavements, Univ. of Michigan, Ann Arbor, Mich., 1967.

1.35 Poulos, H.G., "Stresses and displacements in an elastic layer underlain by a rough rigid base", Geotechnique, Dec. 1967.

1.36 Nielsen, J.P., "Implications of using layered theory in pavement design", ASCE, TE4, Nov. 1970.

1.37 Warren, H. and Dickmann, W.L., "Numerical computation of stresses and strains in a multiple-layer asphalt pavement system" - Computer Program, Unpublished internal report, Chevron Research Corp., USA.

1.38 Peutz, M.G.F., Jones, A., Van Kempen, H.P.M., "Computer program - layered systems under normal surface loads", Shell Research N.V., Koninklijke/Shell-Laboratorium, Amsterdam.

1.39 Thrower, E.N., "Calculation of stresses, strains and displacements in a layered elastic structure", Road Research Laboratory Report LR138, RRL, Crowthorne, Berks., 1968.

1.40 Thrower, E.N., Part II of ref. 1.39, R.R.L. Report LR373, 1971.

1.41 Gerrard, C.M., "The axisymmetric deformation of a homogeneous, cross-anisotropic elastic halfspace", Highway Research Record No. 223, HRB Washington, 1968.

1.42 Cumming, D.A. and Gerrard, C.M., "Computation of stresses in pavements", Proc. 2nd Conf. ARRB, Pt. 2, 729, 1964.

1.43 Gerrard, C.M. and Mulholland, P., "Stress, strain and displacement distributions in cross-anisotropic and two-layer isotropic elastic systems", Proc. 3rd Conf. ARRB, Pt. 2, 1123, 1966.

1.44 Morgan, J.R. and Gerrard, C.M., "Stresses and displacements in a rock mass having stress dependent properties", Proc. Symp. on Rock Mechanics, Vol. 1, pp. 87-91, Univ. of Sydney, 1969.

1.45 Waterhouse, A., "Stresses in layered systems under static and dynamic loads", Proc. 2nd Int. Conf. on the Struct. Design of Asphalt Pavements, Ann Arbor, Mich., 1967.

1.46 Duncan, J.M., Monismith, C.L. and Wilson, E.L., "Finite element analysis of pavements", HRR No. 228, HRB, Washington, 1968.

1.47 Dehlen, G.L., "The effect of non-linear material response on the behaviour of pavements subjected to traffic loads", Ph.D. Thesis, Dept. of Civ. Eng., Univ. of Calif., Berkeley, 1969.

1.48 Pretorius, P.C., "Design considerations for pavements containing soil cement bases", Ph.D. Thesis, Univ. of Calif., Berkeley, April 1970.

1.49 Wilson, E.L., "Analysis of prismatic solids", Unpub. report, Dept. of Civ. Eng., Univ. of Calif., Berkeley, 1968.

2.1 Clough, R.W., "The finite element in structural mechanics", from "Stress Analysis", Zienkiewicz and Hollister, Wiley, 1965.

2.2 Pain, T.H.H., "Derivation of element stiffness matrices by assumed stress distributions", AIAA Journal Vol. 2, pp. 1333-1336, 1964.

2.3 "PAFEC - Program for Automatic Finite Element Calculations", Dept. of Mech. Eng., Univ. of Nottingham, in continuous development 1968 onwards.

2.4 Dunham, R.S., "Stationary principles applied to a class of linear and non-linear boundary value problems in solid mechanics", Ph.D. Thesis, Univ. of California, Berkeley, 1969.

2.5 Wilson, E.L., "A digital computer program for finite element analysis of solids with non-linear properties", Int. Report, Univ. of California, Berkeley, 1965.

2.6 Utku, S. and Akyuz, F.A., "ELAS - A general purpose computer program for the equilibrium problems of linear structures", NASA Tech. Report 32-1240, Jet Propulsion Laboratory, Pasadena, Calif., 1968.

2.7 Utku, S., "Explicit expression for triangular torus element stiffness matrix", AIAA Journal, Vol. 6, pp. 1174, June 1968.

2.8 Zienkiewicz, O.C. and Cheung, Y.K., "The finite element method in structural and continuum mechanics", McGraw-Hill, London 1967.

2.9 Timoshenko, S., "Strength of Materials", Part II, p. 207, Van Nostrand, 1956.

2.10 Taylor, K.L., "Finite element for structural problems", work in partial satisfaction for Part II, B.Sc., Nottingham 1968.

3.1 Domaschuk, L. and Wade, N.H., "A study of the bulk and shear moduli of a sand", ASCE, SM2, March 1969.

3.2 Holubec, I., "Elastic behaviour of cohesionless soils", ASCE, SM6, Nov. 1968.

3.3 Pagen, C.A., "Rheological response of bituminous concrete", Highway Research Record, No. 67, Highway Research Board, Washington, 1964.

3.4 Gandhi, P.M.K. and Gallaway, B.M., "Viscosity effects on stress-strain characteristics of asphalt mixes", Journal of Materials, Vol. 2, No. 1, pp. 27-46, March 1967.

3.5 Hruban, K., "The semi-infinite solid with a non-linear deformation law", Czech Acad. Sci., Feb. 1957.

3.6 Schofield, A. and Wroth, P., "Critical state soil mechanics", McGraw-Hill, 1968.

3.7 Brown, S.F. and Pell, P.S., Closure discussion on "Subgrade stresses and deformations under dynamic load", ASCE, SM4, p. 1039, 1968.

3.8 Huang, Y.H., "Stresses and displacements in non-linear soil media", ASCE, SM1, 1968.

3.9 Clough, R.W. and Woodward, R.J., "Analysis of embankment stresses and deformation", ASCE, SM4, 1967.

3.10 Girijavallabhan, C.V. and Reese, L.C., "Finite element method for problems in soil mechanics", ASCE, SM2, 1968.

3.11 Merkle,J.G. and Merkle,D.H, Discussion on ref. 3.2, ASCE, SM5, p. 1276, 1969.

3.12 Coon,M.D. and Evans R.J, Discussion on ref. 3.2, ASCE, SM5, p. 1281, 1969.

3.13 Girijavallabhan, C.V., Discussion on ref. 3.1, ASCE, SM1, p. 350, Jan. 1970.

3.14 Chowdhury, R.N., Discussion on ref. 3.1, ASCE, SM1, p. 351, Jan. 1970.

3.15 Hardin, B.O. and Black, W.L., "Vibration modulus of normally consolidated clay", ASCE, SM2, March 1968.

3.16 Humphries, W.K., and Wahls, H.E., "Stress history effects on dynamic modulus of clay", ASCE, SM2, March 1968.

3.17 Desai, C.S. and Reese, L.C., "Analysis of circular footings on layered soils", ASCE, SM4, July 1970.

3.18 Duncan, J.M. and Chin Yung Chan, "Non-linear analysis of stresses and strains in soils", ASCE, SM5, 1970.

3.19 Gerrard, C.M., "Some aspects of the stress-strain behaviour of a sand", Aust. Road Research Board, Vol. 3, No. 4, Dec. 1967.

3.20 Pickering, D.J., "Anisotropic elastic parameters for soil", Geot. 20, 3, 1970.

3.21 Šuklje, L., "The equivalent elastic constants of saturated soils exhibiting anisotropy and creep effects", Geot. 13, 1963.

3.22 Hoeg, K., Christian, A.M. and Whitman, R.V., "Settlement of strip load on elastic-plastic soil", ASCE, SM2, 1968.

3.23 Bresler, B. and Pister, K.S., "Strength of concrete under combined stresses", Proc. ACI, Vol. 55, Jul-Dec 1958.

3.24 Bellamy, C.J., "Strength of concrete under conbined stress", Proc. ACI, Vol. 58, 1961.

4.1 Marcal, P.V. and King, I.P., "Elasto-plastic analysis of 2-dimensional stress systems by the finite element method", Int. Jour. Mech. Sciences, Vol. 9, No. 3, March 1967.

4.2 Akyuz, F.A. and Merwin, J.E., "Solution of non-linear problems of elasto-plasticity by the finite element method", AIAA Journal, Vol. 6, No. 10, Oct. 1968.

4.3 Smith, I.M., "Incremental numerical solution of a simple deformation problem in soil mechanics", Geotechnique, 20, No. 4, pp. 357-372, Dec. 1970.

4.4 Smith, I.M., "Plane plastic deformation of soil", Paper presented at Roscoe Memorial Symposium, Cambridge, 1971 (Author: Simon Engineering Laboratories, Univ. of Manchester).

6.1 Brown, S.F. and Pell, P.S., "Developments in the structural design of flexible pavements", Roads and Road Construction, Vol. 48, No. 569, May 1970.

6.2 Southgate, H.F. and Deen, R.C., "Temperature distribution within asphalt pavements and its relationship to pavement design", Highway Research Record 291, pp. 116-131, 1969.

6.3 Galloway, J.W., "Temperature durations at various depths in bituminous roads", RRL Report LR138, 1968.

6.4 Greening, P.A.K., "The estimation of road temperature", RRL Technical Note TN550 (restricted), Oct. 1970.

6.5 Fiddes, D., Personal communication, Climate and

Environment Section, RRL, Crowthorne, 1971.

6.6 Heukelom, W. and Klomp, A.J.G., "Road design and dynamic loading", Proc. Asphalt Paving Technologists", Vol. 33, 1964.

6.7 Monismith, C.L. and Secor, K.E., "Viscoelastic behaviour of asphalt concrete pavements", Proc. 2nd Int. Conf. on the Struct. Design of Asphalt Pavements, Ann Arbor, Mich., 1967.

6.8 Dormon, G.M. and Edwards, J.M., "The design of flexible pavements for road traffic", BITUMEN, Heft 1, Feb. 1966.

7.1 Snaith, M.S., Personal communication, research in progress, Univ. of Nottingham, 1971.

7.2 Balla, A., "Stress conditions in triaxial compression", ASCE, SM6, Dec. 1960.

7.3 Duncan, J.M. and Dunlop, P., "The significance of cap and base restraint", ASCE, SM1, Jan. 1968.

7.4 Rowe, P.W. and Barden, L., "Importance of free ends in triaxial testing", ASCE, SM1, 1964.

7.5 Haythornthwaite, R.M., "Mechanics of the triaxial test for soils", ASCE, SM5, Oct. 1960.

7.6 Zienkiewicz, O.C. and Naylor, D.J., "Discussion on the adaption of critical state soil mechanics for use in finite elements", Roscoe Memorial Symposium, Cambridge 1971.

7.7 Ngo, D. and Scordelis, A.C., "Finite element analysis of R.C. beams", Journal ACI, Vol. 64, March 1967.

7.8 Heukelom, W., "Observations on the rheology and fracture of bitumens and asphalt mixes", Proc. Assoc. Asph. Paving Technologists, Vol. 35, Tech. Session held at Minneapolis, Minnesota, Feb. 1966.

PROGRAM APPENDIX

List of Contents

A.0 INTRODUCTION

The programs developed by the author are listed along with information on the input requirements and the output.

Programs 1, 2.1 and 3 are the basic finite element programs for 3 and 4 node (axisymmetric) and 8 node solid elements. Their form, as listed, would enable an iterative analysis of a single layer, using non-linear elastic properties, to be carried out on the automatically generated meshes shown (Figs. A.1/2/3).

Program 2.2 shows the modifications necessary for an incremental analysis as described in Chapter 4.

Programs 4, 5 and 6 are based on the 4 node axisymmetric rectangle (Program 2.1) but involve modifications extensive enough to warrant separate listings. All three programs were developed so that layered systems could be modelled. Program 6 is the most general; allowing non-linear elastic analysis of a multilayer system, incorporating material characteristics in the form of the Bulk and Shear modulus or Young's Modulus and Poisson's Ratio. The efficient Cholesky solution procedure is listed (Section A.7).

Element number ordering and datageneration

Fig. A.1 3 node axisymmetric triangle (AUTO)

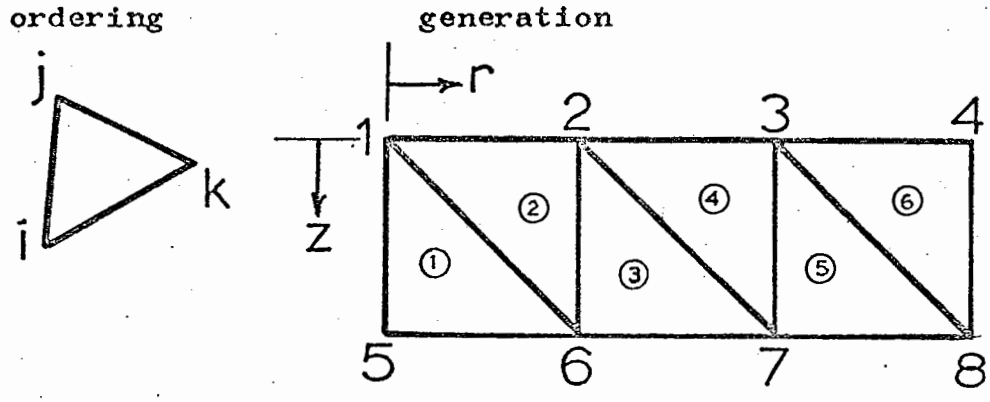

Fig. A.2 3 node axisymmetric rectangle (AUT04:prog 2)
(GEN4N:prog 4)
(GE4NM:prog 5)

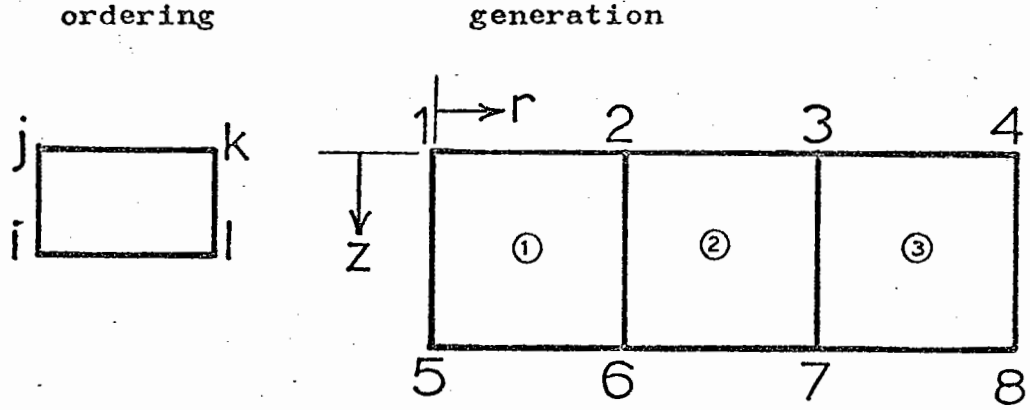

Fig. A.3 8 node rectangular prism (DATGN2)

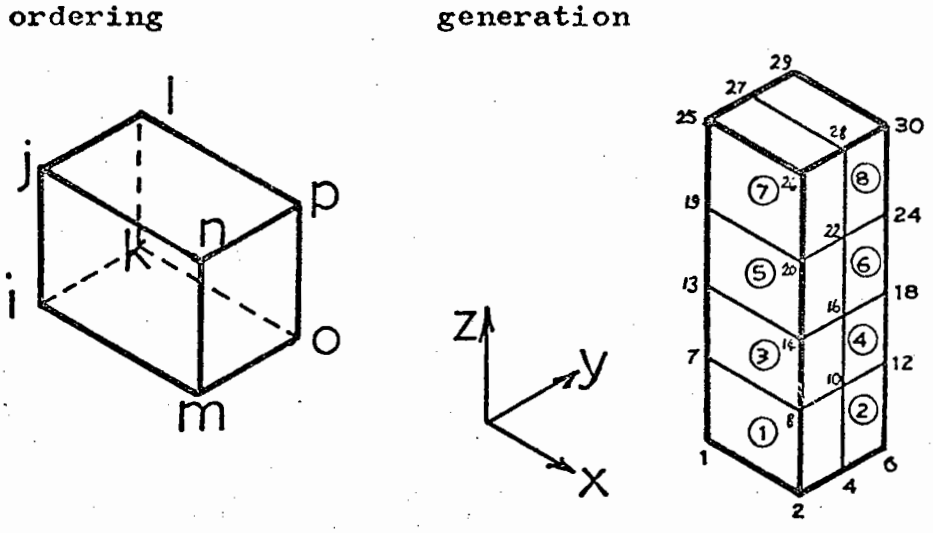

PROGRAM 1 3 Node Axisymmetric Triangle

A1.1 General description

The program is written in modules which are separately compilable (EGDON System, KDF9).

Data to describe an element mesh (Fig. A.1) is generated automatically (procedure AUTO) in matrixes 'ELNOD' and 'NCOORD', given input of the mesh dimensions.

ELNOD(1:EL,1:3) is a matrix with 'EL' (number of elements) rows, each row containing the node numbers for an element.

NCOORD(1:NOD,1:2) contains r and z co-ordinates for each node in turn.

Each module of the program has certain variables and arrays which are common to other modules and must cross intermodular boundaries. This is achieved using a predata device and public variables. The public variables are declared in each module, in this case, by substituting the block (DEC3NBIT) of public variables at the head of the text. All public arrays must have their bounds defined in the predata section thus rendering it impossible to declare arrays dynamically after their bounds have been computed. The calling of procedures 'SUPDV' as the first executable statements in the Main Program is a means whereby the machine address of public arrays is stored within the machine and relates only to the Egdon System on KDF9.

Description of procedures:

NODSTR - stresses at selected element nodes (for checking continuity)

BWCHEK - prints exact bandwidth to check input in PREDATA

AGLOB - (A) matrix in global co-ordinate system (r,z)

INTEG - computation of terms in $2\pi\int_{area} B^T D B r\,d$ area in a general axisymmetric triangular element

TYPE1-5 - integrals called by INTEG

BPOST3 - posts element stiffness to upper band structure stiffness

EXBDIT - boundary conditions, sets relevant rows and columns to zero, 1 on leading diagonal

LOAD - puts radial and vertical loads into load vector (VI)

UD3G00 - calculates nodal loads for a uniformly distributed load on any arbitrary element boundary

SETD - (D) matrix for an element

SETB - (B) matrix for given r and z co-ordinates

A1.2 Input

Sample input for a thick ring (Fig. A.1) is described.

A1.2.1 *Predata

```
*PREDATA
 PUBLIC N,NO,EL,NOD,MM,SS, NCOORD(NOD,2), ELNOD(EL,3),INT(6,6),BD,
1 CS,DD,AREA,
2 A(3),B(3),RR(3),ZZ(3),LP(3),AA(6,6),EK(6,6),SK(N,BD),VI(N,CS),
3K1(2),K2(2),K3(2),K4(1),K5(1),K6(1),K7(1),K8(1),K9(1),K10(2),
4K11(2),K12(2),
5 VI2(N,CS),FX(NFX,3),                    YM(EL),NU(EL),SIGM(EL),
6 NFX,ITER,ITERN,SIGMN,YMI,NUI,MEANST,
7 K13(2),K14(2),K15(1),K16(1),K17(1)
 REAL   MM,SS,NCOORD,INT,A,B,RR,ZZ,LP,AA,EK,SK,VI,DD,AREA,
1 VI2,        YM,NU,SIGMN,YMI,NUI,MEANST,SIGM
 INTEGER N,NO,EL,NOD,ELNOD,BD,CS,
1 FX,NFX,ITER,ITERN
```

NOD = 8 no. of nodes

EL = 6 no. of elements

N = 16 no. of unknowns (2xNOD)

BD = 14 bandwidth

CS = 1 load cases (=1)

NFX = 8 no. of fixed or partly fixed boundary points

PREOUT = 1 (device to leave predata section)

A1.2.2

Data	Description
1	Total number of iterations to full load (ITERN) (only other than 1 if an incremental analysis)
30×10^6 0.3	Young's modulus (YMI), Poisson's Ratio (NUI)
4 2	No. of nodes in radial and z directions
2.0 2.0 2.0 2.0	Width of each element in radial direction and vertical direction
1 1 0 2 1 0 3 1 0 4 1 0 5 1 0 6 1 0 7 1 0 8 1 0	Input to fixity matrix FX(1:NFX,1:3) for each node where some displacement is made zero, 1 row of matrix i.e. (node, r fix, z fix). If r fix = 0 then deletes row and column etc.
1 75400 0	Loading;
5 75400 0 99	node no., r load, z load terminator 99 after last nodal loading

A1.2.3

Input information in program test.

If a non-linear elastic relationship is known for the material, i.e. $E = f(\sigma)$ then:

(1) the precise relationship is written in near the end of main program, where marked,

(2) the number in the equality test (3 lines from end of main program) is changed to equal the desired number of iterations.

A1.3 Output

All input numbers are printed together with descriptive text.

The generated mesh data is printed out.

matrixes ELNOD : element numbering

NCOORD : co-ordinates for each node

All nodal displacements are printed.

If procedure NODSTR is called nodal stresses for any selected element can be printed.

Stresses at all element centroids, in the r, z co-ordinate system, and the first stress invariant are printed together with the new values of E according to equation $E = f(\sigma_{oct})$.

PROGRAM 1: LISTING (main program, 3 node)

```
*SUBSTITUTEDEC3NBIT
 'BEGIN'
 'REAL'          PREAL,LR,LZ$
 'INTEGER' I,J,SM,SN,PINT,LS
 'ARRAY' BB(1'.'6,1'.'6),CC(1'.'6,1'.'6)$

          SUPDV2(NCOORD,K1,NOD,2)$
          SUPDV2(ELNOD,K2,EL,3)$
          SUPDV2(INT,K3,6,6)$
          SUPDV1(A,K4,3)  $
          SUPDV1(B,K5,3)  $
          SUPDV1(RR,K6,3) $
          SUPDV1(ZZ,K7,3) $
          SUPDV1(LP,K8,3)$
          SUPDV2(AA,K9,6,6) $
          SUPDV2(EK,K10,6,6)$
           SUPDV2(SK,K11,N,BD)$
          SUPDV2(VI,K12,N,CS)$
          SUPDV2(VI2,K13,N,CS)$
          SUPDV2(FX,K14,NFX,3)$
          SUPDV1(YM,K15,EL)$
          SUPDV1(NU,K16,EL)$
          SUPDV1(SIGM,K17,EL)$

 'COMMENT' TOTAL NO OF ITERATIONS OF LOAD$
 ININT(ITERN)$
 LINES(1)$ TEXT('(' ITERN'*' ')')$ PRINT(ITERN,3)$

 'COMMENT' INITIALISE YM(NO)                    AND NU
 INREAL(YMI,NUI)$
 LINES(1)$ TEXT('(' YMI'*'AND'*'NUI'*' ')')$ EPRINT(YMI,3)$ SPACES(3)$
 PRINT(NUI,1,2)$

 'FOR' NO=1 'STEP' 1 'UNTIL' EL 'DOBEGIN'
 YM(NO)=YMI$ NU(NO)=NUI$ 'END'$



 'COMMENT' AUTO IS A PROCEDURE TO FORM ELEMENTS IN A HALFSPACE GIVEN-
            NUMBER OF NODES ACROSS TOP OF HALFSPACE
            NUMBER OF NODES DOWN HALFSPACE
           SPACING IN LENGTH UNITS ACROSS
         SPACING IN LENGTH UNITS DOWN   $

 AUTO$


 'FOR' I=1 'STEP' 1 'UNTIL' NOD 'DO BEGIN'
 NCOORD(I,2)=NCOORD(I,2)+10$ 'END'$
```

block of public declarations

dope vectors - for m/c addressing purposes Egdon on KDF9 only

```
'COMMENT' OUTPUT OF ELEMENT NODE MATRIX $
     LINES(2)$ TEXT( '('ELNOD')' )$ LINES(1)$
SM=0$ SN=0$
     'FOR' I = 1 'STEP' 1 'UNTIL' EL 'DO' 'BEGIN'
          'IF' SM 'EQ' 6 'THEN' 'BEGIN' LINES(1)$ SM= 0$ 'END'$
SM=SM+1$
       'IF' SN 'EQ' 24 'THEN' 'BEGIN' LINES(2)$ SN= 0$ 'END'$
SN=SN+1$
     'FOR' J = 1 'STEP' 1 'UNTIL' 3 'DO' 'BEGIN'
     IPRINT(ELNOD(I,J),3)$ SPACES(1)$
'END'$ SPACES(4)$ 'END'$
PAGE$

'COMMENT' OUTPUT OF NODE CO-ORDINATE MATRIX $
     LINES(2)$ TEXT( '(' NCOORD ')' )$  LINES(1)$
SM=0$
      'FOR' I = 1 'STEP' 1 'UNTIL' NOD 'DO' 'BEGIN' SPACES(2)$
'IF' SM 'EQ' 5 'THEN' 'BEGIN' LINES(1)$ SM=0$ 'END'$ SM=SM+1$
     'FOR' J = 1 'STEP' 1 'UNTIL' 2 'DO' 'BEGIN'
     EPRINT(NCOORD(I,J),2)$ SPACES(1)$
     'END'$ 'END'$

BWCHEK$

'COMMENT' READ IN  FIXITY MATRIX $
'FOR' I=1 'STEP' 1 'UNTIL' NFX 'DOBEGIN' 'FOR' J=1,2,3 'DO' ININT
(FX(I,J))$ 'END'$
LINES(1)$ TEXT('(' XXX'*'FIXITY'*'MATRIX'*'XXX ')')$
IMATPR(FX,NFX,3,3)$


ITER=1$
  LAB1'.' PAGE$          LINES(1)$ TEXT('('ITER=')')$ PRINT(ITER,3)$
NULL(SK,N,BD)$


'FOR' NO = 1 'STEP' 1 'UNTIL' EL 'DO' 'BEGIN'
DD=(YM(NO)*NU(NO))/((1+NU(NO))*(1-2*NU(NO)))$
MM= (1-NU(NO))/NU(NO)$
SS=(1-2*NU(NO))/(2*NU(NO))$
AGLOB$
INTEG$
MATCOP (CC,AA,6,6)$
MATINV(PINT,PREAL,BB,CC,6)$
TRANS(EK,BB,6,6)$
MATMUL(CC,EK,INT,6,6,6)$
MATMUL(EK,CC,BB,6,6,6)$
BPOST3$
'END'$
LINES(3)$ TEXT( '(' SK'*'IS'*'DONE')' )$
SPACES(4)$ IPRINT(NO-1,4)$
TEXT('(' '**' ELEMENT'*'STIFFNESSES'*'ADDED')')$
SPACES(8)$TEXT('(' TOTAL'*'HALFSPACE'*'AREA ')')$ SPACES(2)$
PRINT(AREA,4,1)$
AREA=0$
```

element stiffness

```
FXBDIT$
'COMMENT' INCREMENTAL LOADING SEQUENCE INCLUDING 1ST $
'IF' ITER 'EQ' 1 'THEN' 'BEGIN'
NULL(VI,N,CS)$
LOAD$
       'FOR' I=1 'STEP' 1 'UNTIL' N 'DO' VI2(I,1)=VI(I,1)$
       'END'$
NULL(VI,N,CS)$
'FOR' I=1 'STEP' 1 'UNTIL' N 'DO' 'BEGIN'
   'IF' ITER 'LT' ITERN 'THEN' VI(I,1)=(ITER/ITERN)*VI2(I,1)
    'ELSE' VI(I,1)=VI2(I,1)$            'END'$

R51200(N,BD,CS,SK,VI)$ ←—Choleski solution of equations (upper band),
LINES(1)$ TEXT('('DEFLECTIONS')')$          superceeded by PLAGMK3
'FOR' I=1 'STEP' 2 'UNTIL' (N-1) 'DOBEGIN'
SM=(I+1)/2$
LINES(1)$ IPRINT(SM,1)$ SPACES(3)$
EPRINT(VI(I,1),4)$ SPACES(2)$ EPRINT(VI(I+1,1),4)$
'END'$
NODSTR$

PAGES$ TEXT('(' ELEMENT'****'CENTROID'***'R'******'Z'**'STRESSES'***'R
    '****************'TH'****************'Z'****************'TRZ ')')$
'FOR' NO=1 'STEP' 1 'UNTIL' EL 'DOBEGIN'
LR=0$ LZ=0$
'FOR' L=1,2,3 'DOBEGIN'
L1'.'
LR=LR+NCOORD(ELNOD(NO,L),1)$
L2'.'
LZ=LZ+NCOORD(ELNOD(NO,L),2)$
'END'$ LR=LR/3$ LZ=LZ/3$
LINES(1)$ SPACES(4)$ IPRINT(NO,2)$ SPACES(5)$
PRINT(LR,3,1)$ SPACES(2)$ PRINT(LZ,3,1)$
NULL(AA,6,6)$ NULL(BB,6,6)$ NULL(CC,6,6)$
DD=(YM(NO)*NU(NO))/((1+NU(NO))*(1-2*NU(NO)))$
MM= (1-NU(NO))/NU(NO)$
SS=(1-2*NU(NO))/(2*NU(NO))$
SETD(BB,MM,SS)$                          stresses at element centroids
SETB(AA,LR,LZ)$
MATMUL(CC,BB,AA,6,6,6)$ 'COMMENT' C=D.B $
AGLOB$
MATINV(PINT,PREAL,BB,AA,6)$ 'COMMENT' BB=A-1 $
MATMUL(AA,CC,BB,6,6,6)$ 'COMMENT' AA=D.B.A-1 $
NULL(BB,6,6)$
L=1$ 'FOR' I=1 'STEP' 2 'UNTIL' 5 'DOBEGIN'
L3'.'
SM=ELNOD(NO,L)$
L4'.'
BB(I,1)=VI(2*SM-1,1)$BB(I+1,1)=VI(2*SM,1)$
L=L+1$ 'END'$
MATMUL(CC,AA,BB,6,6,6)$ 'COMMENT' CC=D.B.A-1.VI $
'COMMENT' STRESSES IN CC 1,1 TO CC 4,1 $
'FOR' I=1,2,3,4 'DOBEGIN'
SPACES( 4)$ PRINT(CC(I,1),4,2)$CLEAR$ 'END'$
MEANST=0$
'FOR' I=1,2,3 'DO' MEANST=MEANST + CC(I,1)$
MEANST=MEANST/3$
SPACES(2)$ TEXT('(' MN'*'NOR'*'STRSS'*' ')')$ PRINT(MEANST,3,3)$
'COMMENT' MODIFY MODULUS$
SIGM(NO)=MEANST$                         modify Young's modulus according
MEANST=ABS(MEANST)$                      to E = f(σ)
YM(NO)= 7000*MEANST**0.55$
SPACES(1)$ TEXT('('NEW'*'YM ')')$ EPRINT(YM(NO),3)$
'END'$ 'COMMENT' NO=1 TO EL FOR STRESSES$
```

```
LINES(1)$ TEXT('(' MODIFIED'*'MODULUS')')$
LINES(1)$ 'FOR' I=1 'STEP' 1 'UNTIL' EL 'DO' 'BEGIN'
EPRINT(YM(I ),3)$ SPACES(1)$ 'END'$
LINES(1)$ TEXT('(' ALL'*'MEAN'*'STRESSES ')')$
LINES(1)$ 'FOR' I=1 'STEP' 1 'UNTIL' EL 'DOBEGIN' PRINT(SIGM(I ),3)$
SPACES(1)$ 'END'$
'IF' ITER 'EQ' (1) 'THEN' STOP$
ITER=ITER+1$  'GOTO'   LAB1$
STOP$
'END' MAIN 3NBITERATIVE
*PUNCH
*IDENTIFIERNODSTR
*ALGOL

*SUBSTITUTEDEC3NBIT
'PROCEDURE' NODSTR$
'BEGIN'
'REAL' LR,LZ,PREAL$
'INTEGER' I,J,SM,SN,PINT,L$
'ARRAY' BB(1'.'6,1'.'6),CC(1'.'6,1'.'6)$
PAGE$ TEXT('('NODAL'*'STRESSES'*'FOR'*'SOME'*'ELEMENTS ')')$
'COMMENT' 1ST 6 ELEMENTS, NODSTR USES OLD MODULUS$
'FOR' NO=1 ,2,3,4,5,6 'DOBEGIN'
'FOR' L=1,2,3 'DOBEGIN'
LINES(1)$
LR=NCOORD(ELNOD(NO,L),1)$  LZ=NCOORD(ELNOD(NO,L),2)$
LINES(1)$ SPACES(4)$ IPRINT(NO,2)$ SPACES(5)$
PRINT(LR,3,1)$ SPACES(2)$ PRINT(LZ,3,1)$
NULL(AA,6,6)$ NULL(BB,6,6)$ NULL(CC,6,6)$
DD=(YM(NO)*NU(NO))/((1+NU(NO))*(1-2*NU(NO)))$
MM= (1-NU(NO))/NU(NO)$
SS=(1-2*NU(NO))/(2*NU(NO))$
SETD(BB,MM,SS)$
SETB(AA,LR,LZ)$
MATMUL(CC,BB,AA,6,6,6)$ 'COMMENT' C=D.B $
AGLOB$
MATINV(PINT,PREAL,BB,AA,6)$ 'COMMENT' BB=A-1 $
MATMUL(AA,CC,BB,6,6,6)$ 'COMMENT' AA=D.B.A-1 $
NULL(BB,6,6)$
L=1$ 'FOR' I=1 'STEP' 2 'UNTIL' 5 'DOBEGIN'
L3'.'
SM=ELNOD(NO,L)$
L4'.'
BB(I,1)=VI(2*SM-1,1)$BB(I+1,1)=VI(2*SM,1)$
L=L+1$ 'END'$
MATMUL(CC,AA,BB,6,6,6)$ 'COMMENT' CC=D.B.A-1.VI $
'COMMENT' STRESSES IN CC 1,1 TO CC 4,1 $
'FOR' I=1,2,3,4 'DOBEGIN'
SPACES( 4)$ PRINT(CC(I,1),4,2)$       'END'$
MEANST=0$
'FOR' I=1,2,3 'DO' MEANST=MEANST + CC(I,1)$
MEANST=MEANST/3$
SPACES(2)$ TEXT('(' MN'*'NOR'*'STRSS'*' ')')$ PRINT(MEANST,3,3)$
'END'$ 'COMMENT' L=1 2 3 FOR ELEMENT NO$
LINES(1)$
'END'S 'COMMENT' NO=1 TO 6$
'END'  NODSTR
```

change to define no. of iterations

nodal stresses for selected elements

```
*PUNCH
*IDENTIFIERBWCHEK
*ALGOL

*SUBSTITUTEDEC3NBIT
 'PROCEDURE' BWCHEK$                          check and output bandwidth
 'BEGIN'
 'INTEGER' NO,I,R,S,T,BAND$
 'INTEGER ARRAY' P(1':'3)$
 T=0$
 'FOR' NO = 1 'STEP' 1 'UNTIL' EL 'DO' 'BEGIN'
 'FOR' I = 1,2,3 'DO' P(I) = ELNOD(NO,I)$
 R=0$ S=1000$
 'FOR' I = 1,2,3 'DO' 'BEGIN'
 'IF' P(I) 'GT' R 'THEN' R=P(I)$
 'IF' P(I) 'LT' S 'THEN' S=P(I)$
 'END'$
 BAND = 2*(R-S+1)$
 'IF' BAND 'GT' T 'THEN' T = BAND$
 'END'$

 LINES(1)$ TEXT( '('XXX'*'CORRECTED'*'BANDWIDTH'*'XXX')' )$
 SPACES(2)$ TEXT ( '('IS')' )$ SPACES(2)$ IPRINT(T,2)$
 'END' BWCHEK
*PUNCH
*IDENTIFIERAUTO
*ALGOL

*SUBSTITUTEDEC3NBIT
 'PROCEDURE' AUTO$
 'BEGIN'
 'REAL' M$
 'INTEGER' ACROSS,DOWN$
 ININT(ACROSS,DOWN)$
    'BEGIN'
 'INTEGER' I,J,ACI,DUI,ELEM,P $
 'ARRAY' ACVEC(1':'ACROSS-1),DUNVEC(1':'DOWN-1)$
 'REAL' RSUM,ZSUMS

 'FOR' I=1 'STEP' 1 'UNTIL' (ACROSS-1) 'DO' INREAL(ACVEC(I))$
 'FOR' I=1 'STEP' 1 'UNTIL' (DOWN-1) 'DO' INREAL(DUNVEC(I))$

 ELEM=1$  J=1$
 PLO':'ELNOD(ELEM,1) = J+ACROSS$
       ELNOD(ELEM,2) = J$
       ELNOD(ELEM,3) = J+ACROSS+1$      } element node numbering
       ELNOD(ELEM+1,1) =J$
       ELNOD(ELEM+1,2) =J+1$
       ELNOD(ELEM+1,3) = J+1+ACROSS$

 M= ((J+1)/ACROSS) +10$
 P=ENTIER(M)$

 'IF' ABS(M) - ABS(ENTIER(M)) 'LT' ('E'-7) 'THEN' J=J+1$
 'IF' ELEM+1 'EQ' EL 'THEN' 'GOTO' PL1$
 ELEM=ELEM+2$ J=J+1$ 'GOTO' PLO$
```

reverts to zero, if for halfspace problem

```
PL1'.' ELEM=1$ RSUM=6$ ZSUM=0$    ACI=0$  DUI=0$
 'COMMENT' RMIN IE RSUM  6 INCHES $
PL2'.' NCOORD(ELEM,1) = RSUM$
ACI=ACI+1$
RSUM=RSUM+ACVEC(ACI)$
NCOORD(ELEM,2) = ZSUM$
ELEM=ELEM+1$
'IF' ACI 'EQ' (ACROSS-1) 'THEN' 'BEGIN'
NCOORD(ELEM,1)=RSUM$  NCOORD(ELEM,2)=ZSUM$
'IF' DUI 'EQ' (DOWN-1) 'THEN' 'GOTO' PL3$
ELEM=ELEM+1$
ACI=0$
DUI=DUI+1$
ZSUM=ZSUM+DUNVEC(DUI)$
RSUM=6$ 'COMMENT' RSUM SET TO 6  IE R MINIMUM$
'GOTO' PL2$ 'END'$
'GOTO' PL2$
PL3'.' 'END'$
'END' AUTO
```

node co-ordinates

```
*PUNCH
*IDENTIFIERAGLOB
*ALGOL
*SUBSTITUTEDEC3NBIT
 'PROCEDURE' AGLOB$
 'BEGIN'
 'INTEGER' I,J,S,L,D$  'REAL' R,Z$
 NULL(AA,6,6)$
 S=1$
 'FOR' L=1 'STEP' 1 'UNTIL' 3 'DO' 'BEGIN'
 R=NCOORD(ELNOD(NO,L),1)$
 Z=NCOORD(ELNOD(NO,L),2)$

 'FOR' J=1 'STEP' 3 'UNTIL' 4 'DO' 'BEGIN'
 'IF' J 'EQ' 1 'THEN' D=S 'ELSE' D=S+1$
 AA(D,J)=1$ AA(D,J+1)=R$  AA(D,J+2)=Z$
 'END'$
 S=S+2$
 'END'$
 'END' AGLOB
```

```
*PUNCH
*IDENTIFIERINTEG
*ALGOL
*SUBSTITUTEDEC3NBIT
 'PROCEDURE' INTEG$
 'BEGIN'
      'INTEGER' L,I,J$ 'REAL'       TP1,TP2,TP3,TP4,TP5,AREA0$

 NULL(INT,6,6)$
 'FOR' L=1 'STEP' 1 'UNTIL' 3 'DO' 'BEGIN'
 RR(L) = NCOORD(ELNOD(NO,L),1)$
 ZZ(L) = NCOORD(ELNOD(NO,L),2)$
 'END'$
 AREA0= ABS( (RR(1)*(ZZ(2)-ZZ(3))+RR(3)*(ZZ(1)-ZZ(2))
              +RR(2)*(ZZ(3)-ZZ(1)))/2  )$
 'IF' ABS(RR(1)-RR(2)) 'LT' ('E'-10) 'THEN' 'BEGIN'
 A(1)=0$ B(1)=0$ 'GOTO' LAB5$ 'END'$
 A(1) = (RR(2)*ZZ(1)-RR(1)*ZZ(2))/(RR(2)-RR(1))$
 B(1) = (ZZ(2)-ZZ(1))/(RR(2)-RR(1))$
 LAB5'.' 'IF' ABS(RR(2)-RR(3)) 'LT' ('E'-10) 'THEN' 'BEGIN'
 A(2)=0$ B(2)=0$ 'GOTO' LAB6$ 'END'$
 A(2) = (RR(3)*ZZ(2)-RR(2)*ZZ(3))/(RR(3)-RR(2))$
 B(2) = (ZZ(3)-ZZ(2))/(RR(3)-RR(2))$

 LAB6'.' 'IF' ABS(RR(3)-RR(1)) 'LT' ('E'-10) 'THEN' 'BEGIN'
 A(3)=0$ B(3)=0$ 'GOTO' LAB7$ 'END'$
 A(3) = (RR(1)*ZZ(3)-RR(3)*ZZ(1))/(RR(1)-RR(3))$
 B(3) = (ZZ(1)-ZZ(3))/(RR(1)-RR(3))$

 LAB7'.'I=1$
 TLAB1'.' 'IF' ABS(RR(I)) 'LT' ( 'E'-10 ) 'THEN' 'BEGIN'
    LP(I)=0$
 'IF' I 'EQ' 3 'THEN' 'GOTO' TLAB2$
 I=I+1$
 'GOTO' TLAB1$  'END'$
 LP(I)=LN(RR(I))$
 'IF' I 'EQ' 3 'THEN' 'GOTO' TLAB2$
 I=I+1$ 'GOTO'  TLAB1$
 TLAB2'.' INT(1,1) = MM*TYPE1(A,B,RR,LP)$
      INT(1,2) = (1+MM)*AREA0$
      INT(1,6) = AREA0$
      INT(1,3) = MM*TYPE2(A,B,RR,LP)$
      INT(2,2) = 2*(1+MM)*TYPE4(A,B,RR,LP)$
      INT(2,3) = (1+MM)*TYPE5(A,B,RR,LP)$
      INT(2,6) = 2*TYPE4(A,B,RR,LP)$
      INT(3,3) = MM*TYPE3(A,B,RR,LP) + SS*TYPE4(A,B,RR,LP)$
      INT(3,5) = SS*TYPE4(A,B,RR,LP)$
      INT(3,6) = TYPE5(A,B,RR,LP)$
      INT(5,5) = INT(3,5)$
      INT(6,6) = MM*TYPE4(A,B,RR,LP)$

 TP1=TYPE1(A,B,RR,LP)$ TP2=TYPE2(A,B,RR,LP)$ TP3=TYPE3(A,B,RR,LP)$
 TP4=TYPE4(A,B,RR,LP)$ TP5=TYPE5(A,B,RR,LP)$

 'FOR' I = 1 'STEP' 1 'UNTIL' 6 'DO' 'BEGIN'
 'FOR' J = 1 'STEP' 1 'UNTIL' 6 'DO' 'BEGIN'
 INT(J,I) = INT(I,J)$
 'END'$ 'END'$
 'FOR' I=1 'STEP' 1 'UNTIL' 6 'DO BEGIN'
 'FOR' J=1 'STEP' 1 'UNTIL' 6 'DO' INT(I,J)=6.2832*DD*INT(I,J)$ 'END'$
 AREA=AREA+AREA0$
 'END' INTEG
```

if radius zero, de l'Hôpital's rule used in integration

```
*PUNCH
*IDENTIFIERTYPE1
*ALGOL
*SUBSTITUTEDEC3NBIT
 'REAL PROCEDURE' TYPE1(A,B,RR,LP)$ 'ARRAY' A,B,RR,LP$
 'BEGIN'
 'REAL' TYPE$
 TYPE =  A(1)*(LP(2)-LP(1)) + B(1)*(RR(2)-RR(1))
 + A(2)*(LP(3)-LP(2)) + B(2)*(RR(3)-RR(2))
 + A(3)*(LP(1)-LP(3)) + B(3)*(RR(1)-RR(3))$
 TYPE1 = ABS(TYPE)$
 'END'
*PUNCH
*IDENTIFIERTYPE2
*ALGOL
*SUBSTITUTEDEC3NBIT
 'REAL PROCEDURE' TYPE2(A,B,RR,LP)$ 'ARRAY' A,B,RR,LP$
 'BEGIN'
 'REAL' TYPE$
 TYPE =  A(1)**2*(LP(2)-LP(1))/2 + A(1)*B(1)*(RR(2)-RR(1))
               + B(1)**2*(RR(2)**2-RR(1)**2)/4
 + A(2)**2*(LP(3)-LP(2))/2 + A(2)*B(2)*(RR(3)-RR(2))
               + B(2)**2*(RR(3)**2-RR(2)**2)/4
 + A(3)**2*(LP(1)-LP(3))/2 + A(3)*B(3)*(RR(1)-RR(3))
               + B(3)**2*(RR(1)**2-RR(3)**2)/4$
 TYPE2 = ABS(TYPE)$
 'END'
*PUNCH
*IDENTIFIERTYPE3
*ALGOL
*SUBSTITUTEDEC3NBIT
 'REAL PROCEDURE' TYPE3(A,B,RR,LP)$ 'ARRAY' A,B,RR,LP$
 'BEGIN'
 'REAL' TYPE$
 TYPE  = (A(1)**3*(LP(2)-LP(1))          + 3*A(1)**2*B(1)*(RR(2)-RR(1))
 + 3 *A(1)*B(1)**2*(RR(2)**2-RR(1)**2)/2
 + B(1)**3*(RR(2)**3-RR(1)**3)/3
 + A(2)**3*(LP(3)-LP(2))          + 3*A(2)**2*B(2)*(RR(3)-RR(2))
 + 3*A(2)*B(2)**2*(RR(3)**2-RR(2)**2)/2
 + B(2)**3*(RR(3)**3-RR(2)**3)/3
 +A(3)**3*(LP(1)-LP(3))          + 3*A(3)**2*B(3)*(RR(1)-RR(3))
 + 3* A(3)*B(3)**2*(RR(1)**2-RR(3)**2)/2
 + B(3)**3*(RR(1)**3-RR(3)**3)/3)/3$
 TYPE3 = ABS(TYPE)$
 'END'
```

```
*IDENTIFIERTYPE4
*ALGOL
*SUBSTITUTEDEC3NBIT
 'REAL PROCEDURE' TYPE4(A,B,RR,LP)$ 'ARRAY' A,B,RR,LP$
 'BEGIN'
 'REAL' TYPE$
 TYPE =  (A(1)*(RR(2)**2-RR(1)**2)+A(2)*(RR(3)**2-RR(2)**2)
         + A(3)*(RR(1)**2-RR(3)**2))/2
 +(B(1)*(RR(2)**3-RR(1)**3)+B(2)*(RR(3)**3-RR(2)**3)
          +B(3)*(RR(1)**3-RR(3)**3))/3$
 TYPE4 = ABS(TYPE)$
 'END'
*PUNCH
*IDENTIFIERTYPE5
*ALGOL
*SUBSTITUTEDEC3NBIT
 'REAL PROCEDURE' TYPE5(A,B,RR,LP)$ 'ARRAY' A,B,RR,LP$
 'BEGIN'
 'REAL' TYPE$
 TYPE =   (A(1)**2*(RR(2)-RR(1))+ A(1)*B(1)*(RR(2)**2-RR(1)**2)
         +B(1)**2*(RR(2)**3-RR(1)**3)/3
 +A(2)**2*(RR(3)-RR(2))+A(2)*B(2)*(RR(3)**2-RR(2)**2)
             +B(2)**2*(RR(3)**3-RR(2)**3)/3
 + A(3)**2*(RR(1)-RR(3)) +A(3)*B(3)*(RR(1)**2-RR(3)**2)
          + B(3)**2*(RR(1)**3-RR(3)**3)/3)/2$
 TYPE5 = ABS(TYPE)$
 'END' TYPE5
*PUNCH
*IDENTIFIERBPOST3
*ALGOL

*SUBSTITUTEDEC3NBIT
 'PROCEDURE' BPOST3$
 'BEGIN'
 'INTEGER' S,L,I,J,SM,SN$
 'FOR' S=1,2,3 'DOBEGIN'
 'FOR' L=1,2,3 'DOBEGIN'
 I= ELNOD(NO,S)$                    posting element stiffness to upper
 J= ELNOD(NO,L)$                    band
 'FOR' SM=0,1 'DO BEGIN'
 'FOR' SN=0,1 'DO BEGIN'
 'IF' 2*J-SN 'GE' 2*I-SM 'THEN' SK(2*I-SM,2*J-SN-2*I+SM+1) =
 SK(2*I-SM,2*J-SN-2*I+SM+1) + EK(2*S-SM,2*L-SN)$
 'END'$ 'END'$
 'END'$ 'END'$
 'END' BPOST3
```

```
*PUNCH
*IDENTIFIERFXBDIT
*ALGOL

*SUBSTITUTEDEC3NBIT
 'PROCEDURE' FXBDIT$
 'BEGIN'
 'INTEGER' NODE,RSIGN,ZSIGN,I,P$
 'FOR' P=1 'STEP' 1 'UNTIL' NFX 'DOBEGIN'
 NODE = FX(P,1)$  RSIGN = FX(P,2)$  ZSIGN = FX(P,3)$
 'IF' RSIGN 'EQ' 1 'THEN' 'GOTO' A3$
 'FOR' I=2 'STEP' 1 'UNTIL' BD 'DO BEGIN'
 SK(2*NODE-1,I)=0$ 'END'$ SK(2*NODE-1,1)=1$
 'FOR' I=1 'STEP' 1 'UNTIL' (2*NODE-2) 'DO BEGIN'
 'IF' (2*NODE-1) 'GT' (I-1+BD) 'THEN' 'GOTO' A2$
 SK(I,2*NODE-1-I+1)=0$
 A2'.' 'END'$
 A3'.' 'IF' ZSIGN 'E0' 1 'THEN' 'GOTO' A5$
 'FOR' I=2 'STEP' 1 'UNTIL' BD 'DO BEGIN'
 SK(2*NODE,I)=0$ 'END'$ SK(2*NODE,1)=1$
 'FOR' I=1 'STEP' 1 'UNTIL' (2*NODE-1) 'DO BEGIN'
 'IF' (2*NODE) 'GT' (I-1+BD) 'THEN' 'GOTO' A4$
 SK(I,2*NODE-I+1)=0$
 A4'.' 'END'$
 A5'.' 'END'$
 'END'  FXBDIT
*PUNCH
*IDENTIFIERLOAD
*ALGOL
*SUBSTITUTEDEC3NBIT
 'PROCEDURE' LOAD$
 'BEGIN'
 'INTEGER' NO,I$  'REAL' LR,LZ$
 'FOR' I = 1 'STEP' 1 'UNTIL' N 'DO' 'BEGIN' VI(I,1)=0$ 'END'$
 LAB3'.' ININT(NO)$
 'IF' NO 'EQ' 99 'THEN' 'GOTO' LAB4$
 INREAL(LR)$ INREAL(LZ)$
      LINES(2)$ TEXT( '(' LOADING ')' )$ SPACES(5)$TEXT( '('NODE')' )$
      SPACES(1)$ IPRINT(NO,2)$ SPACES(4)$ EPRINT(LR,4)$ SPACES(2)$
     . EPRINT(LZ,4)$
 VI(2*NO-1,1)=LR$
 VI(2*NO,1)=LZ$
 'GOTO' LAB3$
 LAB4'.' 'END' LOAD DOUBLE VI
```

```
*PUNCH
*IDENTIFIERUD3G00


*SUBSTITUTEDEC3NBIT
 'PROCEDURE' UD3G $
 'BEGIN'
 'ARRAY' RE(1'.'6,1'.'1),BB(1'.'6,1'.'6),DUMRE(1'.'6,1'.'1)$
 'REAL' RONE,RTWO,ZONE,ZTWO,SHEAR,NORMAL,A12,B12 $
 'INTEGER' NODE1,NODE2,ELNO,I,J,L$
 'COMMENT' LOADS ON ANY SURFACE EXCEPT A VERTICAL ONE,
        IN THAT CASE USE XX LOAD XX PROCEDURE $
 LINES(1)$
 TEXT('(' XXXXXXXXXXXXXXXXXXXXXXXXXXXXXXXXXXXXXXXXXXXXXXXXXXXXXXXXXX')')$
 LINES(1)$ TEXT('('  UNIFORMALLY'*' DISTRIBUTED'*'LOAD'***'UD3G ')')$
 L1'.' ININT(NO)$
 'IF' NO 'EQ' 888 'THEN' 'GOTO' L2$
    LINES(1)$ TEXT('(' FOR'*'ELEMENT ')')$  IPRINT(NO,2)$
 ININT(NODE1,NODE2)$
    SPACES(1)$ TEXT('('BETWEEN'*'NODES ')')$
 IPRINT(NODE1,2)$ SPACES(1)$ TEXT('(' AND ')')$ IPRINT(NODE2,2)$
 RONE = NCOORD(NODE1,1)$    RTWO = NCOORD(NODE2,1)$
 ZONE = NCOORD(NODE1,2)$ ZTWO = NCOORD(NODE2,2)$
 'IF' ABS(RONE-RTWO) 'LT' ( 'E'-6 ) 'THEN' 'BEGIN'
      LINES(1)$ TEXT('(' HAVE'*'TRIED'*'TO'*'SPECIFY'*'AN'*'R'*'CONSTAN
      '*'SURFACE'*','*'USE'*'THE'*'PROCEDURE'*'LOAD ')')$
      STOP$ 'END'$
 A12 = (RTWO*ZONE-RONE*ZTWO)/(RTWO-RONE)$
 B12 = (ZTWO-ZONE)/(RTWO-RONE)$
       INREAL(SHEAR,NORMAL)$
   SPACES(6)$ TEXT('(' SHEAR ')')$ PRINT(SHEAR,5,1)$
    SPACES(3)$ TEXT('(' NORMAL ')')$ PRINT(NORMAL,5,1)$

 AGLOB$  MATINV(BB,AA,6)$  TRANS(AA,BB,6,6)$
 'COMMENT' AA CONTAINS A-1 TRANSPOSED$
 'FOR' I=1,2,3,4,5,6 'DO' RE(I,1)=0$
 RE(1,1)=RE(4,1)=(RTWO**2-RONE**2)/2$
 RE(2,1)=RE(5,1)=(RTWO**3-RONE**3)/3$
 RE(3,1)=RE(6,1)=A12*(RTWO**2-RONE**2)/2+B12*(RTWO**3-RONE**3)/3$
 'FOR' I=1,2,3 'DO' RE(I,1)=(-6.2832*SHEAR*RE(I,1))$
 'FOR' I=4,5,6 'DO' RE(I,1)=(-6.2832*NORMAL*RE(I,1))$
 MATMUL(DUMRE,AA,RE,6,6,1)$      MATCOP(RE,DUMRE,6,1)$
 LINES(1)$ TEXT('(' RE'*'MATRIX ')')$    EMATPR(RE,6,1,2)$
 I=1$
 'FOR' L=1,2,3 'DOBEGIN'
 ELNO = ELNOD(NO,L)$
 VI(2*ELNO-1,1) = VI(2*ELNO-1,1) + RE(I,1)$
 VI(2*ELNO,1) = VI(2*ELNO,1) + RE(I+1,1)$
 I=I+2$ 'END'$
 'GOTO' L1$
 L2'.' SPACES(2)$TEXT('('VI'*'TO'*'R51200'*'SOLVE ')')$
 'END' UD3
```

```
*PUNCH
*IDENTIFIERSETD
*ALGOL
*SUBSTITUTEDEC3NBIT
 'PROCEDURE' SETD(BB,MM,SS)$ 'ARRAY' BB$  'REAL' MM,SS$
 'BEGIN'
 'INTEGER' I,J$
 BB(1,1)=MM$  BB(1,2)=1$  BB(1,3)=1$
 BB(2,1)=1$  BB(2,2)=MM$  BB(2,3)=1$
 BB(3,1)=1$  BB(3,2)=1$  BB(3,3)=MM$
 BB(4,4)=SS$
 'FOR' I=1,2,3,4,5,6 'DO BEGIN'
 'FOR' J=1,2,3,4,5,6 'DO' BB(I,J)=DD*BB(I,J)$ 'END'$
 'END' SETD
*PUNCH
*IDENTIFIERSETB
*ALGOL
*SUBSTITUTEDEC3NBIT
 'PROCEDURE' SETB(AA,LR,LZ)$ 'ARRAY' AA$  'REAL' LR,LZ$
 'BEGIN'
 AA(1,2)=1$
 AA(2,1)=1/LR$  AA(2,2)=1$  AA(2,3)=LZ/LR$
 AA(3,6)=1$
 AA(4,3)=1$  AA(4,5)=1$
 'END' SETB
```

PROGRAM 2 4 Node Axisymmetric Rectangle

A2.1 Iterative

A2.1.1 General description

The program is written in 1 module using ICL 1900 input/output procedures.

Element data is generated automatically for a cylindrical continuum given the number of mesh nodes in the radial and vertical directions and their spacing (procedure AUTO 4).

Element data calculated in 'AUTO4':

matrix ELNOD(1:EL,1:4), element numbering

" NCOORD(1:NOD,1:2), nodal co-ordinates

Nodes in the structure are numbered as in Fig. A.2. Co-ordinates are calculated using an origin on the mesh axis at element 1. The z-coordinates are reversed, to be increasing upwards from an origin at 10 in. below the base of the structure, in order that integral calculations are performed satisfactorily. The maximum bandwidth of the stiffness matrix is computed (procedure BCHEK4). Storage for the upper band of the stiffness matrix is reserved using bandwidth (BD) and the total number of unknowns (N), calculated from the element numbering data in 'ELNOD'.

Other procedures:

STORE - stores mean normal stress and octahedral shear stress in part of the structural stiffness matrix (when it is redundant after solution of equations has been carried out) for later printout in:

LAYSTR - prints out mean normal and octahedral shear stresses on lineprinter, with spacing proportional to the element mesh to facilitate easy contour sketching.

Procedures in finite element calculations:

AGLOB4 - form (A) matrix for element 'NO' in system co-ordinates

ITINT4 - forms $2\pi\int_{area} B^T D B \, r.d(area)$ using explicit terms calculated from nodal co-ordinates

BPOST4 - posts the relevant part of the element stiffness into the upper band structural stiffness matrix

FXBDIT - boundary conditions; sets the relevant rows and columns of the stiffness matrix to zero: 1 on leading diagonal

LOAD - puts nodal point loads in radial and vertical directions into the load vector

UDOAD4 - calculates the equivalent nodal point loads for a uniformally distributed load (vertical and/or radially symmetric shear loads). The procedure is restricted to the loading of z=constant, element edges

SETD4 - (D) matrix for element 'NO'

SETB4 - (B) matrix for given values of r and z (system co-ordinates)

A2.1.2 Input

Sample input for a thick ring (Fig. A.2) is described:

Data	Description
30×10^6 0.3	Young's Modulus (YMI), Poisson's Ratio (NUI)
1 8	Loads cases (CS), Number of nodes at which boundary conditions are imposed (NFX)
4 2	No. of nodes in radial (ACROSS) and vertical (DOWN) direction
1.0 1.0 1.0	Spacing in radial direction ACVEC (ACROSS-1)
1.0	Spacing in vertical direction DUNVEC (DOWN-1)
1	Total number of iterations or increments to full load (see prog. A.2.2)

Data	Description
1 1 0 2 1 0 3 1 0 4 1 0 5 1 0 6 1 0 7 1 0 8 1 0	Input to boundary fixity matrix FX(1:NFX,1:3); for each node where some displacement is made zero, one row of matrix, i.e. (node, r sign, z sign). If r sign and/or z sign = 0, then deletes relevant row and column, etc.
1 75400 0	Loading:
5 75400 0 99	(node no., r load, z load) and terminator 99 after the last nodal loading

A2.1.3 Input information in program text

If a non-linear elastic relationship is known for the material i.e. $E = f(\sigma_{oct})$, then:

(1) the relationship is defined after label M18

(2) the number in the equality test (6 lines from the end) is changed to equal the desired number of iterations

If a half space problem is being modelled it is important that the minimum radius is set to zero (i.e. in 'AUTO4', RMIN=0).

(NOTE: the sample input was for a thick ring, internal radius 6 in.)

A2.1.4 Output

All input numbers are printed out on the lineprinter together with descriptive text.

The generated mesh data is printed out:

matrixes ELNOD: element numbering

NCOORD: co-ordinates for each node

The total number of unknowns and bandwidth are printed.

All nodal displacements are printed.

Stresses at all the element centroids are printed out.

The new values of modulus are printed, according to $E = f(\sigma_{oct})$.

The mean normal and octahedral shear stresses are outputted on the lineprinter (at iterations 1 and 15) in a form which can be used to sketch contours of equal stress.

PROGRAM 2.1: LISTING (4-node axisymmetric rectangle) (ITERATIVE)

```
*ALGOL
 'BEGIN'
      'INTEGER' NOD,EL,N,CS,NFX, ACROSS,DOWN$
      'REAL' YMI,NUI$
 LTSTAC(20000)$
 YMI=READ$
 NUI=READ$
 CS=READ$                          input data
 NFX=READ$
 ACROSS=READ$
 DOWN=READ$
 'COMMENT' ACROSS IS NODES ACROSS
           DOWN IS NODES DOWN$
 EL = (ACROSS-1)*(DOWN-1)$
 NOD = ACROSS*DOWN$
 N=2*NOD$
 NEWLINE(2)$ WRITETEXT('(' XXX.4.NODE.PROGRAM.XXX ')')$
 'COMMENT' OUTPUT MOST OF THE  INPUT CONSTANTS AND IMPORTANT PARAMETERS$
 NEWLINE(1)$ WRITETEXT('(' INITIAL '('SS')' MODULUS '('21S')' ')')$
 PRINT(YMI,0,4)$
 NEWLINE(1)$ WRITETEXT('(' INITIAL '('SS')' NU      '('27S')' ')')$
 PRINT(NUI,1,4)$
 NEWLINE(1)$ WRITETEXT('(' LOAD '('SS')' CASES '('26S')' ')')$
 PRINT(CS,2,0)$
 NEWLINE(1)$ WRITETEXT('(' NO.'('S')'OF'('S')'FIXITIES '('20S')' ')')$
 PRINT(NFX,3,0)$
 NEWLINE(1)$ WRITETEXT('(' NUMBER.OF.NODES....R,Z..DIRECTIONS ')' )$
 PRINT(ACROSS,2,0)$ SPACE(2)$
 PRINT(DOWN,2,0)$
 NEWLINE(2)$ WRITETEXT('(' ELEMENTS..EL ')')$ SPACE(23)$
 PRINT(EL,5,0)$
 NEWLINE(1)$ WRITETEXT('(' NODES..NOD   ')')$ SPACE(25)$
 PRINT(NOD,5,0)$
 NEWLINE(1)$ WRITETEXT('(' NO.OF.UNKNOWNS...N ')')$ SPACE(17)$
 PRINT(N,5,0)$
 'BEGIN'
 'ARRAY' NCOORD(/1'.'NOD,1'.'2/), INT,AA,BB,CC,EK(/1'.'8,1'.'8/),
 NU,YM(/1'.'EL/), FX(/1'.'NFX,1'.'3/), VI,VI2(/1'.'N,1'.'CS/)$
 'INTEGER' 'ARRAY' ELNOD(/1'.'EL,1'.'4/)$
 'REAL' LR,LZ,EQU,INC,MM,SS,DD,MEANST,TOCT,CR,CT,CZ,CTRZ$
 'INTEGER' I,J,SM,SN,L,NO,ITER,ITERN,BD$
 'INTEGER' II,JJ$
 'PROCEDURE' AUTO4$
 'BEGIN'
 'REAL' M$
 'INTEGER' I,J,ACI,DUI,NODD,P,ELEM$
 'ARRAY' ACVEC(/1'.'ACROSS-1/),DUNVEC(/1'.'DOWN-1/)$
 'REAL' RSUM,ZSUM$
 'FOR' I=1 'STEP' 1 'UNTIL' (ACROSS-1) 'DO' ACVEC(/I/)=READ$
 'FOR' I=1 'STEP' 1 'UNTIL' (DOWN-1) 'DO' DUNVEC(/I/)=READ$
 ELEM=1$  J=1$
 PLO'.'ELNOD(/ELEM,1/) = J+ACROSS$
      ELNOD(/ELEM,2/) = J$
       ELNOD(/ELEM,3/) = J+1$          element node numbering
      ELNOD(/ELEM,4/) = J+ACROSS+1$
 M= ((J+1)/ACROSS) +10$
 P=ENTIER(M)$
 'IF' ABS(M) - ABS(P)          'LT' ('E'-7) 'THEN' J=J+1$
 'COMMENT' NOTE IS ELEM NOT ELEM+1 EQ EL $
 'IF' ELEM   'EQ' EL 'THEN' 'GOTO' PL1$
 ELEM=ELEM+1$ J=J+1$ 'GOTO' PLO$
```

```
PL1'.' PAPERTHROW$
'COMMENT' OUTPUT OF ELEMENT NODE MATRIX $
NEWLINE(2)$ WRITETEXT('(' ELEMENT.NODE.MATRIX...ELNOD ')')$
NEWLINE(1)$
SM=0$  SN=0$
'FOR' I = 1 'STEP' 1 'UNTIL' EL 'DO' 'BEGIN'
'IF' SM 'EQ' 6 'THEN' 'BEGIN' NEWLINE(1)$ SM=0$ 'END'$
SM=SM+1$
'IF' SN 'EQ' 24 'THEN' 'BEGIN' NEWLINE(2)$ SN=0$ 'END'$
SN=SN+1$
'FOR' J=1,2,3,4 'DO' PRINT(ELNOD(/I,J/),3,0)$ SPACE(2)$ 'END'$
      NODD=1$ RSUM=6$ ZSUM=0$    ACI=0$  DUI=0$
  'COMMENT' NOTE RMIN IE RSUM IS 6 INCHES $
PL2'.' NCOORD(/NODD,1/) = RSUM$
ACI=ACI+1$
RSUM=RSUM+ACVEC(/ACI/)$
NCOORD(/NODD,2/) = ZSUM$
NODD=NODD+1$
'IF' ACI 'EQ' (ACROSS-1) 'THEN' 'BEGIN'
NCOORD(/NODD,1/)=RSUM$  NCOORD(/NODD,2/)=ZSUM$      node co-ordinates
'IF' DUI 'EQ' (DOWN-1) 'THEN' 'GOTO' PL3$
NODD=NODD+1$
ACI=0$
DUI=DUI+1$
ZSUM=ZSUM+DUNVEC(/DUI/)$
RSUM=6$ 'COMMENT' RSUM SET TO 6  MIN RADIUS$
'GOTO' PL2$  'END'$
'GOTO' PL2$
PL3'.' PAPERTHROW$
'COMMENT' REARRANGEMENT OF NODE CO-ORDINATES TO BE IN ASCENDING
ORDER OF Z FROM BOTTOM OF HALFSPACE$
'FOR' I=1 'STEP' 1 'UNTIL' NOD 'DO'
            NCOORD(/I,2/)=NCOORD(/I,2/)-NCOORD(/NOD,2/)$
'FOR' I=1 'STEP' 1 'UNTIL' NOD 'DO'
            NCOORD(/I,2/)=ABS(NCOORD(/I,2/))$
'FOR' I=1 'STEP' 1 'UNTIL' NOD 'DO' NCOORD(/I,2/)=NCOORD(/I,2/)+10$
NEWLINE(2)$ WRITETEXT('(' NODE.COORDINATE.MATRIX...NCOORD ')') $
NEWLINE(1)$ SM=0$
'FOR' I = 1 'STEP' 1 'UNTIL' NOD 'DO' 'BEGIN'  SPACE (2)$
'IF' SM 'EQ' 5 'THEN' 'BEGIN' NEWLINE(1)$ SM=0$ 'END'$
SM=SM+1$
'FOR' J=1,2 'DO' PRINT(NCOORD(/I,J/),4,2)$ 'END'$
'END' AUTO4$
'PROCEDURE' BCHEK4$
'BEGIN'
'INTEGER' NO,I,R,S,T,BAND$
'INTEGER' 'ARRAY' P(/1'.'4/)$
T=0$
'FOR' NO = 1 'STEP' 1 'UNTIL' EL 'DO' 'BEGIN'
'FOR' I = 1,2,3,4 'DO' P(/I/) = ELNOD(/NO,I/)$
R=0$ S=1000$
'FOR' I = 1,2,3,4 'DO''BEGIN'
'IF' P(/I/) 'GT' R 'THEN' R=P(/I/,$
'IF' P(/I/) 'LT' S 'THEN' S=P(/I/)$
 'END'$
BAND = 2*(R-S+1)$                          maximum bandwidth
'IF' BAND 'GT' T 'THEN' T = BAND$
 'END'$
BD=T$
'END' BCHEK4$
AUTO4$ 'COMMENT' FORMS ELNOD AND NCOORD (AS SPACE 4 CHOL 3106)
        AND OUTPUTS THEM$
BCHEK4$ 'COMMENT' FORMS BD..BANDWIDTH OF STRUCTURE STIFFNESS MATRIX$
NEWLINE(2)$ WRITETEXT('(' BANDWIDTH..OF.STIFFNESS.MATRIX..BD.OF.SK')')$
SPACE(2)$ PRINT(BD,3,0)$
```

```
    'BEGIN'
'ARRAY' SK(/1'.'N,1'.'BD/)$
'PROCEDURE' STORES$
'BEGIN'
SK(/II,JJ/)=LR$   SK(/II + DOWN -1,JJ/)= ABS(LZ-120)$
SK(/II+ 2*( DOWN -1),JJ/)=MEANST$
SK(/ II+3*(DOWN-1),JJ/)=TOCT$
SK(/II+4*(DOWN-1),JJ/)= MEANST/TOCT$
'IF' JJ 'EQ' (ACROSS-1) 'THEN' 'BEGIN' II=II+1$ JJ=1$ 'END' 'ELSE'
                                                        JJ=JJ+1$
'END' STORE$
'PROCEDURE' LAYSTR$
'BEGIN'
PAPERTHROW$
RMATPR(SK,5*(DOWN-1),ACROSS-1,3,2)$
PAPERTHROW$
'COMMENT' PRINTS OUT MEANST$
WRITETEXT('(' MEAN.NORMAL.STRESS ')')$
NEWLINE(2)$
'FOR' I=1 'STEP' 1 'UNTIL' (DOWN-1) 'DOBEGIN'
'IF' I 'NE' 1 'THEN'
NEWLINE( ENTIER((SK(/I+DOWN-1,1/)-SK(/I-1+DOWN-1,1/))/2) +2)$
'FOR' J=1 'STEP' 1 'UNTIL' (ACROSS-1) 'DOBEGIN'
'IF' J 'NE' 1 'THEN' SPACE(ENTIER((SK(/1,J /)-SK(/1,J -1/))/2))$
PRINT( SK(/I+2*(DOWN-1),J/),2,2)$
'END'$ 'END'$
PAPERTHROW$
WRITETEXT('(' OCT.SHEAR.STRESS ')')$
NEWLINE(2)$
'FOR' I=1 'STEP' 1 'UNTIL' (DOWN-1) 'DOBEGIN'
'IF' I 'NE' 1 'THEN'
NEWLINE( ENTIER((SK(/I+DOWN-1,1/)-SK(/I-1+DOWN-1,1/))/2) +2)$
'FOR' J=1 'STEP' 1 'UNTIL' (ACROSS-1) 'DOBEGIN'
'IF' J 'NE' 1 'THEN' SPACE(ENTIER((SK(/1,J /)-SK(/1,J -1/))/2))$
PRINT( SK(/I+3*(DOWN-1),J/),2,2)$
'END'$ 'END'$
PAPERTHROW$
WRITETEXT('(' RATIO..MEANST.TO.TOCT ')')$
NEWLINE(2)$
'FOR' I=1 'STEP' 1 'UNTIL' (DOWN-1) 'DOBEGIN'
'IF' I 'NE' 1 'THEN'
NEWLINE( ENTIER((SK(/I+DOWN-1,1/)-SK(/I-1+DOWN-1,1/))/2) +2)$
'FOR' J=1 'STEP' 1 'UNTIL' (ACROSS-1) 'DOBEGIN'
'IF' J 'NE' 1 'THEN' SPACE(ENTIER((SK(/1,J /)-SK(/1,J -1/))/2))$
PRINT( SK(/I+4*(DOWN-1),J/),2,2)$
'END'$ 'END'$
'END' LAYSTR$
'PROCEDURE' AGLOB4$
'BEGIN'
'INTEGER' I,J,S,L,D$ 'REAL' R,Z$
NULL(AA,8,8)$
S=1$
'FOR'  L= 1,2,3,4 'DO' 'BEGIN'
R = NCOORD(/ELNOD(/NO,L/),1/)$          (A) matrix
Z = NCOORD(/ELNOD(/NO,L/),2/)$
'FOR' J = 1,5 'DO' 'BEGIN'
'IF' J 'EQ' 1 'THEN' D=S 'ELSE' D=S+1$
AA(/D,J/)=1$ AA(/D,J+1/)=R$ AA(/D,J+2/)=Z$ AA(/D,J+3/)=R*Z$
  'END'$
S=S+2$
 'END'$
'END' AGLOB4$
```

```
'PROCEDURE' ITINT4$
'BEGIN'
'INTEGER' L,I,J$
'REAL' F1OR,FONE,FZOR,FZ,FR,FRZ,FRSQ,FZSQ,FRSQZ,FRCU,FRZSQ,FZSQOR,P,
       R1,R2,Z1,Z2,R21,R221,R231,Z21,Z221,Z231$
'COMMENT' PROVIDED ELEMENT NUMBERED CLOCKWISE STARTING AT BOTTOM LHS
     THEN R1 R2 Z1 Z2 GIVEN AS$
NULL(INT,8,8)$
 R1     = NCOORD(/ELNOD(/NO,1/),1/)$
 R2     = NCOORD(/ELNOD(/NO,4/),1/)$
 Z1     = NCOORD(/ELNOD(/NO,1/),2/)$
 Z2     = NCOORD(/ELNOD(/NO,2/),2/)$
R21=R2-R1$  R221=R2**2-R1**2$  R231=R2**3-R1**3$
Z21=Z2-Z1$  Z221=Z2**2-Z1**2$  Z231=Z2**3-Z1**3$
 'IF' ABS(R1) 'LT' 'E'-6 'OR' ABS(R2) 'LT' 'E'-6 'THEN'
    P=0 'ELSE' P= LN(R2/R1)$
FONE = R21*Z21$
F1OR = ABS( Z21*P )$
FZOR = ABS( Z221*0.5*P )$
FZ = ABS( Z221*R21*0.5 )$
FR = ABS( Z21*R221*0.5 )$
FRZ = ABS(Z221*R221*0.25 )$
FRSQ = ABS( Z21*R231/3 )$
FZSQ = ABS( Z231*R21/3 )$
FRCU = ABS( Z21*R221*(R2**2+R1**2)*0.25 )$
FRSQZ = ABS( Z221*R231/6 )$
FRZSQ = ABS(Z231*R221/6)$
FZSQOR = ABS(Z231*P/3 )$
INT(/1,1/) = MM*F1OR$
INT(/1,2/) = (MM+1)*FONE$
INT(/1,3/) = MM*FZOR$
INT(/1,4/) = (MM+1)*FZ$          explicit integral terms, system
INT(/1,7/) = FONE$               co-ordinates
INT(/1,8/) = FR$
INT(/2,2/) = 2*(MM+1)*FR$
INT(/2,3/) = (MM+1)*FZ$
INT(/2,4/) = 2*(MM+1)*FRZ$
INT(/2,7/) = 2*FR$
INT(/2,8/) = 2*FRSQ$
INT(/3,3/) = MM*FZSQOR + SS*FR$
INT(/3,4/) = (MM+1)*FZSQ + SS*FRSQ$
INT(/3,6/) = SS*FR$
INT(/3,7/) = FZ$
INT(/3,8/) = (SS+1)*FRZ$
INT(/4,4/) = 2*(MM+1)*FRZSQ + SS*FRCU$
'COMMENT' INT 4,4 CHANGED03/11/1969   SS*FRCU  ADDED$
INT(/4,6/) = SS*FRSQ$
INT(/4,7/) = 2*FRZ$
INT(/4,8/) = (2+SS)*FRSQZ$
INT(/6,6/) = SS*FR$
INT(/6,8/) = SS*FRZ$
INT(/7,7/) = MM*FR$
INT(/7,8/)= MM*FRSQ$
INT(/8,8/) = MM*FRCU + SS*FRZSQ$
'FOR' I = 1 'STEP' 1 'UNTIL' 8 'DO'
'FOR' J = 1 'STEP' 1 'UNTIL' 8 'DO' INT(/J,I/)=INT(/I,J/)$
'FOR' I=1 'STEP' 1 'UNTIL' 8 'DO'
'FOR' J=1 'STEP' 1 'UNTIL' 8 'DO' INT(/I,J/)=6.2832*DD*INT(/I,J/)$
'END' INTEG4 $
```

```
'PROCEDURE' BPOST4$
'BEGIN'
'INTEGER' S,L,I,J,SM,SN$
'FOR' S=1,2,3,4 'DO''BEGIN'
I = ELNOD(/NO,S/)$                          post to upper band
'FOR' L=1,2,3,4 'DO''BEGIN'
J = ELNOD(/NO,L/)$
'FOR' SM=0,1 'DO'  'FOR' SN=0,1 'DO'
'IF' 2*J-SN 'GE' 2*I-SM 'THEN'   SK(/2*I-SM,2*J-SN-2*I+SM+1/) =
                                 SK(/2*I-SM,2*J-SN-2*I+SM+1/)+
 EK(/2*S-SM,2*L-SN/)$
 'END'$  'END'$
'END' BPOST4 $
'PROCEDURE' FXBDIT$
'BEGIN'
'INTEGER' NODE,RSIGN,ZSIGN,I,P$   boundary conditions
'FOR' P=1 'STEP' 1 'UNTIL' NFX 'DO''BEGIN'
NODE = FX(/P,1/)$  RSIGN = FX(/P,2/)$  ZSIGN = FX(/P,3/)$
'IF' RSIGN 'EQ' 0 'THEN' 'BEGIN'
'FOR' I=2 'STEP' 1 'UNTIL' BD 'DO'SK(/2*NODE-1,I/)=0$
      SK(/2*NODE-1,1/)=1$
'FOR' I=1 'STEP' 1 'UNTIL' (2*NODE-2) 'DO'
'IF' (2*NODE-1) 'LE' (I-1+BD) 'THEN'SK(/I,2*NODE-1-I+1/)=0$
    'END'$
      'IF' ZSIGN 'EQ' 0 'THEN' 'BEGIN'
'FOR' I=2 'STEP' 1 'UNTIL' BD 'DO' SK(/2*NODE,I/)=0$
     SK(/2*NODE,1/)=1$
'FOR' I=1 'STEP' 1 'UNTIL' (2*NODE-1) 'DO'
'IF' (2*NODE) 'LE' (I-1+BD) 'THEN' SK(/I,2*NODE-I+1/)=0$
'END'$
'END' P$
'END' FXBIT$
'PROCEDURE' LOAD$
'BEGIN'
'INTEGER' NO,I$  'REAL' LR,LZ$
NULL(VI,N,CS)$
NEWLINE(2)$ WRITETEXT('(' XXX.LOADING.OF.SYSTEM.XXX ')')$
LAB3'.' NO=READ$
'IF' NO 'EQ' 99 'THEN' 'GOTO' LAB4$
LR=READ$ LZ=READ$
NEWLINE(1)$ WRITETEXT('(' NODE ')')$ PRINT(NO,3,0)$ SPACE(10)$
WRITETEXT('('R.LOAD')')$ SPACE(2)$ PRINT(LR,0,4)$ SPACE(10)$
WRITETEXT('('Z.LOAD')')$ SPACE(2)$ PRINT(LZ,0,4)$ SPACE(10)$
VI(/2*NO-1,1/)=LR$    VI(/2*NO,1/)=LZ$
'GOTO' LAB3$
'COMMENT' END LOAD VI ARRAY$     load structure
LAB4'.'  'END'$
'PROCEDURE' UDOAD4$
'BEGIN'
'ARRAY' EX(/1'.'8,1'.'2/) ,Q(/1'.'2,1'.'1/), RE(/1'.'8,1'.'1/),BB
(/1'.'8,1'.'8
/),DUMX(/1'.'8,1'.'2/)$
'REAL' RONE,RTWO,ZOTWO,RLOAD,ZLOAD,R221,R231$
'INTEGER' NODE1,NODE2,ELNO,I,L$
NEWLINE(1)$
WRITETEXT( '('XXXXXXXXXXXXXXXXXXXXXXXXXXXXXXXXXXXXXXXXXXXXXXXXX')')$
NEWLINE(1)$
          WRITETEXT( '('XXXXX'*'UNIFORMALLY'*'DISTRIBUTED'*'LOAD')' )$
WRITETEXT( '('XXXXX')' )$
```

```
ULAB1'.' NO=READ$
'IF' NO 'EQ' 888 'THEN' 'GOTO' ULAB2$
  NEWLINE(1)$ WRITETEXT('(' FOR'('S')'ELEMENT ')')$
      PRINT(NO,2,0)$
NODE1=READ$   NODE2=READ$
     SPACE(1)$ WRITETEXT('(' BETWEEN'('S')'NODES ')')$
     PRINT(NODE1,2,0)$ SPACE(1)$ WRITETEXT('(' AND ')')$
     PRINT(NODE2,2,0)$
RONE=NCOORD(/NODE1,1/)$
RTWO=NCOORD(/NODE2,1/)$
ZOTWO=NCOORD(/NODE1,2/)$
'IF' NCOORD(/NODE1,2/)-NCOORD(/NODE2,2/) 'GT' ('E'-6) 'THEN' 'GOTO' ULA
B3$
'GOTO' ULAB4$
ULAB3'.' NEWLINE(1)$ WRITETEXT('(' Z.NOT.CONSTANT.FOR.LOADED.EDGE ')')$
STOP$
ULAB4'.'
RLOAD=READ$  ZLOAD=READ$
     SPACE(6)$ WRITETEXT('('RLOAD')')$ PRINT(RLOAD,0,3)$
     SPACE(3)$ WRITETEXT('('ZLOAD')')$ PRINT(ZLOAD,0,3)$
Q(/1,1/)=RLOAD$ Q(/2,1/)=ZLOAD$
LINES(1)$ EPRINT(Q(/1,1/),3)$ SPACES(1)$ EPRINT(Q(/2,1/),3)$
AGLOB4$
MATINV(BB,AA,8)$
TRANS(AA,BB,8,8)$
'COMMENT' AA NOW CONTAINS INVERT OF A TRANSPOSED$
NULL(EX,8,2)$
'COMMENT' BELOW SETS TERMS OF INTEGRAL, Z CONSTANT$
R221= (RTWO**2-RONE**2)$     R231= (RTWO**3-RONE**3)$
EX(/1,1/) = R221$
EX(/2,1/) = 2*R231/3$
EX(/3,1/) = R221*ZOTWO$
EX(/4,1/) = 2*R231*ZOTWO/3$
EX(/5,2/)=EX(/1,1/)$   EX(/6,2/)=EX(/2,1/)$
EX(/7,2/)=EX(/3,1/)$   EX(/8,2/)=EX(/4,1/)$
MATMUL(DUMX,AA,EX,8,8,2)$
MATMUL(RE,DUMX,Q,8,2,1)$
NEWLINE(2)$ WRITETEXT('('RE=DUMX.Q ')')$ EMATPR(RE,8,1,3)$
'COMMENT' RE CONTAINS IN ITS 8 BY 1 THE LOAD VECTOR FOR NO$
'FOR' I = 1 'STEP' 1 'UNTIL' 8 'DO' RE(/I,1/)=3.14159*RE(/I,1/)$
I=1$
'FOR' L=1,2,3,4 'DOBEGIN'
ELNO=ELNOD(/NO,L/)$
VI(/2*ELNO-1,1/) = VI(/2*ELNO-1,1/) + RE(/I,1/)$
VI(/2*ELNO,1/) = VI(/2*ELNO,1/) + RE(/I+1,1/)$
I=I+2$  'END'$
'GOTO' ULAB1$                          add uniformally distributed loads
ULAB2'.' NEWLINE(1)$                   to load vector
'COMMENT' VI ARRAY UDOADS$
 'END'$
```

```
'PROCEDURE' SETB4 (AA,LR,LZ)$ 'VALUE'LR,LZ$ 'REAL'.LR,LZ$ 'ARRAY' AA$
'BEGIN'
AA(/1,2/)=1$ AA(/1,4/)=LZ$
AA(/2,1/)=1/LR$ AA(/2,2/)=1$ AA(/2,3/)=LZ/LR$ AA(/2,4/)=LZ$
AA(/3,7/)=1$ AA(/3,8/)=LR$
AA(/4,3/)=1$ AA(/4,4/)=LR$ AA(/4,6/)=1$ AA(/4,8/)=LZ$      (B) matrix
 'END'$
'PROCEDURE'SETD4(BB)$ 'ARRAY' BB$
'BEGIN'
'INTEGER' I,J$
BB(/1,1/)=MM$  BB(/1,2/)=1$  BB(/1,3/)=1$
BB(/2,1/)=1$  BB(/2,2/)=MM$  BB(/2,3/)=1$        (D) matrix
BB(/3,1/)=1$  BB(/3,2/)=1$  BB(/3,3/)=MM$
BB(/4,4/)=SS$
'FOR' I=1,2,3,4 'DO'
 'FOR' J=1,2,3,4 'DO' BB(/I,J/)=DD*BB(/I,J/)$
'END' SETD4$
```

```
'COMMENT' TOTAL NO OF ITERATIONS OF LOADS$
 M1'.'
ITERN=READS$ 'COMMENT' INPUT TOTAL ITERATIONS TO FULL LOADS$
NEWLINE(1)$ WRITETEXT('(' ITERN..TO.FULL.LOAD')')$ PRINT(ITERN,3,0)$
'COMMENT' INITIALISE YM(NO) AND NU(NO) $
 M2'.'
              'FOR' I=1 'STEP' 1 'UNTIL' EL 'DO' YM(/I/)=YMI$
              'FOR' I = 1 'STEP' 1 'UNTIL' EL 'DO' NU(/I/)=NUI$
'COMMENT' READ IN FIXITY MATRIX  FX(NFX,3)$
'FOR' I=1 'STEP' 1 'UNTIL' NFX 'DO' 'FOR' J=1,2,3 'DO' FX(/I,J/)=READ
NEWLINE(1)$ WRITETEXT('('XXX.FIXITY.MATRIX.XXX')')$
'FOR' I=1 'STEP' 1 'UNTIL' NFX 'DOBEGIN' NEWLINE(1)$
'FOR' J=1,2,3  'DO' PRINT(FX(/I,J/),3,0)$ 'END'$
 M4'.'
ITER=1$
LAB1'.' PAPERTHROW$
WRITETEXT('(' ITER'('SS')' = ')')$ PRINT(ITER,3,0)$
NULL(SK,N,BD)$
 M5'.'
'FOR' NO = 1 'STEP' 1 'UNTIL' EL 'DO' 'BEGIN'
AGLOB4$
MM=(1-NU(/NO/))/NU(/NO/)$
SS=(1-2*NU(/NO/))/(2*NU(/NO/))$
DD=(YM(/NO/)*NU(/NO/))/((1+NU(/NO/))*(1-2*NU(/NO/)))$
 M6'.'
ITINT4$
MATCOP(CC,AA,8,8)$
MATINV(BB,CC,8)$
TRANS(EK,BB,8,8)$                    element stiffness
MATMUL(CC,EK,INT,8,8,8)$
MATMUL(EK,CC,BB,8,8,8)$
BPOST4$
 'END'$
```

```
 M7'.'
FXBDIT$
 M8'.'
'IF' ITER 'EQ' 1 'THEN BEGIN'
NULL(VI,N,CS)$
 M9'.'
LOAD$
NEWLINE(1)$
WRITETEXT( '('XXXXXXXXXXXXXXXXXXXXXXXXXXXXXXXXXXXXXXXXXXXXXXXXXX')')$
NEWLINE(2)$ WRITETEXT('(' LOAD.VECTORS...VI(N,CS)  ')')$
NEWLINE(1)$
SM=1$ 'FOR' I=1 'STEP' 1 'UNTIL' N 'DOBEGIN' PRINT(VI(/I,1/),0,3)$
'IF' SM 'EQ' 8 'THEN BEGIN' NEWLINE(1)$ SM=1$ 'END' 'ELSE' SM=SM+1$
                                                    'END'$
    'FOR' I=1 'STEP' 1 'UNTIL' N 'DO' VI2(/I,1/)=VI(/I,1/)$
 'END'$
NULL(VI,N,CS)$
'FOR' I=1 'STEP' 1 'UNTIL' N 'DO''BEGIN'
'IF' ITER 'LT' ITERN 'THEN' VI(/I,1/)=(ITER/ITERN)*VI2(/I,1/)
'ELSE' VI(/I,1/)=VI2(/I,1/)$
 'END'$
PLAGMK3(N,BD,CS,SK,VI)$      Choleski solution of equations
CPOUT$
IPRINT(ITER,4)$ SPACES(2)$ EPRINT( VI(/2,1/),6)$
LPOUT$
 M10'.'
NEWLINE(2)$ WRITETEXT('(' DISPLACEMENTS.AT.NODES ')')$
NEWLINE(1)$
'FOR' I = 1 'STEP' 2 'UNTIL' (N-1) 'DO' 'BEGIN'
SM = (I+1)/2$
NEWLINE(1)$ PRINT(SM,3,0)$ SPACE(3)$
'FOR' J=0,1  'DOBEGIN' PRINT(VI(/I+J,1/),0,4)$ SPACE(4)$ 'END'$
'END' I$
 M11'.'
PAPERTHROW$
WRITETEXT('(' ELEM.CENTROID.R...Z.....STR..R
.........   TH ..........Z  .........TRZ
..........MN.STR     .........TOCT       MOD.MODULUS ')')$
 M12'.'
NULL(SK,5*(DOWN-1),ACROSS-1)$
II=1$  JJ=1$
'FOR' NO=1 'STEP' 1 'UNTIL' EL 'DO' 'BEGIN'
LR=0$ LZ=0$
'FOR' L=1,2,3,4 'DO' 'BEGIN'
LR=LR+NCOORD(/ELNOD(/NO,L/),1/)$ LZ=LZ+NCOORD(/ELNOD(/NO,L/),2/)$
 'END'$ LR=LR/4$ LZ=LZ/4$
NEWLINE(1)$ PRINT(NO,3,0)$ SPACE(2)$
PRINT(LR,3,1)$  PRINT(LZ,3,1)$
 M13'.'
NULL(AA,8,8)$ NULL(BB,8,8)$ NULL(CC,8,8)$
MM=(1-NU(/NO/))/NU(/NO/)$
SS=(1-2*NU(/NO/))/(2*NU(/NO/))$
DD=(YM(/NO/)*NU(/NO/))/((1+NU(/NO/))*(1-2*NU(/NO/)))$
M14'.'
SETD4(BB)$
M15'.'
SETB4(AA,LR,LZ)$
MATMUL(CC,BB,AA,8,8,8)$          stresses at element centroid
AGLOB4$
M16'.'
MATINV(BB,AA,8)$
MATMUL(AA,CC,BB,8,8,8)$
```

```
NULL(BB,8,8)$
L=1$ 'FOR' I=1 'STEP' 2 'UNTIL' 7 'DO' 'BEGIN'
SM=ELNOD(/NO,L/)$
BB(/I,1/)=VI(/2*SM-1,1/)$  BB(/I+1,1/)=VI(/2*SM,1/)$
L=L+1$  'END'$
MATMUL(CC,AA,BB,8,8,8)$
'COMMENT' STRESSES ARE IN CC1,1 TO CC 1,4$
'FOR' I=1,2,3,4 'DO'                    PRINT(CC(/I,1/),4,2)$
MEANST=0$
M17'.'
'FOR' I=1,2,3 'DO' MEANST=MEANST + CC(/I,1/)$
MEANST=MEANST/3$
SPACE(4)$ PRINT(MEANST,3,3)$
CR=CC(/1,1/)$  CT=CC(/2,1/)$  CZ=CC(/3,1/)$  CTRZ=CC(/4,1/)$
TOCT= SQRT( ((CR-CT)**2 + (CT-CZ)**2 + (CZ-CR)**2 + 6*CTRZ**2))/3$
PRINT(TOCT,4,2)$
'IF' NO 'EQ' 1 'THEN' 'BEGIN'
CPOUT$
IPRINT(ITER,3)$ SPACES(2)$
EPRINT(CC(/3,1/),6)$ SPACES(2)$
PRINT(MEANST,2,5)$ SPACES(2)$
PRINT(TOCT,2,5)$ SPACES(2)$
LPOUT$    'END'$
'IF' ITER 'EQ' 1 'OR' ITER 'EQ' 15 'THEN'
STORE$ 'COMMENT' PUTS MEANST IN SK, LR, LZ$
M18'.'
MEANST=ABS(MEANST)$          modify Young's Modulus
'COMMENT' X X X X X X X X X X X X X X X X X X X X X X X X X X  $
EQU= 7000*MEANST**0.55$
'COMMENT' X X X X X X X X X X X X X X X X X X X X X X X X X X  $
'COMMENT' DAMP THE MODIFICATION TO MODULUS SO THAT ONLY CHANGE
      BY HALF THE AMOUNT EXPECTED $
'IF' ITER 'GE' ITERN 'THEN BEGIN'
   INC = EQU -YM(/NO/)$
   INC = INC/2$
   YM(/NO/) = YM(/NO/) + INC$
    'END' 'ELSE' YM(/NO/)=EQU$
SPACE(2)$  PRINT(YM(/NO/),0,3)$
'END' NO=1 TO EL FOR STRESSES$
'IF' ITER 'EQ' 1 'OR' ITER 'EQ' 15 'THEN'
LAYSTR$ 'COMMENT' LAYS MEANST ON L/P$
NEWLINE(1)$ WRITETEXT('(' MODIFIED '('SS')' MODULI ')')$
NEWLINE(1)$
         'FOR' I=1 'STEP' 1 'UNTIL' EL 'DO''BEGIN'
PRINT(YM(/I/),0,3)$ SPACE(1)$ 'IF' ABS( I/10-ENTIER(I/10)) 'LT' 'E'-6
'THEN' NEWLINE(1)$ 'END'$
'IF' ITER 'EQ' (1)  'THEN' STOP$
ITER=ITER+1$ 'GOTO' LAB1$      change to define total number of
STOP$                                                  iterations
'END' MAIN 4NVE 200 MODULARISED(2 IN BLOCK)$
 'END' NON MODULARISED HARWELL COMPAT. FROM 4AUTBIG 3313(1 IN BLOCK)$
'END' MAIN PROGRAM 4 NODE ELEMENT AND OUTER BLOCK, 8 NODE COMPATIBLE
```

A2.2 Incremental

A2.2.1 General description

The program is formed similarly to Program A2.1. Modifications in order that displacements and stresses for a 1/(total increments) part of the load are calculated and summed are shown thus: ‖

Procedures, mentioned where they occur in the text, but not listed, are identical to those in Program A2.1.

A2.2.2 Input

The sample input is that for the mesh in Fig. 4.4 and uses initial moduli calculated (as in Chapter 4) from an initial iterative calculation. The load displacement behaviour is shown in Fig. 4.20.

Data	Description
0.5E4 0.4	Dummy variable (YMI), Poisson's Ratio (NUI).
1 43	load cases (CS), no. of fixities (NFX)
11 17	no. of nodes in r direction/z direction
3 3 3 3 3 6 6 20 20	spacing in r direction
3 3 3 3 3 3 3 3 6 6 6 6	spacing in z direction
10 10 20 22	
10	total no. of increments (ITERN)

/contd.

initial tangent moduli:

9.0471E 3	7.9147E 3	4.5599E 3	2.0310E 3
1.4077E 3	1.0202E 3	7.4582E 2	4.4869E 2
4.3356E 2	5.5364E 2	5.8484E 3	5.2584E 3
4.0474E 3	2.7472E 3	1.8131E 3	1.3970E 3
9.9197E 2	6.9402E 2	4.2090E 2	4.9102E 2
4.1780E 3	3.9859E 3	3.3791E 3	2.6643E 3
2.0473E 3	1.5854E 3	1.1936E 3	8.7174E 2
5.5320E 2	4.2078E 2	3.2436E 3	3.1849E 3
2.8709E 3	2.4435E 3	2.0240E 3	1.6750E 3
1.3114E 3	9.9679E 2	6.5085E 2	3.6868E 2
2.6731E 3	2.6576E 3	2.4808E 3	2.2144E 3
1.9275E 3	1.6620E 3	1.3696E 3	1.0758E 3
7.3219E 2	4.7414E 2	2.2954E 3	2.2921E 3
2.1844E 3	2.0101E 3	1.8089E 3	1.6095E 3
1.3802E 3	1.1204E 3	7.9804E 2	5.4567E 2
2.0286E 3	2.0278E 3	1.9571E 3	1.8374E 3
1.6923E 3	1.5408E 3	1.3635E 3	1.1384E 3
8.4989E 2	6.0647E 2	1.8304E 3	1.8297E 3
1.7805E 3	1.6947E 3	1.5870E 3	1.4694E 3
1.3319E 3	1.1388E 3	8.8944E 2	6.5943E 2
1.6090E 3	1.6095E 3	1.5799E 3	1.5262E 3
1.4557E 3	1.3750E 3	1.2794E 3	1.1250E 3
9.2896E 2	7.2411E 2	1.3953E 3	1.3967E 3
1.3819E 3	1.3534E 3	1.3137E 3	1.2657E 3
1.2073E 3	1.0953E 3	9.5992E 2	7.9041E 2
1.2601E 3	1.2608E 3	1.2518E 3	1.2344E 3
1.2098E 3	1.1791E 3	1.1423E 3	1.0625E 3
9.7400E 2	8.3747E 2	1.1707E 3	1.1707E 3
1.1644E 3	1.1526E 3	1.1360E 3	1.1153E 3
1.0907E 3	1.0326E 3	9.7826E 2	8.7016E 2
1.0900E 3	1.0899E 3	1.0860E 3	1.0788E 3
1.0686E 3	1.0558E 3	1.0414E 3	1.0046E 3
9.7724E 2	8.9752E 2	1.0299E 3	1.0298E 3
1.0276E 3	1.0235E 3	1.0179E 3	1.0108E 3
1.0027E 3	9.8247E 2	9.7148E 2	9.1700E 2
9.8738E 2	9.8733E 2	9.8635E 2	9.8456E 2
9.8202E 2	9.7877E 2	9.7548E 2	9.6493E 2
9.6297E 2	9.3033E 2	9.8525E 2	9.8497E 2
9.8418E 2	9.8294E 2	9.8129E 2	9.7934E 2
9.7645E 2	9.7174E 2	9.5724E 2	9.2792E 2

fixity FX(NFX,3)

1 0 1	11 0 1	12 0 1	22 0 1	23 0 1	33 0 1	34 0 1
44 0 1	45 0 1	55 0 1	56 0 1	66 0 1	67 0 1	77 0 1
78 0 1	88 0 1	89 0 1	99 0 1	100 0 1	110 0 1	111 0 1
121 0 1	122 0 1	132 0 1	133 0 1	143 0 1	144 0 1	154 0 1
155 0 1	165 0 1	166 0 1	176 0 1	177 0 0	178 0 0	179 0 0

180 0 0 181 0 0 182 0 0 183 0 0 184 0 0 185 0 0 186 0 0

187 0 0

1 2 1 0 -100	uniformally distributed loading; for each element loaded:
2 3 2 0 -100	(element no./node 2/node 1/r load/ z load)
888	terminator 888

```
*ALGOL
'BEGIN'
     'INTEGER' NOD,EL,N,CS,NFX, ACROSS,DOWN$
     'REAL' YMI,NUI$
LTSTAC(20000)$
YMI=READ$
NUI=READ$
CS=READ$
NFX=READ$
ACROSS=READ$
DOWN=READ$
'COMMENT' ACROSS IS NODES ACROSS
          DOWN IS NODES DOWN$
EL = (ACROSS-1)*(DOWN-1)$
NOD = ACROSS*DOWN$
N=2*NOD$
NEWLINE(2)$ WRITETEXT('(' XXX.4.NODE.PROGRAM.XXX...INCREMENTAL.LOADING
    ...TOTAL.NO.OF.STEPS.IS...ITERN ')')$

'COMMENT' OUTPUT MOST OF THE  INPUT CONSTANTS AND IMPORTANT PARAMETERS$

NEWLINE(1)$ WRITETEXT('(' INITIAL '('SS')' MODULUS '('21S')' ')')$
PRINT(YMI,0,4)$
NEWLINE(1)$ WRITETEXT('(' INITIAL '('SS')' NU      '('27S')' ')')$
PRINT(NUI,1,4)$
NEWLINE(1)$ WRITETEXT('(' LOAD '('SS')' CASES '('26S')' ')')$
PRINT(CS,2,0)$
NEWLINE(1)$ WRITETEXT('(' NO.'('S')'OF'('S')'FIXITIES '('20S')' ')')$
PRINT(NFX,3,0)$
NEWLINE(1)$ WRITETEXT('(' NUMBER.OF.NODES....R,Z..DIRECTIONS ')' )$
PRINT(ACROSS,2,0)$ SPACE(2)$
PRINT(DOWN,2,0)$
NEWLINE(2)$ WRITETEXT('(' ELEMENTS..EL ')')$ SPACE(23)$
PRINT(EL,5,0)$
NEWLINE(1)$ WRITETEXT('(' NODES..NOD   ')')$ SPACE(25)$
NEWLINE(1)$ WRITETEXT('(' NO.OF.UNKNOWNS...N ')')$ SPACE(17)$
PRINT(N,5,0)$
PRINT(NOD,5,0)$

'BEGIN'
'ARRAY' NCOORD(/1'.'NOD,1'.'2/), INT,AA,BB,CC,EK(/1'.'8,1'.'8/),
NU,YM(/1'.'EL/), FX(/1'.'NFX,1'.'3/), VI,VI2(/1'.'N,1'.'CS/)$
'INTEGER' 'ARRAY' ELNOD(/1'.'EL,1'.'4/)$
'REAL' LR,LZ,EQU,INC,MM,SS,DD,MEANST,TOCT,CR,CT,CZ,CTRZ,GUESSM$
'INTEGER' I,J,SM,SN,L,NO,ITER,ITERN,BD$

'ARRAY' STRSUM(/1'.'EL,1'.'4/), DSPSUM(/1'.'N,1'.'CS/)$
'INTEGER' II,JJ$
```

arrays to sum stresses and displacements

XXXXXXXX PROCEDURES

```
AUT04
BWCHEK4
```

AUT04 ← with RSUM=0 in program text

```
AUT04$ 'COMMENT' FORMS ELNOD AND NCOORD (AS SPACE 4 CHOL 3106)
         AND OUTPUTS THEM$
BCHEK4$ 'COMMENT' FORMS BD..BANDWIDTH OF STRUCTURE STIFFNESS MATRIX$
NEWLINE(2)$ WRITETEXT('(' BANDWIDTH..OF.STIFFNESS.MATRIX..BD.OF.SK')')$
SPACE(2)$ PRINT(BD,3,0)$
    'BEGIN'
'ARRAY' SK(/1'.'N,1'.'BD/)$
```

XXXXXXXX PROCEDURES

- STORE
- LAYSTR
- AGLOB4
- ITINT4
- BPOST4
- FXBDIT
- LOAD
- UDOAD4
- SETD4
- SETB4

```
 M1'.'
ITERN=READ$ 'COMMENT' INPUT TOTAL INCREMENTS TO FULL LOAD$
NEWLINE(1)$ WRITETEXT('(' INCREMENTS.TO.FULL.LOAD..ITERN ')')$
PRINT(ITERN,3,0)$
'COMMENT' INITIALISE YM(NO) AND NU(NO) $
 M2'.'

'FOR' I=1 'STEP' 1 'UNTIL' EL 'DOBEGIN'
YMI=READ$ YM(/I/)=YMI      $ 'END'$
NEWLINE(1)$ WRITETEXT('(' INITIAL.TANGENT.MODULI..INPUT ')')$
NEWLINE(1)$
'FOR' I=1 'STEP' 1 'UNTIL' EL 'DOBEGIN'
PRINT(YM(/I/),0,3)$ SPACE(1)$
'IF' ABS( I/10-ENTIER(I/10) ) 'LT' 'E'-6 'THEN' NEWLINE(1)$ 'END'$

              'FOR' I = 1 'STEP' 1 'UNTIL' EL 'DO' NU(/I/)=NUI$
'COMMENT' READ IN FIXITY MATRIX  FX(NFX,3)$
'FOR' I=1 'STEP' 1 'UNTIL' NFX 'DO' 'FOR' J=1,2,3 'DO' FX(/I,J/)=READ$
NEWLINE(1)$ WRITETEXT('('XXX.FIXITY.MATRIX.XXX')')$
 M4'.'
'FOR' I=1 'STEP' 1 'UNTIL' NFX 'DOBEGIN' NEWLINE(1)$
'FOR' J=1,2,3  'DO' PRINT(FX(/I,J/),3,0)$ 'END'$

'COMMENT' NULL STRSUM BEFORE TOTALLING STRESSES IN 1/ITERN PARTS
    NULL DSPSUM BEFORE SUMMING          DISPLACEMENTS              $
NULL(STRSUM,EL,4)$
NULL(DSPSUM,N,CS)$

ITER=1$
LAB1'.' PAPERTHROW$
WRITETEXT('(' ITER'('SS')' = ')')$ PRINT(ITER,3,0)$
NULL(SK,N,BD)$
 M5'.'
'FOR' NO = 1 'STEP' 1 'UNTIL' EL 'DO' 'BEGIN'
AGLOB4$
MM=(1-NU(/NO/))/NU(/NO/)$
SS=(1-2*NU(/NO/))/(2*NU(/NO/))$
DD=(YM(/NO/)*NU(/NO/))/((1+NU(/NO/))*(1-2*NU(/NO/)))$
 M6'.'
ITINT4$
MATCOP(CC,AA,8,8)$
MATINV(BB,CC,8)$
TRANS(EK,BB,8,8)$
MATMUL(CC,EK,INT,8,8,8)$
MATMUL(EK,CC,BB,8,8,8)$
BPOST4$
 'END'$
 M7'.'
FXBDIT$
 M8'.'
```

```
'IF' ITER 'EQ' 1 'THEN BEGIN'
NULL(VI,N,CS)$
 M9'.'
UDOAD4$
NEWLINE(1)$
WRITETEXT( '('XXXXXXXXXXXXXXXXXXXXXXXXXXXXXXXXXXXXXXXXXXXXXXXXXXX')')$
NEWLINE(2)$ WRITETEXT('(' LOAD.VECTORS...VI(N,CS)  ')')$
NEWLINE(1)$
SM=1$ 'FOR' I=1 'STEP' 1 'UNTIL' N 'DOBEGIN' PRINT(VI(/I,1/),0,3)$
'IF' SM 'EQ' 8 'THEN BEGIN' NEWLINE(1)$ SM=1$ 'END' 'ELSE' SM=SM+1$
                                                    'END'$
    'FOR' I=1 'STEP' 1 'UNTIL' N 'DO' VI2(/I,1/)=VI(/I,1/)$
'COMMENT' VI2 HOLDS THE TOTAL LOADS$
 'END'$
NULL(VI,N,CS)$
'FOR' I=1 'STEP' 1 'UNTIL' N 'DO''BEGIN'
'IF' ITER 'LE' ITERN 'THEN' VI(/I,1/)=( 1  /ITERN)*VI2(/I,1/)
'ELSE' VI(/I,1/)=VI2(/I,1/)$
 'END'$
'COMMENT' ITER/ITERN IN  TOTAL LOAD NON INCREMENTAL, IE IN ORDER ONLY
    TO DAMP DOWN THE MATHEMATICAL PROCESS$
PLAGMK3(N,BD,CS,SK,VI)$

'FOR' I=1 'STEP' 1 'UNTIL' N 'DO'
DSPSUM(/I,1/) = DSPSUM(/I,1/) + VI(/I,1/)$      summed displacements

CPOUT$
IPRINT(ITER,4)$ SPACES(2)$ EPRINT( DSPSUM(/2,1/),6)$
'COMMENT' ACCUMULATED Z DISPLACEMENT AT SURFACE$
LPOUT$
 M10'.'
NEWLINE(2)$ WRITETEXT('(' DISPLACEMENTS.AT.NODES ')')$
NEWLINE(1)$
'FOR' I = 1 'STEP' 2 'UNTIL' (N-1) 'DO' 'BEGIN'
SM = (I+1)/2$
NEWLINE(1)$ PRINT(SM,3,0)$ SPACE(3)$
'FOR' J=0,1  'DOBEGIN' PRINT(VI(/I+J,1/),0,4)$ SPACE(4)$ 'END'$
'END' I$
 M11'.'
PAPERTHROW$
WRITETEXT('(' MN.STR...+...TOCT.ARE.FOR.ACCUMULATED.TOTAL.STRESS.LEVEL
 .SO.FAR ')')$
NEWLINE(2)$
WRITETEXT('(' ELEM.CENTROID.R...Z.....STR..R
..........   TH ..........Z  ..........TRZ
..........MN.STR     ..........GUESS.MNST   .....TOCT
  ....MODIFIED.M ODULUS ')')$
 M12'.'

NULL(SK,ACROSS-1,4*(ACROSS-1))$
II=1$  JJ=1$

'FOR' NO=1 'STEP' 1 'UNTIL' EL 'DO' 'BEGIN'
LR=0$ LZ=0$
'FOR' L=1,2,3,4 'DO' 'BEGIN'
LR=LR+NCOORD(/ELNOD(/NO,L/),1/)$ LZ=LZ+NCOORD(/ELNOD(/NO,L/),2/)$
 'END'$ LR=LR/4$ LZ=LZ/4$
NEWLINE(1)$ PRINT(NO,3,0)$ SPACE(2)$
PRINT(LR,3,1)$  PRINT(LZ,3,1)$
```

```
NULL(AA,8,8)$ NULL(BB,8,8)$ NULL(CC,8,8)$ :
MM=(1-NU(/NO/))/NU(/NO/)$
SS=(1-2*NU(/NO/))/(2*NU(/NO/))$
DD=(YM(/NO/)*NU(/NO/))/((1+NU(/NO/))*(1-2*NU(/NO/)))$
M14'.'
SETD4(BB)$
M15'.'
SETB4(AA,LR,LZ)$
MATMUL(CC,BB,AA,8,8,8)$
AGLOB4$
M16'.'
MATINV(BB,AA,8)$
MATMUL(AA,CC,BB,8,8,8)$
NULL(BB,8,8)$
L=1$ 'FOR' I=1 'STEP' 2 'UNTIL' 7 'DO' 'BEGIN'
SM=ELNOD(/NO,L/)$
BB(/I,1/)=VI(/2*SM-1,1/)$  BB(/I+1,1/)=VI(/2*SM,1/)$
L=L+1$  'END'$
MATMUL(CC,AA,BB,8,8,8)$
'COMMENT' STRESSES ARE IN CC1,1 TO CC 1,4$
'COMMENT' THESE ARE THE STRESSES FOR 1/ITERN OF THE TOTAL LOAD
    AT THE ITER STRESS LEVELS IN STRSUM$
'FOR' I=1,2,3,4 'DO'                    PRINT(CC(/I,1/),4,2)$

                              'FOR' I=1,2,3,4 'DO'
STRSUM(/NO,I/)=STRSUM(/NO,I/)+CC(/I,1/)$     summed stresses

MEANST=0$
'FOR' I=1,2,3 'DO' MEANST=MEANST + STRSUM(/NO,I/)$
MEANST=MEANST/3$
SPACE(4)$ PRINT(MEANST,3,3)$
CR=STRSUM(/NO,1/)$ CT=STRSUM(/NO,2/)$ CZ=STRSUM(/NO,3/)$
CTRZ=STRSUM(/NO,4/)$
TOCT= SQRT( ((CR-CT)**2 + (CT-CZ)**2 + (CZ-CR)**2 + 6*CTRZ**2))/3$
PRINT(TOCT,4,2)$

'IF' NO 'EQ' 1 'THEN' 'BEGIN'
CPOUT$
IPRINT(ITER,3)$ SPACES(2)$
EPRINT(CC(/3,1/),6)$ SPACES(2)$
PRINT(MEANST,2,5)$ SPACES(2)$
PRINT(TOCT,2,5)$ SPACES(2)$
LPOUT$    'END'$
'IF' ITER 'EQ' 10 'THEN'
STORE$ 'COMMENT' PUTS MEANST IN SK, LR, LZ$

                                  modified according to tangent
M18'.'                            modulus at new accumulated level
MEANST=ABS(MEANST)$               of stress
'COMMENT' X X X X X X X X X X X X X X X X X X X X X X X X X X X  $
EQU=7000*MEANST**0.55$
'COMMENT' X X X X X X X X X X X X X X X X X X X X X X X X X X X  $
YM(/NO/)=EQU$
SPACE(2)$  PRINT(YM(/NO/),0,3)$
'END' NO=1 TO EL FOR STRESSES$

'IF' ITER 'EQ' 10 'THEN'                  prints octahedral stresses
LAYSTR$ 'COMMENT' LAYS MEANST ON L/P$     after final increment

NEWLINE(1)$ WRITETEXT('(' MODIFIED '('SS')' MODULI ')')$
NEWLINE(1)$
          'FOR' I=1 'STEP' 1 'UNTIL' EL 'DO''BEGIN'
PRINT(YM(/I/),0,3)$ SPACE(1)$ 'IF' ABS( I/10-ENTIER(I/10)) 'LT' 'E'-6
'THEN' NEWLINE(1)$ 'END'$
'IF' ITER 'EQ' ITERN 'THEN' STOP$
ITER=ITER+1$ 'GOTO' LAB1$
STOP$
'END' MAIN 4NVE 200 MODULARISED(2 IN BLOCK)$
 'END' NON MODULARISED HARWELL COMPAT. FROM 4AUTBIG 3313(1 IN BLOCK)$
```

PROGRAM 3: 8-node Rectangular Prism

A3.1 General description

The program is written in 1 module using ICL 1900 input/output.

A solid rectangular mass of elements, each having any mutually compatible dimensions, has element data generated automatically (procedure, DATGN2).

Element data :

matrix ELNOD(1:EL,1:8), element numbering

" NCOORD(1:NOD,1:3), nodal co-ordinate.

The element numbering is always defined as x, y, z increasing, in that order (Fig. A.3). The maximum bandwidth of the stiffness matrix is computed (procedure, BCHEK8).

Storage for upper band of the stiffness matrix is then reserved using bandwidth (BD) and the element mesh data, i.e. array SK(1:N,1:BD).

Other procedures:

ACENT8 - forms (A) matrix for element 'NO', co-ordinates about element centroid

INTEG8 - forms $\int_{vol} B^T D B \, d.vol$ for element 'NO', about the centroid using explicit terms based on the element dimensions

BPOST8 - posts relevant part of element stiffness into upper band structure stiffness matrix

FXBIT8 - boundary conditions; sets relevant rows and columns of stiffness matrix to zero: 1 on leading diagonal

LOAD3D - puts nodal point loads in load vector

SETD8 - (D) matrix for an element, 'NO'

SETB8 - (B) matrix for given values of x, y and z; (X, Y and Z in centroid co-ordinate system).

A3.2 Input

Sample input for steel cantilever (1" x 1" x 4") made up of 16 elements each $\frac{1}{2}$" x $\frac{1}{2}$" x 1" (Fig. A.3).

A3.2.1

Data	Description
30 x 10^6 , 0.15	Young's Modulus (YMI), Poisson's Ratio (NU)
1 6	Load cases (CS), Number of fixities (NFX)
2 , 3 , 9	No. of nodes in x, y and z directions (XND, YND, ZND)
0.0 1.0	Co-ordinates of nodes in x direction X(1:XND)
0.0 0.5 1.0	Co-ordinates of nodes in y direction Y(1:YND)
0.0 0.5 1.0 1.5 2.0 2.5 3.0 3.5 4.0	Co-ordinates of nodes in z direction Z(1:ZND)
1	Total no. of iterations required to full load (ITERN) (only other than 1 if incremental analysis)
1 0 0 0 2 0 0 0 3 0 0 0 4 0 0 0 5 0 0 0 6 0 0 0	Input to fixity matrix FX(1:NFX, 1:4); for each node where some displacement is made zero, 1 row of matrix, i.e. (node, x fix, y fix, z fix). If x fix = 0 then deletes row and column, etc.
49 0 -100 0	Loading;
50 0 -100 0 99	node no., x load, y load, z load terminator, 99 - after last nodal loading

A3.2.2 Input information in program text:

If a non-linear elastic relationship is known for the material i.e. $E = f(\bar{\sigma}_{oct})$, then:

(1) the precise relationship is defined after label M18

(2) the number in the equality test (6 lines from end) is changed to equal the desired number of iterations.

A3.3 Output

All input numbers are printed on lineprinter together with descriptive text.

The generated mesh data is printed out:

matrixes ELNOD: element numbering

and NCOORD: co-ordinates for each node.

All nodal displacements are printed.

Stresses at all element centroids, in the x, y, z co-ordinate system, and the first stress invariant are printed together with the new value of E according to the equation $E = f(\sigma_{oct})$.

Program 3: LISTING (8 node rectangular prism)


```
*ALGOL**
 'BEGIN'
 'INTEGER' NOD,EL,N,NFX,CS,XND,YND,ZND$
 'REAL' YMI,NUI$

 YMI=READ$
 NUI=READ$
 CS=READ$
 NFX=READ$                    model data input
 XND=READ$
 YND=READ$
 ZND=READ$
 EL= (XND-1)*(YND-1)*(ZND-1)$
 NOD= XND*YND*ZND$
 N=3*NOD$

 NEWLINE(2)$ WRITETEXT('(' XXX.8.NODE.PROGRAM.XXX ')')$
 'COMMENT' OUTPUT MOST OF THE  INPUT CONSTANTS AND IMPORTANT PARAMETERS$
 NEWLINE(1)$ WRITETEXT('(' INITIAL '('SS')' MODULUS '('21S')' ')')$
 PRINT(YMI,0,4)$
 NEWLINE(1)$ WRITETEXT('(' INITIAL '('SS')' NU      '('27S')' ')')$
 PRINT(NUI,1,4)$
 NEWLINE(1)$ WRITETEXT('(' LOAD '('SS')' CASES '('26S')' ')')$
 PRINT(CS,2,0)$
 NEWLINE(1)$ WRITETEXT('(' NO.'('S')'OF'('S')'FIXITIES '('20S')' ')')$
 PRINT(NFX,3,0)$
 NEWLINE(1)$ WRITETEXT('(' NUMBER.OF.NODES..X,Y,Z..DIRECTIONS ')' )$
 PRINT(XND,2,0)$ SPACE (2)$
 PRINT(YND,2,0)$ SPACE (2)$
 PRINT(ZND,2,0)$ SPACE (2)$
 NEWLINE(2)$ WRITETEXT('(' ELEMENTS..EL ')')$ SPACE(23)$
 PRINT(EL,5,0)$
 NEWLINE(1)$ WRITETEXT('(' NODES..NOD   ')')$ SPACE(25)$
 PRINT(NOD,5,0)$
 NEWLINE(1)$ WRITETEXT('(' NO.OF.UNKNOWNS...N ')')$ SPACE(17)$
 PRINT(N,5,0)$

     'BEGIN'
 'ARRAY' NCOORD(/1'.'NOD,1'.'3/), INT,AA,BB,CC,EK(/1'.'24,1'.'24/),
 NU,YM(/1'.'EL/), FX(/1'.'NFX,1'.'4/), VI,VI2(/1'.'N,1'.'CS/)$
 'INTEGER ARRAY' ELNOD(/1'.'EL,1'.'8/)$
 'REAL' LX,LY,LZ,EQU,INC ,MM,SS,DD,MEANST$
 'INTEGER' I,J,SM,SN,L, NO,ITER,ITERN,BD$
 'PROCEDURE' DATGN2$
 'BEGIN'
 'ARRAY'                          X(/1'.'XND/),Y(/1'.'YND/),Z(/1'.'ZND/)$
 'INTEGER' IX,IY,IZ,XYND,IXYZ,P,Q,R,I,J,PP,QQ,RR,SM,SN$
 'FOR' I=1 'STEP' 1 'UNTIL' XND 'DO' X(/I/)=READ$
 'FOR' I=1 'STEP' 1 'UNTIL' YND 'DO' Y(/I/)=READ$
 'FOR' I=1 'STEP' 1 'UNTIL' ZND 'DO' Z(/I/)=READ$
 I=1$ R=0$ P=0$ Q=0$
 XYND= XND*YND$
 'FOR' IZ=P 'STEP' 1 'UNTIL' ZND-2+P 'DOBEGIN'
 'FOR' IY=Q 'STEP' 1 'UNTIL' YND-2+Q 'DOBEGIN'
 'FOR' IX= R 'STEP' 1 'UNTIL' XND-2+R 'DOBEGIN'
 IXYZ = 1+IX+IY+IZ$
 ELNOD(/I,1/) = IXYZ$
 ELNOD(/I,2/) = IXYZ +1$
 ELNOD(/I,3/) = IXYZ +XND$          element node numbering
 ELNOD(/I,4/) = IXYZ +XND+1$
 ELNOD(/I,5/) = IXYZ +XYND$
 ELNOD(/I,6/) = IXYZ +XYND+1$
 ELNOD(/I,7/) = IXYZ +XYND+XND$
 ELNOD(/I,8/) = IXYZ +XYND+XND+1$
```

```
'IF' I 'EQ' EL 'THEN GOTO' L1$
I=I+1$
RR=R$
'END' IX$
R=RR$ R=R+XND-1$
QQ=Q$
'END' IY$
Q=QQ$  Q=Q+YND-1$    R=R+XND-1$
'END' IZ$
L1'.' NEWLINE(1)$
WRITETEXT('(' ELNOD..ELEMENT.NODE.NUMBERING ')')$
NEWLINE(1)$
SM=0$ SN=0$
'FOR' I=1 'STEP' 1 'UNTIL' EL   'DOBEGIN'
'IF' SM 'EQ' 3 'THEN BEGIN' NEWLINE(1)$ SM=0$ 'END'$
SM=SM+1$
'IF' SN 'EQ' 12 'THEN BEGIN' NEWLINE(2)$ SN=0$ 'END'$
SN=SN+1$
'FOR' J=1,2,3,4,5,6,7,8 'DO'        PRINT(ELNOD(/I,J/),3,0)$
SPACE (2)$ 'END'$

P=1$  Q=1$  R=1$
'FOR' I=1 'STEP' 1 'UNTIL' NOD 'DOBEGIN'
NCOORD(/I,1/) = X(/P/)$
NCOORD(/I,2/) = Y(/Q/)$          node co-ordinates
NCOORD(/I,3/) = Z(/R/)$
P=P+1$
'IF' ABS( I/XND - ENTIER(I/XND) ) 'LE' 'E'-6 'THEN BEGIN'
P=1$ Q=Q+1$ 'END'$
'IF' ABS( I/(XND*YND) - ENTIER(I/(XND*YND)) ) 'LE' 'E'-6 'THEN BEGIN'
Q=1$ R=R+1$ 'END'$
'END' I 1 TO NOD$
NEWLINE(3)$
WRITETEXT('(' NCOORD..COORDINATE.VALUES ')')$
NEWLINE(1)$ SM=0$
'FOR' I=1 'STEP' 1 'UNTIL' NOD 'DOBEGIN'
'IF' SM 'EQ' 4 'THEN BEGIN' NEWLINE(1)$ SM=0$ 'END'$
PRINT(I,4,0)$
SM=SM+1$
'FOR' J=1,2,3 'DO'       PRINT(NCOORD(/I,J/),3,2)$
SPACE(1)$ 'END'$

'END'                    PROCEDURE DATA GENERATION & NODE *
```

```
'PROCEDURE' BCHEK8$
'BEGIN' 'INTEGER' NO,I,R,S,T,BAND$ 'INTEGERARRAY' P(/1'.'8/)$
T=0$
'FOR' NO=1 'STEP' 1 'UNTIL' EL 'DOBEGIN'
'FOR' I=1,2,3,4,5,6,7,8 'DO' P(/I/)=ELNOD(/NO,I/)$
R=0$ S=1000$
'FOR' I=1,2,3,4,5,6,7,8 'DOBEGIN'
'IF' P(/I/) 'GT' R 'THEN' R=P(/I/)$
'IF' P(/I/) 'LT' S 'THEN' S=P(/I/)$
'END'$
BAND=3*(R-S+1)$                          maximum bandwidth
'IF' BAND 'GT' T 'THEN' T=BAND$
'END'$
BD=T$
'END' BCHEK8$
PAPERTHROW$
DATGN2$ 'COMMENT' FORMS ELNOD AND NCOORD$
BCHEK8$ 'COMMENT' PRODUCES BD (BANDWIDTH)$
NEWLINE(2)$          WRITETEXT('(' BANDWIDTH..BD ')')$ PRINT(BD,5,0)$
     'BEGIN'
'ARRAY' SK(/1'.'N,1'.'BD/)$
'PROCEDURE' ACENT8$
'BEGIN' 'REAL' X,Y,Z,CX,CY,CZ$     'INTEGER' I,J,S,L,P,D$
'FOR' I=1 'STEP' 1 'UNTIL' 24 'DO' 'FOR' J=1 'STEP' 1 'UNTIL' 24 'DO'
                                        AA(/I,J/)=0$
CX=0$ CY=0$ CZ=0$
'FOR' L=1,2,3,4,5,6,7,8 'DOBEGIN'
P=ELNOD(/NO,L/)$
CX=CX+NCOORD(/P,1/)$ CY=CY+NCOORD(/P,2/)$ CZ=CZ+NCOORD(/P,3/)$
'END'$
CX=CX/8$ CY=CY/8$ CZ=CZ/8$
'COMMENT' CENTROID CX,CY,CZ$
S=1$
'FOR' L=1,2,3,4,5,6,7,8 'DOBEGIN'
P=ELNOD(/NO,L/)$
X=NCOORD(/P,1/) - CX$                    (A) matrix
Y=NCOORD(/P,2/) - CY$
Z=NCOORD(/P,3/) - CZ$
'FOR' J=1,9,17 'DOBEGIN'
'IF' J 'EQ' 1 'THEN' D=S 'ELSE'
'IF' J 'EQ' 9 'THEN' D=S+1 'ELSE' D=S+2$
AA(/D,J/)=1$ AA(/D,J+1/)=X$ AA(/D,J+2/)=Y$ AA(/D,J+3/)=Z$
AA(/D,J+4/)=X*Y$ AA(/D,J+5/)=Y*Z$ AA(/D,J+6/)=X*Z$
AA(/D,J+7/)=X*Y*Z$
'END'$ S=S+3$ 'END'$
'END' ACENT8$
```

```
'PROCEDURE' INTEG8$
'BEGIN'
'INTEGER' F,G,I,J$
'REAL' A,B,C,X2,Y2,Z2,X2Y2,Y2Z2,X2Z2$

F=ELNOD(/NO,1/)$  G=ELNOD(/NO,8/)$
A=ABS( NCOORD(/F,1/)-NCOORD(/G,1/) )/2$
B=ABS( NCOORD(/F,2/)-NCOORD(/G,2/) )/2$
C=ABS( NCOORD(/F,3/)-NCOORD(/G,3/) )/2$

X2 = A**2/3$  Y2 = B**2/3$    Z2 = C**2/3$
X2Y2=A**2*B**2/9$  Y2Z2=B**2*C**2/9$  X2Z2=A**2*C**2/9$
'FOR' I=1 'STEP' 1 'UNTIL' 24 'DO'
'FOR' J=1 'STEP' 1 'UNTIL' 24 'DO' INT(/I,J/)=0$

      INT(/2,2/) =MM$
      INT(/3,3/) =SS$
      INT(/4,4/) =SS$
      INT(/5,5/) =MM*Y2 +SS*X2$
      INT(/6,6/) =SS*(Y2+Z2)$
      INT(/7,7/) =MM*Z2 +SS*X2$
      INT(/8,8/) =MM*Y2Z2 +SS*(X2Z2+X2Y2)$
      INT(/10,3/) =SS$
      INT(/10,10/) =SS$
      INT(/11,2/) = 1$
      INT(/11,11/) =MM$
      INT(/12,12/) =SS$
      INT(/13,13/) =MM*X2 +SS*Y2$
      INT(/14,14/) =MM*Z2 +SS*Y2$
      INT(/15,6/) =SS*Z2$
      INT(/15,15/) =SS*(X2+Z2)$
      INT(/16,16/) =MM*X2Z2 +SS*(Y2Z2+X2Y2)$
      INT(/18,4/) =SS$
      INT(/18,18/) =SS$
      INT(/19,12/) =SS$
      INT(/19,19/) =SS$
      INT(/20,2/) =1$
      INT(/20,11/) =1$
      INT(/20,20/) =MM$
      INT(/21,6/) =SS*Y2$
      INT(/21,15/) =SS*X2$
      INT(/21,21/) =SS*(X2+Y2)$
      INT(/22,5/) =Y2$
      INT(/22,22/) =MM*Y2 +SS*Z2$
      INT(/23,13/) =X2$
      INT(/23,23/) =MM*X2 +SS*Z2$
      INT(/24,24/) = MM*X2Y2 + SS*(X2Z2+Y2Z2)$

'COMMENT' MULT LOWER TRIANGLE BY DD AND VOLUME= 8*A*B*C  $
'FOR' I=1 'STEP' 1 'UNTIL' 24 'DO'
'FOR' J=1 'STEP' 1 'UNTIL' I 'DO' INT(/I,J/) = 8*A*B*C*DD*INT(/I,J/)$
'COMMENT' PUT UPPER TRIANGLE EQUAL TO LOWER$
'FOR' I=1 'STEP' 1 'UNTIL' 24 'DO'
'FOR' J=I 'STEP' 1 'UNTIL' 24 'DO' INT(/I,J/)=INT(/J,I/)$
'END' INTEG8 $
```

integral about centroid

```
'PROCEDURE' BPOST8$
'BEGIN' 'INTEGER' S,L,I,J,SM,SN$
'FOR' S=1,2,3,4,5,6,7,8 'DOBEGIN'
      I=ELNOD(/NO,S/)$
'FOR' L=1,2,3,4,5,6,7,8 'DOBEGIN'                    post to upper band
      J=ELNOD(/NO,L/)$
'FOR' SM=0,1,2 'DO'
'FOR' SN=0,1,2 'DO'
'IF' 3*J-SN 'GE' 3*I-SM 'THEN'
SK(/3*I-SM,3*J-SN-3*I+SM+1/) =
SK(/3*I-SM,3*J-SN-3*I+SM+1/) + EK(/3*S-SM,3*L-SN/)$
'END'$ 'END'$
'END' BPOST8$
'PROCEDURE' FXBIT8$
'BEGIN' 'INTEGER' NODE,XSIGN,YSIGN,ZSIGN,I,P$
'FOR' P=1 'STEP' 1 'UNTIL' NFX 'DOBEGIN'
NODE=FX(/P,1/)$
XSIGN=FX(/P,2/)$ YSIGN=FX(/P,3/)$ ZSIGN=FX(/P,4/)$      boundary conditions

'IF' XSIGN 'EQ' 0 'THEN BEGIN'
'FOR' I=2 'STEP' 1 'UNTIL' BD 'DO' SK(/3*NODE-2,I/)=0$
                               SK(/3*NODE-2,1/)=1$
'FOR' I=1 'STEP' 1 'UNTIL' (3*NODE-3) 'DO'
'IF' (3*NODE-2) 'LE' (I-1+BD) 'THEN' SK(/I,3*NODE-2-I+1/)=0$
'END'$

      'IF' YSIGN 'EQ' 0 'THEN BEGIN'
'FOR' I=2 'STEP' 1 'UNTIL' BD 'DO' SK(/3*NODE-1,I/)=0$
                               SK(/3*NODE-1,1/)=1$
'FOR' I=1 'STEP' 1 'UNTIL' (3*NODE-2) 'DO'
'IF' (3*NODE-1) 'LE' (I-1+BD) 'THEN' SK(/I,3*NODE-1-I+1/)=0$
'END'$

      'IF' ZSIGN 'EQ' 0 'THEN BEGIN'
'FOR' I=2 'STEP' 1 'UNTIL' BD 'DO' SK(/3*NODE,I/)=0$
                           SK(/3*NODE,1/)=1$
'FOR' I=1 'STEP' 1 'UNTIL' (3*NODE-1) 'DO'
'IF' (3*NODE) 'LE' (I-1+BD) 'THEN' SK(/I,3*NODE-I+1/)=0$
'END'$
'END' P$
'END' FXBIT8$
'PROCEDURE' LOAD3D$
'BEGIN' 'INTEGER' NO,I$ 'REAL' XLOAD,YLOAD,ZLOAD$
NULL(VI,N,CS)$
NEWLINE(2)$ WRITETEXT('(' LOADING'('S')'OF'('S')' SYSTEM ')')$
LAB3':' NO=READ$
'IF' NO 'EQ' 99 'THEN' 'GOTO' LAB4$
XLOAD=READ$  YLOAD=READ$  ZLOAD=READ$
NEWLINE(1)$ WRITETEXT('('NODE')')$ PRINT(NO,3,0)$ SPACE (10)$
WRITETEXT('(' XLOAD ')')$ SPACE (2)$ PRINT(XLOAD,0,4)$ SPACE (10)$
WRITETEXT('(' YLOAD ')')$ SPACE (2)$ PRINT(YLOAD,0,4)$ SPACE (10)$
WRITETEXT('(' ZLOAD ')')$ SPACE (2)$ PRINT(ZLOAD,0,4)$ SPACE (10)$
VI(/3*NO-2,1/)=XLOAD$
VI(/3*NO-1,1/)=YLOAD$
VI(/3*NO,1/)=ZLOAD$                          load structure
'GOTO' LAB3$
LAB4':' 'END' LOAD3D, VI ARRAY$
```

```
'PROCEDURE' SETD8(D)$ 'ARRAY' D$
'BEGIN'  'INTEGER' I,J$
D(/1,1/)=MM$D(/1,2/)=1$ D(/1,3/)=1$
D(/2,1/)=1$ D(/2,2/)=MM$D(/2,3/)=1$
D(/3,1/)=1$ D(/3,2/)=1$ D(/3,3/)=MM$
D(/4,4/)=D(/5,5/)=D(/6,6/)=SS$
'FOR' I=1,2,3,4,5,6 'DO'
'FOR' J=1,2,3,4,5,6 'DO' D(/I,J/)=DD*D(/I,J/)$
'END' SETD8$
```

(D) matrix

```
'PROCEDURE' SETB8(B,X,Y,Z)$ 'VALUE' X,Y,Z$ 'REAL' X,Y,Z$ 'ARRAY' B$
'BEGIN'
B(/1,2/)=1$ B(/1,5/)=Y$ B(/1,7/)=Z$ B(/1,8/)=Y*Z$
B(/2,11/)=1$ B(/2,13/)=X$ B(/2,14/)=Z$ B(/2,16/)=X*Z$
B(/3,20/)=1$ B(/3,22/)=Y$ B(/3,23/)=X$ B(/3,24/)=X*Y$

B(/4,3/)=1$ B(/4,5/)=X$ B(/4,6/)=Z$ B(/4,8/)=X*Z$
B(/4,10/)=1$ B(/4,13/)=Y$ B(/4,15/)=Z$ B(/4,16/)=Y*Z$

B(/5,12/)=1$ B(/5,14/)=Y$ B(/5,15/)=X$ B(/5,16/)=X*Y$
B(/5,19/)=1$ B(/5,21/)=X$ B(/5,22/)=Z$ B(/5,24/)=Y*Z$

B(/6,4/)=1$ B(/6,6/)=Y$ B(/6,7/)=X$ B(/6,8/)=X*Y$
B(/6,18/)=1$ B(/6,21/)=Y$ B(/6,23/)=Z$ B(/6,24/)=Y*Z$
'END' SETB8$
```

(B) for given x,y,z

```
ITERN=READ$  'COMMENT' INPUT TOTAL NO. OF ITERATIONS TO FULL LOAD$
M2'.'
NEWLINE(1)$ WRITETEXT('(' TOTAL.ITERATIONS.TO.FULL.LOAD '('SS')' ')')$
PRINT(ITERN,4,0)$

'COMMENT' INITIAL    YM(NO) AND NU(NO)$
            'FOR' I=1 'STEP' 1 'UNTIL' EL 'DO' YM(/I/)=YMI$
            'FOR' I=1 'STEP' 1 'UNTIL' EL 'DO' NU(/I/)=NUI$

'COMMENT' READ IN FIXITY MATRIX  FX(NFX,4)$
'FOR' I=1 'STEP' 1 'UNTIL' NFX 'DO'      'FOR' J=1,2,3,4 'DO'
 FX(/I,J/)=READ$
M4'.'
NEWLINE(2)$ WRITETEXT('('XXX'('S')'FIXITY'('S')'MATRIX'('S')'XXX')')$
'FOR' I=1 'STEP' 1 'UNTIL' NFX 'DOBEGIN' NEWLINE(1)$
'FOR' J=1,2,3,4 'DO'  PRINT(FX(/I,J/),3,0)$ 'END'$
ITER=1$
LAB1'.' PAPERTHROW$
NEWLINE(1)$
WRITETEXT('(' ITER'('SS')'= ')')$ PRINT(ITER,3,0)$
NULL(SK,N,BD)$
M5'.'
'FOR' NO=1 'STEP' 1 'UNTIL' EL 'DOBEGIN'
ACENT8$
MM= (1-NU(/NO/))/NU(/NO/)$
SS= (1-2*NU(/NO/))/(2*NU(/NO/))$
DD = (YM(/NO/)*NU(/NO/))/((1+NU(/NO/))*(1-2*NU(/NO/)))$
M6'.'
INTEG8$
MATCOP(CC,AA,24,24)$
MATINV(BB,CC,24)$
TRANS(EK,BB,24,24)$
MATMUL(CC,EK,INT,24,24,24)$
MATMUL(EK,CC,BB,24,24,24)$
BPOST8$
'END'$
M7'.'
```

element stiffness

```
FXBIT8$
M8'.'
'IF' ITER 'EQ' 1 'THENBEGIN'
NULL(VI,N,CS)$
M9'.'
LOAD3D$
NEWLINE(1)$
WRITETEXT('(' X X X X X X X X X X X X X X X X X X X X X X X X X X X ')')$
NEWLINE(2)$ WRITETEXT('(' VI.TO.EQN.SOLVE ')')$
SM=1$
'FOR' I=1 'STEP' 1 'UNTIL' N 'DOBEGIN' PRINT(VI(/I,1/) ,0,3)$
'IF' SM 'EQ' 8 'THEN BEGIN' NEWLINE(1)$ SM=1$ 'END' 'ELSE'
                                        SM=SM+1$ 'END'$
'FOR' I=1 'STEP' 1 'UNTIL' N 'DO' VI2(/I,1/)=VI(/I,1/)$
'END'$
NULL(VI,N,CS)$
'FOR' I=1 'STEP' 1 'UNTIL' N 'DO'
'IF' ITER 'LT' ITERN 'THEN' VI(/I,1/)=(ITER/ITERN)*VI2(/I,1/)
'ELSE' VI(/I,1/)=VI2(/I,1/)$
PLAGMK3(N,BD,CS,SK,VI)$          Choleski solution of equations
M10'.'
NEWLINE(2)$ WRITETEXT('(' DISPLACEMENTS '('S')' AT '('S')' NODES')')$
NEWLINE(1)$
'FOR' I=1 'STEP' 3 'UNTIL' (N-2) 'DOBEGIN'
SM=ABS( (I+2)/3 )$
NEWLINE(1)$ PRINT(SM,3,0)$ SPACE(3)$
'FOR' J=0,1,2 'DOBEGIN' PRINT(VI(/I+J,1/),0,4)$ SPACE(4)$ 'END'$
'END' I$
M11'.'
PAPERTHROW$
WRITETEXT
    ('(' ELEM '('4S')' CENTROID '('6S')' X '('6S')' Y '('6S')' Z
'('2S')' STRESSES '('14S')' X '('6S')' Y '('6S')' Z '('6S')' TXY
'('6S')' TYZ '('6S')' TXZ '('4S')' MN.NOR.STRS '('2S')' NEW.YM ')')$
M12'.'
'FOR' NO=1 'STEP' 1 'UNTIL' EL 'DOBEGIN'
LX=0$ LY=0$ LZ=0$ 'COMMENT' THE CENTROIDS$
     'FOR' L=1,2,3,4,5,6,7,8 'DOBEGIN'
     LX=LX+NCOORD(/ELNOD(/NO,L/),1/)$
     LY=LY+NCOORD(/ELNOD(/NO,L/),2/)$
     LZ=LZ+NCOORD(/ELNOD(/NO,L/),3/)$
     'END'$ LX=LX/8$ LY=LY/8$ LZ=LZ/8$
     NEWLINE(1)$ SPACE (1)$
     PRINT(NO,3,0)$ SPACE (2)$
    PRINT(LX,0,4)$ PRINT(LY,0,4)$ PRINT(LZ,0,4)$
     LX=0$ LY=0$ LZ=0$ 'COMMENT' THE CENTROID IN CENTROID COORDS$
M13'.'
NULL(AA,24,24)$ NULL(BB,24,24)$ NULL(CC,24,24)$
MM= (1-NU(/NO/))/NU(/NO/)$
SS= (1-2*NU(/NO/))/(2*NU(/NO/))$
DD = (YM(/NO/)*NU(/NO/))/((1+NU(/NO/))*(1-2*NU(/NO/)))$
M14'.'
SETD8(BB)$
M15'.'
SETB8(AA,LX,LY,LZ)$
MATMUL(CC,BB,AA,24,24,24)$       stresses at element centroid
ACENT8$
MATINV(BB,AA,24)$
MATMUL(AA,CC,BB,24,24,24)$
NULL(BB,24,24)$
```

```
L=1$ 'FOR' I=1 'STEP' 3 'UNTIL' 22 'DOBEGIN'
SM=ELNOD(/NO,L/)$
BB(/I,1/)=VI(/3*SM-2,1/)$
BB(/I+1,1/)=VI(/3*SM-1,1/)$
BB(/I+2,1/)=VI(/3*SM,1/)$
L=L+1$ 'END'$
MATMUL(CC,AA,BB,24,24,24)$
'COMMENT' STRESSES ARE IN CC1,1 TO CC6,1$
'FOR' I=1,2,3,4,5,6 'DO' PRINT(CC(/I,1/),5,2)$
MEANST=0$
M17'.'
'FOR' I=1,2,3 'DO' MEANST=MEANST + CC(/I,1/)$
MEANST=MEANST/3$
SPACE (2)$ PRINT(MEANST,3,3)$
M18'.'                                   modify Young's modulus
MEANST=ABS(MEANST)$                          <-
'COMMENT' X X X X X X X X X X X X X X X X X X X X X X X X X X X $
EQU= 7000*MEANST**0.55$
'COMMENT' X X X X X X X X X X X X X X X X X X X X X X X X X X X $
'COMMENT' DAMP THE MODIFICATION TO MODULUS SO THAT IS ONLY
      CHANGED BY HALF THE AMOUNT CALCULATED$
'IF' ITER 'GE' ITERN 'THENBEGIN'
INC=EQU-YM(/NO/)$
INC=INC/2$
YM(/NO/)=YM(/NO/) + INC$
'END' 'ELSE' YM(/NO/) = EQU$
SPACE (2)$ PRINT(YM(/NO/),0,3)$
'END' NO=1 TO EL FOR STRESSES $,
NEWLINE(2)$ WRITETEXT('(' MODIFIED '('S')' MODULI ')')$
NEWLINE(1)$
          'FOR' I=1 'STEP' 1 'UNTIL' EL 'DOBEGIN'
PRINT(YM(/I/),0,3)$ SPACE (1)$
'IF' ABS( I/10 - ENTIER(I/10) ) 'LT' 'E'-6 'THEN' NEWLINE(1)$ 'END'$
'IF' ITER 'EQ' 1 'THEN' STOP$
ITER=ITER+1$ 'GOTO' LAB1$                <-  change to define no. of iterations
STOP$
'END' 2 IN  BLOCK$
'END' 1 IN BLOCK$
'END' MAIN PROGRAM 8 NODE ELEMENT AND OUTER BLOCK
```

PROGRAM 4: 4 node axisymmetric rectangle (TEMPERATURE)

Effect of temperature on the stiffness of the top layer

A4.1 General Description

The program is modified from Program 2.1 to incorporate layers of different materials. Procedures which are common to program 2.1 are not listed but simply named at the position in the program where they must be declared.

A layer description is read into a matrix RELAT(1:NLAYS,1:2). One row of this matrix refers to each of the (NLAYS) layers. Into the first location of a row is read the lowest element number in the layer and the second, the highest. By reference to this matrix the program can establish which layer contains a particular element.

The program as presented carries out two computations:

(i) an analysis using constant moduli for each layer in a 2-layer system

(ii) an analysis using modulus values modified in the top layer according to the stiffness-with-depth relationship given in the procedure 'LAYMOD'

Procedures not described in Section A2.1.1:

GEN4N - generates the element mesh data using input of mesh-line co-ordinates instead of mesh spacing (AUTO4)

LAYMOD - given the layer number (LAYER) as input, the procedure recalculates the Young's modulus YM(NO) for an element (NO) according to some criteria:

In this case:

$\text{Temp}^\circ\text{F} = f_1(z)$ z = depth

$\text{Temp}^\circ\text{C} = f_2(^\circ\text{F})$

$E = f_3(\text{Temp}^\circ\text{C})$

Depth must be defined from the surface. The co-ordinates were generated as increasing upward from 10 in. below the bottom boundary (440 in. below surface in the text) and thus 'depth' = (450-LZ) in the text of 'LAYMOD'.

A4.2 Input

Sample input for a 12 in. layer overlying a halfspace (similar to Fig. 6.5) is given - the total mesh dimensions have, however, been changed to 280 in. radial x 440 in. depth:-

Data	Description
1 43	Load cases (CS), no. of nodes at which boundary fixities are imposed (NFX)
11 17	No. of nodes in radial (r) direction (XND). No. of nodes in vertical (z) direction (YND)
2	Number of layers (NLAYS)
0 3 6 9 12 20 45 75 130 200 280	Co-ordinates of mesh points in the radial direction X(1:XND)
0 3 6 9 12 15 25 40 60 95 130 170 220 270 325 380 440	Co-ordinates of mesh points in the vertical direction Y(1:YND)
1	(ITERN) - total iterations to full load - redundant in this program; keep as 1
1 40 41 160	RELAT(1:NLAYS, 1:2) i.e. elements 1 to 40 are in row 1 elements 41 to 160 are in row 2
6.1828×10^5 1.0×10^4	Young's modulus of each layer, i.e. E_1, E_2
0.4 0.4	Poisson's Ratio of each layer, i.e. ν_1, ν_2

/contd.

1 0 1 11 0 1 12 0 1 22 0 1 33 0 1 34 0 1 44 0 1 45 0 1 .... etc. exactly as input in Section A2.2.2 up to 187 0 0	Fixity matrix FX(1:NFX,1:3) as described in A2.1.1
1 2 1 0 -100 2 3 2 0 -100	uniformally distributed loading, for each element loaded:- (element no./node 2/node 1/ r load/z load)
888	terminator

A4.3 Input Information in the Program Text

The procedure LAYMOD is the device by which the change in modulus is defined after each calculation of the element centroid stresses. The equations, defining the change in modulus with temperature and depth (here) or stress level (Prog. 6) within each layer, are included in the procedure text.

A4.4 Output

Card output was produced of some of the critical stresses and strains on the load axis. This provided data for the automatic plotting of certain of the graphs in Chapter 6. These instructions may be removed.

Otherwise the lineprinter output is substantially the same as that described in section A2.1.4 for Program 2.1.

PROGRAM 4 LISTING (4 node axisymmetric rectangle) (TEMPERATURE)

The effect of temperature on the stiffness of the top layer

```
*ALGOL

'BEGIN'
     'INTEGER' NOD,EL,N,CS,NFX, XND,YND, NLAYS$
     'REAL' YMI,NUI$
LTSTAC(20000)$
CS=READS
NFX=READS
XND=READS
YND=READS
NLAYS=READS$ <-- number of layers
'COMMENT' XND IS NODES ACROSS   YND IS NODES DOWN$
EL= (XND-1)*(YND-1)$
NOD= XND*YND$
N=2*NOD$
NEWLINE(2)$ WRITETEXT('(' 4.NODE.PROGRAM..LAYERED.TEMPERATURE.NON.LINEA
R.ELASTIC '('SS')' NO.FRICTION.OPTION ')')$

'COMMENT' OUTPUT MOST OF THE  INPUT CONSTANTS AND IMPORTANT PARAMETERS$

NEWLINE(1)$ WRITETEXT('(' LOAD '('SS')' CASES '('26S')' ')')$
PRINT(CS,2,0)$
NEWLINE(1)$ WRITETEXT('(' NO.'('S')'OF'('S')'FIXITIES '('20S')' ')')$
PRINT(NFX,3,0)$
NEWLINE(1)$ WRITETEXT('(' NUMBER.OF.NODES....R,Z..DIRECTIONS ')' )$
PRINT(XND,2,0)$ SPACE(2)$
PRINT(YND,2,0)$
NEWLINE(2)$ WRITETEXT('(' NO.OF.LAYERS...NLAYS ')')$ PRINT(NLAYS,5,0)$
NEWLINE(2)$ WRITETEXT('(' ELEMENTS..EL ')')$ SPACE(23)$
PRINT(EL,5,0)$
NEWLINE(1)$ WRITETEXT('(' NODES..NOD   ')')$ SPACE(25)$
PRINT(NOD,5,0)$
NEWLINE(1)$ WRITETEXT('(' NO.OF.UNKNOWNS...N ')')$ SPACE(17)$
PRINT(N,5,0)$

'BEGIN'
'ARRAY' NCOORD(/1'.'NOD,1'.'2/), INT,AA,BB,CC,EK(/1'.'8,1'.'8/),
NU,YM(/1'.'EL/), FX(/1'.'NFX,1'.'3/), VI,VI2(/1'.'N,1'.'CS/)$
'INTEGER' 'ARRAY' ELNOD(/1'.'EL,1'.'4/) , RELAT(/1'.'NLAYS,1'.'2/)$
'REAL' LR,LZ,EQU,INC,MM,SS,DD,MEANST,TOCT,CR,CT,CZ,CTRZ,TEMPF,TEMPC$
'INTEGER' I,J,SM,SN,L,NO,ITER,ITERN,BD,LAYER$

'INTEGER' II,JJ$
```

matrix to assign elements to layers

```
'PROCEDURE' GEN4N $
'BEGIN'
'ARRAY' X(/1'.'XND/), Y(/1'.'YND/)$
'INTEGER' I,IX,IY,P,Q,R,IXY,RR,QQ,NULFAC,NF$
'FOR' I=1 'STEP' 1 'UNTIL' XND 'DO' INREAL( X(/I/) )$
'FOR' I=1 'STEP' 1 'UNTIL' YND 'DO' INREAL( Y(/I/) )$

'COMMENT' GEN4NM IS A MODIFICATION OF GEN4N
TO NUMBER INTERFACE ROWS OF ELEMENTS TWICE, INPUT IS
 ROWZ(1 TO ROWS)  ROWS IS NO OF ROWS WITH FRICTION
                  ROWZ CONTAINS ROW NO AFTER WHICH FRICTION
INTERFACE OCCURS $
'COMMENT' GEN4NM MOD LEFT IN 4TRIAX PROGRAM$

I=1$ Q=0$ R=0$
          NF=1$
'FOR' IY=Q 'STEP' 1 'UNTIL' YND-2+Q 'DOBEGIN'
'FOR' IX=R 'STEP' 1 'UNTIL' XND-2+R 'DOBEGIN'
IXY=1+IX+IY$
ELNOD(/I,1/)=IXY+XND$
ELNOD(/I,2/)=IXY$                    element numbering
ELNOD(/I,3/)=IXY+1$
ELNOD(/I,4/)=IXY+XND+1$
'IF' I 'EQ' EL 'THEN GOTO' L1$
I=I+1$
RR=R$
'END' IX$

R=RR$ R=R+XND-1$
QQ=Q$
'END' IY$
L1'.' LINES(1)$

P=1$ Q=1$
'FOR' I=1 'STEP' 1 'UNTIL' NOD 'DOBEGIN'
NCOORD(/I,1/)= X(/P/)$
NCOORD(/I,2/)= Y(/Q/)$      node co-ordinates
P=P+1$
'IF' ABS( I/XND-ENTIER(I/XND) ) 'LE' 'E'-6 'THEN BEGIN'
P=1$ Q=Q+1$ 'END'$
'END'$ 'COMMENT' I IS 1 TO NOD$
NEWLINE(3)$
'END' GEN4N     $
'PROCEDURE' BCHEK4$
'BEGIN'
'INTEGER' NO,I,R,S,T,BAND$
'INTEGER' 'ARRAY' P(/1'.'4/)$
T=0$
'FOR' NO = 1 'STEP' 1 'UNTIL' EL 'DO' 'BEGIN'
'FOR' I = 1,2,3,4 'DO' P(/I/) = ELNOD(/NO,I/)$
R=0$ S=1000$
'FOR' I = 1,2,3,4 'DO''BEGIN'
'IF' P(/I/) 'GT' R 'THEN' R=P(/I/)$
'IF' P(/I/) 'LT' S 'THEN' S=P(/I/)$
 'END'$
BAND = 2*(R-S+1)$
'IF' BAND 'GT' T 'THEN' T = BAND$
 'END'$
BD=T$
'END' BCHEK4$
```

```
GEN4N$ 'COMMENT' FORMS ELNOD AND NCOORD (AS SPACE 4 CHOL 3106)
        AND OUTPUTS THEM$
PAGE$ TEXT('(' NCOORD'*'FROM'*'GEN4N ')')$ LINES(1)$
'COMMENT' REARRANGEMENT OF NODE CO-ORDINATES TO BE IN ASCENDING
ORDER OF Z FROM BOTTOM OF HALFSPACES    + 10 in.
'FOR' I=1 'STEP' 1 'UNTIL' NOD 'DO'
            NCOORD(I,2)=NCOORD(I,2)-NCOORD(NOD,2)$
'FOR' I=1 'STEP' 1 'UNTIL' NOD 'DO'
            NCOORD(I,2)=ABS(NCOORD(I,2))$
'FOR' I=1 'STEP' 1 'UNTIL' NOD 'DO' NCOORD(I,2)=NCOORD(I,2)+10$

PAGE$
'COMMENT' OUTPUT OF ELEMENT NODE MATRIX $
LINES(2)$ TEXT( '(' ELNOD ')' )$
LINES(1)$
SM=0$  SN=0$
'FOR' I = 1 'STEP' 1 'UNTIL' EL 'DO' 'BEGIN'
'IF' SM 'EQ' 6 'THEN' 'BEGIN' LINES(1)$ SM=0$ 'END'$
SM=SM+1$
'IF' SN 'EQ' 24 'THEN' 'BEGIN' LINES(2)$ SN=0$ 'END'$
SN=SN+1$
'FOR' J=1,2,3,4 'DOBEGIN'
IPRINT(ELNOD(I,J),3)$ SPACES(1)$ 'END'$
SPACES(4)$ 'END'$

PAGE$
'COMMENT' OUTPUT OF NODE CO-ORDINATE MATRIX$
LINES(2)$ TEXT('(' NCOORD ')')$ LINES(1)$ SM=0$
'FOR' I = 1 'STEP' 1 'UNTIL' NOD 'DO' 'BEGIN'  SPACES(2)$
'IF' SM 'EQ' 5 'THEN' 'BEGIN' LINES(1)$ SM=0$ 'END'$
SM=SM+1$
'FOR' J=1,2 'DOBEGIN'
PRINT(NCOORD(I,J),3,2)$ SPACES(1)$
'END'$ 'END'$

BCHEK4$ 'COMMENT' FORMS BD..BANDWIDTH OF STRUCTURE STIFFNESS MATRIX$
NEWLINE(2)$ WRITETEXT('(' BANDWIDTH..OF.STIFFNESS.MATRIX..BD.OF.SK')')$
SPACE(2)$ PRINT(BD,3,0)$
    'BEGIN'
'ARRAY' SK(/1'.'N,1'.'BD/)$
```

XXXXXXXXXX PROCEDURES

STORE, LAYSTR,
AGLOB4, ITINT4, BPOST4,
FXBDIT, LOAD, UDOAD4,
SETD4,SETB4.

modified Young's Modulus for each element (layer number already established)

```
'PROCEDURE' LAYMOD(LAYER,EQU)$ 'INTEGER' LAYER$ 'REAL' EQU$
'BEGIN'
 'IF' LAYER 'EQ' 1 'THEN BEGIN'
 'COMMENT' 5 AM SUMMER 4507B$
 TEMPF= 68 + 0.75*(450-LZ)$SPACE(2)$ PRINT(TEMPF,3,1)$
 TEMPC=(5/9)*(TEMPF-32)$ SPACE(2)$ PRINT(TEMPC,3,1)$
 EQU=EXP(14.64802-0.04352*TEMPC-0.00066*TEMPC**2)$
 YM(/NO/)=EQU$  'END'$
'END' LAYMOD$
```

```
'COMMENT' TOTAL NO OF ITERATIONS OF LOADS$
 M1'.'
ITERN=READS$ 'COMMENT' INPUT TOTAL ITERATIONS TO FULL LOADS$
 M2'.'
NEWLINE(1)$ WRITETEXT('(' ITERN..TO.FULL.LOAD')')$ PRINT(ITERN,3,0)$

'COMMENT' READ IN LAYER DESCRIPTION RELATS$
'FOR' I=1 'STEP' 1 'UNTIL' NLAYS 'DOBEGIN'
'FOR' J=1,2 'DO' RELAT(/I,J/)=READS$ 'END'$
NEWLINE(2)$
WRITETEXT('(' LAYER.DESCRIPTION..RELAT(NLAYS,2) ')')$
NEWLINE(2)$
'FOR' I=1 'STEP' 1 'UNTIL' NLAYS 'DOBEGIN'
'FOR' J=1,2 'DOBEGIN' PRINT(RELAT(/I,J/),4,0)$ SPACE(2)$
'END'$ NEWLINE(1)$ 'END'$

'COMMENT' READ IN AND SET INITIAL LAYER MODULIS
NEWLINE(2)$ WRITETEXT('(' LAYER.YOUNGS.MODULI ')')$ NEWLINE(1)$
'FOR' I=1 'STEP' 1 'UNTIL' NLAYS 'DOBEGIN'  YMI=READS$
PRINT(YMI,0,3)$ SPACE(2)$
'FOR' SM=RELAT(/I,1/) 'STEP' 1 'UNTIL' RELAT(/I,2/) 'DO'
YM(/SM/)=YMIS 'END'$

'COMMENT' READ IN AND SET LAYER POISSONS RATIOS
NEWLINE(2)$ WRITETEXT('(' LAYER.POISSONS.RATIO ')')$ NEWLINE(1)$
'FOR'I=1 'STEP' 1 'UNTIL' NLAYS 'DOBEGIN'  NUI=READS$
PRINT(NUI,1,3)$ SPACE(2)$
'FOR' SM= RELAT(/I,1/) 'STEP' 1 'UNTIL' RELAT(/I,2/) 'DO'
NU(/SM/)=NUIS 'END'$

'COMMENT' READ IN FIXITY MATRIX  FX(NFX,3)$
'FOR' I=1 'STEP' 1 'UNTIL' NFX 'DO' 'FOR' J=1,2,3 'DO' FX(/I,J/)=READ
NEWLINE(1)$ WRITETEXT('('XXX.FIXITY.MATRIX.XXX')')$
'FOR' I=1 'STEP' 1 'UNTIL' NFX 'DOBEGIN' NEWLINE(1)$
'FOR' J=1,2,3  'DO' PRINT(FX(/I,J/),3,0)$ 'END'$
 M4'.'
ITER=1$
LAB1'.' PAPERTHROW$
WRITETEXT('(' ITER'('SS')' = ')')$ PRINT(ITER,3,0)$
NULL(SK,N,BD)$
 M5'.'
'FOR' NO = 1 'STEP' 1 'UNTIL' EL 'DO' 'BEGIN'
AGLOB4$
MM=(1-NU(/NO/))/NU(/NO/)$
SS=(1-2*NU(/NO/))/(2*NU(/NO/))$
DD=(YM(/NO/)*NU(/NO/))/((1+NU(/NO/))*(1-2*NU(/NO/)))$
 M6'.'
ITINT4$
MATCOP(CC,AA,8,8)$
MATINV(BB,CC,8)$
TRANS(EK,BB,8,8)$
MATMUL(CC,EK,INT,8,8,8)$
MATMUL(EK,CC,BB,8,8,8)$
BPOST4$
 'END'$
```

element stiffnesses using latest known Young's Modulus and Poisson's Ratio

```
 M7'.'
FXBDIT$
 M8'.'
'IF' ITER 'EQ' 1 'THEN BEGIN'
NULL(VI,N,CS)$
 M9'.'
UDOAD4$
NEWLINE(1)$
WRITETEXT( '('XXXXXXXXXXXXXXXXXXXXXXXXXXXXXXXXXXXXXXXXXXXXXXXXXXXXXXXX')')$
NEWLINE(2)$ WRITETEXT('(' LOAD.VECTORS...VI(N,CS)  ')')$
NEWLINE(1)$
SM=1$ 'FOR' I=1 'STEP' 1 'UNTIL' N 'DOBEGIN' PRINT(VI(/I,1/),0,3)$
'IF' SM 'EQ' 8 'THEN BEGIN' NEWLINE(1)$ SM=1$ 'END' 'ELSE' SM=SM+1$
                                                    'END'$
    'FOR' I=1 'STEP' 1 'UNTIL' N 'DO' VI2(/I,1/)=VI(/I,1/)$
 'END'$
NULL(VI,N,CS)$
'FOR' I=1 'STEP' 1 'UNTIL' N 'DO''BEGIN'
'IF' ITER 'LT' ITERN 'THEN' VI(/I,1/)=(ITER/ITERN)*VI2(/I,1/)
'ELSE' VI(/I,1/)=VI2(/I,1/)$
 'END'$
PLAGMK3(N,BD,CS,SK,VI)$     Choleski solution of equations
 M10'.'
NEWLINE(2)$ WRITETEXT('(' DISPLACEMENTS.AT.NODES ')')$
NEWLINE(1)$
'FOR' I = 1 'STEP' 2 'UNTIL' (N-1) 'DO' 'BEGIN'
SM = (I+1)/2$
NEWLINE(1)$ PRINT(SM,3,0)$ SPACE(3)$
'FOR' J=0,1  'DOBEGIN' PRINT(VI(/I+J,1/),0,4)$ SPACE(4)$ 'END'$
'END' I$

'IF' ITER 'EQ' 2 'THEN BEGIN'
'COMMENT' CARD OUTPUT OF AXIS NODE NO, ZCOORD, VERT DISPL$
CPOUT$
'FOR' I=1 'STEP' XND 'UNTIL' XND*(YND-1)+1 'DOBEGIN'
NEWCRD$
PRINT(I,4,0)$ SPACE(2)$
PRINT(NCOORD(/I,2/),4,3)$ SPACE(2)$
PRINT(VI(/2*I,1/),0,7)$ SPACE(2)$
'END' I$
LPOUT$ 'END' ITER2$
```

```
 M11'.'
PAPERTHROW$
WRITETEXT('(' ELEM.CENTROID.R...Z.....STR..R
.........   TH .........Z  .........TRZ
..........MN.STR     .........TOCT       MOD.MODULUS ')')$
 M12'.'

NULL(SK,5*(XND -1),YND   -1)$
II=1$  JJ=1$

'FOR' NO=1 'STEP' 1 'UNTIL' EL 'DO' 'BEGIN'
LR=0$ LZ=0$
'FOR' L=1,2,3,4 'DO' 'BEGIN'
LR=LR+NCOORD(/ELNOD(/NO,L/),1/)$ LZ=LZ+NCOORD(/ELNOD(/NO,L/),2/)$
 'END'$ LR=LR/4$ LZ=LZ/4$
NEWLINE(1)$ PRINT(NO,3,0)$ SPACE(2)$
PRINT(LR,3,1)$  PRINT(LZ,3,1)$
 M13'.'
NULL(AA,8,8)$ NULL(BB,8,8)$ NULL(CC,8,8)$
MM=(1-NU(/NO/))/NU(/NO/)$
SS=(1-2*NU(/NO/))/(2*NU(/NO/))$
DD=(YM(/NO/)*NU(/NO/))/((1+NU(/NO/))*(1-2*NU(/NO/)))$
M14'.'
SETD4(BB)$
M15'.'
SETB4(AA,LR,LZ)$
MATMUL(CC,BB,AA,8,8,8)$          stresses at element centroids
AGLOB4$
M16'.'
MATINV(BB,AA,8)$
MATMUL(AA,CC,BB,8,8,8)$
NULL(BB,8,8)$
L=1$ 'FOR' I=1 'STEP' 2 'UNTIL' 7 'DO' 'BEGIN'
SM=ELNOD(/NO,L/)$
BB(/I,1/)=VI(/2*SM-1,1/)$  BB(/I+1,1/)=VI(/2*SM,1/)$
L=L+1$  'END'$
MATMUL(CC,AA,BB,8,8,8)$
'COMMENT' STRESSES ARE IN CC1,1 TO CC 1,4$
'FOR' I=1,2,3,4 'DO'                    PRINT(CC(/I,1/),4,2)$
MEANST=0$
M17'.'
'FOR' I=1,2,3 'DO' MEANST=MEANST + CC(/I,1/)$
MEANST=MEANST/3$
SPACE(4)$ PRINT(MEANST,3,3)$
CR=CC(/1,1/)$  CT=CC(/2,1/)$  CZ=CC(/3,1/)$  CTRZ=CC(/4,1/)$
TOCT= SQRT( ((CR-CT)**2 + (CT-CZ)**2 + (CZ-CR)**2 + 6*CTRZ**2))/3$
PRINT(TOCT,4,2)$

'IF' ITER 'EQ' 2 'THEN BEGIN'
'COMMENT' STRESSES CENTRELINES$
'IF' NO 'EQ' 1 'OR'
ABS( (NO-1)/(XND-1) - ENTIER( (NO-1)/(XND-1) ) ) 'LT' 'E'-6 'THENBEGIN'
CPOUT$
NEWCRD$
PRINT(NO,4,0)$ SPACE(2)$
PRINT(LZ,4,3)$ SPACE(2)$
PRINT(CC(/1,1/),5,5)$ SPACE(2)$      card output of stresses near
PRINT(CC(/3,1/),5,5)$ SPACE(2)$      centreline
NEWCRD$
PRINT(NO,4,0)$ SPACE(2)$
PRINT(LZ,4,3)$ SPACE(2)$
PRINT(MEANST,5,5)$ SPACE(2)$
PRINT(TOCT,5,5)$ SPACE(2)$
LPOUT$ 'END'$   'END' ITER2$
```

```
'IF' ITER 'EQ' 1 'OR' ITER 'EQ' 2  'THEN'
STORE(XND,YND)$ 'COMMENT' PUTS MEANST IN SK, LR, LZ $

M18'.'                          establish which layer element is in
MEANST=ABS(MEANST)$
'COMMENT' X X X X X X X X X X X X X X X X X X X X X X X X X X X X  $
'COMMENT' MODIFY MODULUS IN CORRECT LAYER$
'FOR' I=1 'STEP' 1 'UNTIL' NLAYS 'DOBEGIN'
'IF' NO 'EQ' RELAT(/I,1/) 'AND' NO 'LE' RELAT(/I,2/) 'THEN BEGIN'
LAYER=I$ 'GO TO' LAYE$ 'END'$ 'END'$
LAYE'.' LAYMOD(LAYER,EQU)$
'COMMENT' X X X X X X X X X X X X X X X X X X X X X X X X X X X X  $
                calculate element modulus for next analysis

SPACE(2)$  PRINT(YM(/NO/),0,3)$
'END' NO=1 TO EL FOR STRESSES$

'IF' ITER 'EQ' 1 'OR' ITER 'EQ' 2  'THEN'
LAYSTR(XND,YND)$ 'COMMENT'  LAYS MEANST ON L/P$

NEWLINE(1)$ WRITETEXT('(' MODIFIED '('SS')' MODULI ')')$
NEWLINE(1)$
          'FOR' I=1 'STEP' 1 'UNTIL' EL 'DO''BEGIN'
PRINT(YM(/I/),0,3)$ SPACE(1)$ 'IF' ABS( I/10-ENTIER(I/10)) 'LT' 'E'-6
'THEN' NEWLINE(1)$ 'END'$
'IF' ITER 'EQ' 2  'THEN' STOP$
ITER=ITER+1$ 'GOTO' LAB1$          terminates after 2 analyses
STOP$
'END' MAIN 4NVE 200 MODULARISED(2 IN BLOCK)$
 'END' NON MODULARISED HARWELL COMPAT. FROM 4AUTBIG 3313(1 IN BLOCK)$
'END' MAIN PROGRAM 4 NODE ELEMENT AND OUTER BLOCK, 8 NODE COMPATIBLE
```

PROGRAM 5: 4 node axisymmetric rectangle (FRICTION/TRIAXIAL)

Friction and linkage forces and modelling the triaxial specimen

A5.1 General Description

The program is written in separately compilable modules (see Prog. 1) so that well established procedures could be retained in binary form and not waste extra compiling time during the development of this lengthy program. The form is basically that of Program 2.1, modified to consider a layer system in the way described in Program 4. The theoretical approach to the linkage stiffnesses between nodes, the release of certain of these, and mobilisation of frictional forces at layer interfaces, is described in Chapter 7.

If frictional forces are to be mobilised, then an iterative procedure involving more than 1 solution of the structural equations is necessary. For this purpose the iteration counter (ITER) was conveniently used, the process being terminated after 5 iterations.

Card output is produced both at the centreline of loading and at the structure edge, with depth to facilitate the automatic plotting of some of the graphs in Chapter 7.

At iteration 1 and 5 (zero friction forces, and stable mobilised friction forces) the mean and shear stress invariants are outputted to the lineprinter to enable countour sketching (Figs. 7.6/7/8).

Certain procedures which are common with those in Program 2.1 are named in the position in the program where they should be declared.

Important comments within the program text have been underlined and others added.

A5.1.1 Extra storage requirements (these are declared in the 'predata' section)

Matrix Name	Purpose
ROWZ(ROWS)	to store the no. of rows vertically down from upper surface of structure, to the upper row of elements at each interface where frictional forces are to be mobilised
LINEK(4,4)	a matrix of linkage stiffnesses to be added to the structural stiffness matrix, computed for each pair of nodes so joined at each interface
FORCE(XND,ROWS)	matrix which stores the mobilised friction forces - one row of the matrix for each interface
LDAR(NOLOAD,3)	storage for the (node no./r load/z load) for each external load - used in the modified external load procedure 'LOADM'

A5.1.2 Additional procedures

LOADM — places the external structural load(s), stored in LDAR, into the load vector (VI)

LOADFR — adds the latest frictional forces (stored in FORCE), to the load vector

FORCES — calculates the frictional forces mobilised at the layer interfaces using latest known displacements (as described in Chapter 7)

LINK — calculates the linkage stiffnesses, LINEK(4,4), at the layer interfaces and adds them to the upper band of the overall structural stiffness matrix

FXTEST — deletes any load in (VI) which has been applied in a restrained direction (e.g. frictional forces on the axis of load)

GEN4NM — as GEN4N (Prog. 4) but increments the element numbering in order to provide a double row of elements at the layer interfaces, as defined by ROWZ(ROWS,2)

A5.2 Input

Sample input is given for the problem in Fig. 7.1 (with a 6 in. long specimen). Frictional forces are mobilised at the two layer interfaces as shown.

```
*PREDATA
      PUBLIC N,NO,EL,NOD,MM,SS,NCOORD(NOD,2),ELNOD(EL,4),INT(8,8),
     1       A(2),B(2),AA(8,8),EK(8,8),SK(N,BD),VI(N,CS),VI2(N,CS),
     2   FX(NFX,3),BD,CS, NLAYS,RELAT(NLAYS,2),ROWZ(ROWS),ROWS,
     3       K1(2),K2(2),K3(2),K4(1),K5(1), K9(2),K10(2),K11(2),K12(2),
     4       YM(EL),          NU(EL),DD,NFX, XND,YND,LINEK(4,4),KH,KV,
     5        K13(2),K14(2),K15(1),K16(1),K17(2),K18(1),K19(2),K20(2),
     6       ITER,ITERN,    YMI,NUI,MEANST,MU,FORCE(XND,ROWS),
     7     LDAR(NOLOAD,3),NOLOAD, K21(2)
      REAL MM,SS,NCOORD,INT,A,B,AA,EK,SK,VI,VI2,
     1       YM,LINEK,KH,KV,     DD,NU, LDAR,MEANST,YMI,NUI,MU,FORCE
      INTEGER N,NO,EL,NOD,ELNOD,FX,NFX,ITER,ITERN,BD,CS,NLAYS,RELAT,
     1         ROWZ,ROWS,XND,YND,NOLOAD
      NOD=288   no. of nodes
      EL=232    no. of elements
      N=576     no. of unknowns (2xNOD)
      BD=22     bandwidth
      CS=1      load cases
      NFX=41    no. of boundary fixities
      ROWS=2    no. of rows where 2 rows of nodes are necessary
      NLAYS=3   no. of layers
      XND=9     no. of nodes in radial direction
      NOLOAD=1  no. of externally loaded nodes
      PREOUT=1  device to leave predata section
```

Data	Description
1	(ITERN) redundant, keep as 1
1 32 33 224 225 232	RELAT(NLAY,2) - 1st and last element numbers in each of the 'NLAYS' layers (here, 3)
30×10^6 2×10^5 30×10^6	Young's Modulus of each of the 'NLAYS' layers
0.3 0.35 0.3	Poisson's Ratio of each of the layers
0.25	Coefficient of friction (μ) - the same for each interface
9 32	No. of nodes in the radial direction (XND), total no. of nodes in the vertical direction, <u>including</u> the two nodes at each interface (YND)

Data	Description
5 30	ROWZ(ROWS) - the number of nodes vertically downward to the top node of each of the 'ROWS' interfaces
0 .25 .5 .75 1.0 1.25 1.5 1.75 2.0	Radial co-ordinates of nodes X(1:XND)
0 0.25 0.5 0.75 1.0 1.0 1.25 1.5 1.75 2.0 2.25 2.5 2.75 3.0 3.25 3.5 3.75 4.0 4.25 4.5 4.75 5.0 5.25 5.5 5.75 6.0 6.25 6.5 6.75 7.0 7.0 7.5	Vertical co-ordinates of each node, including two at interfaces Y(1:YND)
	Fixity matrix FX(1:NFX,1:3) as described in Program 2.1
1 0 1 10 0 1 19 0 1 28 0 1 37 0 1 46 0 1 55 0 1 64 0 1 73 0 1 82 0 1 91 0 1 100 0 1 109 0 1 118 0 1 127 0 1 136 0 1 145 0 1 154 0 1 163 0 1 172 0 1 181 0 1 190 0 1 199 0 1 208 0 1 217 0 1 226 0 1 235 0 1 244 0 1 253 0 1 262 0 1 271 0 1 280 0 0 281 0 0 282 0 0 283 0 0 284 0 0 285 0 0 286 0 0 287 0 0 288 0 0 279 0 0	
0 10^{10} 0 10^{10}	K_h and K_v for each row: (note: K_h=0 if radial frictional forces are to be mobilised or no degree of radial restraint is required at the interface)
1 0 -1257	LDAR(NOLOAD,3): in this case only 1 load, i.e. at node no. 1 :- r load = 0, z load = -1257 lbf

A5.3 Output

The frictional forces calculated at each iteration are printed out, as are displacements and stresses. This enabled the iterative procedure to be monitored as well as the effect

on stresses of further iterations. Output is thus essentially the same as for program 2.1, except that the extra procedures associated with the calculation of linkage stiffnesses and frictional forces output the important quantities K_h, K_v and the linkage stiffness matrix.

```
      PUBLIC N,NO,EL,NOD,MM,SS,NCOORD(NOD,2),ELNOD(EL,4),INT(8,8),
     1       A(2),B(2),AA(8,8),EK(8,8),SK(N,BD),VI(N,CS),VI2(N,CS),
     2   FX(NFX,3),BD,CS, NLAYS,RELAT(NLAYS,2),ROWZ(ROWS),ROWS,
     3       K1(2),K2(2),K3(2),K4(1),K5(1), K9(2),K10(2),K11(2),K12(2),
     4       YM(EL),          NU(EL),DD,NFX, XND,YND,LINEK(4,4),KH,KV,
     5        K13(2),K14(2),K15(1),K16(1),K17(2),K18(1),K19(2),K20(2),
     6       ITER,ITERN,   YMI,NUI,MEANST,MU,FORCE(XND,ROWS),
     7      LDAR(NOLOAD,3),NOLOAD, K21(2)
      REAL MM,SS,NCOORD,INT,A,B,AA,EK,SK,VI,VI2,
     1       YM,LINEK,KH,KV,     DD,NU, LDAR,MEANST,YMI,NUI,MU,FORCE
      INTEGER N,NO,EL,NOD,ELNOD,FX,NFX,ITER,ITERN,BD,CS,NLAYS,RELAT,
     1         ROWZ,ROWS,XND,YND,NOLOAD
'BEGIN'
'REAL' LR,LZ,PREAL, CR,CT,CZ,CTRZ,TOCT$
'REAL' EXPM,INC,EQU$
'INTEGER' I,J, SM,SN,L,PINT,LAYER$
'INTEGER' II,JJ$
'ARRAY' BB(1'.'8,1'.'8),CC(1'.'8,1'.'8)$
'PROCEDURE' STORE(ACROSS,DOWN)$ 'INTEGER' ACROSS,DOWN$
'BEGIN'
SK(/II,JJ/)=LR$   SK(/II + DOWN -1,JJ/)= ABS(LZ-120)$
SK(/II+ 2*( DOWN -1),JJ/)=MEANST$
SK(/ II+3*(DOWN-1),JJ/)=TOCT$
SK(/II+4*(DOWN-1),JJ/)= MEANST/TOCT$
'IF' JJ 'EQ' (ACROSS-1) 'THEN' 'BEGIN' II=II+1$ JJ=1$ 'END' 'ELSE'
                                                        JJ=JJ+1$
'END' STORE$

'PROCEDURE' LAYSTR(ACROSS,DOWN)$ 'INTEGER' ACROSS,DOWN$
'BEGIN'
PAPERTHROW$
RMATPR(SK,5*(DOWN-1),ACROSS-1,3,2)$
PAPERTHROW$
'COMMENT' PRINTS OUT MEANST$
WRITETEXT('(' MEAN.NORMAL.STRESS ')')$
NEWLINE(2)$
'FOR' I=1 'STEP' 1 'UNTIL' (DOWN-1) 'DOBEGIN'
'IF' I 'NE' 1 'THEN'
NEWLINE( ENTIER((SK(/I+DOWN-1,1/)-SK(/I-1+DOWN-1,1/))/2) +2)$
'FOR' J=1 'STEP' 1 'UNTIL' (ACROSS-1) 'DOBEGIN'
'IF' J 'NE' 1 'THEN' SPACE(ENTIER((SK(/1,J /)-SK(/1,J -1/))/2))$
PRINT( SK(/I+2*(DOWN-1),J/),2,2)$
'END'$ 'END'$

PAPERTHROW$
WRITETEXT('(' OCT.SHEAR.STRESS ')')$
NEWLINE(2)$
'FOR' I=1 'STEP' 1 'UNTIL' (DOWN-1) 'DOBEGIN'
'IF' I 'NE' 1 'THEN'
NEWLINE( ENTIER((SK(/I+DOWN-1,1/)-SK(/I-1+DOWN-1,1/))/2) +2)$
'FOR' J=1 'STEP' 1 'UNTIL' (ACROSS-1) 'DOBEGIN'
'IF' J 'NE' 1 'THEN' SPACE(ENTIER((SK(/1,J /)-SK(/1,J -1/))/2))$
PRINT( SK(/I+3*(DOWN-1),J/),2,2)$
'END'$ 'END'$

PAPERTHROW$
WRITETEXT('(' RATIO..MEANST.TO.TOCT ')')$
NEWLINE(2)$
'FOR' I=1 'STEP' 1 'UNTIL' (DOWN-1) 'DOBEGIN'
'IF' I 'NE' 1 'THEN'
NEWLINE( ENTIER((SK(/I+DOWN-1,1/)-SK(/I-1+DOWN-1,1/))/2) +2)$
'FOR' J=1 'STEP' 1 'UNTIL' (ACROSS-1) 'DOBEGIN'
'IF' J 'NE' 1 'THEN' SPACE(ENTIER((SK(/1,J /)-SK(/1,J -1/))/2))$
PRINT( SK(/I+4*(DOWN-1),J/),2,2)$
'END'$ 'END'$
'END' LAYSTR$
```

```
SUPDV2(SK,K11,N,BD)$
SUPDV2(NCOORD,K1,NOD,2)$
SUPDV2(ELNOD,K2,EL,4)$
SUPDV2(INT,K3,8,8)$
SUPDV1(A,K4,3)$
SUPDV1(B,K5,3)$
SUPDV2(AA,K9,8,8)$
SUPDV2(EK,K10,8,8)$
SUPDV2(VI,K12,N,CS)$
SUPDV2(VI2,K13,N,CS)$
SUPDV2(FX,K14,NFX,3)$
SUPDV1(YM,K15,EL)$
SUPDV1(NU,K16,EL)$
SUPDV2(RELAT,K17,NLAYS,2)$
SUPDV1(ROWZ,K18,ROWS)$
SUPDV2(LINEK,K19,4,4)$
SUPDV2(FORCE,K20,XND,ROWS)$
SUPDV2(LDAR,K21,NOLOAD,3)$
'COMMENT' TOTAL NO OF ITERATIONS OF LOADS$

ININT(ITERN)$
LINES(1)$ TEXT('(' ITERN ')')$   IPRINT(ITERN,3)$
'COMMENT' READ IN RELAT, THE LAYER DESCRIPTIONS$

'FOR' I=1 'STEP' 1 'UNTIL' NLAYS 'DOBEGIN'
'FOR' J=1,2 'DO' ININT(RELAT(I,J))$ 'END'$
     LINES(1)$TEXT('('RELAT')')$LINES(1)$ IMATPR(RELAT,NLAYS,2,3)$
'COMMENT' READ IN AND SET THE NLAYS MODULI$
     LINES(1)$ TEXT('('LAYER'*'MODULI'*****'..')')$ LINES(1)$
M21'.'
'FOR' I=1 'STEP' 1 'UNTIL' NLAYS 'DOBEGIN'
INREAL(YMI)$
     EPRINT(YMI,3)$ SPACES(2)$
'FOR' SM= RELAT(  I  ,1) 'STEP' 1 'UNTIL' RELAT(  I  ,2) 'DO'
YM(SM)= YMI$
'END'$
'COMMENT' READ IN AND SET THE  NLAYS  NU$
     LINES(1)$ TEXT('(' LAYER'*'POISSONS'*'RATIO ')')$ LINES(1)$
M22'.'
'FOR' I=1 'STEP' 1 'UNTIL' NLAYS 'DOBEGIN'
INREAL(NUI)$
     PRINT(NUI,1,3)$ SPACES(2)$
'FOR' SM=RELAT(  I  ,1) 'STEP' 1 'UNTIL' RELAT(  I  ,2) 'DO'
NU(SM)=NUI$
'END'$
M23'.'
LINES(1)$
J=1$
'FOR' I=1 'STEP' 1 'UNTIL' EL 'DOBEGIN'
EPRINT(YM(I),3)$ SPACES(2)$
'IF' J 'EQ' 10 'THEN' 'BEGIN' J=0$ LINES(1)$ 'END'$ J=J+1$
'END'$
LINES(1)$
J=1$
          'FOR' I=1 'STEP' 1 'UNTIL' EL 'DOBEGIN'
EPRINT(NU(I),3)$ SPACES(2)$
'IF' J 'EQ' 10 'THEN' 'BEGIN' J=0$ LINES(1)$ 'END'$ J=J+1$
'END'$
INREAL(MU)$ 'COMMENT' LAYER FRICTION FACTORS$
```

procedures called for machine addressing purposes (includes all arrays)

```
LINES(1)$ TEXT('(' FRICTION.MU ')')$ PRINT(MU,1,3)$
'COMMENT' AUTOMATIC GENERATION OF THE HALFSPACE USED IN  4CHOL3106$
 M3'.'←(000430)
ININT(XND)$ ININT(YND)$
LINES(1)$ TEXT('(' XND..YND ')')$ IPRINT(XND,3)$ IPRINT(YND,3)$
LINES(1)$ TEXT('(' NO.OF.FRICTION.INTERFACES..ROWS= ')')$
          IPRINT(ROWS,3)$
'FOR' I=1 'STEP' 1 'UNTIL' ROWS 'DO' ININT( ROWZ(/I/) )$
LINES(1)$ TEXT('(' ROWZ(ROWS) ')')$ IVECPR(ROWZ,ROWS,2)$
GEN4NM$
PAGE$ TEXT('(' NCOORD'*'FROM'*'GEN4N ')')$ LINES(1)$
'COMMENT' REARRANGEMENT OF NODE CO-ORDINATES TO BE IN ASCENDING
ORDER OF Z FROM BOTTOM OF HALFSPACE$
'FOR' I=1 'STEP' 1 'UNTIL' NOD 'DO'
            NCOORD(I,2)=NCOORD(I,2)-NCOORD(NOD,2)$
'FOR' I=1 'STEP' 1 'UNTIL' NOD 'DO'
            NCOORD(I,2)=ABS(NCOORD(I,2))$
'FOR' I=1 'STEP' 1 'UNTIL' NOD 'DO' NCOORD(I,2)=NCOORD(I,2)+10$

PAGE$
'COMMENT' OUTPUT OF ELEMENT NODE MATRIX $
LINES(2)$ TEXT( '(' ELNOD ')' )$←(000290)
LINES(1)$
SM=0$  SN=0$
'FOR' I = 1 'STEP' 1 'UNTIL' EL 'DO' 'BEGIN'
'IF' SM 'EQ' 6 'THEN' 'BEGIN' LINES(1)$ SM=0$ 'END'$
SM=SM+1$
'IF' SN 'EQ' 24 'THEN' 'BEGIN' LINES(2)$ SN=0$ 'END'$
SN=SN+1$
'FOR' J=1,2,3,4 'DOBEGIN'
IPRINT(ELNOD(I,J),3)$ SPACES(1)$ 'END'$
SPACES(4)$ 'END'$
PAGE$
'COMMENT' OUTPUT OF NODE CO-ORDINATE MATRIX$
LINES(2)$ TEXT('(' NCOORD ')')$ LINES(1)$ SM=0$
'FOR' I = 1 'STEP' 1 'UNTIL' NOD 'DO' 'BEGIN'  SPACES(2)$
'IF' SM 'EQ' 5 'THEN' 'BEGIN' LINES(1)$ SM=0$ 'END'$
SM=SM+1$
'FOR' J=1,2 'DOBEGIN'
PRINT(NCOORD(I,J),3,2)$ SPACES(1)$
'END'$ 'END'$
BCHEK4$
'COMMENT' READ IN FIXITY MATRIX$
'FOR' I=1 'STEP' 1 'UNTIL' NFX 'DOBEGIN' 'FOR' J=1,2,3 'DO'
ININT(FX(I,J))$ 'END'$
LINES(1)$ TEXT('('XXX'*'FIXITY'*'MATRIX'*'XXX ')')$
IMATPR(FX,NFX,3,3)$
 M4'.'←(000460)
```

```
ITER=1$
LAB1'.' PAGE$ LINES(1)$ TEXT('(' ITER= ')')$IPRINT(ITER,3)$
NULL(SK,N,BD)$
 M5'.'←(000480)
'FOR' NO=1 'STEP' 1 'UNTIL' EL 'DOBEGIN'
AGLOB4$
MM=(1-NU(NO))/NU(NO)$
SS=(1-2*NU(NO))/(2*NU(NO))$
DD=(YM(NO)*NU(NO))/((1+NU(NO))*(1-2*NU(NO)))$
 M6'.'←(000500)
ITINT4$
MATCOP(CC,AA,8,8)$
MATINV(PINT,PREAL,BB,CC,8)$
TRANS(EK,BB,8,8)$←(001850)
MATMUL(CC,EK,INT,8,8,8)$←(001860)
MATMUL(EK,CC,BB,8,8,8)$
BPOST4$ ←—— post element stiffnesses
'END'$
LINK$ ←—— post linkage stiffnesses
'COMMENT' INPUT KH AND KV FOR EACH$
 M7'.'←(000520)
'IF' ITER 'EQ' 1 'THEN' 'BEGIN'
LINES(1)$ TEXT('(' LEADING'*'DIAGONAL ')')$
LINES(1)$ 'FOR' I=1 'STEP' 1 'UNTIL' N 'DOBEGIN'
       SPACES(1)$ EPRINT(SK(I,1),2)$ 'END'$
'END'$
 M8'.'←(000540)
FXBDIT$
'IF' ITER 'EQ' 1 'THEN' 'BEGIN'
NULL(VI,N,CS)$
 M9'.'←(000590)
LOADM$ 'COMMENT'          STORES LOADS IN LDAR
LINES(1)$
     TEXT( '('XXXXXXXXXXXXXXXXXXXXXXXXXXXXXXXXXXXXXXXXXXXXXXXXXXX')')$
LINES(2)$ TEXT( '('VI'*'TO'*'EQN'*'SOLVE')' )$EVECPR(VI,N,3)$
    'FOR' I=1 'STEP' 1 'UNTIL' N 'DO' VI2(I,1)=VI(I,1)$
'END' 'ELSE'
'BEGIN'
NULL(VI,N,CS)$
LOADM$ 'COMMENT' 1ST IT STORES LOADS IN LDAR, LOADS VI EACH ITER$
LOADFR$ 'COMMENT' RADIAL FORCES$
LINES(2)$ TEXT('(' VI.TO.SOLUTION.ROUTINE ')')$ EVECPR(VI,N,3)$
'END'$
FXTEST$
PLAGMK3(N,BD,CS,SK,VI)$
 M10'.'←(000610)
LINES(2)$ TEXT( '(' DEFLECTIONS ')' )$ LINES(1)$←(000700)
'FOR' I = 1 'STEP' 2 'UNTIL' (N-1) 'DO' 'BEGIN'←(000720)
SM = (I+1)/2$←(000730)
LINES(1)$ IPRINT(SM,1)$ SPACES(3)$←(000740)
EPRINT(VI(I,1),4)$ SPACES(2)$ EPRINT(VI(I+1,1),4)$
'END'$←(000770)
'COMMENT' RADIAL AND VERTICAL DISPLACEMENTS ON C LINE AND EDGE
      OUTPUT ON CARDS WITH VERTICAL COORDINATES$
'IF' ITER 'EQ' 1 'OR' ITER 'EQ'5'THENBEGIN'
CPOUT$
'COMMENT' CENTRE LINES$
'FOR' I=1 'STEP' XND 'UNTIL' XND*(YND-1)+1 'DOBEGIN'
NEWCRD$
IPRINT(I,4)$ SPACES(2)$
PRINT(NCOORD(/I,2/),4,3)$ SPACES(2)$
EPRINT(VI(/2*I-1,1/),7)$ SPACES(2)$
EPRINT(VI(/2*I  ,1/),7)$ SPACES(2)$
'END' I$
```

```
'COMMENT' EDGE$
'FOR' I=XND 'STEP' XND 'UNTIL' XND*YND 'DOBEGIN'
NEWCRD$
IPRINT(I,4)$ SPACES(2)$
PRINT(NCOORD(/I,2/),4,3)$ SPACES(2)$
EPRINT(VI(/2*I-1,1/),7)$ SPACES(2)$
EPRINT(VI(/2*I  ,1/),7)$ SPACES(2)$
'END' I$
LPOUT$
'END'$
FORCES$ 'COMMENT' CALCULATES FORCES ON ROWS INTERFACES$
LINES(2)$ TEXT('(' FORCES ')')$ LINES(1)$ EMATPR(FORCE,XND,ROWS,4)$
 M11'.'←(000630)
PAGE$ TEXT( '('ELEMENT'****'CENTROID'********'R'**********'Z'**'
STRESSES'**********'R
'*******'TH'*******'Z'*******'TRZ ')')$
SPACES(3)$ TEXT('(' MEANST '('3S')' TOCT ')')$

NULL( SK, 5*(XND-1), YND-1)$
II=1$   JJ=1$

'FOR' NO=1 'STEP' 1 'UNTIL' EL 'DO BEGIN'
LR=0$ LZ=0$
'FOR' L=1,2,3,4 'DO BEGIN'
LR=LR+NCOORD(ELNOD(NO,L),1)$ LZ=LZ+NCOORD(ELNOD(NO,L),2)$
'END'$ LR=LR/4$ LZ=LZ/4$
LINES(1)$ TEXT('('EL     ')')$ SPACES(1)$
IPRINT(NO,2)$ SPACES(2)$
TEXT('('CEN·     ')')$ SPACES(1)$
EPRINT(LR,4)$ SPACES( 1)$ EPRINT(LZ,4)$
 M13'.'
NULL(AA,8,8)$ NULL(BB,8,8)$ NULL(CC,8,8)$
MM=(1-NU(NO))/NU(NO)$
SS=(1-2*NU(NO))/(2*NU(NO))$
DD=(YM(NO)*NU(NO))/((1+NU(NO))*(1-2*NU(NO)))$
 M14'.'
AGLOB4$
MATINV(BB,AA,8)$
NULL(AA,8,8)$
SETB4(AA,LR,LZ)$
MATMUL(CC,AA,BB,8,8,8)$
NULL(BB,8,8)$
L=1$ 'FOR' I=1 'STEP' 2 'UNTIL' 7 'DO BEGIN'
SM=ELNOD(NO,L)$
BB(I,1)=VI(2*SM-1,1)$  BB(I+1,1)=VI(2*SM,1)$
L=L+1$ 'END'$
NULL(AA,8,8)$
MATMUL(AA,CC,BB,8,8,8)$
'FOR' I=1 'STEP' 1 'UNTIL' 4 'DOBEGIN'
EPRINT(AA(/I,1/),2)$ 'END'$
NULL(BB,8,8)$                    element centroid stresses
SETD4(BB,MM,SS)$
MATMUL(CC,BB,AA,8,8,8)$
'COMMENT' STRESSES ARE IN CC1,1 TO CC 1,4$
'FOR' I=1,2,3,4 'DOBEGIN' SPACES(1)$ PRINT(CC(I,1),4,2)$ 'END'$
MEANST=0$
M17'.'←(000810)
'FOR' I=1,2,3 'DO' MEANST=MEANST + CC(I,1)$
MEANST=MEANST/3$
SPACES(2)$   PRINT(MEANST,3,3)$
CR=CC(/1,1/)$ CT=CC(/2,1/)$ CZ=CC(/3,1/)$ CTRZ=CC(/4,1/)$
TOCT= SQRT(( (CR-CT)**2 + (CT-CZ)**2 + (CZ-CR)**2 +6*CTRZ**2 ))/3$
PRINT(TOCT,2,2)$
```

```
'IF' ITER 'EQ' 1 'OR' ITER 'EQ'5 'THEN' STORE(XND,YND)$ 'COMMENT'
 MEANST AND TOCT IN SK          $

'IF' ITER 'EQ' 1 'OR' ITER 'EQ'5'THENBEGIN'
'COMMENT' OUTPUT OF         STRESSES CENTRE LINE AND EDGES$
'IF' NO 'EQ' 1 'OR'
ABS( (NO-1)/(XND-1) -ENTIER( (NO-1)/(XND-1) ) ) 'LT' 'E'-6 'THENBEGIN'
CPOUT$
NEWCRD$
IPRINT(NO,4)$ SPACES(2)$
PRINT(LZ,4,3)$ SPACES(2)$
PRINT(CC(/1,1/),5,5)$ SPACES(2)$
PRINT(CC(/2,1/),5,5)$ SPACES(2)$
PRINT(CC(/3,1/),5,5)$ SPACES(2)$
NEWCRD$
PRINT(NO,4,0)$ SPACES(2)$                    card output of stresses
PRINT(LZ,4,3)$ SPACES(2)$                    for plotting
PRINT(MEANST,5,5)$ SPACES(2)$
PRINT(TOCT  ,5,5)$ SPACES(2)$
LPOUT$
'END'$
'COMMENT' EDGES$
'IF' ABS(NO/(XND-1) -ENTIER(NO/(XND-1) ) ) 'LT' 'E'-6 'THEN BEGIN'
CPOUT$
NEWCRD$
IPRINT(NO,4)$ SPACES(2)$
PRINT(LZ,4,3)$ SPACES(2)$
PRINT(CC(/1,1/),5,5)$ SPACES(2)$
PRINT(CC(/2,1/),5,5)$ SPACES(2)$
PRINT(CC(/3,1/),5,5)$ SPACES(2)$
NEWCRD$
PRINT(NO,4,0)$ SPACES(2)$
PRINT(LZ,4,3)$ SPACES(2)$
PRINT(MEANST,5,5)$ SPACES(2)$
PRINT(TOCT  ,5,5)$ SPACES(2)$
LPOUT$
'END'$
'END' ITER5$
M18'.'
```

```
                    MEANST=ABS(MEANST)$
'COMMENT' MODIFY MODULUS IN THE LAYERS
'FOR' I=1 'STEP' 1 'UNTIL' NLAYS 'DOBEGIN'
'IF' NO 'GE' RELAT(I,1) 'AND'      NO 'LE' RELAT(I,2) 'THEN'
 'BEGIN'
 LAYER=I$                  | dummy statements - moduli in layers are
 'GOTO' LAY$               | unchanged;  (they could be modified if
 'END'$                    | desired)
'END'$
'COMMENT' X X X X X X X X X X X X X X X X X X X X XX X X X X $
LAY'.' 'IF' LAYER 'EQ' 2 'THEN' EQU = 2*('E'+5)              'ELSE'
   EQU= 30*('E'+6)$
'COMMENT' X X X X X X X X X X X X X X X X X X X X XX X X X X $
'IF' ITER 'GE' ITERN 'THEN' 'BEGIN'
INC = EQU - YM(NO)$
INC = INC/2$
YM(NO) = YM(NO) + INC$
'END' 'ELSE' 'BEGIN'
YM(NO) = EQU$ 'END'$
SPACES(1)$ TEXT('('      YM')')$ EPRINT(YM(NO),3)$
'END'$ 'COMMENT' NO=1 TO EL FOR STRESSES$

'IF' ITER'EQ' 1 'OR' ITER 'EQ' 5 'THEN' LAYSTR(XND,YND)$

LINES(1)$ TEXT('(' MODIFIED'*'MODULUS ')')$
LINES(1)$ 'FOR' I=1 'STEP' 1 'UNTIL' EL 'DOBEGIN'
EPRINT(YM(I),3)$ SPACES(1)$ 'END'$
'IF' ITER 'EQ' 5 'THEN' STOP$
ITER=ITER+1$ 'GOTO' LAB1$
STOP$
'END' MAIN 4NVE 200 ETC
```

XXXXXXXXX PROCEDURES

- AGLOB4
- BPOST4
- FXBDIT
- SETD4
- SETB4

```
'PROCEDURE'LOADM$
'BEGIN'
 'INTEGER'          I,J,P$
 LINES(1)$ TEXT('(' NO.OF.LOADS..NOLOAD ')')$ IPRINT(NOLOAD,6)$
 'IF' ITER 'EQ' 1 'THEN'
 'FOR' I=1 'STEP' 1 'UNTIL' NOLOAD 'DO'
 'FOR' J=1,2,3 'DO' INREAL(LDAR(/I,J/))$
 LINES(1)$ RMATPR(LDAR,NOLOAD,3,4,1)$
 'FOR' I=1 'STEP' 1 'UNTIL' NOLOAD 'DOBEGIN'
 P=ENTIER( LDAR(/I,1/))$
 VI(/2*P-1,1/)=LDAR(/I,2/)$
 VI(/2*P , 1/)=LDAR(/I,3/)$
 'END'$
       'END' LOADM
```

```
'PROCEDURE' FORCES$
'BEGIN'
'INTEGER' I,J,REFND,REFEL,L,SM,P,O$
'REAL' FA,FB$
'ARRAY' BB,CC(/1'.'8,1'.'8/)$
'COMMENT' CALCULATES RADIAL FORCES ON UPPER BOUNDARY OF EACH
INTERFACE USING COEFFICIENT OF FRICTION WHICH IS READ IN AT BEG.
OF PROGRAM $
NULL(FORCE,XND,ROWS)$
'FOR' I=1 'STEP' 1 'UNTIL' ROWS 'DOBEGIN'
REFND=XND*(ROWZ(/I/)-1)+1$
LINES(1)$ TEXT('(' REFND ')')$ IPRINT(REFND,5)$
REFEL=(XND-1)*(ROWZ(/I/)-I-1)+1$
SPACES(2)$ TEXT('(' REFEL ')')$ IPRINT(REFEL,5)$
'COMMENT' STIFFNESS;THEN FORCES FOR EACH ELEMENT IN UPPER ROW AT
INTERFACES$
'FOR' NO=REFEL 'STEP' 1 'UNTIL' REFEL+XND-2 'DOBEGIN'
AGLOB4$
MM=(1-NU(/NO/))/NU(/NO/)$
SS=(1-2*NU(/NO/))/(2*NU(/NO/))$
DD=(YM(/NO/)*NU(/NO/))/((1+NU(/NO/))*(1-2*NU(/NO/)))$
ITINT4$
MATCOP(CC,AA,8,8)$
MATINV(BB,CC,8)$
TRANS(EK,BB,8,8)$
MATMUL(CC,EK,INT,8,8,8)$
MATMUL(EK,CC,BB ,8,8,8)$
'COMMENT' ELEMENT STIFFNESS IN .EK. $
L=1$ 'FOR' J=1 'STEP' 2 'UNTIL' 7 'DOBEGIN'
SM=ELNOD(/NO,L/)$
BB(/J  ,1/)=VI(/2*SM-1,1/)$
BB(/J+1,1/)=VI(/2*SM  ,1/)$
L=L+1$ 'END'$
MATMUL(CC,EK,BB,8,8,8)$ 'COMMENT' FORCES IN CC $
'COMMENT' RADIAL FORCES ONLY ADDED IN, IE MU X VERTICAL FORCES$
FA=CC(/2,1/)$
FB=CC(/8,1/)$
P=NO-REFEL+1$
FORCE(/P  ,I/)=MU*FA+FORCE(/P  ,I/)$
FORCE(/P+1,I/)=MU*FB+FORCE(/P+1,I/)$
'END' NO$
'IF' I 'EQ' 2 'THEN FOR' J=1 'STEP' 1 'UNTIL' XND 'DO'
   FORCE(/J,2/)=-FORCE(/J,2/)$
          'END' I ROWS$
'END' FORCES
```

```
'PROCEDURE' LOADFR$
'BEGIN'
'INTEGER' I,J,P,Q,REFND$
'COMMENT' PUT RADIAL FORCES FROM FORCE(XND,ROWS) INTO LOAD VECTOR
 VI, SO THAT EQUAL AND OPPOSITE RADIAL LOADS TOP AND BOTTOM LAYER
 OF NODES IN EACH INTERFACE      $
'FOR' I=1 'STEP' 1 'UNTIL' ROWS 'DOBEGIN'
REFND=XND*(ROWZ(/I/)-1)+1$
'FOR' J=REFND 'STEP' 1 'UNTIL' REFND+XND-1 'DOBEGIN'
P=J-REFND+1$
Q=2*J-1$
VI(/Q    ,1/)=VI(/Q    ,1/)+   FORCE(/P,I/)$
VI(/Q+2*XND,1/)=VI(/Q+2*XND,1/) - FORCE(/P,I/)$
'COMMENT' RADIALS ONLY$
'END' J$   'END' I$
'END' LOADFR
```

```
'PROCEDURE' LINK$
'BEGIN'
'INTEGER' I,J,SM,SN,ND1,ND2,REFND,S,L$
'INTEGER ARRAY' LKEL(/1'.'2/)$
PAGE$
'FOR' I=1 'STEP' 1 'UNTIL' ROWS 'DOBEGIN'
REFND=XND*( ROWZ(/I/)-1 ) +1$
LINES(1)$ TEXT('(' REFND ')')$ IPRINT(REFND,4)$
'IF' ITER 'EQ' 1 'THEN BEGIN'
INREAL(KH)$ INREAL(KV)$ 'END'$
LINES(1)$ TEXT('(' KH..KV.. ')')$ EPRINT(KH,3)$ EPRINT(KV,3)$
LINES(1)$ TEXT('(' J ')')$
 'FOR' J=REFND 'STEP' 1 'UNTIL' REFND+XND-1 'DOBEGIN'
LINES(1)$ IPRINT(J,3)$ SPACES(1)$
LKEL(/1/)=J$  LKEL(/2/)=J+XND$
'COMMENT' GIVEN KH,KV AND LINEK(4,4) DECLARED$
NULL(LINEK,4,4)$
LINEK(/1,1/)=LINEK(/3,3/)=KH$
LINEK(/1,3/)=LINEK(/3,1/)=-KH$
LINEK(/2,2/)=LINEK(/4,4/)=KV$
LINEK(/2,4/)=LINEK(/4,2/)=-KV$
'COMMENT' IF LEADING DIAGONAL TERM IS ZERO, CHANGE TO 1 $
'FOR' L=1,2,3,4 'DO' 'IF' ABS(LINEK(/L,L/) ) 'LT' 'E'-12 'THEN'
   LINEK(/L,L/)=1$
'COMMENT' POST TO SK$
'FOR' S=1,2 'DOBEGIN'
ND1=LKEL(/S/)$
'FOR' L=1,2 'DOBEGIN'
ND2=LKEL(/L/)$
'FOR' SM=0,1 'DO' 'FOR' SN=0,1 'DO'
'IF' 2*ND2-SN 'GE' 2*ND1-SM 'THEN'
SK(/2*ND1-SM,2*ND2-SN-2*ND1+SM+1/)=
SK(/2*ND1-SM,2*ND2-SN-2*ND1+SM+1/)+ LINEK(/2*S-SM,2*L-SN/)$
'END'$ 'END'$
LINES(1)$ TEXT('(' LINEK ')')$ EMATPR(LINEK,4,4,3)$
'END' J$ 'END' I$
'END' LINK
```

```
'PROCEDURE' FXTEST$
'BEGIN'
'INTEGER' II,FXD$
LINES(2)$ TEXT('(' SET.TO.ZERO..BECAUSE.LOADED.AT.BOUNDARY ')')$
'FOR' II=1 'STEP' 1 'UNTIL' NFX 'DOBEGIN'
   FXD=2*FX(II,1)$
'IF' ABS( VI(FXD-1,1) ) 'GT' ('E'-6) 'AND' FX(II,2) 'EQ' 0
'THEN BEGIN'
     VI(FXD-1,1)=0$
     LINES(1)$ TEXT('('RADIAL '('5S')' NODE.... ')')$
     PRINT( (ABS(FXD/2)),3)$ 'END'$
'IF' ABS( VI(FXD  ,1) ) 'GT' ('E'-6) 'AND' FX(II,3) 'EQ' 0
'THEN BEGIN'
     VI(FXD,1)=0$
     LINES(1)$ TEXT('(' Z '('10S')' NODE.... ')')$
     PRINT((FXD/2),3)$ 'END'$
'END' TO NFX$
'END'
```

```
'PROCEDURE' GEN4NM$
'BEGIN'
'ARRAY' X(/1'.'XND/), Y(/1'.'YND/)$
'INTEGER' I,IX,IY,P,Q,R,IXY,RR,QQ,NULFAC,NF$
'FOR' I=1 'STEP' 1 'UNTIL' XND 'DO' INREAL( X(/I/) )$
'FOR' I=1 'STEP' 1 'UNTIL' YND 'DO' INREAL( Y(/I/) )$
'COMMENT' GEN4NM IS A MODIFICATION OF GEN4N
TO NUMBER INTERFACE ROWS OF ELEMENTS TWICE, INPUT IS
 ROWZ(1 TO ROWS)  ROWS IS NO OF ROWS WITH FRICTION
                  ROWZ CONTAINS ROW NO AFTER WHICH FRICTION
INTERFACE OCCURS $
I=1$ Q=0$ R=0$
NULFAC=0$ NF=1$
'FOR' IY=Q 'STEP' 1 'UNTIL' YND-2+Q 'DOBEGIN'
'FOR' IX=R 'STEP' 1 'UNTIL' XND-2+R 'DOBEGIN'
IXY=1+IX+IY+ NULFAC$ 'COMMENT' NULFAC IS INCREMENT FOR DOUBLE ROW$
ELNOD(/I,1/)=IXY+XND$
ELNOD(/I,2/)=IXY$
ELNOD(/I,3/)=IXY+1$                    element node numbering
ELNOD(/I,4/)=IXY+XND+1$
'IF' I 'EQ' EL 'THEN GOTO' L1$
I=I+1$
RR=R$
'END' IX$
'IF' ELNOD(/I-1,4/) 'EQ' XND*ROWZ(/NF/) 'THEN BEGIN'
   NULFAC=NULFAC+XND$
   'IF' NF 'NE' ROWS 'THEN' NF=NF+1$ 'END'$
'COMMENT' NULFAC IS A DEVICE TO INCREASE NODE NUMBERS BY XND WHERE TWO
      ROWS OF NODES NEEDED TO MODEL FRICTION$
R=RR$ R=R+XND-1$
QQ=Q$
'END' IY$
L1'.' LINES(1)$
P=1$ Q=1$
'FOR' I=1 'STEP' 1 'UNTIL' NOD 'DOBEGIN'
NCOORD(/I,1/)= X(/P/)$
NCOORD(/I,2/)= Y(/Q/)$        node co-ordinate numbering
P=P+1$
'IF' ABS( I/XND-ENTIER(I/XND) ) 'LE' 'E'-6 'THEN BEGIN'
P=1$ Q=Q+1$ 'END'$
'END'$ 'COMMENT' I IS 1 TO NOD$
LINES(3)$
'END' GEN4N
```

```
'PROCEDURE' BCHEK4$
'BEGIN'
'INTEGER' NO,I,R,S,T,BAND$
'INTEGER ARRAY' P(1'.'4)$
T=0$
'FOR' NO = 1 'STEP' 1 'UNTIL' EL 'DO' 'BEGIN'
'FOR' I = 1,2,3,4 'DO' P(I) = ELNOD(NO,I)$
R=0$ S=1000$
'FOR' I = 1,2,3,4 'DOBEGIN'
'IF' P(I) 'GT' R 'THEN' R=P(I)$
'IF' P(I) 'LT' S 'THEN' S=P(I)$
'END'$                          a check of calculated
BAND = 2*(R-S+1)$               bandwidth
'IF' BAND 'GT' T 'THEN' T = BAND$
'END'$
LINES(1)$ TEXT( '('XXX'*'CORRECTED'*'BANDWIDTH'*'XXX')' )$
SPACES(2)$ TEXT ( '('IS')' )$ SPACES(2)$ IPRINT(T,2)$
'END' BCHEK4
```

PROGRAM 6 Iterative Analysis of a Horizontally Layered System: 4 node axisymmetric rectangle

A6.1 General description

The program is intended to enable the analysis of systems consisting of horizontal layers of linear or non-linear elastic materials. The materials in the system may be characterised either by the Young's Modulus (E) and Poisson's Ratio (ν) or by the Bulk Modulus (K) and Shear Modulus (G) depending on the choice of a control integer. The self weight of the materials may be considered.

The program form is substantially that of Program 2 (Section A2.1.1) with certain procedures amended and others added. The layers to which elements belong are defined in the same way as described in Section A4.1.

A6.1.1 Procedures amended:

ITINT4 - the integral terms are calculated (for the i^{th} element) using either E (YMKM(i)) and ν (NU(i)) or K (YMKM(i)) and G (GM(i)) depending on whether the integer KGYC is 1 or 2 respectively.

UDOAD4 - the procedure is amended to allow for the case where the maximum radius of loaded area does not coincide with a mesh point.

SETD4 - amended to calculate (D) matrix for E, ν or K, G functional approaches.

LAYMOD - the procedures calls on the appropriate functional relationship between modulus and stress for each element, given the layer (LAY) in which it is situated, and calculates the modified modulus for the element. For each different layered problem this procedure must be rewritten and define modulus either as $E = f(\sigma,\tau)$ or $K, G = f(\sigma,\tau)$.

i.e. if KGYC = 1 then EQU = $f(\sigma,\tau)$
if KGYC = 2 then EQUK = $f(\sigma,\tau)$
EQUG = $f(\sigma,\tau)$

A6.1.2 Procedures added:

OVLD4 - given the overburden density for each layer, the equivalent nodal loads for each element are calculated by integration and added to the relevant part of the load vector (VI).

FXTEST - as described in Section A5.1.2

A6.1.3 Special features and difficulties

The program text is presented as run on the Science Research Council, Chilton Atlas Computer and incorporates dumping of a copy of the program to tape NO313 after each 10 minutes of computing to guard against loss by machine breakdown. The matrix procedures declared at the beginning of the program call on the Atlas matrix library. ICL 1900 series input/output procedures are used. Removal of the ATLAS JOB heading cards and library calls and the substitution of a suitable set of matrix procedures would enable the program's use with any Algol 60 compiler.

The Chilton Atlas Computer was used in preference to the Nottingham University KDF9 since it has a larger core store and allowed greater refinement of finite element mesh. Difficulties were encountered at Atlas in the use of integration procedures to calculate the equivalent nodal forces for both uniformly distributed loads (UDOAD4) and overburden loads (OVLD4). As a result it was found necessary to calculate these forces on KDF9 and input them to Atlas on cards. It is suspected that the inversion of the (A) matrix is performed in a less general way on Atlas and that provision of a routine such as that available at Nottingham would eliminate the overflow in the matrix inversion routine.

A6.2 Input

Sample input is given for the 3 layer system in Fig. 5.7.

Data	Description
2	Control integer (KGYC); if 1 then E, ν if 2 then K, G
1 54	No. of load cases (CS), Number of nodes at which boundary conditions are imposed (NFX)
14 21	No. of nodes in radial (ACROSS) and vertical (DOWN) directions
3	No. of layers (NLAYS)
1 1 1 1 1 1 1 3 5 5 8 8 12	Spacing in radial direction ACVEC (ACROSS-1)
1 1 1 1 1 1 1 2 2 1 2 2 2 2 5 5 5 10 13 14	Spacing in vertical direction from surface downward DUNVEC(DOWN-1)
1	Total no. of iterations to full load (or increments, section A2.2)
1 39 40 130 131 260	Layer description RELAT(1:NLAYS, 1:2) i.e. layer 1 contains elements 1 to 39 inclusive layer 2 contains elements 40 to 130 inclusive layer 3 contains elements 131 to 260 inclusive
228200 48900	K_1 G_1 initial bulk and shear
10000 4000	K_2 G_2 moduli
825600 1195000	K_3 G_3 (if 'E,ν' then read in as E_1, E_2, E_3 and ν_1, ν_2, ν_3)

/contd.

Data	Description
	Boundary fixity FX(1:NFX, 1:3)
1 0 1 14 0 0 15 0 1 28 0 0 29 0 1 42 0 0 43 0 1	
56 0 0 57 0 1 70 0 0 71 0 1 84 0 0 85 0 1 98 0 0	
99 0 1 112 0 0 113 0 1 126 0 0 127 0 1 140 0 0 141 0 1	
154 0 0 155 0 1 168 0 0 169 0 1 182 0 0 183 0 1 196 0 0	
197 0 1 210 0 0 211 0 1 224 0 0 225 0 1 238 0 0 239 0 1	
252 0 0 253 0 1 266 0 0 267 0 1 280 0 0 281 0 1 294 0 0	
282 0 0 283 0 0 284 0 0 285 0 0 286 0 0 287 0 0 288 0 0	
289 0 0 290 0 0 291 0 0 292 0 0 293 0 0	
6 80	Radius of loaded area (AAA) in. Vertical distributed load (UDL) lbf/in^2
1 2 1 0 80	
2 3 2 0 80	Uniformly distributed load of 80 lbf/in^2 on 1st 6 elements from axis of symmetry i.e. for each: (element no./node 2/node 1/radial load/vertical load) terminator 888
3 4 3 0 80	
4 5 4 0 80	
5 6 5 0 80	
6 7 6 0 80	
0 0.08102	Overburden density for each layer (radial "density", vertical density) expressed in compatible units (lbf/in^3)
0 0.06713	
0 0.06944	

A6.3 Input in program text

The procedure LAYMOD, which defines the new modulus in non-linear layers, must contain a statement of the elastic modulus in linear layers. (e.g. in layer 1 of the following program text K = 2.82×10^5, G = 4.890×10^4). This is essential since the program modifies moduli by half the predicted amount at each iteration and to remain general does not differentiate

between linear and non-linear layers in performing this for a particular element. The procedure hence conveniently exists as a concise reminder of all the layer properties.

The total number of iterations desired must be specified in three places: at the calls of STORE and LAYSTR (to provide output of the mean and octahedral shear stresses at the final iteration) - these are underlined; for termination of the program, 8 lines from the end of the program text.

A6.4 Output

All input quantities are output to the lineprinter together with descriptive text. The generated element mesh and node co-ordinates are printed together with the calculated bandwidth. In the case KGYC = 2 (for K and G = $f(\sigma,\tau)$) the initial moduli and implied Poisson's ratio are output.

All nodal displacement are printed together with the appropriate node number.

Strains and stresses are printed out at all element centroids together with the mean stress and octahedral shear stress. In order to compare results with insitu tests (Chapter 5), "normalised" values of strain and stresses are calculated. The new moduli based on the mean stresses are printed for each element. Thus for each element the output is as follows:

element no./radial co-ordinate/vertical co-ordinate (measured from an origin 10 units below bottom boundary)/$\varepsilon_r/\varepsilon_\theta/\varepsilon_z/\gamma_{rz}$/ $\sigma_r/\sigma_\theta/\sigma_z/\tau_{rz}$/Mean normal stress ($\sigma$)/Octahedral shear stress (τ)/ $r/a/z/a$ (z is measured from surface)/$\varepsilon_r/p/\varepsilon_\theta/p/\varepsilon_z/p/\gamma_{rz}/p$/

σ_r/p%/σ_θ/p%/σ_z/p%/τ_{rz}/p%/modified K/modified G.
(in the case KGYC = 1, modified E is printed here not K,G)
At chosen iterations the mean normal and actahedral shear stresses at centroids are printed with spacing proportional to the element mesh dimensions to enable approximate contour plotting.

After stress and strain calculations the new Bulk and Shear moduli (together with the new implied Poisson's Ratios) are printed. Alternatively, if (E,ν) relationships have been used these are printed out.

PROGRAM 6: LISTING (4 node axisymmetric triangle) GENERAL ITERATIVE program as run on Chilton Atlas

```
JOB
VV115 KEN TAYLOR H4605 3 LAYER 80 PSI  6 IN RAD OVLD4 LAY   H4600 PROG
COMPUTING 60 MINUTES
STORE 120/175 BLOCKS
INPUT 1 TAYLOR
OUTPUT 0 LINEPRINTER 80000 LINES
OUTPUT 1 CARDS 1000 LINES
TAPE 99 ALGOLIB*INHIBIT
TAPE 1 NO313 RENEWED HOPE
COMPILER ALGOL
INPUT KDF9 CARDS WITH ICT I/O PROCEDURES.
LIST ON LINEPRINTER$
  'BEGIN'
 'LIBRARY' ICT5$
 'LIBRARY' ICT6$
 'LIBRARY' ICT7$
 'LIBRARY' ICT8$
 'LIBRARY' ICT9$
 'LIBRARY' ICT10$
 'LIBRARY' ICT11$
 'LIBRARY' ICT13$
 'LIBRARY' ICT40$
 'LIBRARY' ICT48$
      'INTEGER' NOD,EL,N,CS,NFX, ACROSS,DOWN,NLAYS,KGYC$
      'REAL' YMI,NUI,GMI,KMI$
 'PROCEDURE'NULL(A,M,N)$'ARRAY'A$'INTEGER'M,N$NULLARRAY(A)$
'PROCEDURE' TRANS(A,B,M,N)$ 'ARRAY' A,B$ 'INTEGER' M,N$
EQUTRANSMX(A,B)$
 'PROCEDURE'MATADD(A,B,C,M,N)$'ARRAY'A,B,C$'INTEGER'M,N$ADDXARRAY(A,B,1
  ,C)$
 'PROCEDURE'MATINV(A,B,N)$'ARRAY'A,B$'INTEGER'N$'BEGIN''ARRAY'
C(/1'.'N,1'.'N/)$ ADDXARRAY(A,B,0,C)$ INVERT(A,0)$ 'END'$
 'PROCEDURE'MATMUL(A,B,C,M,N,P)$'ARRAY'A,B,C$'INTEGER'M,N,P$
 MULTMX(A,B,C)$
 'PROCEDURE'MATCOP(A,B,M,N)$'ARRAY'A,B$'INTEGER'M,N$'BEGIN'
'ARRAY' C(/1'.'M,1'.'N/)$  ADDXARRAY(A,B,0,C)$ 'END'$
'PROCEDURE' STOP$ 'BEGIN' BREAK OUTPUT(0)$
                          BREAK OUTPUT(1)$   'END'$
'PROCEDURE' LPOUT$ SELECTOUTPUT(0)$
'PROCEDURE' CPOUT$ SELECTOUTPUT(1)$
SELECT INPUT(1)$
SELECT OUTPUT(0)$
KGYC=READ$
CS=READ$
NFX=READ$
ACROSS=READ$
DOWN=READ$
NLAYS=READ$
'COMMENT' ACROSS IS NODES ACROSS
          DOWN IS NODES DOWN$
EL = (ACROSS-1)*(DOWN-1)$
NOD = ACROSS*DOWN$
N=2*NOD$
NEWLINE(2)$ WRITETEXT('(' XXX.4.NODE.PROGRAM.XXX ')')$
```

Atlas Job heading

matrix procedures made to call Atlas procedures

input of control integer and element mesh dimensions

```
'COMMENT' OUTPUT MOST OF THE  INPUT CONSTANTS AND IMPORTANT PARAMETERS$

NEWLINE(1)$ WRITETEXT('(' KGYC..CONTROL.INTEGER..IF.1.THEN
   .YOUNGS.MODULUS..IF.2.THEN.BULK.AND.SHEAR ')')$
SPACE(5)$ PRINT(KGYC,3,0)$
NEWLINE(1)$ WRITETEXT('(' LOAD '('SS')' CASES '('26S')' ')')$
PRINT(CS,2,0)$
NEWLINE(1)$ WRITETEXT('(' NO.'('S')'OF'('S')'FIXITIES '('20S')' ')')$
PRINT(NFX,3,0)$
NEWLINE(1)$ WRITETEXT('(' NUMBER.OF.NODES....R,Z..DIRECTIONS ')' )$
PRINT(ACROSS,2,0)$ SPACE(2)$
PRINT(DOWN,2,0)$
NEWLINE(2)$ WRITETEXT('(' NO.OF.LAYERS...NLAYS ')')$
PRINT(NLAYS,5,0)$
NEWLINE(2)$ WRITETEXT('(' ELEMENTS..EL ')')$ SPACE(23)$
PRINT(EL,5,0)$
NEWLINE(1)$ WRITETEXT('(' NODES..NOD   ')')$ SPACE(25)$
PRINT(NOD,5,0)$
NEWLINE(1)$ WRITETEXT('(' NO.OF.UNKNOWNS...N ')')$ SPACE(17)$
PRINT(N,5,0)$

'BEGIN'
     'REAL' AAA,UDL,TIME,TIME2$
     'INTEGER' IDUMP,JDUMP$
'ARRAY' NCOORD(/1'.'NOD,1'.'2/), INT,AA,BB,CC,EK(/1'.'8,1'.'8/),
                FX(/1'.'NFX,1'.'3/), VI,VI2(/1'.'N,1'.'CS/),
               GM,YMKM,NU(/1'.'EL/)$
'INTEGER' 'ARRAY' ELNOD(/1'.'EL,1'.'4/),RELAT(/1'.'NLAYS,1'.'2/)$
'REAL' LR,LZ,EQU,INC,MM,SS,DD,GG,KK,MEANST,TOCT,CR,CT,CZ,CTRZ,
  INCG,INCK,EQUG,EQUK$
'INTEGER' I,J,SM,SN,L,NO,ITER,ITERN,BD,LAYER$

'INTEGER' II,JJS

        PROCEDURES   - AUTO4
                       BCHEK4

AUTO4$ 'COMMENT' FORMS ELNOD AND NCOORD (AS SPACE 4 CHOL 3106)
       AND OUTPUTS THEM$
BCHEK4$ 'COMMENT' FORMS BD..BANDWIDTH OF STRUCTURE STIFFNESS MATRIX$
NEWLINE(2)$ WRITETEXT('(' BANDWIDTH..OF.STIFFNESS.MATRIX..BD.OF.SK')')$
SPACE(2)$ PRINT(BD,3,0)$
    'BEGIN'
'ARRAY' SK(/1'.'N,1'.'BD/)$

'PROCEDURE' FXTEST$
'BEGIN'
'INTEGER' II,FXD$
NEWLINE(2)$ WRITETEXT('(' SET.TO.ZERO..SINCE.LOADED.AT.BOUNDARY ')')$
'FOR' II=1 'STEP' 1 'UNTIL' NFX 'DOBEGIN'
  FXD=2*FX(/II,1/)$
'IF' ABS( VI(/FXD-1,1/) ) 'GT' ('E'-6) 'AND' FX(/II,2/) 'EQ' 0
'THEN BEGIN'
     VI(/FXD-1,1/)=0$
NEWLINE(1)$ WRITETEXT('(' RADIAL '('5S')' NODE.... ')')$
PRINT( (ABS(FXD/2)),3,0)$ 'END'$
'IF' ABS( VI(/FXD,1/) ) 'GT' ('E'-6) 'AND' FX(/II,3/) 'EQ' 0
'THEN BEGIN'
     VI(/FXD,1/)=0$
NEWLINE(1)$ WRITETEXT('(' VERTICAL'('4S')'NODE.... ')')$
     PRINT((FXD/2),3,0)$ 'END'$
'END' TO NFX$
'END'$
```

```
'PROCEDURE' OVLD4$
'BEGIN'
'ARRAY' EX,RE(/1'.'8,1'.'1/), EQN(/1'.'4/), BB(/1'.'8,1'.'8/),
OLD(/1'.'NLAYS,1'.'2/)$              |storage of overburden loads
'REAL' RONE,RTWO,ZONE,ZTWO,REQU,RO$
'INTEGER' N1,N2,   N4,I,L,ELNO$
NEWLINE(1)$ WRITETEXT('(' OVERBURDEN '('2S')' LOADINGS ')')$
'FOR' I=1 'STEP' 1 'UNTIL' NLAYS 'DO'
'FOR' J=1,2 'DO' OLD(/I,J/)=READ$
NEWLINE(1)$ WRITETEXT('(' OVERBURDEN..RADIAL..VERTICAL.. ')')$
'FOR' I=1 'STEP' 1 'UNTIL' NLAYS 'DOBEGIN'
'FOR' J=1,2 'DO' PRINT(OLD(/I,J/),0,3)$ NEWLINE(1)$ 'END'$
NEWLINE(1)$
'FOR' NO=1 'STEP' 1 'UNTIL' EL 'DOBEGIN'  |count through elements
N1=ELNOD(/NO,1/)$ N2=ELNOD(/NO,2/)$ N4=ELNOD(/NO,4/)$
RONE=NCOORD(/N1,1/)$ RTWO=NCOORD(/N4,1/)$
ZONE=NCOORD(/N1,2/)$ ZTWO=NCOORD(/N2,2/)$
EQN(/1/)= (RTWO**2-RONE**2)*(ZTWO-ZONE)/2$
EQN(/2/)= (RTWO**3-RONE**3)*(ZTWO-ZONE)/3$
EQN(/3/)= (RTWO**2-RONE**2)*(ZTWO**2-ZONE**2)/4$
EQN(/4/)= (RTWO**3-RONE**3)*(ZTWO**2-ZONE**2)/6$

'COMMENT' WHICH LAYER$
'FOR' I=1 'STEP' 1 'UNTIL' NLAYS 'DOBEGIN'
'IF' NO 'EQ' RELAT(/I,1/) 'AND' NO 'LE' RELAT(/I,2/) 'THEN BEGIN'
LAYER=I$ 'GOTO' ESC$
'END'$ 'END'$                        |assign density of appropriate layer
                                     |for this element
ESC'.' 'FOR' I=1,2,3,4 'DO'
EX(/I,1/)=OLD(/LAYER,1/)*EQN(/I/)$
'FOR' I=5,6,7,8 'DO'
EX(/I,1/)=OLD(/LAYER,2/)*EQN(/I-4/)$      matrix inversion
AGLOB4$   MATINV(BB,AA,8)$  TRANS(AA,BB,8,8)$
'COMMENT' AA CONTAINS AA-1.TRANSPOSED $
MATMUL(RE,AA,EX,8,8,1)$
'FOR' I=1 'STEP' 1 'UNTIL' 8 'DO' RE(/I,1/)=-6.28318*RE(/I,1/)$
'FOR' I=1 'STEP' 1 'UNTIL' 4 'DOBEGIN'
PRINT( ELNOD(/NO,I/),3,0)$ SPACE(1)$ 'END'$
'FOR' I=1 'STEP' 1 'UNTIL' 8 'DO'  PRINT(RE(/I,1/),0,3)$
NEWLINE(1)$
I=1$                                 |add equivalent nodal
'FOR' L=1 'STEP' 1 'UNTIL' 4 'DOBEGIN'  |loads to load vector
ELNO=ELNOD(/NO,L/)$
VI(/2*ELNO-1,1/) = VI(/2*ELNO-1,1/) + RE(/I,1/)$
VI(/2*ELNO  ,1/) = VI(/2*ELNO  ,1/) + RE(/I+1,1/)$
I=I+2$ 'END'$
'END' NO=1 TO EL$
NEWLINE(1)$ WRITETEXT('(' VI '('S')' AFTER '('2S')' OVLD4 ')')$
'FOR' I=1 'STEP' 1 'UNTIL' N 'DOBEGIN'
'IF' ABS( (I-1)/10 - ENTIER((I-1)/10) ) 'LT' ('E'-4) 'THEN'
NEWLINE(1)$
PRINT(VI(/I,1/),0,3)$
'END'$
'END' OVLD4  $
```

PROCEDURES - STORE
LAYSTR
AGLOB4

```
'PROCEDURE' ITINT4$
'BEGIN'
'INTEGER' L,I,J$
'REAL' F1OR,FONE,FZOR,FZ,FR,FRZ,FRSQ,FZSQ,FRSQZ,FRCU,FRZSQ,FZSQOR,P,
       R1,R2,Z1,Z2,R21,R221,R231,Z21,Z221,Z231$
'COMMENT' PROVIDED ELEMENT NUMBERED CLOCKWISE STARTING AT BOTTOM LHS
     THEN R1 R2 Z1 Z2 GIVEN AS  BELOW $
NULL(INT,8,8)$
MM=(1-NU(/NO/))/NU(/NO/)$

'IF' KGYC 'EQ' 1 'THEN BEGIN'
DD=(YMKM(/NO/)*NU(/NO/))/((1+NU(/NO/))*(1-2*NU(/NO/)))$
SS=(1-2*NU(/NO/))/(2*NU(/NO/))$
'END ELSE BEGIN'
KK=3*YMKM(/NO/)*NU(/NO/)/(1+NU(/NO/))$
SS=GM(/NO/)/KK$
'END'$

 R1     = NCOORD(/ELNOD(/NO,1/),1/)$
 R2     = NCOORD(/ELNOD(/NO,4/),1/)$
 Z1     = NCOORD(/ELNOD(/NO,1/),2/)$
 Z2     = NCOORD(/ELNOD(/NO,2/),2/)$
R21=R2-R1$  R221=R2**2-R1**2$  R231=R2**3-R1**3$
Z21=Z2-Z1$  Z221=Z2**2-Z1**2$  Z231=Z2**3-Z1**3$
 'IF' ABS(R1) 'LT' 'E'-6 'OR' ABS(R2) 'LT' 'E'-6 'THEN'
    P=0 'ELSE' P= LN(R2/R1)$
FONE = R21*Z21$
F1OR = ABS( Z21*P )$
FZOR = ABS( Z221*0.5*P )$
FZ = ABS( Z221*R21*0.5 )$
FR = ABS( Z21*R221*0.5 )$
FRZ = ABS(Z221*R221*0.25 )$
FRSQ = ABS( Z21*R231/3 )$
FZSQ = ABS( Z231*R21/3 )$
FRCU = ABS( Z21*R221*(R2**2+R1**2)*0.25 )$
FRSQZ = ABS( Z221*R231/6 )$
FRZSQ = ABS(Z231*R221/6)$
FZSQOR = ABS(Z231*P/3 )$
INT(/1,1/) = MM*F1OR$
INT(/1,2/) = (MM+1)*FONE$
INT(/1,3/) = MM*FZOR$
INT(/1,4/) = (MM+1)*FZ$
INT(/1,7/) = FONE$
INT(/1,8/) = FR$
INT(/2,2/) = 2*(MM+1)*FR$
INT(/2,3/) = (MM+1)*FZ$
INT(/2,4/) = 2*(MM+1)*FRZ$
INT(/2,7/) = 2*FR$
INT(/2,8/) = 2*FRSQ$
INT(/3,3/) = MM*FZSQOR + SS*FR$
INT(/3,4/) = (MM+1)*FZSQ + SS*FRSQ$
INT(/3,6/) = SS*FR$
INT(/3,7/) = FZ$
INT(/3,8/) = (SS+1)*FRZ$
INT(/4,4/) = 2*(MM+1)*FRZSQ + SS*FRCU$

INT(/4,6/) = SS*FRSQ$
INT(/4,7/) = 2*FRZ$
INT(/4,8/) = (2+SS)*FRSQZ$
INT(/6,6/) = SS*FR$
INT(/6,8/) = SS*FRZ$
INT(/7,7/) = MM*FR$
INT(/7,8/)= MM*FRSQ$
INT(/8,8/) = MM*FRCU + SS*FRZSQ$
```

```
 'FOR' I = 1 'STEP' 1 'UNTIL' 8 'DO'
 'FOR' J = 1 'STEP' 1 'UNTIL' 8 'DO' INT(/J,I/)=INT(/I,J/)$
 'IF' KGYC 'EQ' 1 'THEN'
'BEGIN'
 'FOR' I=1 'STEP' 1 'UNTIL' 8 'DO'
 'FOR' J=1 'STEP' 1 'UNTIL' 8 'DO' INT(/I,J/)=6.2832*DD*INT(/I,J/)
'END'
 'ELSE'
'BEGIN'
 'FOR' I=1 'STEP' 1 'UNTIL' 8 'DO'
 'FOR' J=1 'STEP' 1 'UNTIL' 8 'DO' INT(/I,J/)=6.2832*KK*INT(/I,J/)$
'END'$
 'END'        $
```

PROCEDURES - BPOST4
FXBDIT
LOAD

```
      'PROCEDURE' UDOAD4$
      'BEGIN'
'ARRAY' EX(/1'.'8,1'.'2/), Q(/1'.'2,1'.'1/), RE(/1'.'8,1'.'1/),
   BB(/1'.'8,1'.'8/), DUMX(/1'.'8,1'.'2/)$
       'REAL' RONE,RTWO,ZOTWO,RLOAD,ZLOAD$
       'INTEGER' NODE1,NODE2,ELNO,I,L$
NEWLINE(1)$ WRITETEXT('(' XXXXXXXXXXXXXXXXXXXXXX '('2S')'
UNIFORMALLY'('2S')' DISTRIBUTED '('2S')' LOAD '('2S')'
 XXXXXXXXXXXXXXXXXXXXXXXXXXXXXXXXXXXXXXXX ')')$
 ULAB1'.' NO=READS$
       'IF' NO 'EQ' 888 'THEN' 'GOTO' ULAB2$
NEWLINE(1)$ WRITETEXT('(' FOR '('S')' ELEMENT ')')$
PRINT(NO,2,0)$
NODE2=READS$ NODE1=READS$
SPACE(1)$ WRITETEXT('(' BETWEEN '('S')' NODES ')')$
PRINT(NODE2,2,0)$ SPACE(1)$ WRITETEXT('(' AND ')')$
PRINT(NODE1,2,0)$
       RONE=NCOORD(/NODE1,1/)$
'COMMENT' INCLUDES THE CASE OF PART LOADED EDGE$
'IF' NODE2 'EQ' 300 'THEN' RTWO=READ    'ELSE' RTWO=NCOORD(/NODE2,1/)$
       ZOTWO=NCOORD(/NODE1,2/)$
'IF' NODE2 'EQ' 300 'THEN BEGIN' NEWLINE(2)$
WRITETEXT('(' MAXIMUM'('S')' RADIUS '('S')' ')')$ PRINT(RTWO,2,0)$
'END'$
'IF' ABS( NCOORD(/NODE1,2/)-NCOORD(/NODE2,2/) ) 'GT' ('E'-6)
'AND' NODE2 'NE' 300 'THEN' 'GOTO' ULAB3$
       'GOTO' ULAB4$
ULAB3'.' NEWLINE(1)$
WRITETEXT('(' Z '('S')' NOT '('S')' CONSTANT '('S')' FOR '('S')' LOADED
'('S')' EDGE ')')$
ULAB4'.' RLOAD=READS$  ZLOAD=READS$
SPACE(6)$ WRITETEXT( '(' RLOAD ')')$ PRINT(RLOAD,0,3)$
SPACE(3)$ WRITETEXT( '(' ZLOAD ')')$ PRINT(ZLOAD,0,3)$
       Q(/1,1/)=RLOADS$ Q(/2,1/)=ZLOADS$
       AGLOB4$
MATCOP(CC,AA,8,8)$
NULL(BB,8,8)$
'FOR' I=1 'STEP' 1 'UNTIL' 8 'DO'
'FOR' L=1 'STEP' 1 'UNTIL' 8 'DO'
CC(/I,L/)=CC(/I,L/)/('E'+15)$
 MATINV(BB,CC,8)$
'FOR' I=1 'STEP' 1 'UNTIL' 8 'DO'
'FOR' L=1 'STEP' 1 'UNTIL' 8 'DO'
BB(/I,L/)= BB(/I,L/)/('E'+15)$
       TRANS(AA,BB,8,8)$
       'COMMENT' AA NOW CONTAINS INVERT OF A TRANSPOSED$
```

```
        NULL(EX,8,2)$
        'COMMENT' BELOW SETS TERMS OF INTEGRAL, Z CONSTANT$
      EX(/1,1/) = (RTWO**2-RONE**2)$
      EX(/2,1/) = 2*(RTWO**3-RONE**3)/3$
      EX(/3,1/) = (RTWO**2-RONE**2)*ZOTWOS
      EX(/4,1/) = 2*(RTWO**3-RONE**3)*ZOTWO/3$
    EX(/5,2/)=EX(/1,1/)$   EX(/6,2/)=EX(/2,1/)$
    EX(/7,2/)=EX(/3,1/)$    EX(/8,2/)=EX(/4,1/)$
        MATMUL(DUMX,AA,EX,8,8,2)$
        MATMUL(RE,DUMX,0,8,2,1)$
        'COMMENT' RE CONTAINS IN ITS 8 BY 1 THE LOAD VECTOR FOR NO$
 NEWLINE(1)$
 'FOR' I=1 'STEP' 1 'UNTIL' 8 'DOBEGIN' RE(/I,1/)=-3.14159*RE(/I,1/)$
 PRINT(RE(/I,1/),0,3)$ 'END'$
        I=1$
        'FOR'  L= 1 'STEP' 1 'UNTIL' 4 'DO' 'BEGIN'
          ELNO=ELNOD(/NO,L/)$
          VI(/2*ELNO-1,1/) = VI(/2*ELNO-1,1/) + RE(/I,1/)$
          VI(/2*ELNO,1/) = VI(/2*ELNO,1/) + RE(/I+1,1/)$
          I=I+2$  'END'$
        'GOTO' ULAB1$
 ULAB2'.' NEWLINE(1)$
        'COMMENT' VI ARRAY UDOAD$
         'END'$
 'PROCEDURE' SETB4 (AA,LR,LZ)$ 'VALUE'LR,LZ$ 'REAL' LR,LZ$ 'ARRAY' AA$
 'BEGIN'
 AA(/1,2/)=1$ AA(/1,4/)=LZ$
 AA(/2,1/)=1/LR$ AA(/2,2/)=1$ AA(/2,3/)=LZ/LR$ AA(/2,4/)=LZ$
 AA(/3,7/)=1$ AA(/3,8/)=LR$
 AA(/4,3/)=1$ AA(/4,4/)=LR$ AA(/4,6/)=1$ AA(/4,8/)=LZ$
  'END'$
 'PROCEDURE'SETD4(BB)$ 'ARRAY' BB$
 'BEGIN'
 'INTEGER' I,J$

 MM=(1-NU(/NO/))/NU(/NO/)$
 'IF' KGYC 'EQ' 1 'THEN BEGIN'
 SS=(1-2*NU(/NO/))/(2*NU(/NO/))$
 DD=(YMKM(/NO/)*NU(/NO/))/((1+NU(/NO/))*(1-2*NU(/NO/)))$
 'END ELSE BEGIN'
 KK=3*YMKM(/NO/)*NU(/NO/)/(1+NU(/NO/))$
 SS=GM(/NO/)/KK$
 'END'$

 BB(/1,1/)=MM$  BB(/1,2/)=1$  BB(/1,3/)=1$
 BB(/2,1/)=1$  BB(/2,2/)=MM$  BB(/2,3/)=1$
 BB(/3,1/)=1$  BB(/3,2/)=1$  BB(/3,3/)=MM$
 BB(/4,4/)=SS$
 'IF' KGYC 'EQ' 1 'THEN'
'BEGIN'
 'FOR' I=1 'STEP' 1 'UNTIL' 4 'DO'
 'FOR' J=1 'STEP' 1 'UNTIL' 4 'DO' BB(/I,J/)=DD*BB(/I,J/) 'END' 'ELSE'
'BEGIN'
 'FOR' I=1 'STEP' 1 'UNTIL' 4 'DO'
 'FOR' J=1 'STEP' 1 'UNTIL' 4 'DO' BB(/I,J/)=KK*BB(/I,J/)$
'END'$
 'END' SETD4$
```

PROCEDURES - PLAGMK3
CHODET
CHOSOL

```
'PROCEDURE' LAYMOD(LAY,EQQN)$ 'INTEGER' LAY,EQQN$
'BEGIN'
'IF' LAY 'EQ' 1 'THEN BEGIN'
EQUK=2.282*('E'+5)$
EQUG=4.890*('E'+4)$            'END'$
'IF' LAY 'EQ' 2 'THEN BEGIN'
'IF' MEANST 'GE' 35.0 'THEN' MEANST=35.0$
EQUK=('E'+6)/(107-2.8*MEANST)$
   EQUG=('E'+6)/(276-5*TOCT)$ 'END'$
'IF' LAY 'EQ' 3 'THEN BEGIN'
EQUK= ('E'+6)/(1.2+0.09*MEANST)$
EQUG= ('E'+6)/0.5-0.2*TOCT+0.08*TOCT**2)$
'IF' 3*EQUK-2*EQUG 'LE' ('E'-6) 'THEN BEGIN'
EQUK=8.27129*('E'+5)$      EQUG=1.19646*('E'+6)$  'END'$
 'COMMENT' VALUES FOR MEANST=0.1  TOCT=3.6$
'END'$
'END' LAYMOD$
'COMMENT' TOTAL NO OF ITERATIONS OF LOAD$
ITERN=READ$ 'COMMENT' INPUT TOTAL ITERATIONS TO FULL LOAD$
NEWLINE(1)$ WRITETEXT('(' ITERN..TO.FULL.LOAD')')$ PRINT(ITERN,3,0)$


 'COMMENT' READ IN LAYER DESCRIPTION  RELAT$
 'FOR' I=1 'STEP' 1 'UNTIL' NLAYS 'DOBEGIN'
 'FOR' J=1,2 'DO' RELAT(/I,J/)=READ$ 'END'$
 NEWLINE(2)$
 WRITETEXT('(' LAYER.DESCRIPTION..RELAT(NLAYS,2)  ')')$
 NEWLINE(2)$
 'FOR' I=1 'STEP' 1 'UNTIL' NLAYS 'DOBEGIN'
 'FOR' J=1,2 'DOBEGIN' PRINT(RELAT(/I,J/),4,0)$ SPACE(2)$
 'END'$ NEWLINE(1)$ 'END'$

 'IF' KGYC 'EQ' 1 'THEN BEGIN'
 'COMMENT' READ IN AND SET LAYER INITIAL YOUNGS MODULI $
 NEWLINE(2)$ WRITETEXT('(' LAYER.YOUNGS.MODULI ')')$ NEWLINE(1)$
 'FOR' I=1 'STEP' 1 'UNTIL' NLAYS 'DOBEGIN'   YMI=READ$
 PRINT(YMI,0,3)$ SPACE(2)$
 'FOR' SM= RELAT(/I,1/) 'STEP' 1 'UNTIL' RELAT(/I,2/) 'DO'
 YMKM(/SM/)=YMI$ 'END'$          'END' 'ELSE' 'BEGIN'
 'COMMENT' READ IN AND SET INITIAL BULK AND SHEAR MODULI$
 NEWLINE(2)$ WRITETEXT('(' LAYER.BULK...SHEAR.MODULI..INITIAL ')')$
 NEWLINE(1)$
 'FOR' I=1 'STEP' 1 'UNTIL' NLAYS 'DOBEGIN'  KMI=READ$ GMI=READ$
 PRINT(KMI,0,3)$ SPACE(1)$    PRINT(GMI,0,3)$ SPACE(5)$
 'FOR' SM= RELAT(/I,1/) 'STEP' 1 'UNTIL' RELAT(/I,2/) 'DO BEGIN'
 YMKM(/SM/)=KMI$  GM(/SM/)=GMI$   'END'$'END'$'END' IF KGYC BLOCK$

 'IF' KGYC 'EQ' 1 'THEN BEGIN'
 'COMMENT' READ IN AND SET NLAYS POISSONS RATIOS    NU(EL)  $
 NEWLINE(2)$ WRITETEXT('(' LAYER.POISSONS.RATIO ')')$ NEWLINE(1)$
 'FOR' I=1 'STEP' 1 'UNTIL' NLAYS 'DOBEGIN'  NUI=READ$
 PRINT(NUI,1,3)$ SPACE(2)$
 'FOR'  SM= RELAT(/I,1/) 'STEP' 1 'UNTIL' RELAT(/I,2/) 'DO'
 NU(/SM/)=NUI$  'END'$
 'END' NU KGYC IF$
```

```
'COMMENT' OUTPUT TO LP YM OR KM AND GM    ALSO NU
  NOTE THAT KM IS STORED IN YMKM,AS IS YM$
NEWLINE(2)$
'IF' KGYC 'EQ' 1 'THEN' WRITETEXT('(' INITIAL.YM.S ')')  'ELSE'
    WRITETEXT('(' INITIAL. BULK.MODULUS ')')$
NEWLINE(1)$ J=1$
'FOR' I=1 'STEP' 1 'UNTIL' EL 'DOBEGIN'
PRINT(YMKM(/I/),0,3)$ SPACE(2)$
'IF' J 'EQ'  5 'THEN' 'BEGIN' J=0$ NEWLINE(1)$ 'END'$ J=J+1$ 'END'$
'IF' KGYC 'EQ' 2 'THEN  BEGIN'
NEWLINE(2)$ WRITETEXT('('  INITIAL.SHEAR.MODULUS ')')$
NEWLINE(1)$ J=1$
'FOR' I=1 'STEP' 1 'UNTIL' EL 'DOBEGIN'
PRINT(GM(/I/),0,3)$ SPACE(2)$
'IF' J 'EQ'  5 'THENBEGIN' J=0$ NEWLINE(1)$ 'END'$ J=J+1$
'END'$      'END' KGYC EQ 2$
'IF' KGYC 'EQ' 1 'THEN BEGIN'
NEWLINE(2)$ WRITETEXT('(' INITIAL.POISSONS.RATIOS ')')$
NEWLINE(1)$ J=1$
'FOR' I=1 'STEP' 1 'UNTIL' EL 'DOBEGIN'
PRINT(NU(/I/),0,3)$ SPACE(2)$
'IF' J 'EQ'  5 'THEN BEGIN' J=0$ NEWLINE(1)$ 'END'$ J=J+1$ 'END'$
'END ELSE BEGIN'
NEWLINE(2)$
WRITETEXT('(' CALCULATED.INITIAL.VALUES.OF.POISSONS.RATIOS')')$
'FOR' I=1 'STEP' 1 'UNTIL' EL 'DO'
NU(/I/)= (3*YMKM(/I/)-2*GM(/I/))/(6*YMKM(/I/)+2*GM(/I/))$
NEWLINE(1)$
J=1$
'FOR' I=1 'STEP' 1 'UNTIL' EL 'DOBEGIN'
PRINT(NU(/I/),0,3)$ SPACE(2)$
'IF' J 'EQ' 5 'THEN BEGIN'
J=0$ NEWLINE(1)$
'END'$ J=J+1$ 'END'$
'END' NU KGYC IF  IF 1 OR 2 $

'COMMENT' READ IN FIXITY MATRIX  FX(NFX,3)$
    'FOR' I=1 'STEP' 1 'UNTIL' NFX 'DO' 'FOR' J=1,2,3 'DO' FX(/I,J/)=RE
 AD$
NEWLINE(1)$ WRITETEXT('('XXX.FIXITY.MATRIX.XXX')')$
'FOR' I=1 'STEP' 1 'UNTIL' NFX 'DOBEGIN' NEWLINE(1)$
'FOR' J=1,2,3  'DO' PRINT(FX(/I,J/),3,0)$ 'END'$
'COMMENT' INPUT NORMALISING CONSTANTS$
AAA=READS   UDL=READS$
NEWLINE(1)$
WRITETEXT('(' RADIUS .OF.LOADED.AREA ')')$     SPACE(2)$
PRINT(AAA,2,2)$
NEWLINE(1)$ WRITETEXT('(' UD.LOAD..FOR.NORMALISING.PURPOSES ')')$
SPACE(2)$ PRINT(UDL,3,2)$
ITER=1$
IDUMP=1000$     JDUMP=4800$  TIME2=600$
LAB1'.' PAPERTHROW$
TIME=ELAPSED TIME$ NEWLINE(1)$ PRINT(TIME,5,1)$
    'IF' TIME 'GT' TIME2 'THEN BEGIN'
        TIME2=TIME2+600$
        DUMP PROGRAM(1,IDUMP,JDUMP)$
NEWLINE(1)$ WRITETEXT('(' I....J.... ')')$
SPACE(3)$
 PRINT(IDUMP,3,0)$ SPACE(2)$ PRINT(JDUMP,3,0)$
        IDUMP=JDUMP+1$
JDUMP=4800$
```

each 10 minutes dump copy of program to tape to enable re-start in the event of m/c breakdown

```
          BREAK OUTPUT(0)$
          BREAK OUTPUT(1)$
      'END'$
WRITETEXT('(' ITER'('SS')' = ')')$ PRINT(ITER,3,0)$
NULL(SK,N,BD)$
'FOR' NO = 1 'STEP' 1 'UNTIL' EL 'DO' 'BEGIN'
AGLOB4$
ITINT4$
MATCOP(CC,AA,8,8)$
MATINV(BB,CC,8)$
TRANS(EK,BB,8,8)$                    |element stiffness
MATMUL(CC,EK,INT,8,8,8)$
MATMUL(EK,CC,BB,8,8,8)$
BPOST4$
 'END'$
FXBDIT$
'IF' ITER 'EQ' 1 'THEN BEGIN'

NULL(VI,N,CS)$
LOAD$   }
OVLD4$  }  <-------loading
FXTEST$
NEWLINE(1)$
WRITETEXT( '('XXXXXXXXXXXXXXXXXXXXXXXXXXXXXXXXXXXXXXXXXXXXXXXXXXX')')$
NEWLINE(2)$ WRITETEXT('(' LOAD.VECTORS...VI(N,CS)  ')')$
NEWLINE(1)$
SM=1$ 'FOR' I=1 'STEP' 1 'UNTIL' N 'DOBEGIN' PRINT(VI(/I,1/),0,3)$
'IF' SM 'EQ' 5 'THEN BEGIN' NEWLINE(1)$ SM=1$ 'END' 'ELSE' SM=SM+1$
                                                    'END'$
    'FOR' I=1 'STEP' 1 'UNTIL' N 'DO' VI2(/I,1/)=VI(/I,1/)$
 'END'$
NULL(VI,N,CS)$
'FOR' I=1 'STEP' 1 'UNTIL' N 'DO''BEGIN'
'IF' ITER 'LT' ITERN 'THEN' VI(/I,1/)=(ITER/ITERN)*VI2(/I,1/)
'ELSE' VI(/I,1/)=VI2(/I,1/)$
 'END'$
PLAGMK3(N,BD,CS,SK,VI)$   |solution of equations by Choleski
                          | decomposition
CPOUT$
PRINT(ITER,4,0)$ SPACE(2)$ PRINT(VI(/2,1/),0,6)$
LPOUT$
NEWLINE(2)$ WRITETEXT('(' DISPLACEMENTS.AT.NODES ')')$
NEWLINE(1)$
'FOR' I = 1 'STEP' 2 'UNTIL' (N-1) 'DO' 'BEGIN'
SM = (I+1)/2$
NEWLINE(1)$ PRINT(SM,3,0)$ SPACE(3)$
'FOR' J=0,1  'DOBEGIN' PRINT(VI(/I+J,1/),0,4)$ SPACE(4)$ 'END'$
'END' I$
PAPERTHROW$
WRITETEXT ('(' ELEMENT '('4S')' CENTROID '('8S')' R '('11S')' Z
'('3S')' STRAINS...R.TH.Z.TRZ ')')$
SPACE(10)$ WRITETEXT('(' STRESSES...R.TH.Z.TRZ....MEAN.STRESS ')')$
NEWLINE(1)$ SPACE(100)$ WRITETEXT('(' OCT.SHEAR.STRESS ')')$

NULL(SK,5*(DOWN-1),ACROSS-1)$   |provide storage in redundant
II=1$  JJ=1$                    |stiffness matrix for mean and shear
                                |stresses
```

```
'FOR' NO=1 'STEP' 1 'UNTIL' EL 'DO' 'BEGIN'
LR=0$ LZ=0$
'FOR' L=1 'STEP' 1 'UNTIL' 4 'DO BEGIN'
LR=LR+NCOORD(/ELNOD(/NO,L/),1/)$ LZ=LZ+NCOORD(/ELNOD(/NO,L/),2/)$
 'END'$ LR=LR/4$ LZ=LZ/4$
NEWLINE(1)$ PRINT(NO,3,0)$
PRINT(LR,2,2)$ PRINT(LZ,2,2)$
NULL(AA,8,8)$ NULL(BB,8,8)$ NULL(CC,8,8)$
AGLOB4$
MATINV(BB,AA,8)$
NULL(AA,8,8)$
SETB4(AA,LR,LZ)$
MATMUL(CC,AA,BB,8,8,8)$
NULL(BB,8,8)$
L=1$ 'FOR' I=1 'STEP' 2 'UNTIL' 7 'DO' 'BEGIN'
SM=ELNOD(/NO,L/)$
BB(/I,1/)=VI(/2*SM-1,1/)$  BB(/I+1,1/)=VI(/2*SM,1/)$
L=L+1$  'END'$
NULL(AA,8,8)$
MATMUL(AA,CC,BB,8,8,8)$
'COMMENT' STRAINS OUT$
'FOR' I=1,2,3,4 'DOBEGIN'
PRINT(AA(/I,1/),0,1)$ 'END'$
NULL(BB,8,8)$
SETD4(BB)$
MATMUL(CC,BB,AA,8,8,8)$
'COMMENT' STRESSES ARE IN CC1,1 TO CC 1,4$
'FOR' I=1 'STEP' 1 'UNTIL' 4 'DO'      PRINT(CC(/I,1/),3,2)$
MEANST=0$
'FOR' I=1 'STEP' 1 'UNTIL' 3 'DO' MEANST=MEANST + CC(/I,1/)$
MEANST=MEANST/3$
CR=CC(/1,1/)$  CT=CC(/2,1/)$  CZ=CC(/3,1/)$  CTRZ=CC(/4,1/)$
TOCT= SQRT( ((CR-CT)**2 + (CT-CZ)**2 + (CZ-CR)**2 + 6*CTRZ**2))/3$
PRINT(MEANST,3,2)$
PRINT(TOCT  ,3,2)$

'IF' NO 'EQ' 1 'THEN' 'BEGIN'
CPOUT$
PRINT(ITER,3,0)$ SPACE(2)$
 PRINT(CC(/3,1/),3,5)$ SPACE(2)$
PRINT(MEANST,2,5)$ SPACE (2)$
PRINT(TOCT,2,5)$ SPACE (2)$
LPOUT$    'END'$
'IF' ITER 'EQ' 1 'OR' ITER 'GE' 12 'THEN'
STORE$ 'COMMENT' PUTS MEANST IN SK, LR, LZ$

'FOR' I=1,2,3,4 'DOBEGIN' AA(/I,1/)=('E'+6)*AA(/I,1/)/UDL$
                          CC(/I,1/)=100* CC(/I,1/)/UDL$ 'END'$
LR=LR/AAA$  LZ=(82-LZ)/AAA$     (82 is total mesh depth + 10)
NEWLINE(1)$ SPACE(5)$ PRINT(LR,2,2)$
        PRINT(LZ,2,2)$
'FOR' I=1,2,3,4 'DOBEGIN'
 PRINT(AA(/I,1/),3,3)$              'END'$
'FOR' I=1,2,3,4 'DO' PRINT(CC(/I,1/),2,2)$

MEANST=ABS(MEANST)$
'COMMENT' X X X X X X X X X X X X X X X X X X X X X X X X X X X  $
'COMMENT' MODIFY MODULI IN CORRECT LAYER$
'FOR' I=1 'STEP' 1 'UNTIL' NLAYS 'DOBEGIN'
'IF' NO 'EQ' RELAT(/I,1/) 'AND' NO 'LE' RELAT(/I,2/) 'THEN' 'BEGIN'
LAYER=I$ 'GOTO' LAYE$ 'END'$ 'END'$
LAYE'.' LAYMOD(LAYER,KGYC)$
```

```
'COMMENT' X X X X X X X X X X X X X X X X X X X X X X X X X X X $
'COMMENT' DAMP THE MODIFICATION TO MODULUS SO THAT ONLY CHANGE
      BY HALF THE AMOUNT EXPECTED $

'IF' KGYC 'EQ' 1 'THEN BEGIN'
INC=EQU-YMKM(/NO/)$ INC=INC/2$ YMKM(/NO/)=YMKM(/NO/)+INC$
          PRINT(YMKM(/NO/),0,3)$   'END ELSE BEGIN'
INCG=EQUG-GM(/NO/)$ INCG=INCG/2$ GM(/NO/)=GM(/NO/)+INCG$
INCK=EQUK-YMKM(/NO/)$ INCK=INCK/2$ YMKM(/NO/)=YMKM(/NO/)+INCK$
          PRINT(YMKM(/NO/),0,3)$
          PRINT(GM(/NO/),0,3)$
NU(/NO/) = (3*YMKM(/NO/)-2*GM(/NO/))/(2*GM(/NO/)+6*YMKM(/NO/))$
'END'$

'END' NO=1 TO EL FOR STRESSES$

'IF' ITER 'EQ' 1 'OR' ITER 'GE' 12 'THEN'
LAYSTRS$ 'COMMENT' LAYS MEANST ON L/P$

'COMMENT' OUTPUT TO LP YM OR KM AND GM-   ALSO NU
  NOTE THAT KM IS STORED IN YMKM AS IS YM$
NEWLINE(2)$
'IF' KGYC 'EQ' 1 'THEN' WRITETEXT('('          YM.S ')')  'ELSE'
   WRITETEXT('('          BULK.MODULI ')')$
NEWLINE(1)$ J=1$
'FOR' I=1 'STEP' 1 'UNTIL' EL 'DOBEGIN'
PRINT(YMKM(/I/),0,3)$ SPACE(2)$
'IF' J 'EQ'  5 'THEN' 'BEGIN' J=0$ NEWLINE(1)$ 'END'$ J=J+1$ 'END'$
'IF' KGYC 'EQ' 2 'THEN  BEGIN'
NEWLINE(2)$ WRITETEXT('('          SHEAR.MODULUS ')')$
NEWLINE(1)$ J=1$
'FOR' I=1 'STEP' 1 'UNTIL' EL 'DOBEGIN'
PRINT(GM(/I/),0,3)$ SPACE(2)$
'IF' J 'EQ'  5 'THENBEGIN' J=0$ NEWLINE(1)$ 'END'$ J=J+1$
'END'$      'END' KGYC EQ 2$
NEWLINE(2)$ WRITETEXT('('          POISSONS.RATIOS')')$
NEWLINE(1)$ J=1$
'FOR' I=1 'STEP' 1 'UNTIL' EL 'DOBEGIN'
PRINT(NU(/I/),0,3)$ SPACE(2)$
'IF' J 'EQ'  5 'THEN BEGIN' J=0$ NEWLINE(1)$ 'END'$ J=J+1$ 'END'$
'IF' ITER 'EQ' 12 'THEN GOTO' L99$
ITER=ITER+1$ 'GOTO' LAB1$                    change to equal max. desired
'END' MAIN 4NVE 200 MODULARISED(2 IN BLOCK)$      no. of iterations
 'END' NON MODULARISED HARWELL COMPAT. FROM 4AUTBIG 3313(1 IN BLOCK)$
L99'.'
STOP$
  'END'$ 'END'$ 'END'$ 'END'$ 'END'$
'END' MAIN PROGRAM 4 NODE ELEMENT AND OUTER BLOCK, 8 NODE COMPATIBLE
```

A.7 CHOLESKY BANDED DECOMPOSITION

The procedure PLAGMK3 is a standard Cholesky decomposition for a banded symmetric matrix modified and made to be efficient and easy to use in structural problems. The procedure requires storage equal to the upper band of the structural stiffness matrix and places the solution(s) into the load vector(s).

Input parameters:

ID - total no. of unknowns

IW - bandwidth

ILO - number of load cases

S - stiffness matrix, S(1:ID, 1:IW)

LO - load vector(s)/solution vector(s) LO(1:ID, 1:ILO)

If the stiffness matrix is non-positive definite a failure message "FAILURE IN CHODET" is printed, usually signifying faulty data.

```
'PROCEDURE' PLAGMK3(ID,IW,ILO,S,LO)$   'VALUE' ID,IW,ILO$
'ARRAY' S,LO$ 'INTEGER' ID,IW,ILO$
'BEGIN' 'INTEGER' IMM,INN$
'FOR' IMM=ID 'STEP' -1 'UNTIL' 1 'DO'
'FOR' INN=IW 'STEP' -1 'UNTIL' 1 'DO'
'IF' (IMM+INN) 'GT' IW 'THEN'
S(/IMM,INN/)=S(/IMM+INN-IW,IW-INN+1/)$
CHODET(ID,IW,S,S)$
CHOSOL(ID,IW,ILO,S,LO,LO)$
'END' PLAGMK3
*IDENTIFIERCHODET
*ALGOL
'PROCEDURE' CHODET(N,M,A,L)$       'VALUE' N,M$
'ARRAY' A,L$ 'INTEGER' N,M$
'BEGIN'
'INTEGER' P,Q,R,S,MA,I,J,K$    'REAL' Y$
MA=M-1$
'FOR' I=1 'STEP' 1 'UNTIL' N 'DOBEGIN'
'IF' I 'GT' MA 'THEN' P=1 'ELSE' P=M-I+1$
R=I-M+P$
'FOR' J=P 'STEP' 1 'UNTIL' M 'DOBEGIN'
S=J-1$  Q=M-J+P$
Y=A(/I,J/)$
'IF' P 'LE' S 'THEN'
'FOR' K=P 'STEP' 1 'UNTIL' S 'DOBEGIN'
Y=Y-L(/I,K/)*L(/R,Q/)$
Q=Q+1$ 'END'$
'IF' J 'EQ' M 'THEN BEGIN'
'IF' Y 'LT' 0 'THEN BEGIN'
NEWLINE(2)$ WRITETEXT('(' FAILURE.IN.CHODET..Y.LT.0 ')')$ STOP$ 'END'$
L(/I,J/)=1/SQRTF(Y)$ 'END' 'ELSE' L(/I,J/)=Y*L(/R,M/)$ R=R+1$
'END' J$ 'END' I$
'END' CHODET
*IDENTIFIERCHOSOL
*ALGOL
'PROCEDURE' CHOSOL(N,M,R,L,B,X)$ 'VALUE' N,M,R$
'ARRAY' L,B,X$ 'INTEGER' N,M,R$
'BEGIN'
'INTEGER' P,Q,  S,MA,I,J,K,KA,IA$
'REAL' Y$
S=M-1$  MA=M-1$
'FOR' J=1 'STEP' 1 'UNTIL' R 'DOBEGIN'
'COMMENT' SOLUTION OF LY=B$
'FOR' I=1 'STEP' 1 'UNTIL' N 'DOBEGIN'
'IF' I 'GT' MA 'THEN' P=1 'ELSE' P=M-I+1$   Q=I$
Y=B(/I,J/)$
'IF' P 'LE' S 'THEN'
'FOR' K=P 'STEP' 1 'UNTIL' S 'DOBEGIN'
KA=S-K+P$
Q=Q-1$
Y=Y-L(/I,KA/)*X(/Q,J/)$
'END' K$     X(/I,J/)=Y*L(/I,M/)$
'END' I$
'COMMENT' SOLUTION OF UX=Y $
'FOR' I=1 'STEP' 1 'UNTIL' N 'DOBEGIN'
IA=N+1-I$
'IF' (N-IA) 'GT' MA 'THEN' P=1 'ELSE' P=M-N+IA$
Y=X(/IA,J/)$
Q=IA$
'IF' P 'LE' S 'THEN'
'FOR' K=P 'STEP' 1 'UNTIL' S 'DOBEGIN'
KA=S-K+P$  Q=Q+1$
Y=Y-L(/Q,KA/)*X(/Q,J/)$
'END' K$  X(/IA,J/)=Y*L(/IA,M/)$
'END' I$ 'END' J$
'END' CHOSOL AND PLAGMK3 MODULES
```